# Boiling in Mini and Micro-Channels

A Thesis
Presented to
The Academic Faculty

by

Nurudeen O. Olayiwola

In Partial Fulfillment
of the Requirements for the Degree
Master of Science in the
School of Mechanical Engineering

Georgia Institute of Technology
August 2005

Boiling in Mini and Micro-Channels

Approved by:

Dr. S. Mostafa Ghiaasiaan, Chair
School of Mechanical Engineering
*Georgia Institute of Technology*

Dr. Said I. Abdel Khalik
School of Mechanical Engineering
*Georgia Institute of Technology*

Dr. Sheldon M. Jeter
School of Mechanical Engineering
*Georgia Institute of Technology*

Date Approved: June 22, 2005

**ACKNOWLEDGEMENT**

As customary and indeed appropriate, I would like to thank the Almighty God, for without Him nothing is possible. Secondly I would like to thank my advisor, Dr. S. M Ghiaasiaan. This work would not have been possible without him. Last but not least I would like to thank all my colleagues, my entire family, especially my wife, who has been tremendous and supportive.

**TABLE OF CONTENTS**

LIST OF TABLES

Table

LIST OF FIGURES

Figure

## Nomenclature

### Greek Letters

$a_k$ = void fraction of phase k

$\bar{r}$ = mixture, two phase density (kg/m$^3$)

$r_h$ = homogeneous density (kg/m$^3$)

$r_G$ = gas density (kg/m$^3$)

$r_L$ = liquid density (kg/m$^3$)

$n_L$ = liquid specific volume (m$^3$/kg)

$n_G$ = gas specific volume (m$^3$/kg)

$s$ = surface tension (N/m)

µ = kinematic viscosity (kg/ms)

$a_l$ = thermal diffusivity of the liquid

$q$ = dependant parameter

$t$ = shear stress (N/m$^2$)

### Symbols

A = area (m$^2$)

$M_k$ = signal from sensor to show present phase

t = time (s)

z = position (m)

r = radius (m)

G = Mass flux (kg/m$^2$s)

j = superficial velocity (m/s)

x = quality

h = convective heat trans. Coefficient ($W/m^2K$)

T = temperature (K)

e = specific energy (J/kg)

P = pressure (Pa)

$P_H$ = Heated perimeter

$q''$ = heat flux ($W/m^2$)

$\dot{q}$ = heat rate ($W/m^3$)

U = phase velocity (m/s)

Re = Reynolds number

Pr = Prandtl number

k = conductivity (W/mK)

D = diameter (m)

$B_o$ = boiling number

$X_{tt}$ = Martinelli parameter

$N_u$ = Nusselt numer

$D_h$ = Hydraulic diameter (m)

L = length (m)

$h_{mac}$ = macro heat transfer coefficient ($W/m^2K$)

$h_{fg}$ = latent heat of vaporization (J/kg)

$T_{sat}$ = saturation temperature (K)

$T_w$ = wall temperature (K)

$\Delta T_b$ = change in bulk temperature (K)

$\Delta T_s$

$F_{fl}$ = Fluid dependent parameter given by Kandlikar [21, 22]

f = friction factor

$\dot{m}$ = mass flux (kg/s)

F= forced convection heat transfer enhancement factor

S = suppression factor

$c_{pl}$ = specific heat (J/kg.K)

Co = Convective number

Bo = Boiling number

E = Enhancement factor

Fr = Froude number

g = acceleration due to gravity ($m^2s$)

M = mass (kg)

$B_M$ = fluid specific constant

Ra = wall roughness (µm)

$Ra_0$ = wall roughness under normalized conditions

X = martinelli factor

L = length (m)

$Re_m$ = mixture Reynolds number

$Pe_*$ = modified peclet number

**Definition of subscripts**

0 = initial

G = gas phase

L = liquid phase

l = liquid only

tp = two phase

w = wall

sat = saturated

nb = nucleate boiling

cb = convective boiling

nbo = nucleate boiling only

mac = macro

mic = micro

tur = turbulent

f = fluid

g = gas/ vapor

FC = forced convection

B = boiling

b = bulk

lo = liquid only

NBD = nucleate boiling

CBD = convective boiling

vv = viscous-viscous

v-t = viscous-turbulent

PB = pool boiling

exp = experimental

corr = correlation

# Summary

**Boiling heat transfer in Mini and Micro-channels**

Cooling systems that consist of mini-channels (hydraulic diameters in the 0.5 mm-2.0 mm range) and micro-channels (hydraulic diameters in the 100 µm-500 µm range) can dispose of extremely large volumetric thermal loads that are well beyond the feasible range of conventional cooling methods. Mini/micro-channel systems that utilize boiling fluids are particularly useful due to the superiority of boiling heat transfer mode over convection. Although forced flow boiling in mini and micro-channels has been investigated by several groups in the past, a reliable predictive method is not yet available.

In this study, the capability of a large number of forced flow boiling correlations for application to mini channels is examined by comparing their predictions with three experimental data sets. The tested correlations include well-established methods for conventional boiling systems, as well as correlations recently proposed for mini-channels.

The experimental data all represent mini-channels. Based on these comparisons, the most accurate existing predictive method for mini-channel boiling is identified. The deficiencies of the predictive methods and the potential causes that underlie these deficiencies are also discussed.

# CHAPTER 1: Introduction

## 1.1 General Remarks about Mini and Micro-Channels

The advantages of using mini and micro-channels in high demand cooling systems could not be over emphasized, especially with the advent of micro technology. This trend is present in many branches of industry. There is for example, a great need in the automotive industry, particularly in the heavy machinery industry, for small and highly efficient cooling systems, that could only be met by micro-channel-based devices. Potential applications of mini and micro-channel based systems include the heat exchangers in the home refrigeration systems. These systems currently take up considerable space. There is also an obvious need to reduce the cooling system size in small powerful laptops as well as in other micro computers.

Thus, the main reason mini and micro channels are a focus of attention in various industries is because of their efficiency in heat transfer and the advantage these small scale ducts have the regular size pipes with respect to material cost. When used with a well suited fluid, the small channels provide for higher heat transfer, save space, and reduce material cost. It is worth emphasizing that the use of mini and micro channels enables us to conserve space as well. This is a major factor in the design of many contemporary electronic devices, office spaces, automobiles and a vast array of other applications.

Due to the aforementioned benefits, many researchers have spent a great deal of effort aimed at understanding single and two phase flow and heat transfer phenomena, and the development of reliable modeling procedures for mini and micro-channels. Nevertheless, it is widely accepted that there is still a lack of a comprehensive understanding of the trends and the dominant factors affecting the flow and transport process in mini and micro-channels. Poorly understood basic phenomena are many, and worldwide attempts aimed at their resolution are underway. An example that is relevant to this thesis is the heat transfer mechanism in boiling. Bubble nucleation (nucleate boiling) and evaporation convection both can contribute to boiling heat transfer. However, there is a debate about the dominant component from these two heat transfer component.

## 1.2 Objectives of this Work

A critical study of the available correlations for forced-flow boiling heat transfer, with respect to their applicability to mini and micro-channels is done in this Thesis. This is to enable us to focus attention in the identification of well grounded starting point in a new phase of studying mini and micro-channels. Boiling in commonly-applied tubes and channels (typically with hydraulic diameters larger that about 3mm) has of course been exhaustively studied in the past, and a number of relatively accurate correlations exist. Some of widely-referenced correlations have indeed limited numbers of data points in their data bases that can be considered mini-channel data. The applicability of these correlations to mini and micro-channels is by no means certain. This is because the hydrodynamic and transport phenomena in mini and micro-channels are likely to be different than large channels due to the effects of the reduction in channel size. As a result, macro-scale models and correlations often do not fully explain all the heat transfer trends in mini and micro-channels. Notwithstanding, these correlations and modeling procedures are widely used to analyze mini and micro-channels. The focus of this thesis is thus on the examination of the most widely-referenced boiling heat transfer correlation with respect to their relevance to mini and micro channels, and identify the most appropriate correlation among them for use in mini and micro-channel analysis and to demonstrate the need of performing more in-depth experiments in the field of mini and micro-channel boiling and heat transfer. To this end, experimental data from several sources will be compared with the predictions of the most widely-used correlations. This comparison will elucidate the shortcomings of the existing models and/or correlations, and help provide the background for the development of a correlation tailored for the boiling heat transfer in mini and micro-channels. Reliable correlations, once available, will provide for the full use of the advantages of mini and micro-channels.

## Chapter 2: Review of Literature

### 2.1 Two Phase Flow Regimes and Models

In forced-flow boiling, the flow of the fluid in a heated conduit is generally in the form of a complex two-phase flow. Numerous studies have been conducted in the past to understand the characteristics of these types of flow. Many of these studies were done to understand and model the flow patterns. The main purpose of modeling usually is to produce tools for predicting the behavior of these systems, and thereby make the control of these flow types possible. Due to complicated hydrodynamic effects, however, boiling two-phase flow regimes are generally more complicated than adiabatic flows.

The study of most gas-liquid two-phase flow regimes in principle revolves around the combined flow of gas and liquid phases in a duct. A brief review of adiabatic gas-liquid two-phase flow regimes is therefore a rational starting point for the discussion of boiling regimes. These flows have been widely studied for a century, and extensive research has been performed in order to understand the regimes in two phase flow. Since buoyancy plays an important role in gas-liquid two-phase flow in commonly-applied channels (i.e., excluding mini and micro-channels), the flow regimes are generally sensitive to the channel orientation. Most of the industrial two-phase flow applications involve either horizontal or vertical channels, however. The bulk of the past studies have therefore been focused on these orientations.

There are several major flow regimes in both vertical and horizontal pipes, which are often separated from each other by regime transition regions in flow regime maps. Horizontal pipes have been observed to depict at least eight major regimes. The transition from one regime to the next is mainly dependent on the hydrodynamic parameters of the channel flow as well as heat transfer patterns. The main flow regimes in a horizontal pipe are as follows; Bubbly flow, Plug flow, Stratified flow, Wavy flow, Slug flow, Semi-annular, Annular, and Spray. Figure 2.1 shows the morphological shapes of these flow regimes in a horizontal pipe.

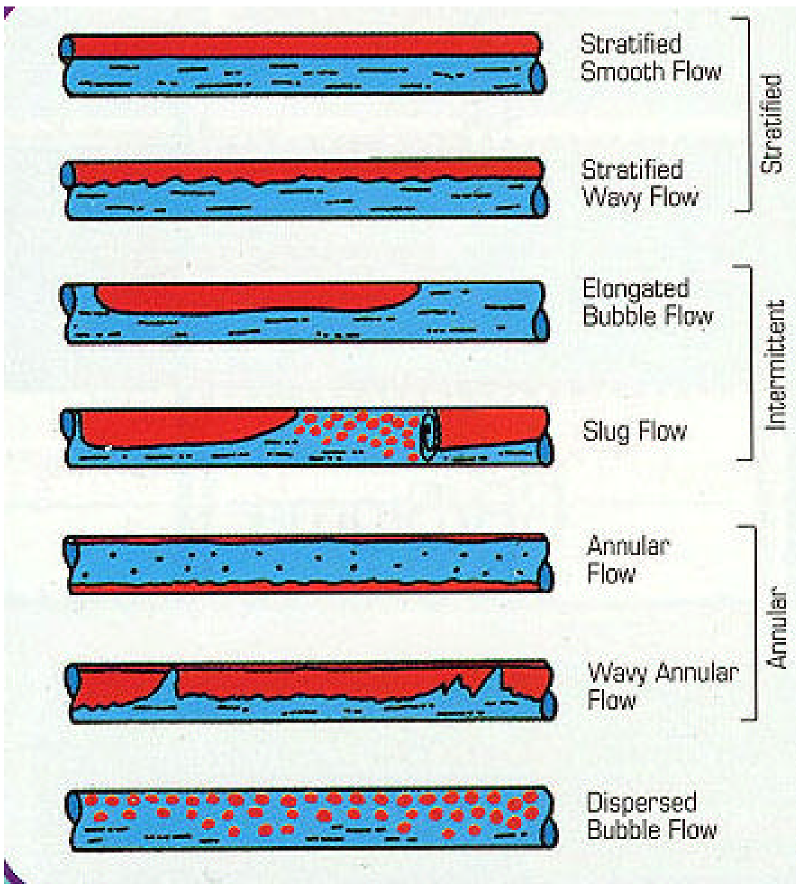


Figure 2.1: Flow regimes in a horizontal pipe.[69]

A relatively small inclination with respect to the horizontal plane usually has a big impact on the flow regimes. Figure 2.2 shows the flow regime categories in inclined pipes. In vertical pipes there are four main flow regimes, as shown in Fig. 2.3. The main observed flow regimes in vertical channels are: Bubbly flow, Slug flow, Churn flow and Annular /dispersed flow.

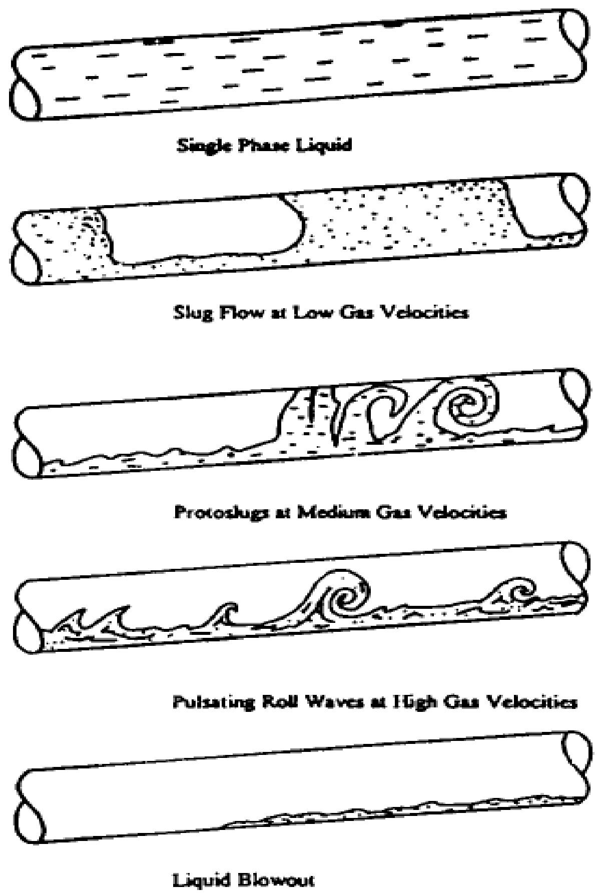


Figure 2.2: Flow regimes in an inclined pipe. [69]

The schematics in Figs (2.1- 2.3) are rather self explanatory with regards to the major morphological characteristics of each major flow regime. Therefore, they will not be discussed further. A flow regime that occurs in both adiabatic and boiling channels, and has similar characteristics in both types of systems, is the annular/dispersed flow. The annular/dispersed flow regime is characterized by the occurrence of a liquid film on the wall, while dispersed droplets are entrained by a gaseous core flow. However, a flow pattern that can only occur in heated (boiling) channels is the inverted annular regime. This flow regime is characterized by a thin vapor layer on the heated wall, and a liquid core flow that often contains entrained bubbles.

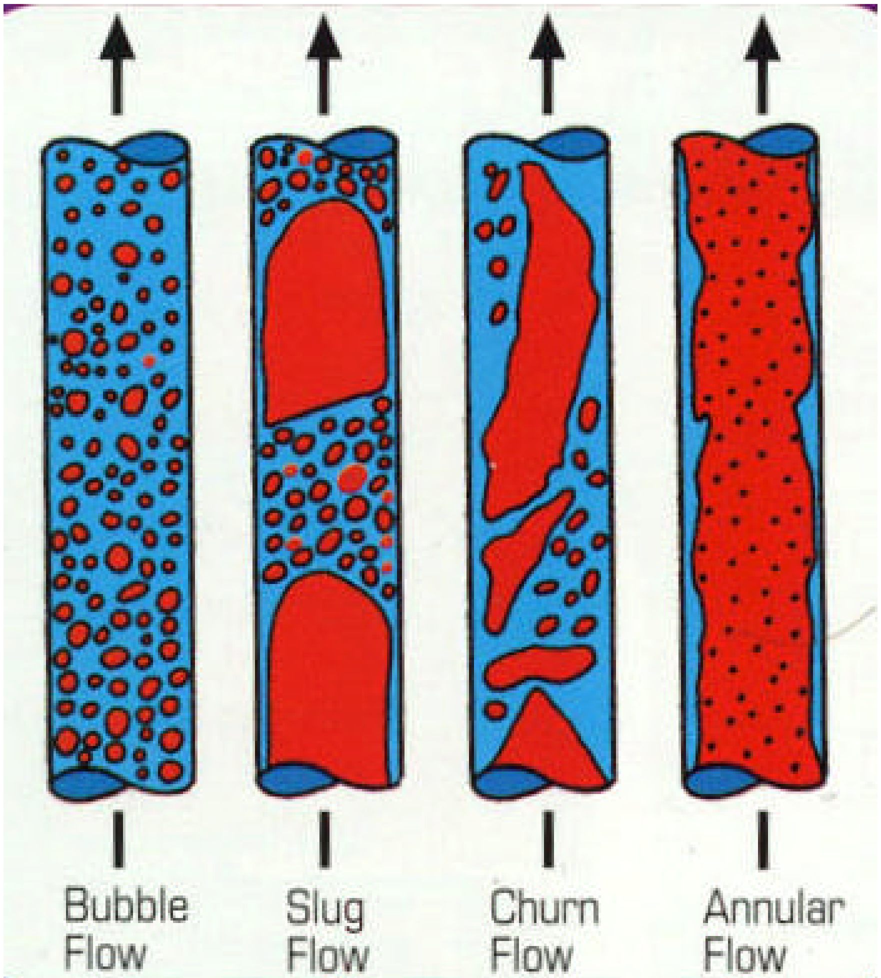


Figure 2.3: Flow regimes in vertical channels. [69]

Despite the importance of two phase flow regimes, attaining a full understanding about them has been very difficult. As correctly stated by Lowe et al [1], most of the analysis done has been subjective. The methods used to determine flow regimes can be classified into two categories: Direct methods and indirect methods. The direct methods involve the use of the human eye in one way or the other. Although in most cases fast movie or video cameras have been used, these methods nevertheless rely on a physical observation of the flow in the pipe and are to some extent subjective. The indirect methods involve using numerical and empirical tools to determine the transition from one regime to another.

Despite all the problems and difficulties, it can be said that the subject of adiabatic gas-liquid flow in commonly used channels is mature, and the predictive methods are reasonably well-developed. The difficulty in studying two-phase flow in ducts is increased when the flow in micro and mini channels is considered. There are a relatively large number of correlations used to evaluate the flow in mini and micro channels. However, the accuracy of these correlations is doubtful. Many correlations were in fact initially developed to study flow patterns in regular ducts.

One of the major factors that play a crucial role in the flow patterns in narrow passages is surface tension, as emphasized by Ghiaasiaan and Abdul-Khalik [2], and Kandlikar [3]. It has been argued that the major flow regimes in mini and micro-channels that are larger than a few hundred micro meters in diameter are somewhat similar to the flow regimes in large channels, at least with respect to their overall morphology. As stated by Lin et al. [4], the current procedures and correlations cannot be confidently used to predict heat transfer, pressure drop and flow regimes in micro channels. This fact can be understood by a close look at the continuity, momentum as well as energy balance equations and closure relations. It can be seen that the diameter of the pipe has a significant effect on the flow patterns as well as other important flow regime-dependent parameters.

An important issue about two-phase flow models and correlations is averaging. The local and instantaneous parameters are generally highly fluctuating in two phase flow, and are difficult to measure or predict. As a result of this issue the only practical method for obtaining measurable and easily calculable parameters is averaging. Averaging could be done on time, volume, and flow area. Averaging in fact refers to a low pass filter whereby the fluctuations with high frequency are obscured. Arguments behind averaging, and the basic mathematical tools for its implementation can be found in many standard textbooks (e.g. Collier and Thome [5] 1996; Carey [6] 1992) and will not be repeated here. An example of averaging is the in-citu volume fraction of the phase k in a channel, defined as a time and cross section average quantity.

$$a_k(t_0, z_0)_A = \frac{1}{\Delta t A}\int^t dt \int M_k(r, q, t) dA \tag{2.1}$$

where $M_k = 1$ when the point is in phase $k$, otherwise $M_k$ is 0.

The most commonly used predictive tools for flow regimes are flow regime maps. A flow regime map is usually a two dimensional diagram with each coordinate representing an easily quantifiable flow parameter, or a combination of such parameters. The ranges of occurrence of the major flow regimes are specified on the flow regime map by flow regime transition lines. There are many flow regime maps available in the literature. These maps are used to empirically determine flow regimes based on the macroscopic characteristics of the flow. The following are two of the most widely applied flow regime maps.

The flow regime map of Hewitt and Robert [7] is among the most widely used for flow in vertical pipes. This map is shown in fig 2.4. The map of Baker [8] is known as a reliable flow regime map for horizontal flow in pipes. Fig 2.5 shows the Baker [8] flow regime map.

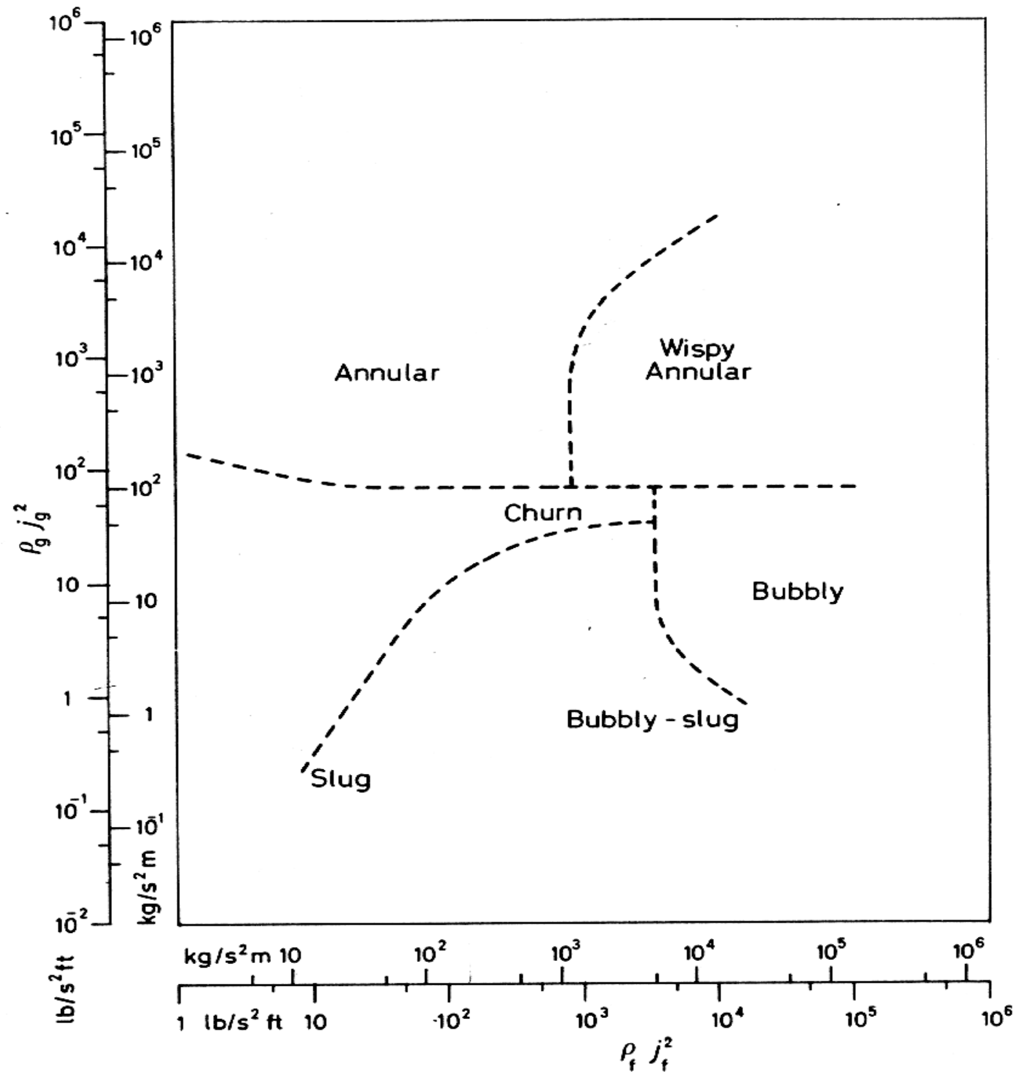


Figure 2.4: Flow regime map of Hewitt and Roberts [7] for vertical tubes.

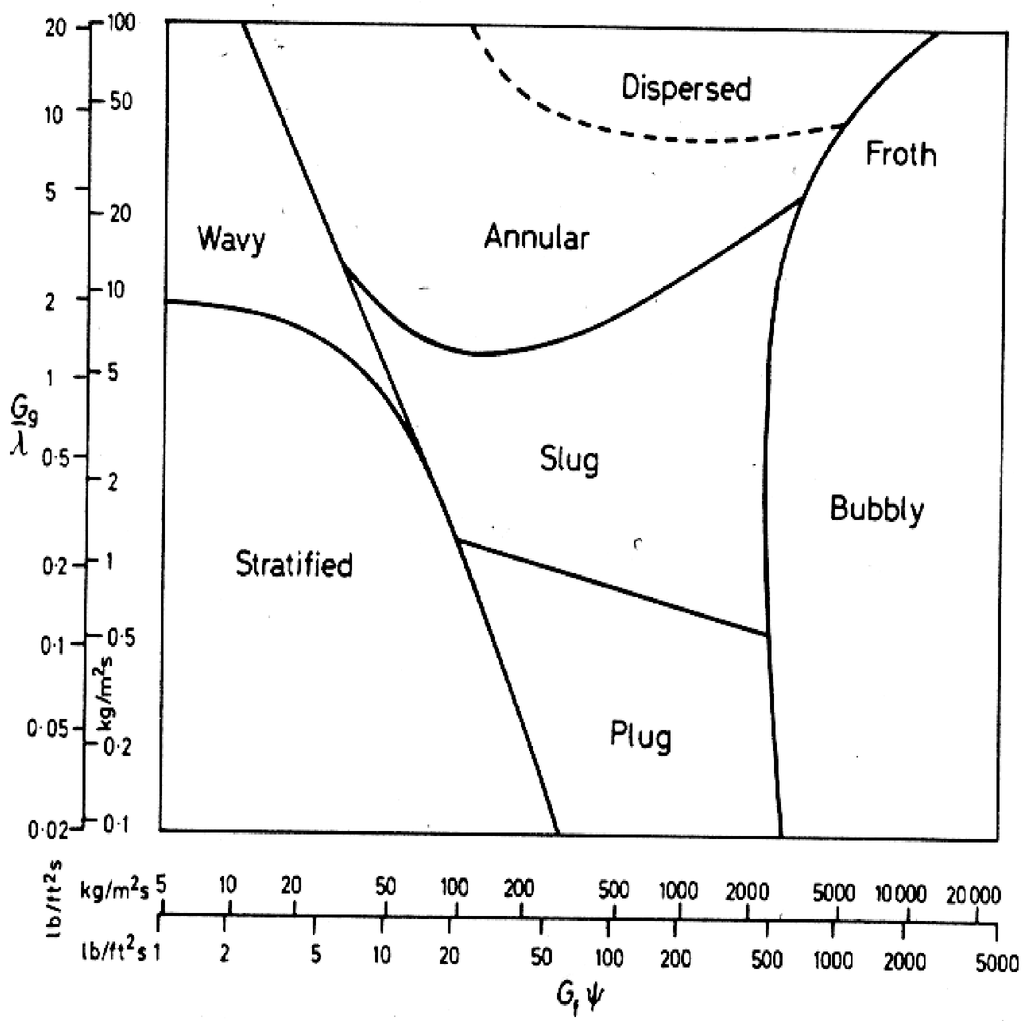


Figure 2.5: Flow regime map of Baker [8] for horizontal tubes.

A brief discussion regarding the two-phase flow conservation equations is now presented.

The emergence of powerful computers and robust numerical techniques in the last few decades has made the numerical solution of properly averaged two-phase conservation equations possible. Model conservation equations are needed before mechanistic modeling of a two-phase system can be attempted, however. Several modeling techniques exist in literature for two phase flow. Some of the most widely used are, Drift Flux Model (DFX), Two Fluid Model (TFM), Multi Fluid Flow Model (MFM) and the Homogeneous Mixture Model (HEM).

Generally, there are three main categories of two-phase flow modeling that are widely used in thermal-hydraulic computer codes. The three categories are briefly described below.

**Homogeneous Mixture Model:** In this model the two phases are assumed to be well mixed and most of the fundamental properties, like velocity and thermodynamic properties are assumed to be the same at all locations in the flow pipe. The HEM model is derived from this simple modeling technique and it only requires one momentum equation for the entire flow. HEM model is thus practical for certain applications involving little phase separation and velocity slip. The fundamental relations that underlie the HEM model are as follows;

The mixture or homogeneous density is defined as:

$$\bar{r} = r_h = \frac{G}{j} = a r_G + (1 - a) r_L = [v_L + x(v_G - v_L)]^{-1} \tag{2.2}$$

The following relation exists between quality and void fraction.

$$\frac{x}{1-x} = \frac{r_G a}{r_L (1-a)} \tag{2.3}$$

The mixture mass conservation equation for channels with uniform flow area can be written as:

$$\frac{D_j}{Dt} r_h + r_h \frac{\partial j}{\partial z} = 0 \tag{2.4}$$

The momentum conservation equation is:

$$\frac{\partial}{\partial t}\left(r_h j\right)+\frac{\partial}{\partial z}\left(r_h j^2\right)=-\frac{\partial P}{\partial z}-g r_h \sin q+\frac{p_f t_w}{A} \tag{2.5}$$

where j is the total volumetric flux. The mixture enthalpy is defined as:

$$\bar{h}=\frac{\left[r_G a h_G + r_L(1-a)h_L\right]}{\bar{r}}=h_L+x\left(h_G-h_L\right) \tag{2.6}$$

Thermodynamic equilibrium between the two phases requires that:

$$T_L=T_G \tag{2.7}$$

The HEM indeed treats the two-phase mixture as a pseudo-single phase. The conservation equations become simple, and resemble the familiar single phase flow equations (Collier and Thome [5], 1996). As an example, the energy conservation equation can be presented as,

$$A\frac{\P}{\P t}\left(r_h e-P\right)+\frac{\P}{\P z}\left(A r_h je\right)-P_H q''-A\dot{q}=0 \tag{2.8}$$

where *e* is the total specific energy.

**Multi-Fluid Models**: In these models, each phase is represented by its own specific momentum, mass, and energy equations. In other words, each phase is treated as a separate “fluid”. In order to reduce the number of unknowns, an assumption of thermal equilibrium is sometimes made between the phases or a saturation condition for one of the phases is assumed. A separate momentum equation is always written for each “fluid”, nevertheless.

The Two-Fluid Model is one of the most widely used two phase flow models. In this method, each of the gas (vapor) and liquid phases is represented as a single “fluid”. A more complicated model is the three fluid models, where three sets of equations are written; one for the contiguous liquid phase, one for contiguous gas phase, and one for the dispersed phase of either gas bubbles or liquid bubbles. In the development of this model, stratified or annular flow pattern is usually used to demonstrate the various terms. When a single component fluid is considered, one of the phases could be assumed to be saturated with respect to the local pressure. Only one energy equation is required in this situation. The fundamental two fluid model equations are given below.

Equation (2.9) is the mixture mass conservation equation. This is a combination of the liquid and vapor mass conservation equations.

$$\frac{\partial}{\partial t}\left[r_L(1-a)+r_G a\right]+\frac{1}{A}\frac{\partial}{\partial t}\left(A\left[r_L(1-a)U_L+r_G a U_G\right]\right)=0 \tag{2.9}$$

the mixture momentum conservation equation is given by

$$\frac{\partial G}{\partial t}+\frac{1}{A}\frac{\partial}{\partial z}\left(A\frac{G^2}{r'}\right)=-\frac{\partial P}{\partial z}-rg\sin q-t_w\frac{P_f}{A} \tag{2.10}$$

$$r'=\left[\frac{(1-x)^2}{r_L(1-a)}+\frac{x^2}{r_G a}\right]^{-1}\text{momentum density} \tag{2.11}$$

The energy conservation equation is given by:

$$\begin{aligned}&\frac{\partial}{\partial t}\left(\overline{r\,h}\right)+\frac{\partial}{\partial t}\left(\frac{G^2}{2r'}\right)+\frac{1}{A}\frac{\partial}{\partial z}(AGh)+\frac{1}{A}\frac{\partial}{\partial z}\left(A\frac{G^3}{2r'''^2}\right)+g\sin qG-\frac{\partial P}{\partial t}\\&=p_H\frac{q_W''}{A}+\left[\dot{q}_{v,L}(1-a)+\dot{q}_{v,G}\,a\right]\end{aligned} \tag{2.12}$$

where:

$$\bar{h}=\frac{\left[r_L(1-a)h_L+r_G a h_G\right]}{\bar{r}} \tag{2.13}$$

$$\bar{r}=a\,r_G+(1-a)r_L \tag{2.14}$$

$$h=xh_G+(1-a)h_L=h_L+h_{LG} \tag{2.15}$$

$$\rho'''^{2} = \left[ \frac{(1-x)^{3}}{\rho_{L}^{2}(1-\alpha)^{2}} + \frac{x^{3}}{\rho_{G}^{2}\alpha^{2}} \right]^{-1} \tag{2.16}$$

**Diffusion Models**: This is the third category of models for two phase flow. In this method only one momentum (the mixture momentum equation), in the form of a differential equation, is used. An algebraic equation representing the relative velocity of one phase with respect to the other velocity (or with respect to the mixture) replaces the second momentum equation needed for the closure of the equations. The Drift Flux model is the most well-known diffusion model. DFM is useful in solving two-phase conservation equation, when lowering the computational cost is important.

## 2.2 Forced flow boiling

Boiling occurs when a liquid changes phase to vapor. Flow boiling is characterized by the process of boiling in a moving liquid. The prevalent cause of flow boiling is heating, and it is this type of boiling that this thesis is concerned with. It is noted, however, that evaporation under forced convection could occur due to different causes, such as variations in temperature, velocity, or even contact angle Som et al. 9. Forced flow boiling has been extensively studied and there is abundant literature available dealing with different aspects of flow boiling.

In flow boiling experiments, for simplicity, the flow channel must be placed under one of two known boundary conditions: known heat flux on the wall, or known wall temperature. The known wall heat flux condition is a better representation of most practical situations and is easier to implement. As a result, much of the experimental data in the literature pertain to this type of boundary condition. Under the condition of known wall heat flux there are several correlations that are currently used widely. These correlations will be highlighted in section 3.4.

As mentioned earlier, evaporation can be caused by the addition of heat to a channel, or by a number of other parameters. Indeed, evaporation can occur in an adiabatic channel with no net heat exchange with surrounding. Adiabatic boiling (evaporation) occurs only due to velocity variations, mass flow rate variations, or variations in void distribution within the channel. For example, evaporation occurs with a decrease in the pressure from the saturation pressure, in a single component flow.

In the more familiar adiabatic flow boiling, boiling occurs on the walls of the channels. Forced flow boiling is accompanied by an increasing void fraction, and gives rise to flow pattern transitions even when the temperature and/or heat flux are kept constant.

The modeling methods for the solution of conservation equations in forced-flow boiling are in principle similar to adiabatic two-phase flow. The closure relations are different than those in adiabatic two-phase flow, however. A convenient way of characterizing the two-phase hydrodynamics of a boiling channel is by correlation of the slip ratio, defined as S = $U_g/U_L$. Many of the widely used slip ratio correlations for boiling of water can be obtained from Butterworth [10]. The slip velocity or relative velocity is related to the slip ratio according to:

$$U_r = U_G - U_L = U_L(S-1) \tag{2.17}$$

As mentioned earlier, evaporation, even rapid boiling (flashing), can occur if there is sufficient drop in pressure. Various parametric effects on boiling have been performed. For example Klimenko [11], [12] meticulously evaluated the effect of pressure variations.

Most of the past studies of boiling deal with pure fluids. Numerous correlations have been developed for forced -flow boiling of pure liquids. These correlations will be discussed in Section 3.4. Boiling of binary mixtures of liquids is also encountered in some industrial systems. Many investigators, including Kandlikar [13] have studied boiling in binary mixtures.

As previously stated, flow boiling could occur in both saturated and sub-cooled conditions. Sub-cooled flow boiling typically occurs when the wall temperature is significantly greater than the bulk liquid saturation temperature. Research in the area of sub-cooled boiling has shown the occurrence of three important thresholds: (1) The onset of nucleate boiling (ONB), (2) the point of net vapor generation (NVG), or the onset of significant void (OSV), and (3) the location where the equilibrium quality becomes zero. The heat transfer region upstream the ONB point is single phase flow heat transfer, the regime between the ONB and the net vapor generation point is called partial boiling, and fully developed boiling occurs downstream the net vapor generation boiling point. Downstream the point where the bulk fluid becomes saturated, the heat transfer regime is called bulk boiling. Kandlikar [13] states that in the fully developed region of sub cooled boiling, the effect of convective heat transfer is insignificant and the heat transfer is mainly due to nucleate boiling. Most other researchers have argued that convective boiling both contribute to nucleate boiling heat transfer, however. The map of different regions in flow boiling under low quality is shown in Fig. 2.6.

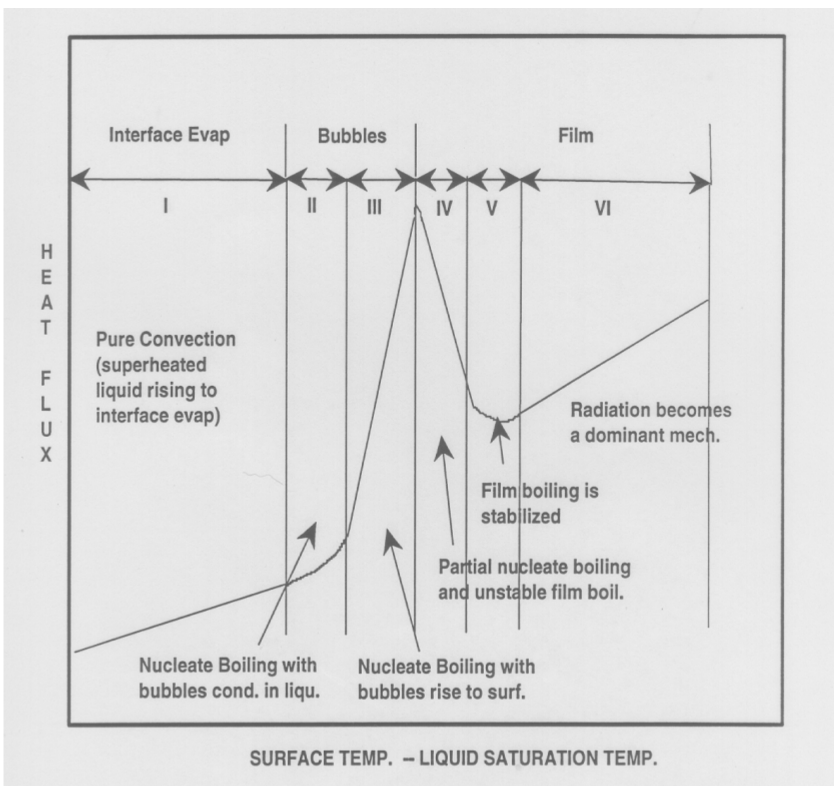


Figure 2.6: Regions in flow boiling.

# CHAPTER 3.

## Forced-Flow Boiling Correlations

A large number of correlations have been proposed for heat transfer in flow boiling. Reviews and compilations of boiling heat transfer correlations and textbooks dealing with boiling and two phase flow are numerous, and include Collier and Thome [5], Tong 14 and Carey [6], among others. However, there are several recently-published correlations that are not discussed in the aforementioned books. Many of these correlations were generated empirically, often without solid theoretical foundations, or sufficiently wide experimental databases. However several researchers have developed correlations that over time have been proven to be relatively accurate. The most recent correlations indeed include experimental data obtained recently with highly sophisticated test facilities. Some of these correlations have experimental data obtained with mini channels in their databases, and are thus more likely to apply to mini and micro-channels. A brief review of the latter group of correlations is provided in this chapter.

### 3.1 Flow boiling Correlations

As mentioned above, flow boiling correlations are numerous. However, user experience has led to the identification of the most accurate among them. For example, Gungor and Winterton [15] give a list of investigators who have presented relatively successful correlations for both sub-cooled and saturated boiling. They have also developed a table that qualifies their listed correlations with respect to their accuracy. Most of the forthcoming correlations are in fact included among the correlations listed by Gungor and Winterton [15].

Generally speaking, the forced flow boiling correlations can be divided into three groups, Thome [16]. The oldest, and probably the most successful group, at least with respect to forced flow boiling in macro-scale, are based on what can be referred to as the Chen summation rule. In these correlations, in view of the fact that nucleate boiling and forced convection mechanisms both contribute to the total heat transfer, the heat transfer coefficient is presented as the summation of two terms, one accounting for nucleate boiling, the other for forced convection.

The second group of correlations can be called asymptotic models, (Thome [16]). These correlations also explicitly account for additive nature of nucleate boiling and forced convection contributions, and are formulated such that at the limit of $x_e$? 0, they asymptotically approach pure nucleate boiling, while at $x_e$? 1 they approach pure convection. The most widely used generic form of these correlations is

$$h_{TP} = \left(h_{nb}^{n} + h_{cb}^{n}\right)^{\frac{1}{n}} \qquad (3.1)$$

where n is often an integer.

Finally, the third group of correlations can be referred to as flow pattern dependent. In these correlations, as the name suggests, the heat transfer process is modeled semi-mechanistically, with attention to the two-phase flow pattern. It should be mentioned, however, that the latter group of correlations are less popular in comparison with the aforementioned two groups of correlations, primarily due to their complexity and the difficulties associated with the prediction of two-phase flow regimes in boiling systems. The forthcoming correlations in fact all belong to the first two categories.

Chen 17 presented one of the most successful and widely-referenced correlations for heat transfer in flow boiling. Like most of the successful forced flow boiling correlations that deal with macro-scale, the correlation of Chen [17] is a summation type correlation and assumes that forced flow boiling and nucleate boiling heat transfer mechanisms both contribute to the total heat transfer. However the contribution of nucleate boiling is diminished while the forced convection effect increases as the flow quality in increased. The correlation of Chen [17] is

$$
\begin{aligned}
h &= 0.00122 \frac{k_l^{0.79} c_{pl}^{0.45} r_l^{0.49}}{s^{0.5} m_l^{0.29} H_{fg}^{0.24} r_g^{0.24}} \left(T_W - T_S\right)^{0.24} \Delta P^{0.75} S \\
&+ 0.023 \left[\frac{DG(1-x)}{m_l}\right]^{0.8} \left(\frac{c_{pl} m_l}{k_l}\right) \frac{k_l}{D} F
\end{aligned}
\tag{3.2}
$$

Where S is the suppression factor and F is a parameter that accounts for the two-phase nature of flow.

More recently, Gungor and Winterton [15] attempted to improve Chen's [17] correlation and developed the following summation type correlation that is meant to be applicable to both sub-cooled and saturated flow boiling, using an extensive databank:

$$h_{tp} = Eh_l + Sh_{pool} \tag{3.3}$$

$$h_l = 0.023\,\mathrm{Re}^{0.8}\,\mathrm{Pr}^{0.4}\left(\frac{k_l}{d}\right) \tag{3.4}$$

$$\mathrm{Re} = \frac{G(1-x)d}{m_l} \tag{3.5}$$

$$E = f\left(X_{tt}, Bo\right) \tag{3.6}$$

The parameter $h_{pool}$ represents the pool boiling heat transfer coefficient. Parameter E is an enhancement factor and S is a suppression factor that accounts for the suppression of nucleate boiling as quality is increased. Empirical expressions for E and S are provided by Gungor and Winterton [15]

Shah $\boxed{18}$ developed the following correlation dealing with saturated boiling;

$$q = \left[230\left(\dot{m}h_{lv}\right)^{-0.5} h_{lo}\left(\Delta T_{sat}\right)\right]^2 \tag{3.7}$$

where $h_{lo}$ is obtained from the Dittus-Boelter [23] correlation, assuming that all coolant is saturated liquid:

$$h_{lo}\frac{d}{k_{lo}} = 0.023\,\mathrm{Re}_{lo}^{0.8}\,\mathrm{Pr}_{lo}^{0.4} \tag{3.8}$$

In 1982, Bjorge et al $\boxed{19}$ proposed the following asymptotic type correlation for saturated flow boiling:

$$q = q_{FC} + q_B\left[1 - \left(\frac{(T_w - T_{sat,ib})}{T_w - T_{sat}}\right)^3\right] \tag{3.9}$$

where $q_{FC}$ is the forced convection heat flux, subscript ib represents the point of incipient boiling (the same as the point of onset of nucleate boiling, ONB), and $q_B$ is the nucleate boiling contribution to the total heat flux. The form of the correlation of Bjorge et al [19] is such that any reasonable correlation can be used for calculating $q_{FC}$ and $q_B$.

Klimenko [11, 12] also presented a correlation for flow boiling. This correlation is applicable for both vertical and horizontal channels. According to Klimenko [11, 12],

$$h_{tp} = h_{NB} \quad \text{for} \quad N_{CB} < 1.2 \times 10^4 \tag{3.10}$$

$$h_{tp} = \quad \text{the larger of } h_{NB} \text{ and } h_{CB} \tag{3.11}$$

for $1.2 \times 10^4 = N_{CB} = 2 \times 10^4$ and

$$h_{tp} = h_{CB} \text{ for } N_{CB} > 2 \times 10^4 \tag{3.12}$$

where:

$$h_{NB} = C\left(\frac{k_l}{b}\right) Pe_*^{\,0.6} \left(\frac{pb}{s}\right)^{0.54} \Pr^{-.033} \left(\frac{k_w}{k_l}\right)^{0.12} \tag{3.13}$$

$$h_{CB} = 0.087\left(\frac{k_l}{b}\right) \mathrm{Re}_m^{\,0.6} \Pr_l^{0.167} \left(\frac{r_v}{r_l}\right)^{0.2} \left(\frac{k_w}{k_l}\right)^{0.09} \tag{3.14}$$

$$N_{CB} = \frac{Gh_{fg}}{q}\left[1 + x\left(\frac{r_l}{r_v} - 1\right)\right]\left(\frac{r_v}{r_l}\right)^{\frac{1}{3}} \tag{3.15}$$

$Pe_*$ is a modified Peclet number, defined as shown in Equation (3.16) and $\mathrm{Re}_m$ is the mixture Reynolds number defined as shown in Equation (3.17).

$$Pe = \frac{qb}{c_p r_g a_l} \tag{3.16}$$

$$\mathrm{Re}_m = \frac{U_m b}{m_l} \tag{3.17}$$

where $a_l$ is the liquid thermal diffusivity $\mathrm{Re}_m$ is the two phase mixture velocity given in Equation (3.17) and $m_l$ is defined as the kinematic viscosity of liquid at saturation.

$$U_m = \frac{G}{r_l}\left[1 + x\frac{r_l}{r_g} - 1\right] \tag{3.18}$$

The above correlations are valid for cases in which $\frac{D}{b} > 1.5$, where b is the Laplace constant, defined as

$$b = \left[\frac{s}{g\Delta r}\right]^{\frac{1}{2}} \tag{3.19}$$

The coefficient C in Equation (3.15) is a constant that depends on the fluid. Table 3.1 depicts the values of this constant for several fluids.

Table 3.1: The values of the constant C to be used in the correlation of Klimenko [11, 12]

| **Fluid** | **C** | **$Pr_l$** |
|---|---|---|
| Freon | $7.6 \times 10^{-3}$ | 3.8 ± 2.5 |
| Organic Fluids | $6.8 \times 10^{-3}$ | 3.5 ± 1.3 |
| Cryogenic fluids | $6.1 \times 10^{-3}$ | 1.6 ± 1.0 |
| Water | $4.9 \times 10^{-3}$ | 1.2 ± 0.4 |

Liu and Winterton have [20] recently proposed the following frequently referenced correlation for heat transfer in flow boiling:

$$h_{tp} = \sqrt{(Eh_l)^2 + (Sh_{pool})}^2 \tag{3.20}$$

where

$$E = \left[ 1 + x \Pr_l \left( \frac{r_l}{r_v} - 1 \right) \right]^{0.35} \tag{3.21}$$

$$S = \frac{1}{1 + 0.055 E^{0.1} \operatorname{Re}_l^{0.16}} \tag{3.22}$$

A comparison between Equations (3.21) and (3.6) confirms that the former correlation indeed a modification of the latter.

Kandlikar and co-workers [21], [22] have developed widely-referenced correlations for flow boiling. Kandlikar [21, 22] correlation of 1990 is:

$$h = \max\{h_{NBD}, h_{CBD}\} \tag{3.23}$$

$$h_{NBD} = 0.6683 Co^{-0.2} (1-x)^{0.8} f_2(Fr_{lo}) h_{lo} + 1058 Bo^{0.7} (1-x)^{0.8} F_{fl} h_{lo} \tag{3.24}$$

$$h_{CBD} = 1.136 Co^{-0.9} (1-x)^{0.8} f_2(Fr_{lo}) h_{lo} + 667.2 Bo^{0.7} (1-x)^{0.8} f_2(Fr_{lo}) h_{lo} \tag{3.25}$$

where

$$f_2(Fr_{lo}) = \min\{1, 25 Fr_{lo}\} \tag{3.26}$$

The parameter $Fr_{lo}$ is the Froude number defined as

$$Fr_{lo} = \frac{G^2}{r^2 g D_H} \tag{3.27}$$

The parameter $h_{lo}$ is calculated from Dittus-Boelter [23] or the correlations of Gnielinski [24] and Petukov [25], depending on the magnitude of the $Re_{lo}$, and $F_{fl}$ a fluid dependent parameter, the values of which for selected fluids are listed in Table 3.2 below. For the fluids that are not listed in the table, Forster and Zuber $\boxed{26}$ correlation for nucleate boiling heat transfer may be used in order to calculate $h_{CBD}$. The parameters $Co$ and $Bo$ are convection number and boiling number, respectively, and are defined as:

$$Bo = \frac{q}{Gh_{lv}} \tag{3.28}$$

$$Co = \left(\frac{r_v}{r_l}\right)^{0.5} \left[\frac{(1-x)}{x}\right]^{0.8} \tag{3.29}$$

Table 3.2: Recommended values of the fluid dependent parameter $F_{fl}$

| | |
|---|---|
| Water | 1.0 |
| R-11 | 1.3 |
| R-12 | 1.5 |
| R-13 B1 | 1.31 |
| R-22 | 2.20 |
| R-113 | 1.30 |
| R-114 | 1.24 |
| R-134a | 1.63 |
| R-152a | 1.10 |
| R-32/R-132<br>60%-40% wt. | 3.30 |
| Kerosene | 0.488 |

Steiner and Taborek [27] also developed the following widely-used asymptotic type correlation,

$$h_{tp} = \left( h_{nb}{}^{n} + h_{cb}{}^{n} \right)^{\frac{1}{n}} \tag{3.30}$$

where

$$h_{nb} = h_{nbo} F_{nb} \tag{3.31}$$

$$F_{nb} = F_p \left( \frac{q}{q_o} \right)^{m} \left( \frac{D}{D_o} \right)^{-0.4} \left( \frac{Ra}{Ra_0} \right)^{0.133} F(m) \tag{3.32}$$

$$h_{cb} = h_{lo} F_{tp} \tag{3.33}$$

In the above expression, $D_0$ is diameter at normalized condition Ra is the wall roughness given in µm and $Ra_0$ is the wall roughness under normalized condition. The parameter $q_0$ is given for different fluids in Table 3.3 Thome [28]. More details about this correlation will be provided later in section 3.4.

Table 3.3: Values of $q_0$ for different fluids as given by Steiner and Taborek [27]. Standard Nucleate Flow Boiling Coefficients $a_{nb,0}$ in $W/m^2 \cdot K$ at $p_r = 0.1$ for $q_0$ in $W/m^2$ and $R_{p,0} = 1\,\mu m$ with $p_{crit}$ in bar (http://www.knovel.com/knovel2/Toc.jsp?BookID=725)

| Fluid | $p_{crit}$ | $M$ | $q_0$ | $\alpha_{nb,0}$ |
|---|---|---|---|---|
| Methane | 46.0 | 16.04 | 20,000 | 8,060 |
| Ethane | 48.8 | 30.07 | 20,000 | 5,210 |
| Propane | 42.4 | 44.10 | 20,000 | 4,000 |
| *n*-Butane | 38.0 | 58.12 | 20,000 | 3,300 |
| *n*-Pentane | 33.7 | 72.15 | 20,000 | 3,070 |
| Isopentane | 33.3 | 72.15 | 20,000 | 2,940 |
| *n*-Hexane | 29.7 | 86.18 | 20,000 | 2,840 |
| *n*-Heptane | 27.3 | 100.2 | 20,000 | 2,420 |
| Cyclohexane | 40.8 | 84.16 | 20,000 | 2,420 |
| Benzene | 48.9 | 78.11 | 20,000 | 2,730 |
| Toluene | 41.1 | 92.14 | 20,000 | 2,910 |
| Diphenyl | 38.5 | 154.2 | 20,000 | 2,030 |
| Methanol | 81.0 | 32.04 | 20,000 | 2,770 |
| Ethanol | 63.8 | 46.07 | 20,000 | 3,690 |
| *n*-Propanol | 51.7 | 60.10 | 20,000 | 3,170 |
| Isopropanol | 47.6 | 60.10 | 20,000 | 2,920 |
| *n*-Butanol | 49.6 | 74.12 | 20,000 | 2,750 |
| Isobutanol | 43.0 | 74.12 | 20,000 | 2,940 |
| Acetone | 47.0 | 58.08 | 20,000 | 3,270 |
| R-11 | 44.0 | 137.4 | 20,000 | 2,690 |
| R-12 | 41.6 | 120.9 | 20,000 | 3,290 |
| R-13 | 38.6 | 104.5 | 20,000 | 3,910 |
| R-13B1 | 39.8 | 148.9 | 20,000 | 3,380 |
| R-22 | 49.9 | 86.47 | 20,000 | 3,930 |
| R-23 | 48.7 | 70.02 | 20,000 | 4,870 |
| R-113 | 34.1 | 187.4 | 20,000 | 2,180 |
| R-114 | 32.6 | 170.9 | 20,000 | 2,460 |
| R-115 | 31.3 | 154.5 | 20,000 | 2,890 |
| R-123 | 36.7 | 152.9 | 20,000 | 2,600 |
| R-134a | 40.6 | 102.0 | 20,000 | 3,500 |
| R-152a | 45.2 | 66.05 | 20,000 | 4,000 |
| R-226 | 30.6 | 186.5 | 20,000 | 3,700 |
| R-227 | 29.3 | 170.0 | 20,000 | 3,800 |
| RC318 | 28.0 | 200.0 | 20,000 | 2,710 |
| R-502 | 40.8 | 111.6 | 20,000 | 2,900 |
| Chloromethane | 66.8 | 50.49 | 20,000 | 4,790 |
| Tetrachloromethane | 45.6 | 153.8 | 20,000 | 2,320 |
| Tetrafluoromethane | 37.4 | 88.00 | 20,000 | 4,500 |
| Helium[a] | 2.275 | 4.0 | 1,000 | 1,990 |
| Hydrogen (para) | 12.97 | 2.02 | 10,000 | 12,220 |
| Neon | 26.5 | 20.18 | 10,000 | 8,920 |
| Nitrogen | 34.0 | 28.02 | 10,000 | 4,380 |
| Argon | 49.0 | 39.95 | 10,000 | 3,870 |
| Oxygen | 50.8 | 32.00 | 10,000 | 4,120 |
| Water | 220.6 | 18.02 | 150,000 | 25,580 |
| Ammonia | 113.0 | 17.03 | 150,000 | 36,640 |
| Carbon dioxide[b] | 73.8 | 44.01 | 150,000 | 18,890 |
| Sulfur hexafluoride | 37.6 | 146.1 | 150,000 | 12,230 |

[a]Physical properties at $p_r = 0.3$ rather than 0.1.

[b]Calculated with properties at $T_{crit}$.

A simple correlation, proposed by Gungor and Winterton [15] in 1987 should also be mentioned here. This correlation can be represented as:

$$\frac{h_{tp}}{h_l} = 1 + 3000 Bo^{0.86} + 1.12 \left( \frac{x}{1-x} \right)^{0.75} \left( \frac{r_l}{r_v} \right)^{0.41} \tag{3.34}$$

It must be emphasized that the applicability of the afore-mentioned widely-used forced flow boiling correlations to micro-channels is questionable. These correlations are all essentially empirical and are based on data that at best include only limited mini-channel boiling data. The issue has been noted and emphasized by some investigators. For example, Agostini et al 29 have noted that old and classical correlations generally under predict the performance of mini-channels.

### 3.2 General Remarks About Flow Boiling in Micro Channels

In the contemporary literature on mini and micro channels, there is considerable interest in boiling heat transfer. This is due to the wide potential applications of micro-channels and the savings that would arise from using mini and micro-channels in many industrial systems. Some examples of micro-channel utilization are fuel cells, refrigeration units, chemical process equipment, and microelectronics cooling.

The precise definition of micro-channels is the subject of disagreement. One of the earliest definitions is due to Suo and Griffith [30], according to which a cylindrical channel with diameter D is a micro-channel if D = 0.3b (Ghiaasiaan and Abdul-Khalik [31], 2001), where b is the Laplace length scale, and has been defined earlier in equation (23). More recently, however, other definitions have been proposed, and currently the most popular classification method appears to be as follows:

Micro-channels: 50 µm = D = 0.5 mm

Mini-channels: 0.5 mm = D = 3 mm

Macro channels D = 3 mm

However, direct experimental observations, Ghiaasiaan and Abdul-Khalik [31], have shown that with air-water and steam-water type fluid pairs, near circular channels with 0.1 mm = $D_H$ =1 mm should be considered as a single category, while channels with 10 µm = $D_H$=100 µm and $D_H$= 1 mm should constitute two other size categories. In this sense, the recommendations of Mehendale et al [32], are more reasonable, according to which

Micro-channels: 1 µm = D = 100 µm (micro heat exchangers)

Mini (meso) channels: 100 µm = D = 1 mm (meso heat exchangers)

Macro channels 1 mm = D = 6 mm (compact heat exchangers)

Conventional channels D> 6 mm (conventional)

Following the aforementioned popular definitions, the term micro-channels is applied here to conduits with hydraulic diameters of 100 μm ~ *0.5 mm* range. Mini-channels are characterized here as channels with hydraulic diameter between *0.5 mm* and *3 mm*. We will limit our consideration of boiling heat transfer data to 2 mm, however.

Most studies dealing with mini and micro-channels have shown that nucleate and convective boiling both contribute to heat transfer. This observation is in principle consistent with what has been well known about boiling in conventional large channels. The trends in the micro-channel boiling data, however, have not been consistent and as will be discussed later, indicate that there are major differences between micro-channels and conventional channels. Studies carried out in large channels include the use of available sophisticated technology, which is utilized to obtain valuable information about the heat transfer coefficient, bulk fluid temperature, wall temperature, and quality. In the case of micro-channels, such detailed measurements are of course very difficult. Vlassie et al [33] have observed that the majority of flow boiling experiments have measured local boiling heat transfer coefficient or heat flux as a function of $x_e$, the equilibrium vapor quality. In a study, Tran et al [34] observed that local heat transfer coefficient in the evaporation of R-113 in their small diameter horizontal channel was dependent on the heat flux, with little dependence on mass flux or quality. This trend suggests the predominance of nucleate boiling. In the work of Lin et al [35], on the other hand, the observed results showed that the heat transfer coefficient increases with a decrease in quality. This trend indicates the predominance of forced convection.

There are many technical difficulties that make the study of boiling in mini and micro-channels challenging. Agostini et al $\boxed{36}$ has highlighted one of the major difficulties in the study of boiling in mini and micro channels. They stated that the lack of detailed information about geometry and other tube characteristics is a challenge for a full understanding of the characteristics of mini and micro channels. Furthermore, they point out some flaws in using the available correlations. (These correlations are also examined in this project). The discrepancy between micro-channel data and these classical correlations is of course primarily due to the fact that they were developed in principle for channels with D > 3 mm.

It must be mentioned that there is considerable controversy even with respect to single phase flow heat transfer in micro-channels. While some researchers have reported that macro scale correlations for turbulent flow disagree with micro-channel experimental data, others have observed reasonable agreement.

Agostini et al [29], for example observed agreement between their data and with Gnielinski [24] correlation. This widely-respected correlation has been shown to accurately predict the heat transfer coefficient in both regular ducts and mini channels. The correlation is given in the forthcoming Equation [31], and its range of validity is listed below.

$$Nu = \frac{\frac{f}{2}\left(\mathrm{Re}-1000\right)\mathrm{Pr}}{1+12\sqrt{\left(\frac{f}{2}\left(\mathrm{Pr}-1\right)\right)}} \tag{3.35}$$

The range of validity of Gnielinski [24] correlation is $2300 < \mathrm{Re} < 10^6;\ \mathit{and}\ \ 0.6 < \mathrm{Pr} < 10^5$.

Lee and Mudawar [37] recently performed a careful and detailed review of the past experimental studies dealing with boiling in mini and micro-channels. They noted that the past researchers could be divided into two groups. The first group believes that in micro-channels nucleate boiling is the dominant heat transfer mechanism. This conclusion was based on the observation that in their experiments the local heat transfer coefficient was a function of heat flux, but was insensitive to mass flux and quality. Among the authors in this group are Lazarek and Black [38], Wambsgass et al [34], Tran et al [34], Bao et al [39], Mehendale and Jacobi [32] and Yu et al [40]. The second group of authors has reported on observations that indicate the predominance of annular flow regime, hence the convective boiling mechanism. Observations supporting this view include decreasing local heat transfer coefficient with increasing quality, and increasing local heat transfer coefficient with increasing mass flux. Authors in this group include Kew and Cornwell [41], Raviguguruajan [42], Lee and Lee [43], Lin, Kew and Cornwell [44], Warrier et al [45], Wen et al [46], and Huo et al [47]. Lee and Mudawar [37], however, noted that the observations of both groups are in fact reasonable, since they hold under different ranges of parameters. They also developed an empirical prediction method for boiling heat transfer in micro-channels, which will be discussed later.

### 3.3 Recent Experimental Studies Dealing with Boiling in Micro-Channels

Some important, recent investigations dealing with flow boiling in mini and micro-channels are now reviewed in some detail.

Ravigururajan [42] studied the effect of micro-channel geometry on two-phase flow heat transfer. Using R-124 refrigerant purified with 10 µm filter, he performed steady-state experiments in a micro-channel with rectangular cross section that was 1 mm wide and 270 µm deep. Since experimentation with a single micro-channel is difficult, Ravigururajan [42] constructed 54 identical, parallel micro-channels, with a length of 20.5 cm that were connected at both ends to common plenums. He reported liquid single-phase, and liquid-vapor two-phase heat transfer coefficients, as well as pressure drop data. However, it is not clear what types of measurements were performed in this study, and how the channel inner wall temperature was measured. It is also not clear how the effects of channel exit pressure losses were accounted for.

Hapke et al. [48] performed Onset Nucleate Boiling (ONB) experiments, using degassed de-ionized water, in a vertical micro tube with 0.5 mm inner diameter. They noted that, for the same heat flux in comparison with well established ONB correlations for macro-scale, their data indicated that ONB occurred at a larger wall temperature. Their data primarily covered the laminar flow regime. They argued that, near the ONB point, heat transfer is augmented by fluctuations in mass flux and pressure, early laminar-turbulent transition and by the heterogeneously-generated bubbles themselves. They attempted to derive empirical correlations for the prediction of ONB, based on their own experimental data.

The ONB, as well as the Onset of Significant Void (OSV) and Onset of Flow Instability (OSI) had been studied earlier by Kennedy et al [49], Chedester and Ghiaasiaan [50] and Ghiaasiaan and Chedester [50]. Kennedy et al [49] experimentally studied the ONB and OFI phenomenon in heated micro-channels with 1.17 mm and 1.45 mm inner diameters, using water. They noted that the widely used macro scale correlations for ONB overall over-predicted the ONB heat flux for micro-channels. Ghiaasiaan and Chedester [50] speculated that a major contributor to the different behavior of macro scale systems and micro-channels is the significance of thermo capillary effect in the latter. Thermo capillary effect refers to the non-uniformity of surface tension distribution over the liquid-vapor inter-phase for the heterogeneously-generated micro-bubbles, itself a result of the non-uniformity of the interfacial temperature distribution. Ghiaasiaan and Chedester [50] developed an ONB model, based on the modification of the ONB model of Davis and Anderson [51], empirically accounting for the effect of thermo capillary phenomenon. Chedester and Ghiaasiaan [50] developed a model for OSV in micro-channels using a similar argument.

Bao et al [39] performed flow boiling experiments using R-11 and HCFC-123 refrigerants as the working fluids, in a horizontal test section that had an inner diameter of 1.95 mm. The heated segment of the test section was 270 mm long, and was preceded by 400 mm long unheated segment that was meant to eliminate the hydrodynamic entrance effects. Temperature measurements were performed in metallic heating blocks that encased the test section, within 2 mm from the micro-channel inner surface. The mass flux and heat flux ranges were 50-1800 $kg/m^2s$ and 5-200 $kW/m^2$, respectively. The vapor quality range for their reported data was 0.3 to 0.9. The experiment thus covered both sub-cooled and saturated boiling, under low flow conditions. They observed little effect of mass flux under sub-cooled boiling conditions, suggesting negligible convective contribution to heat transfer.

For saturated boiling conditions, Bao et. al [39] noted that mass flux and quality both had little effect on the heat transfer coefficient, once again suggesting that nucleate boiling was the main component of heat transfer, while the convective heat transfer had little contribution. In the saturated boiling region, furthermore, the heat transfer coefficient was a strong function of heat flux. Bao et al [39] compared their experimental data with several forced-flow boiling correlations. Neither correlation could predict their entire data reasonably well, however.

Haynes and Fletcher $\boxed{52}$ more recently reported on an experimental study of sub-cooled and saturated flow boiling, using R-11 and HCFC-123 refrigerants, in heated micro-tubes with 0.92 and 1.95 mm inner diameters. The experimental rig was the same as the one used earlier by Bao et al [39]. The mass and heat flux ranges in these experiments were 110-1840 $kg/m^2s$ and 11-170 $kW/m^2$, respectively, implying that the test series were in the low-flow and low-heat flux category. The Reynolds number at inlet varied in the 450 to 12,000 range. They noted that in laminar developing flow, their liquid single phase heat transfer coefficients agreed with theory within only 10%. They noted the same level of agreement between their data and well established correlations for transitional and turbulent flow. Overall, Haynes and Fletcher [52] produced more than 2000 data points. For saturated boiling, they compared their data with several correlations, with the correlation of Gorenflo $\boxed{53}$ providing the best result. They noted a weak contribution of convection in the saturated boiling regime. They proposed the following composite correlation for sub-cooled boiling:

$$q'' = h_{lo}\left(Tw - \overline{T}_l\right) + h_{pb}\left(Tw - T_{sat}\right) \tag{3.36}$$

where $T_l$ is the local average temperature and $h_{pb}$ represents the pool boiling contribution and can be calculated using the correlation of Gorenflo [53].

Bubble nucleation and nucleate boiling in micro-channels with hydraulic diameters in the = 100µm range have also been investigated in the past. Included among these studies are Koo et al [54] and Zhang et al [55]. Although micro-channels in this size range are not the focus of this investigation, a brief review of the latter studies is provided. Koo et al [54] developed a simple model that addressed the flow field and conduction in the solid structure. The fluid flow model considered a liquid single-phase flow regime followed by a dispersed droplet regime, and utilized the correlation of Kandlikar for boiling. Zhang et al [55] conducted experiments, using deionized water, in single heated micro-channels that are 10-150 µm wide, and 10-200 µm deep, and had a length of 2 cm. By inserting etches with controlled parameters on the channel walls, Zhang et al [55] could examine the effect of wall roughness (wall crevice) on bubble nucleation. They demonstrated that bubble nucleation is heterogeneous when crevices are present. For very small channels ($D_h$ = 50 µm) onset of boiling was accompanied by sudden eruption of bubbles that lead to the development of dispersed flow regime, but needed high wall superheats ($T_w - T_{sat}$ = 20°C), to occur. For $D_H$ = 100 µm, onset of nucleate boiling occurred at $T_w - T_{sat}$ ˜ 5°C, however. The aforementioned “eruption boiling” was apparently due to the absence of viable cavities on the channel walls.

An extensive and carefully designed experimental study of boiling and pressure drop in heated micro-tubes was recently reported by Yen et al $\boxed{56}$. These authors used insulated stainless steel test sections which were 28 cm in length, with inner diameters equal to 0.19, 0.13 and 0.51 mm. Heating was provided by Jules heating of the test section itself, and in all tests the inlet liquid was about 10 K sub-cooled. Tests were performed with HCFC123 and FC72 as the working fluids. A multitude of thermocouples were used to measure the test section wall temperatures, and coolant inlet pressure and temperature. By careful control of various parameters, the uncertainty in the inferred heat transfer coefficients were maintained within +/-10%. The pressure distribution in the test section in each experiment was obtained by assuming linear pressure variation in the sub-cooled and saturated fluid lengths of the test section. Yen et al. [56] studied the inner surfaces of their test sections using a scanning electron microscope (SEM). The cavities were typically 3 ~ 4 μm across, and groves were 1 ~ 3μm wide. Their experiments targeted relatively low flow and low wall heat flux conditions. ($G = 50\sim300$ kg/m$^2$; $q'' = 1\sim13$ kW/m$^2$). With respect to liquid single phase flow, Yen et al. [56] noticed that the laminar flow theory for tubes agreed with their data well.

A very interesting observation by Yen et al [56] was the occurrence of highly superheated liquid in the experiments (i.e., occurrence of superheated liquid before bubble nucleation takes place). Superheats up to 70 K were noted, and the maximum superheat increased with decreasing channel diameter, but was insensitive to heat flux. Based on an extrapolation of the data, the data of Yen et al [56] show that the liquid superheat needed for bubble nucleation becomes equal to the liquid spinodal temperature at a capillary diameter of about 0.1 mm. Their observations are consistent with the observations of Roach et al. [57] in their experimental study of critical heat flux in micro-channels, under low flow conditions as discussed in detail by Ghiaasiaan and Abdul-Khalik [31].

With respect to boiling heat transfer (i.e., heat transfer in saturated flow region), Yen et al [56] compared their data with several correlations. The results are shown in Fig 3.1, borrowed from Yen et al. [56] and as noted they shown that all the tested correlations failed to agree with the data. However, Yen at al. [56] noticed that the correlation of

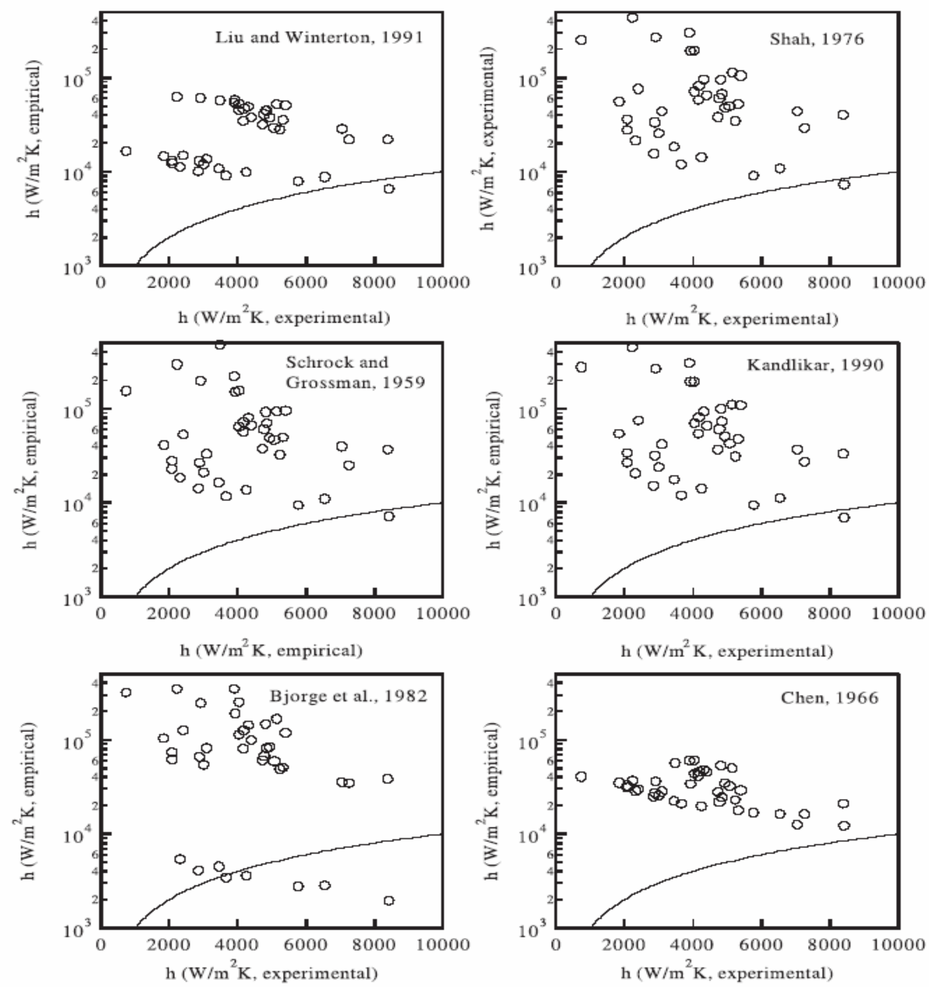


Fig 3.1: Comparison of the data of Yen et al. [56] obtained using HCFC123, with the predictions of several forced-flow boiling correlations.

Kandlikar [21, 22] agreed with their data well, provided that the term representing forced convection in the latter correlations was completely ignored. Based on this, Yen et al [56], concluded that boiling in micro-channels under low flow and low heat flux conditions is dominated by nucleate boiling. The boiling heat transfer coefficient monotonically decreased with increasing local quality up to a quality of about 0.3 and became insensitive to quality for higher qualities.

Lee and Mudawar [37] recently published an extensive experimental investigation into boiling in micro-channels, under high mass flux and high heat flux conditions, using R-134a as the coolant. Their test section consisted of 53 parallel, and presumably identical, rectangular channels (231 µm x 713 µm) constructed into an oxygen-free copper block. The channels were 2.5 cm long, and were all connected to large plena at inlet and outlet. This arrangement, namely multiple parallel channels connected to common plena, can cause parallel-channel flow oscillations, although Lee and Mudawar [37] have indicated that there oscillations were kept small. Temperature measurements and heat transfer calculations were made for the point half way along the heated channel, using parameters that properly represented the average among the 53 channels.

Lee and Mudawar [37] noted important differences between their data with R-134a, and the data previously generated using the same test section with water. Whereas proper bubbly flow had been observed with water, with R-134a the bubbly flow regime in fact contained bubbles as well as vapor slugs. The difference was attributed to the low surface tension of R-134a. Based on their data and their trends, Lee and Mudawar [37] concluded that three distinct boiling regimes must be considered in micro-channels: a low quality regime ($0 = x_e = 0.05$); a medium quality regime ($0.05 = x_e = 0.55$) where the flow field is dominated by elongated bubbles that are sometimes separated from one another by very thin liquid regions; and a high quality regime ($x_e$=0.55) where annular flow regime characterized by very thin liquid film occurs. In the low quality range, heat transfer is predominantly by nucleate boiling. Lee and Mudawar [37] compared their data with several macro and small channel correlations. Macro channel correlations generally over-predict the data at high qualities, but under-predicted the data at low qualities. The small channel correlations, on the other hand, all performed poorly, in particular for the data in the high quality (annular flow regime) range. Lee and Mudawar [37] developed three separate correlations for the aforementioned three regimes. These correlations will be presented in the next section. However, they did not compare their correlations with other investigators' data.

An important shortcoming in the experiments of Lee and Mudawar [37], as well as many other investigators who have used multiple parallel channels, must be emphasized. In the experiments of Lee and Mudawar [37], the parallel channels were connected at both ends to common manifolds. With the configuration parallel channel instabilities and oscillations, and perhaps more importantly non-uniform flow distribution among the channels is inevitable. The data produced in the studies of this type, which are usually present for "average channel", must therefore be treated with caution.

Sumith et al [58] performed an experimental study of forced flow boiling in a vertical tube that had an inner diameter of 1.45 mm, and a length of 100 mm. The working fluid was de-ionized water. By comparing their data with the predictions of the correlation of Stephan and Abdulsalam [59], they noticed that their measured heat fluxes were actually higher than what would be expected in a macro channel. The compared their data with the correlations of Chen [17], Klimenko [11,12] and Liu and Winterton [20]. The correlations all performed poorly at low heat fluxes, but their argument with data improved considerably at high heat fluxes. The low heat flux data corresponds to slug and slug-annular flow regimes. The high heat flux data, on the other hand, represented forced convective evaporation, and corresponded to annular-dispersed two-phase flow regime. Based on the parametric trends in their data, Sumith et al. [58] evolved an empirical correlation which will be presented later in section 3.4.

## 3.4 Boiling Heat Transfer Correlations for Small Channels

In this section we will revisit some of the available correlations with additional details that describe the methods that were used to develop these correlations, as well as the range of applicability of each correlation. With a few exceptions, the correlations revisited in this section will be tested against mini and micro-channel flow boiling data later. Although some of the correlations that are discussed in this section have been reviewed in section 3.1, their review in this section will be based on a different point of view. In Chapter 4, we will show a comparison of most of these correlations with actual available experimental data from Bao et al [39] and Baird et al [60], and Yan and Lin [61],

Agostini et al [29], conducted an experimental study to evaluate the friction factor in mini channels. The experimental set up included a liquid pump, glycol-water mixture, and a channel made of extruded Al. The test section was a rectangular channel (3.28 mm x 1.4 mm) with a hydraulic diameter of 2.01 mm, and was thermally insulated.

It must be mentioned that comparison between widely-used correlations and mini and micro-channel experimental data have been performed before by some investigators. As mentioned before, Vlassie et al [33] have provided a table shown in Figure 3, this highlights the available correlations used in the analysis of mini and micro-channels. These were correlations that Vlassie et. al. [33] themselves compared with the data that had been generated by Kew and Cornwell [62]. These correlations were as follows: (i) Liu and Winterton [20]; (ii). Cooper [63]; (iii) Lazarek and Black [38]; (iv) Kew and Cornwell [62], and (v) Tran et al [34]. Lee and Mudawar [37] have also compiled flow boiling correlations, and have compared the predictions of the compiled correlations with their experimental data. Furthermore, Lee and Mudawar [37] developed a set of three correlations for micro-channels flow boiling in low, medium and high quality ranges. These correlations will also be reviewed. Thus, as can be noted, the above-mentioned studies either compared the correlations with large-channel data, or compared the predictions of correlations with one mini and micro-channel data set only.

Table 3.4: A table from Vlasie et al [33]; correlations used by the authors

| Reference | Equation number | Correlation (in SI units) |
|---|---|---|
| Liu and Winterton [29] | (6) | $h^2 = (S \cdot h_{nph})^2 + (F \cdot h_L)^2$ |
| Cooper [30] | (7) | $h = 55 \cdot p_r^{0.12} \cdot (-\log_{10} \cdot p_r)^{-0.55} M^{-0.5} \cdot q^{0.67}$ |
| Cooper [31] | (8) | $h = 35 \cdot p_r^{0.12} \cdot (-\log_{10} \cdot p_r)^{-0.55} M^{-0.5} \cdot q^{0.67}$ |
| Lazarek and Black [7] | (9) | $Nu = 30 \cdot \mathrm{Re}^{0.857} \cdot Bo^{0.714}$ |
| Kew and Cornwell [13] (modified Lazarek and Black) | (10) | $Nu = 30 \cdot \mathrm{Re}^{0.857} \cdot Bo^{0.714} \cdot (1 - x)^{-0.143}$ |
| Tran et al. [14] | (11) | $h = 840 \cdot 10^3 \cdot (Bo^2 \cdot We_l)^{0.3} (\rho_l / \rho_v)^{-0.4}$ |

In this review, the following correlations will thus be discussed: (i) Liu and Winterton [20]; (ii) Kandlikar [13]; (iii) Chen [17]; (iv) Shah [18]; (v) Thome et al [64]; (vi) Gungor and Winterton [15]; (vii) Bjorge et al [19]; (viii) Klimenko [11, 12]; (ix) Steiner and Taborek [27]; (x) Tran et al [34]; (xi) Yen et al [56]; (xii) Lee and Mudawar [37] ; (xiii) Haynes and Fletcher [52]; Sumith et.al [58]

The method of Thome et al. 64 formulated a model to predict local dynamic heat transfer coefficients. The focus of this model is on what happens at a fixed point on the wall of a channel subject to a vapor-liquid flow regime dominated by elongated bubbles and a constant wall heat flux boundary condition. They concluded that nucleate boiling is not the major player in boiling in mini and micro-channels. Based on a three zones evaporation model, Thome et al showed that transient evaporation of the thin liquid film surrounding elongated bubbles is the dominant heat transfer mechanism. The input parameters for their model are the local equilibrium quality $x_e$, heat flux, tube diameter, mass flow rate, and fluid thermo-physical properties at local saturation pressure. The model assumes that bubbles nucleate quickly and grow to become of the order of the channel size. These bubbles trap a liquid film between them and the inner tube wall. Thome et al [64] showed that the thickness of the film plays a major role in heat transfer. The 3 zones considered by Thome et al. [64] are as follows: liquid slug; elongated bubble; and vapor slug, as shown in Fig. 3.2. A fixed point on the channel wall is thus periodically subjected to the passage of these three zones, in sequence. The average heat transfer coefficient for the fixed point is then obtained based on some empirical model for each zone. Thome et al. [64] used the homogenous model to obtain the void fraction, and a two-phase mixture velocity, based on several assumptions about the conditions of the liquid, gas and channel. For the liquid and vapor slugs zone, heat transfer coefficient was calculated from a local Nusselt number correlation for forced convection, applied to the respective lengths, with the liquid flow assumed to be hydro-dynamically and thermally developed. For laminar forced convection (Re< 2300), Thome et al [64] used the following correlation that was borrowed from Shah [18]:

$$Nu_{lam}(z) = 0.455\sqrt[3]{\Pr}\sqrt{\frac{d\,\mathrm{Re}}{L(z)}} \tag{3.37}$$

$$Nu = 2Nu_{lam}(z) \tag{3.38}$$

$$Nu_{trans}(z) = \frac{\left(\frac{x}{8}\right)[\mathrm{Re}-1000]\mathrm{Pr}}{1+12.7\sqrt{\left(\frac{x}{8}\right)}\left(\mathrm{Pr}^{2/3}-1\right)}\left[1+\frac{1}{3}\left(\frac{d}{L(z)}\right)^{\frac{2}{3}}\right] \tag{3.39}$$

The friction factor to be used in Equation 39 is found from

$$x = (1.82\log_{10}\mathrm{Re}-1.64)^{-2} \tag{3.40}$$

A large number of assumptions are made for the derivation of this model, including: a) Onset of nucleate boiling occurs at the axial location where the fluid is saturated liquid, b) Bubbles that grow and depart at the ONB point act as “shutters”, that divide the flow field into liquid slugs separated by bubbles. The bubbles keep growing at the expense of the liquid slugs, however, c) The bubble ebullition process does not include a waiting period, but has a growth period that can be modeled according to Plesset and Zwick [65]. The bubble departs when it forms a sphere with a diameter equal to the heated tube diameter.

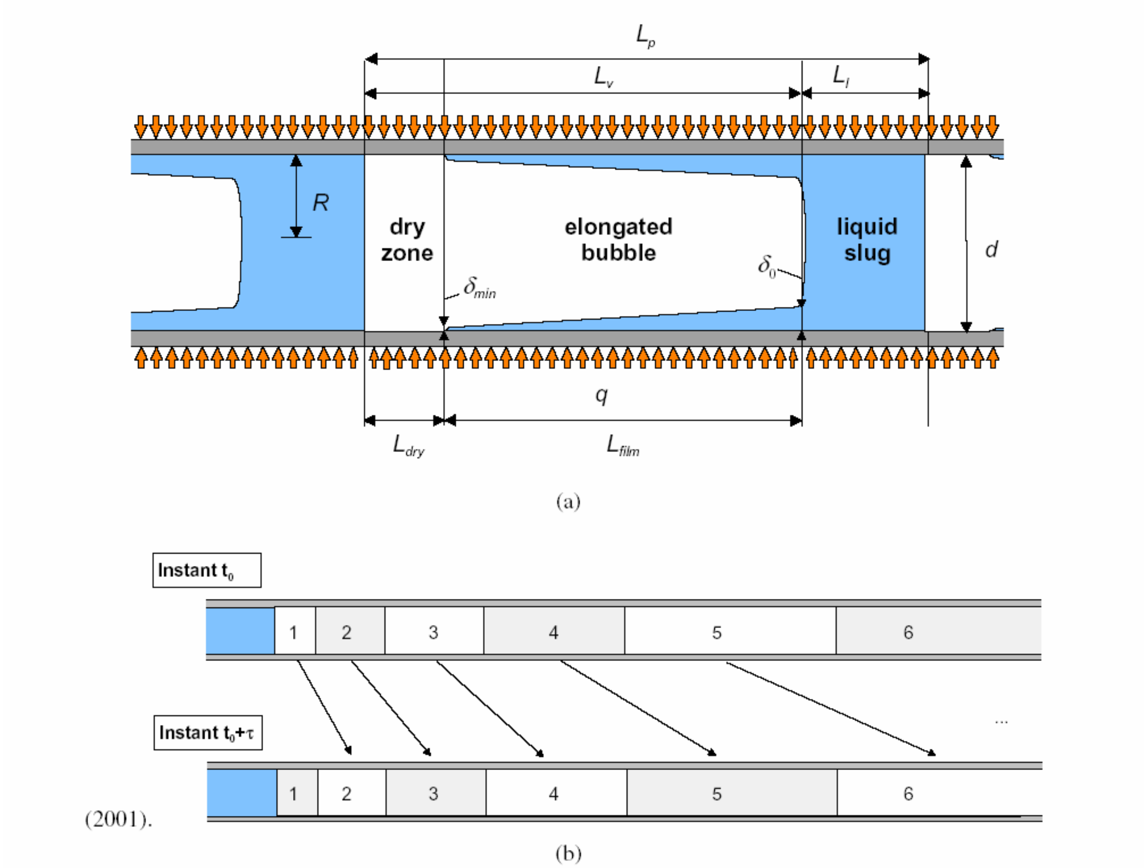


Figure 3.2: The three zones of Thome et al [64]

The phenomenological picture, for a fixed point on the channel wall downstream from the ONB point, according to Thome et al. [64] is thus as follows. Liquid slugs and elongated bubbles pass over the point, in turn. During the passage of the liquid slug, wall heat transfer can be found from correlations representing fully-developed pipe flow. During the passage of an elongated bubble the fixed point is covered by a thin liquid film formed from the liquid slug. The heat transfer is governed by the heat conduction and surface evaporation in the liquid film. Should the liquid film be disrupted before the arrival of the next liquid film, furthermore, for a period of the time the fixed point will be subject to single-phase vapor forced convection, and the latter is represented by fully-developed pipe flow. The model of Thome et al. [64] is thus a "three zone" model, and the time average heat transfer coefficient at a fixed point should accordingly be obtained from:

$$h(z)=\frac{t_1}{t}h_1(z)+\frac{t_{film}}{t}h_{film}(z)+\frac{t_{dry}}{t}h_v(z) \tag{3.41}$$

where $t_l$, $t_{film}$ and $t_{dry}$ represent the time periods during which the fixed point is covered by a liquid slug, the liquid film underneath an elongated bubble, and pure vapor , respectively , and $t = t_l + t_{film} + t_{dry}$. ( Note that $t_{dry}$ can be equal to zero).

Despite its interesting phenomelogical background, the model of Thome et al [64] does not appear to be a promising predictive tool. The model needs three adjustable coefficients that are difficult to predict. The parameters that need adjustment are the minimum liquid film thickness at dry out; a correction factor for the prediction of initial film thickness; and a pair frequency, which is a function of the bubble formation process. Thome et al. [64] applied their model to the data from several different sources, and found out that the aforementioned adjustable parameters varied from case to case. They developed a "general model" as well, where the adjustable coefficients were chosen to provide the best possible fit to the entire data base they had used. Furthermore, as mentioned earlier, the model is limited to the elongated bubbles regime.

**The correlation of Liu and Winterton** [20]:

This is a widely used correlation for the prediction of flow boiling heat transfer coefficient. Like most correlations dealing with forced flow boiling, the correlation is in fact the addition of two heat transfer coefficients, one representing nucleate boiling and the other convection heat transfer. The nucleate boiling heat transfer component is calculated using Cooper's [63] correlations while the Dittus-Boelter [23] correlation is used to evaluate the convective heat transfer component.

Liu and Winterton [20] employed a method suggested by Kutateladize [66] to combine the effects of nucleate boiling and convection. A forced convection enhancement factor F and a nucleate boiling suppression factor S are defined where:

$$h_{TP} = \sqrt{\left(\left[\frac{h_{\exp}}{h_{pool}}\right]^2 - \left[\frac{Fh_l}{h_{pool}}\right]^2\right)} \tag{3.42}$$

where F and S themselves are correlated as:

$$F = \left[1 + x\Pr_l\left(\frac{r_l}{r_v} - 1\right)\right]^{0.35} \tag{3.43}$$

$$S = \left(1 + 0.055F^{0.1}\operatorname{Re}_l^{0.16}\right)^{-1} \tag{3.44}$$

When applied to saturated flow, heat flux is calculated from

$$q = h_{TP}(T_w - T_s) \tag{3.45}$$

where:

$$h_{TP} = \sqrt{(Fh_l)^2 + (Sh_{pool})^2} \tag{3.46}$$

If the heated tube is horizontal and the Froude number defined in equation 3.47 is less than 0.05, $Fh_l$ and $Sh_{pool}$ in equation 3.50 must be multiplied by respectively by the expressions in equations 3.48 and 3.49.

$$Fr = \frac{G^2}{r_l^{\,2} g D_h} \tag{3.47}$$

$$e_f = Fr^{0.1-2Fr} \tag{3.48}$$

$$e_s = \sqrt{Fr} \tag{3.49}$$

In sub-cooled boiling, the correlation is as follows:

$$q = \sqrt{\left( \left( Fh_l \Delta T_b \right)^2 + \left( Sh_{pool} \Delta T_s \right)^2 \right)} \tag{3.50}$$

$$\Delta T_b = T_w - T_s$$
$$\Delta T_s = T_w - T_s \tag{3.51}$$

**<u>The correlation of Kandlikar</u>** [21, 22]

The correlation of Kandlikar [21], [22] was presented earlier in equations (3.23) to (3.29). The correlation is recommended for application to channels with water and refrigerants as the working fluid. The all-liquid forced convection heat transfer coefficient $h_{lo}$ is calculated from Gnielinski [24], or Petukov and Popov's[25] correlation, depending on the value of $Re_{l0}$. The parameter $F_{fl}$ is the fluid surface parameter given by Kandlikar [21, 22] and its values for several fluid-solid pairs were given earlier in Table 3.2. Recently (Kandlikar ,2003) Kandlikar [21, 22] examined the applicability of this correlation to boiling in mini-channels (i.e. channels with $D_H$ = 400 µm~ 2.97 mm). He noted that the parameter $f_2(Fr_{lo})$ in his correlation is meant to account for the effect of flow stratification in horizontal channels , and therefore $f_2(Fr_{lo})$= 1 is appropriate for mini-channels where stratification does not occur. Comparing his correlation with the data from four different sources, he arrived at the following major conclusions:

a) The correlation does quite well when $Re_{lo}$ is less than 1600, provided that $h_{lo}$ is obtained from appropriate laminar flow forced convection correlations.

b) For 1600 < $Re_{lo}$ = 3000, where transition from laminar to turbulent flow takes place, deviation occurs between the correlation and data. An appropriate interpolation technique is needed for the calculation of $h_{lo}$, and there is the need for more experimental data.

c) For $Re_{lo}$ greater than 3000 the correlation is probably adequate, as long as $h_o$ is calculated using a turbulent channel flow correlation.

**<u>The correlation of Chen</u> [17]**

Chen's [17] correlation is one of the most widely referenced correlations in the field of boiling. The heat transfer coefficient is obtained from:

$$h = h_{mic} + h_{mac} \tag{3.52}$$

where $h_{mic}$ and $h_{mac}$ represent the micro (nucleate boiling) and macro (conventional) convective terms.

Chen [17] was interested in saturated boiling. The approach by Chen [17] was to treat the forced convection (macro heat transfer) by a modified Dittus-Boelter [23] equation according to:

$$h_{mac} = 0.023(\mathrm{Re})^{0.8}(\mathrm{Pr})^{0.4}\left(\frac{k}{D}\right) \tag{3.53}$$

where *Pr,* and *Re* represent effective values associated with the two-phase fluid. For the two-phase part of the flow field, the equation is written as equation,

$$h_{mac} = 0.023(\mathrm{Re}_l)^{0.8}(\mathrm{Pr}_l)^{0.4}\left(\frac{k_l}{D}\right)F \tag{3.54}$$

Where $Pr_l$ and $Re_l$ are the liquid Prandtl and Reynolds numbers, respectively. The Parameter $F$ is the ratio of the two-phase Reynolds number to the liquid Reynolds number based on liquid fraction of the flow, namely $Re_l$, and is meant to account for the macro contribution to the convection heat transfer. The micro contribution (i.e., the nucleate boiling contribution) is given by the correlation of Forster and Zuber [26], modified for the bubble nucleate suppression due to forced convection. This correlation was given earlier in Equation 3.2, and is repeated below for convenience:

$$h = 0.00122 \frac{k_l^{0.79} c_{pl}^{0.45} r_l^{0.49}}{s^{0.5} m_l^{0.29} H_{fg}^{0.24} r_g^{0.24}} (T_W - T_S)^{0.24} \Delta P^{0.75} S + 0.023 \left[ \frac{DG(1-x)}{m_l} \right]^{0.8} \left( \frac{c_{pl} m_l}{k_l} \right) \frac{k_l}{D} F \tag{3.55}$$

where:

$$\Delta T = T_w - T_s \tag{3.56}$$

$$\Delta P = T_{sat}(T_w - P) \tag{3.57}$$

The parameter S is a suppression factor and is defined as $S = \left( \frac{\Delta T_e}{\Delta T} \right)^{0.99}$. The following equations are used to evaluate $\Delta T_e$ and S:

$$(\Delta T_e)^{0.99} = \left( \frac{T_e}{l\, r_{vj}} \right)_{T_e, l}^{0.75} (\Delta T_e)^{0.24} (\Delta P_e)^{0.75} \tag{3.58}$$

$$S = \left( \frac{\Delta T_e}{\Delta T} \right)^{0.24} \left( \frac{\Delta P_e}{\Delta P} \right)^{0.75} \tag{3.59}$$

Chen [17] subsequently obtained the numerical values for F and S, and represented F and S graphically, as functions of $\frac{1}{X_{tt}}$ and $\mathrm{Re}_l F^{1.25}$, respectively. These graphical representations were subsequently fitted to the empirical expressions of Equations (3.7) and (3.8), respectively.

**<u>The correlation of Shah</u> [18]**

In 1976, Shah [18] also developed a correlation for saturated flow boiling; the fluids for which the correlation is recommended are R-11, R-12, R-113 and water (in the pressure range of 15 to 2500 psia). The correlation is:

$$\frac{h_{tp}}{h_l} = f(Co, Bo, Fr_l) \tag{3.60}$$

Where $h_l$ is obtained from the Dittus-Boelter [23] correlation, and:

$$Co = \left(\frac{1}{x} - 1\right)^{0.8} \left(\frac{r_v}{r_l}\right)^{0.5} \tag{3.61}$$

$$Bo = \frac{q}{Gh_{fg}} \tag{3.62}$$

$$Fr_l = \frac{G^2}{r_l^2 gD} \tag{3.63}$$

This correlation was proposed for a wide range of pipe orientations as well as annular flow channels.

In 1982, Shah [18] published the following widely-applied macro-channel correlation

$$h_{tp} = Max(E, S) h_{sp} \tag{3.64}$$

$$h_{sp} = Nu \frac{k_f}{D_h} \tag{3.65}$$

*where* Nu represents the Nusselt number when all the fluid mixture is liquid, and $D_h$ is the flow passage hydraulic diameter.

$$Nu_{tur} = 0.023 \, \mathrm{Re}_f^{0.8} \, \mathrm{Pr}_f^{0.4} \tag{3.66}$$

$$For\ 0.1 < N, S = 1.8/N^{0.8}, E = 230Bo^{0.5}\ for\ Bo > 3\times10^{-5}$$
$$or\ E = 1 + 46Bo^{0.5}\ for\ Bo < 3\times10^{-5} \tag{3.67}$$

$$\begin{aligned} &For\ 0.1 < N \le 1.0, S = 1.8/N^{0.8} \\ &E = FBo^{0.5}\exp(2.47N^{-0.1}) \end{aligned} \tag{3.68}$$

The parameter N is defined as follows. For vertical tubes, and for horizontal tubes with $Fr_l > 0.04$, N = Co. For horizontal tubes when $Fr_l < 0.04$,

$$N = 0.38 Fr_l^{-0.3} Co \tag{3.69}$$

where $\Pr = \dfrac{P}{Pcr}$ with Pcr representing the fluids critical pressure, and M is the molecular mass number of the fluid.

This correlation is not applicable to metallic fluids and Re numbers greater 10,000. Shah [18] (82) also suggests caution when using this correlation for annular channels with a clearance less than 4 mm. Shah [18]suggests that to use this correlation with annuli with clearance less than 4 mm, the heated perimeter should be used. The overall standard deviation of the correlation of Shah [18] is ±30%.

**The correlation of Gungor and Winterton [14, 15]**

Gungor and Winterton [15] modified the correlation of Chen [17] and developed a correlation for flow boiling inside horizontal and vertical tubes, as well as annuli. The correlation is:

$$h_{tp} = Eh_l + Sh_{pool} \tag{3.70}$$

where E is calculated from:

$$E = 1 + 24000Bo^{1.16} + 1.23\left(\frac{1}{X_{tt}}\right)^{0.86} \tag{3.71}$$

The parameter $X_{tt}$ is the turbulent-turbulent Martinelli factor, and is defined as:

$$X_{tt} = \left(\frac{1-x_g}{x_g}\right)^{0.9} \left(\frac{r_g}{r_l}\right)^{0.5} \left(\frac{m_l}{m_g}\right)^{0.1} \tag{3.72}$$

The correlation of Cooper [63] is used to evaluate $h_{pool}$, and this is the main difference with Chen's [17] correlation (recall that the correlation by Foster and Zuber [26] was used by Chen [17] in his original correlation). The correlation of Cooper [63] is repeated here for convenience.

$$h_{pool} = 55 P_r^{\,0.12} \left(-\log P_r\right)^{-0.55} M^{-0.5} q''^{0.67} \tag{3.73}$$

**<u>The correlation of Bjorge et al. [19]</u>**

Bjorge et al [19] developed the following simple, empirical correlation:

$$q = q_{FC} + q_B \left[ 1 - \left( \frac{(T_w - T_{sat})_{ib}}{(T_w - T_{sat})} \right)^3 \right] \tag{3.74}$$

The correlation is evidently the superposition of convection and boiling components. The forced convection component is found from:

$$q_{FC} = \frac{\mathrm{Re}_l^{0.9}\, \mathrm{Pr}_l\, F(X_{tt}) k_l}{F_2 D} (T_W - T_{sat}) \tag{3.75}$$

where

$$F(X_{tt}) = 0.15 \left[ \frac{1}{X_{tt}} + 2.0 \left( (\frac{1}{X_{tt}}) \right)^{0.32} \right] \tag{3.76}$$

where $X_{tt}$ is the turbulent-turbulent Martinelli factor, and

$$\mathrm{Re}_l = \frac{GD(1-x)}{m_l} \tag{3.77}$$

The parameter $F_2$ is defined as:

$$F_2 = 5\mathrm{Pr}_l + 5\ln(1+\mathrm{Pr}_l) + 2.5\ln(0.0031\mathrm{Re}_l^{\ 0.812}) \ for\, \mathrm{Re}_l > 1125 \tag{3.78}$$

$$F_2 = 5\mathrm{Pr}_l + 5\ln[1+\mathrm{Pr}_l(0.0964\mathrm{Re}_l^{0.585}-1)] \text{ for } 50 < \mathrm{Re}_l < 1125 \tag{3.79}$$

While for $\mathrm{Re}_l < 50$

$$F_2 = 0.0707\,\mathrm{Pr}_l\,\mathrm{Re}_l^{0.5} \tag{3.80}$$

For sub-cooled and low quality regions. Bjorge et al [19] recommend the following equation to evaluate the forced convection contribution, shown in Equation 3.82.

$$\left(\frac{h_{FC}D}{k_b}\right) = 0.023\left(\frac{GD}{m_f}\right)^{0.8}\left(\frac{m_f C_{pb}}{k_b}\right)^{1/3} \tag{3.81}$$

$$q_{FC} = h_{FC}[(T_w - T_{sat}) + (\Delta T_{sc})] \tag{3.82}$$

Properties with subscript b are to be calculated at liquid bulk temperature. The subscript f indicates the evaluation of the property at the film temperature defined as:

$$T_f = \frac{T_w - T_b}{2} \tag{3.86}$$

$$\frac{q_B}{m_f h_{fg}}\left(\frac{s}{g(r_l - r_v)}\right)^{\frac{1}{2}} = B_M \frac{k_l^{1/2} r_l^{17/8} C_{pl}^{19/8} r_v^{1/8}}{m_l h_{fg}(r_l - r_v)^{9/8} s^{5/8} T_{sat}^{1/8}} \Delta T_{sat}^3 \tag{3.83}$$

where $B_M$ is a dimensionless constant given as 1.89 * $10^{-14}$ in SI units and 0.0000213 in engineering units, for water. The wall superheat at the boiling incipience is found from

$$\Delta T_{sat,ib} = \frac{8sT_{sat} b u_{fg} h_{FC}}{k_l h_{fg}} \tag{3.84}$$

The correlation is valid for qualities above 5 %.

**<u>The correlation of Klimenko</u> [11], [12]**

Klimenko [11], [12] also developed a highly respected correlation for forced convection boiling heat transfer. He recommended his correlation for both horizontal and vertical pipes. The original correlation from 1988 [11] was later revised in 1990 [12]. The new correlation is not applicable for dry out situations discussed in sufficient detail in section 3.1, and will not be repeated here. The range of applicability of the correlation is also given in Table 3. Klimenko [11, 12] stated that this correlation was tested with 3000 data points and agreed with the data with a standard deviation of 14.4%.

**<u>The correlation of Steiner and Taborek</u> [27]**

Steiner and Taborek [27], developed a correlation that falls into the category of asymptotic correlations. This correlation is based on the power type addition of Kutateladze [65]. The power-type addition sums the nucleate and convective boiling components, and has been used by many investigators. For example, Churchill 67 used the method of power-type summation to develop a correlation for transition between forced convection and natural convection boiling heat transfer. The factor $F_{nb}$, shown in the forthcoming Equation (3.85), determines which component is more dominant between the two convection modes. The general form of the correlation of Steiner and Taborek [27] was given earlier in section 3.1, and is repeated here for convenience:

$$h_{tp} = \left(h_{nb}{}^{n} + h_{cb}{}^{n}\right)^{\frac{1}{n}} \tag{3.85}$$

where

$$h_{nb} = h_{nbo}F_{tp} \tag{3.86}$$

The quantity $h_{nbo}$ is the nucleate pool boiling heat transfer coefficient. The factor $F_{nb}$ is given by:

$$F_{nb} = F_{tp}\left(\frac{q}{q_o}\right)^{m}\left(\frac{D}{D_o}\right)^{-0.4}\left(\frac{R_a}{R_{ao}}\right)^{0.133} F(m) \tag{3.87}$$

$$h_{cb} = h_{lo}F_{tb} \tag{3.88}$$

The parameter $h_{lo}$ is the purely convective heat transfer coefficient for total liquid flow. The parameter $F_{tp}$ is the two phase flow multiplier, and is defined as:

$$F_{tp} = \left[(1-x)^{1.5} + 1.9(x)^{0.6}\left(\frac{r_l}{r_G}\right)^{0.35}\right]^{1.1} \quad \text{for x = 0.6} \tag{3.89}$$

The above expression ensures that $F_{tp}$? *1 as x? 0. (see Fig. 3.3). For x > 0.6,* one must ensure that $F_{tp}$? $\frac{h_{go}}{h_{lo}}$ as for x ? 1 and this is provided by the equation below,

$$\frac{h_{cb}}{h_{lo}} = F_{tp} = \left(\left[(1-x)^{1.5} + 1.9(x)^{0.6}(1-x)^{0.01}\times\left(\frac{r_l}{r_G}\right)^{0.35}\right]^{-2.2} + \left\{\left(\frac{h_{go}}{h_{lo}}\right)(x)^{0.01}\times\left[1+8(1-x)^{0.7}\left(\frac{r_l}{r_G}\right)^{0.67}\right]\right\}^{-2}\right)^{-0.5} \tag{3.90}$$

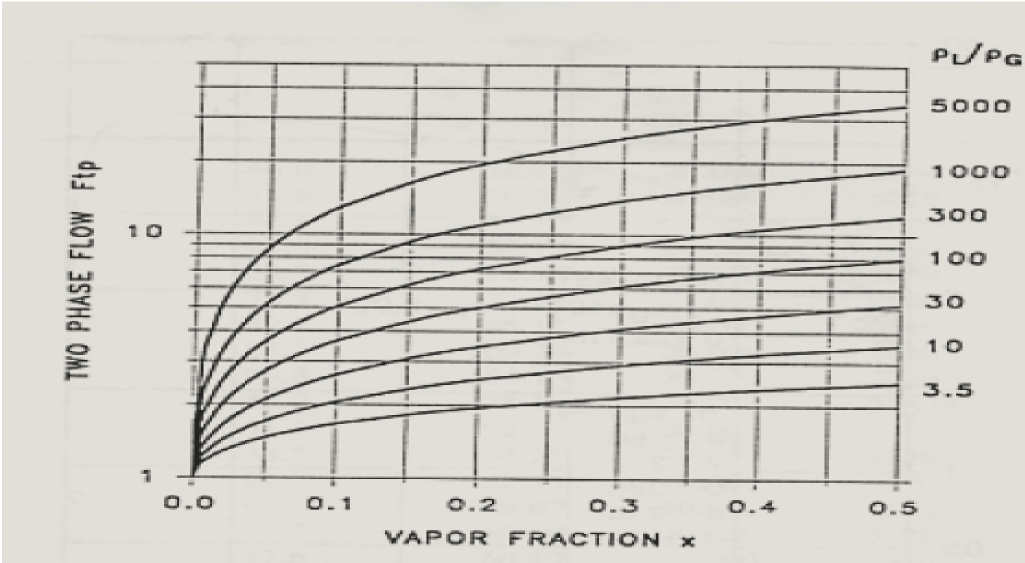


Figure 3.3: Relationship between quality and Ftp for Steiner and Taborek [27]

**The correlation of Kandlikar and Steinke [68]**

Kandlikar [21, 22] also proposed a correlation for flow boiling in vertical and horizontal channels. The correlation of Kandlikar [21, 22] in its original form was given and discussed in section 3.1. Kandlikar and Steinke [68] examined the applicability of the correlation to mini-channels, and argued that, for mini-channels $f_2(Fr_{lo}) = 1$. They also indicated that for $Re_{lo} < 1600$, $h_{lo}$ must be found from an appropriate laminar flow regime correlation, which for $Re_{lo}$ the correlation of Gnielinski [24] for single-phase turbulent flow is probably adequate. For the transition range $1600 < Re_{lo} < 3000$, there appears to be the need for more experimental data

Thus the heat transfer coefficient $h_{tp}$ is the large of $h_{nbd}$ and $h_{cbd}$, where:

$$h_{NBD} = 0.6683 Co^{-0.2} h_{lo} + 1058.0 Bo^{0.7} F_{fl} h_l o \tag{3.91}$$

$$h_{CBD} = 1.1360 Co^{-0.9} h_{lo} + 667.2 Bo^{0.7} F_{fl} h_{lo} \tag{3.92}$$

The parameter $F_{fl}$ values for certain fluids were listed earlier in Table 3.2, and for other fluids, Forster and Zuber [26] correlation for boiling heat transfer may be used. The latter correlation can also be used for boiling when $F_{rl}$ is less than 0.04. The first term in the equation for $h_{NBD}$ must be multiplied by $e_f = (25F_{rl})^{0.3}$ when $F_{rl}$ is less than 0.04.

This correlation was developed by Kandlikar [21, 22] using a data set of 5000 points. The correlations of Chen [17], Shah [18] and Gungor and Winterton [15], when compared with the same 5000 data points, had standard deviations of 29.6%, 17.9% and 20.7%, respectively.

**The correlation of Tran et. al. [34]**

The correlation of Tran et. al [34] were developed based on their own date that were obtained in a circular channel with 2.46 mm diameter, and a rectangular channel with a hydraulic diameter of 2.40 mm, using refrigerant R-12. Their correlation can be represented as

$$h_{tp} = \left[ 8.4\times10^{5}(Bo^{2}We_{fo})^{0.3}\left(\frac{v_g}{v_f}\right)^{-0.4} \right] \tag{3.93}$$

where term $We_{fo}$ is given in equation (3.103)

$$We_{fo} = \frac{n_f G^2 D_h}{s} \tag{3.94}$$

**The correlation of Lee and Mudawar [37]**

A detailed discussion of the experimental investigation of Lee and Mudawar [37] has already been given in the previous section. They divided the entire boiling heat transfer regimes in Microchannels into low, medium and high quality zones, and for each zone they developed a separate correlation. Their correlations are as follows:

for $x_e$ = 0.0 to 0.05

$$h_{tp} = 3.856X^{0.267}h_{sp,f} \tag{3.95}$$

where X is the Martinelli's factor:

$$X^2 = \frac{(dp/dz)_f}{(dp/dz)_g} \tag{3.96}$$

$$h_{sp,f} = \frac{Nuk_f}{D_h} \tag{3. 97}$$

The test section of Lee and Mudawar [37] was composed of rectangular channels with three sides heated. They used an appropriate correlation for Nu for their data. For circular channels, evidently $Nu = \frac{48}{11}$ can be assumed for known wall heat flux conditions.

In defining the Martinelli's factor, Lee and Mudawar [37] considered the viscous-viscous and viscous-turbulent regimes both, thereby defined:

$$X_{vv} = \left(\frac{m_f}{m_g}\right)^{0.5}\left(\frac{1-x_e}{x_e}\right)^{0.5}\left(\frac{v_f}{v_g}\right)^{0.5} \tag{3.98}$$

$$X_{vt} = \left(\frac{f_f \operatorname{Re}_g^{0.25}}{0.079}\right)^{0.5}\left(\frac{1-x_e}{x_e}\right)^{0.5}\left(\frac{v_f}{v_g}\right)^{0.5} \tag{3.99}$$

$$\operatorname{Re}_g = \frac{G x_e D_h}{m_g} \tag{3.100}$$

For $x_e$=0.05-0.55:

$$h_{tp} = 436.48 Bo^{0.522} We_{fo}^{0.351} X^{0.665} h_{sp,f} \tag{3.101}$$

$$Bo = \frac{q''}{G h_{fg}} \tag{3.102}$$

$$We_{fo} = \frac{v_f G^2 D_h}{s} \tag{3.103}$$

For $x_e$=0.55 to 1.0:

$$h_{tp} = \max\{(108.6 X^{1.665} h_{sp,g}), h_{sp,g}\} \tag{3.104}$$

In laminar flow,

$$h_{sp,g} = \frac{Nu_3 k_g}{D_h} \tag{3.105}$$

and for turbulent flow,

$$h_{sp,g} = 0.023\,\mathrm{Re}_g^{0.8}\,\mathrm{Pr}_g^{0.4} \tag{3.106}$$

**<u>Haynes and Fletcher</u> [52]**

This correlation was developed based on the authors' own experimental data representing sub-cooled and saturated forced flow boiling of refrigerants R-11 and HCFC-123 in copper tubes with diameters 0.92 and 1.95 mm, under low-flow (110 ~ 1840 kg/m$^2$s ; 450 = $\mathrm{Re}_{lo}$ = 1200) and low heat flux (11~170 KW/m$^2$) conditions. The correlation is

$$h = h_{FC} + h_{PB}\frac{\Delta T_{sat}}{\Delta T_{mean}} \tag{3.107}$$

The forced convection component is to be found from macro scale forced –flow correlations with due attention to laminar and turbulent regimes based on $\mathrm{Re}_{lo}$. The pool boiling heat transfer coefficient is found from the boiling component of the correlation of Gorenflo [53] [1993]. To use Gorenflo's [53] method, the reference heat transfer coefficients

$h_o$ =2.8kW/m$^2$K and $h_o$ = 2.6 kW/m$^2$K were used for R-11 and HCFC-123 respectively.

The correlation of Gorenflo [53] is given below in Equation (3.108).

$$h_{nb} = h_0 F_{PF}\left(\frac{q}{q_0}\right)^n \left(\frac{R_p}{R_{po}}\right)^{0.133} \tag{3.108}$$

where $F_{PF}$, the pressure correction factor is given as:

$$F_{PF} = 1.2\,p_r^{\;0.27} + 2.5\,p_r + \frac{p_r}{1 - p_r}$$

$$n = 0.9 - 0.3\,p_r^{\;0.3}$$

The fluid specific value for $h_o$ is given by Gorenflo [53].

The value for $R_p$ is set to 0.4 µm when unknown. The Equation (109 ) for $F_{PF}$ is for all fluids except for helium and water. For these two fluids the following equation is to be implemented

$$F_{PF} = 1.73 p_r^{0.27} + \left(6.1 + \frac{0.68}{1 - p_r}\right) p_r^{2} \tag{3.109}$$

$$n = 0.9 - 0.3 p_r^{0.15} \tag{3.110}$$

### 3.5 Available Mini and Micro-Channel data

Despite the importance of a full understanding of flow boiling in mini and micro channels, there is relatively little data available. Furthermore, unfortunately most researchers are often reluctant to provide their data for others to use for testing with available correlations.

As mentioned by Dupont et al [64], only Bao et al [39] and Baird et al [60] made their data available for testing by the former author's correlations. The data of Bao et al [39] and Baird et al. [60] were also used by Dupont et.al [64], in the development of their 3 zone model.

Due to the unavailability of data, some data sets were electronically extracted for the present study. The method used is explained below. The graphs shown by the authors in their publications were scanned using an Epson TWAIN scanner. Each image was then digitized with grids placed on it. This was done so as to be able to obtain reasonably accurate data points. Unfortunately, most of data extracted in this way were found to be unsuitable for use, due to the lack of confidence in the obtained points as well as other missing essential parameters that were not provided in the papers.

It must therefore be emphasized that there are not enough data to conclusively test the available correlations, and more extensive work is required to obtain accurate and reliable data in mini and micro-channels. This is necessary so that accurate and efficient correlations could be developed to deal with different effects and causes important to flow boiling in min and micro-channels. Future experiments should not only deal with boiling of water in mini and micro-channels, but should also utilize different fluids.

The following is a brief description of the experimental procedures use to acquire the available data.

**Bao et al. [39]**

Bao et al. [39] used the test facility shown in figure 3.4 to perform their experiments. Their test section was composed of a smooth tube made from copper, with an inner diameter of 1.95 mm. The heated length of their test section was 270 mm. A boiler was used to create the vapor with the required pressure in the fluid. The test fluids were, R11 and HCFC123; the range of heat flux was 5-200 kW/m$^2$; and the range of mass flux was 50-1800 kg/m$^2$s. The quality varied in the 0-0.9 range. The pressure range was 200-800 kPa, and the experimental heat transfer coefficients calculate to be in the 1-18 kW/m$^2$K range.

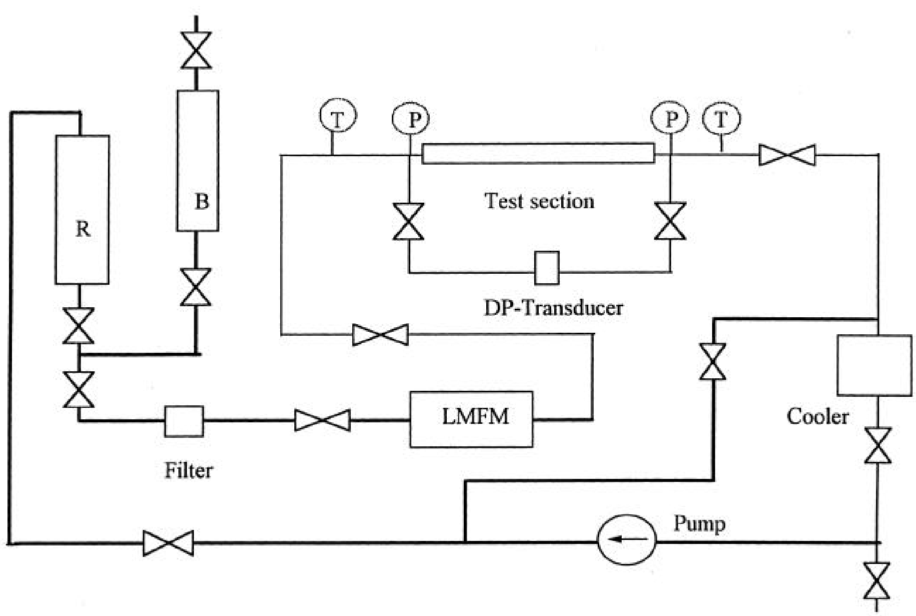


Figure 3.4: The test section used by Bao et al. [39], (LMFM: liquid mass flow meter).

**Baird et al. [60]**

These experiments were performed using a new and sophisticated test section shown in Figure 3.5. The test section setup allowed for a good control and easy measurement of local heat transfer parameters. The two fluids used in these experiments are R11 and HCFC123, and their study let to the collection of more than 2000 data points. The channel diameters were 1.95 mm and 0.92 mm, fabricated from copper. The heated length in the experiments was 30 mm, with an entrance length of 270 mm and exit length of 150 mm. The test mass fluxes were in the range 70-600 kg/m$^2$; the heat flux range was 15-110 kWm$^2$; and pressure set range was between 120-410 kPa.

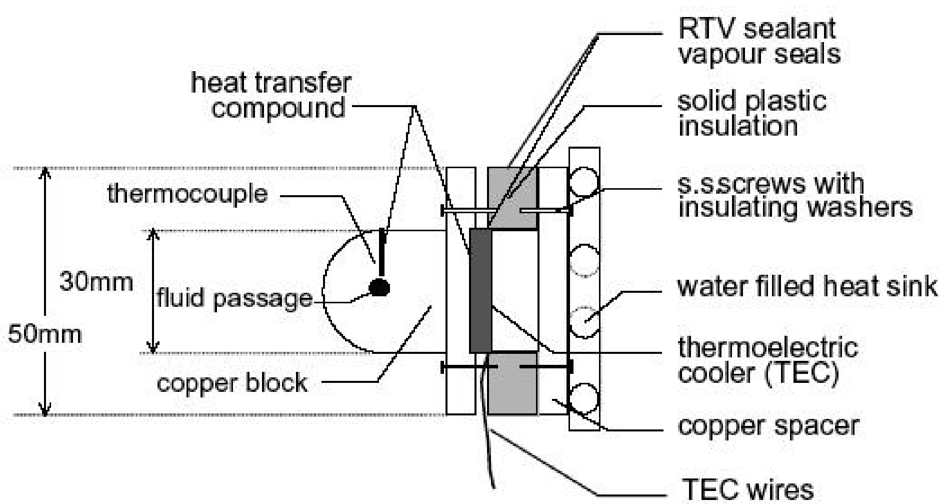


Figure 3.5: The test facility of Baird et al [60]

The test section was divided into separate regions, which were independently cooled. A TEC (Thermoelectric Cooler) was used because of its ease in obtaining temperature readings in small conduits.

Copper blocks were attached to each section and the temperature of each block in the different zones was assumed to be equal to the bulk fluid temperature. In order to eliminate the hydrodynamic entrance and exit effects, two unheated sections with the actual test flow area were connected to the two ends of the test section.

The local fluid properties and temperature were calculated as a function of the local fluid enthalpy and an estimated pressure at each location. Baird et al [60] assert that there is further work needed in the area, so as to obtain more information about the trends in mini and micro-channels.

**Yan and Lin [61]**

Yan and Lin [61] performed an experimental investigation to measure the heat transfer coefficients associated with boiling of R134a in a tube with an inner diameter of 2 mm. Their experimental setup in shown in Figure 3.6. It consists of 3 loops, a DC power supply and a data acquisition system. The working fluid was a mixture of water and glycol. By varying the ratio of the two components, they could vary the properties of the test fluid.

In order to minimize error and to obtain accurate measurements, 28 parallel pipes with hydraulic diameter of 2 mm were placed side by side, as shown in Figure3.7. Thermocouples were connected to the pipes to obtain their temperatures. The test setup in its entirety was calibrated in order to minimize experimental errors and obtain reliable data. Table 3.5 shows a summary of the important uncertainties in the experiment of Yan and Lin [61]. Many fundamental assumptions were made in the data acquisition process however, and these assumptions are mainly applicable to flow channels with geometrically regular cross-sections.

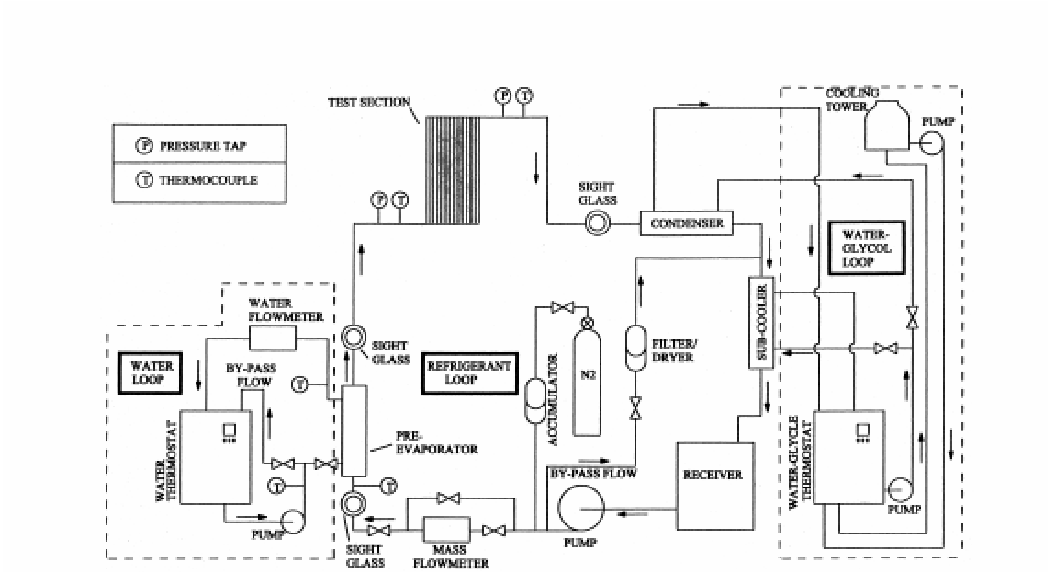


Figure 3.6: The test section of Yan and Lin [61].

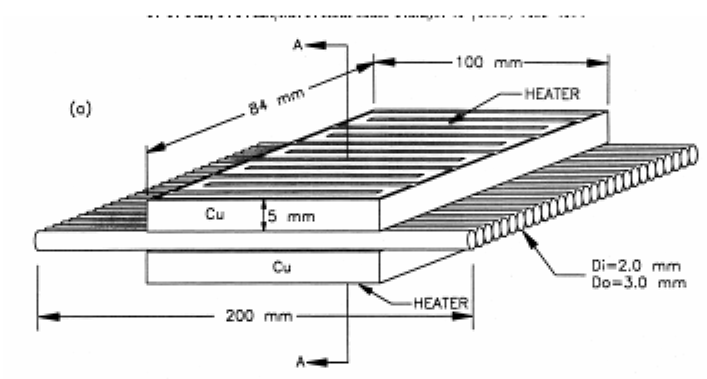


Figure 3.7: The arrangement of the test channels of Yan and Lin [61].

Table 3.5: The uncertainties in the experiment of Yan and Lin [61].

| Parameter | Uncertainty |
| --- | --- |
| Length, width and thickness (m) | ±0.5% |
| Area ($m^2$) | ±1% |
| Temperature, $T$ | ±0.1°C |
| $\Delta T$ | ±0.14°C |
| Pressure, $P$ | ±0.001 MPa |
| Measured pressure drop, $\Delta P_{exp}$ | ±40 Pa |
| Water flow rate in pre-evaporator, $W_{w,p}$ | ±2% |
| Mass flux of refrigerant, $G$ | ±2% |
| Heat transfer rate of test section, $Q_t$ | ±0.5% |
| Heat transfer of pre-evaporator, $Q_{w,p}$ | ±4% |
| Vapor quality, $X$ | ±0.03 |
| Single liquid phase heat transfer coefficient, $h$ | ±6% |
| R-134a evaporation heat transfer coefficient, $h_r$ | ±6% |
| Two-phase friction factor, $f_{tp}$ | ±10% |

## Lee and Mudawar [37] [2004]

Lee and Mudawar [37] recently performed an experiment to study two phase flow and heat transfer. The size of the channel used was 231 μm by 713 μm; 53 of these channels were placed side by side. Proper insulation was provided by the use of a transparent cover, this also allowed for visualization of the flow within the channels. The calculation of uncertainty are shown in the Table 3.5 below. An isenthalpic throttling valve was used to set the enthalpy of the refrigerant. The refrigerant was used to supply the two phase mixture. The mass flow rate was calculated using conventional methods. The outlet quality coming from the evaporator was calculated from the Equation 3.111 given below.

$$x_{e,out} - x_{e,in} = \frac{4q^{''}L}{Gd_h h_{fg}} \tag{3.111}$$

The experimental conditions were within the following ranges; $x_{e,in}$ 0.001-0.25, $x_{e,out}$ 0.49. The flow rate was in the range of G = 127-634 kg/m$^2$.s; heat flux $q''$ was in the range from 159 to 938 kW/m$^2$, the pressure range was the range of 1.44 to 6.60 bar. The test facility is shown in figure 3.8 below.

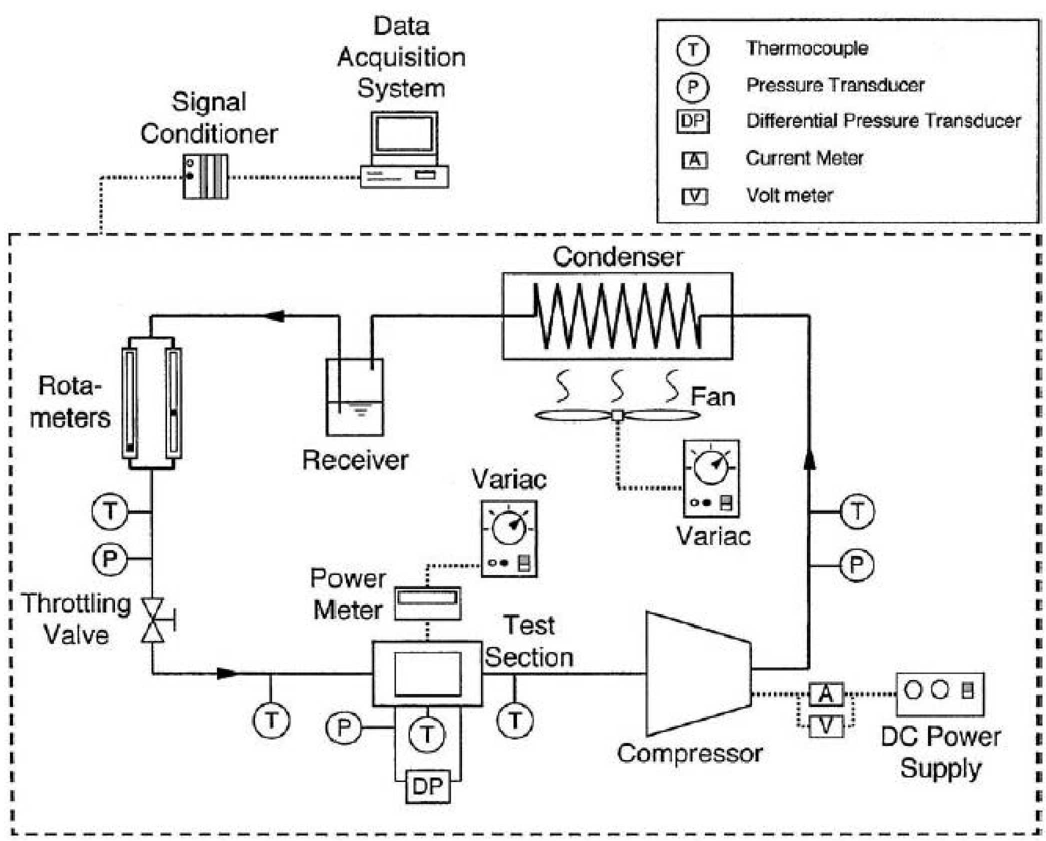


Figure 3.8: The refrigeration loop for Lee and Mudawar [37]

# Chapter 4: Results and Discussion

## 4.1 Introductory Remarks

Three sets of data are used for the assessment of forced flow boiling correlations with respect to their applicability to mini-channels. These data include the data of Bao et al. [39]; Baird et al. [60], and Yan and Lin [61]. These data all correspond to the mini-channel size range. The experimental test facilities of these investigators were discussed in Section 3.5. The source of data was limited to the three reported, mainly due to challenge of obtaining data from different sources. Most authors were not forthcoming in providing their data. Furthermore, the presented data were selected for comparison because they had the most detailed fundamental parameters needed for a critical comparison with individual correlations. All the data points used here are tabulated in Tables B-1 through B-3 in Appendix B.

The predictive methods that are examined include the correlations of Liu and Winterton [20]; Kandlikar[21,22]; Kandlikar and Steinke [68]; Chen [17]; Shah [18]; Gungor and Winterton [15]; Bjorge et al [19]; Klimenko [11,12]; Steiner and Taborek [27]; Tran et al. [34]; Lee and Mudawar [37]; Haynes and Fletcher [52]; and Sumith et al. [58]. These correlations have been discussed in some detail in section 3.4. Among them, only the correlation of Tran et al. [34], Lee and Mudawar [37], and the correlation of Kandlikar [21,22] with the modifications suggested by Kandlikar and Steinke [68], are specifically based on mini-channel data. However, as must be noted that most of the other correlations are based on vast data bases that include mini-channel data points as well.

In what follows, the data of Bao et al. [39] is used for comparison with correlations in section 4.2. In section 4.3, the data of Baird et al. [60] is utilized for this purpose. Finally, in section 4.4, the data of Yan and Lin [61] are utilized. Concluding remarks regarding the suitability of the correlations for mini-channel boiling will be presented in section 4.5.

In the forthcoming discussions, the following statistic is used:

$$x = \frac{h_{corr} - h_{\exp}}{h_{\exp}} \tag{4.1}$$

Where $h_{corr}$ and $h_{exp}$ represent the predicted and experimental heat transfer coefficients, respectively. The mean, $\bar{x}$, and standard deviation, s?, of this statistic will be used to facilitate the quantitative assessment of the performance of correlations.

## 4.2 The Experimental Data of Bao et al. [39]

Figure 4.1 compares the predictions of the correlation of Liu and Winterton [20] with the data. As noted the correlation under-predicts the overwhelming majority of the data points. For this correlation, $\bar{x}$ = -57.38 %, and $s_{?}$ = 39.20 %.

The correlation of Kandlikar [21, 22], with modifications suggested by Kandlikar and Steinke [68] is compared with the data in Fig. 4.2. There is remarkably good agreement between the correlation and the data, and $\bar{x}$ = -14.30 %, and $s_{?}$ = 31 % only.

The correlation of Chen [17], depicted in Fig. 4.3, agrees with the data reasonably well at low heat fluxes, but under-predicts the data monotonically, and rather significantly as the heat flux is increased. For this correlation $\bar{x}$ = -52.40 %, and $s_{?}$ = 22.90 %.

In Fig. 4.4, the predictions by the correlation of Shah [18] are compared with the data. Evidently, the correlation performs poorly, and systematically under-predicts the data. The average under-prediction leads to $\bar{x}$ = -40 %.

The correlation Gungor and Winterton [15] is compared with the data in Fig. 4.5. The correlation is in excellent agreement with the data ($\bar{x}$ = -6.44 % only). There is also very little scatter, $s_{?}$ = 17 %.

Figure 4.6 displays the predictions of the correlation of Bjorge et al. [19]. This correlation over-predicts the data significantly ($\bar{x}$ = 26.1 %), and leads to a wide scatter ($s_{?}$ = 28.25 %).

The correlation of Klimenko [11, 12] is compared with data in Fig. 4.7. Overall, the correlation performs reasonably well in predicting the average data ($\bar{x}$ = -33.93 %), although the scatter of the comparison points is rather large (s ? = 33.99 %).

The correlation of Steiner and Taborek [27] is depicted in Fig. 4.8. Some of the experimental data that were outside the range of applicability of the correlation, as emphasized by the authors themselves have been left out. As noted, although the correlation does very well in terms of average of discrepancies ($\bar{x}$ =

-3.90 %), very large scatter is evidently occurs (s ? = 81.80 %).

The correlations of Tran et al. [34] and Lee and Mudawar [37] are compared with the data in Figures 4.9 and 4.10, respectively. Both correlations do poorly. The correlation of Tran et al [34], in particular, over-predicts the data consistently. An opposite trend is observed with respect to the correlation of Lee and Mudawar [37]. It should be emphasized that these two correlations are both based on experimented data obtained with rectangular cross-section channels. Furthermore, both correlations were developed based on only one set of data, namely, the data of the authors of the correlations.

The predictions of the correlation of Haynes and Fletcher [52] are compared with the data in Fig. 4.11. In this case, the average error, and scatter are both relatively small ($\bar{x}$ = -37.40 %, and s? = 15.34 %). However, the correlation evidently systematically under-predicts the data.

Finally, the predictions of the correlation of Sumith et al [58] are compared with the data in Fig. 4.12. In this case, the average error, and scatter are both relatively small ($\bar{x}$ = 128 %, and s ? = 28.70 %).

The above comparisons utilize the data, without consideration of the flow and boiling regimes. Empirical correlations are often based on certain implied assumptions regarding the flow and boiling regimes. (Please see the discussion in section 3.3.) Comparison between the data and correlations with due attention to flow and heat transfer regimes would require detailed information about the experimented data. However, in view of the fact that mass flux, G and quality, x, are the most important flow property with respect to the most important regime change, namely the transition from bubbly or slug flow to annular-dispersed regime, examination of the correlation predictions as a function of quality can provide useful information about the performance of the correlations. One should recall that at low qualities the two-phase flow regime is typically bubbly or slug, and nucleate boiling prevails. At high qualities, on the other hand, the flow regime is likely to be annular-dispersed, and forced convective evaporation is the dominant mechanism.

Figures 4.13 through 4.18 depict the variations of $\frac{h_{corr}}{h_{\exp}}$ as a function of x, with G as a parameter, for most of the aforementioned correlations. The correlation of Kandlikar and Steinke $\boxed{68}$ (Fig. 4.13) performs best when x < 0.3, where nucleate boiling is predominant, and its performance deteriorates as x is increased and hence forced convection becomes more prevalent.

The correlation of Chen [17], depicted in Fig. 4.14, performs more or less similarly throughout.

The correlation of Shah [18], displayed in Fig. 4.15 shows the following interesting trends. With respect to its average deviation from data, it behaves approximately the same over the entire quality range. The scatter, however, is diminished noticeably as x is increased.

The correlation of Gungor and Winterton [15] is displayed in Fig. 4.16. The correlation does reasonably well for $x < 0.5$, but increasingly under-predicts the data for higher qualities.

Figures 4.17 and 4.18 display the correlations of Klimenko [11, 12], and Steiner and Taborek [27], respectively. Both correlations appear to perform similarly over the entire quality range.

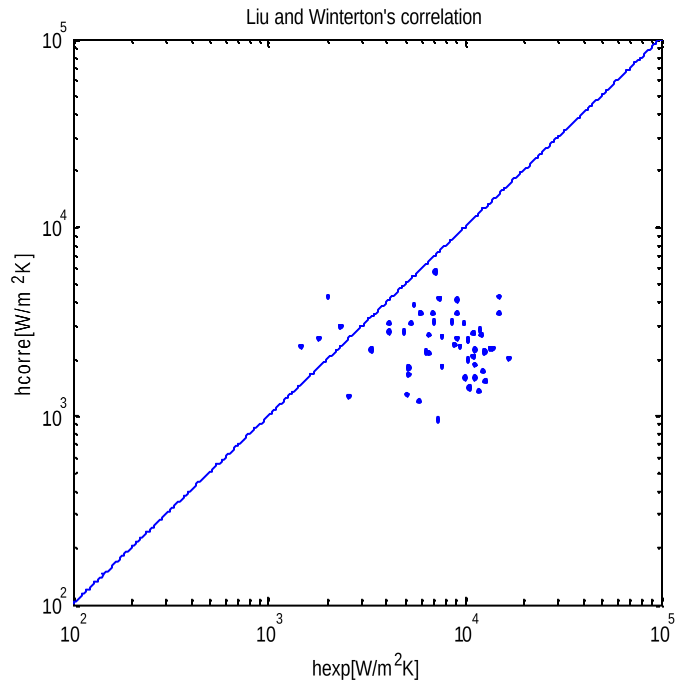


Figure 4.1: Comparison between the experimental data of Bao et al. [39] and the correlation of Liu and Winterton [20]

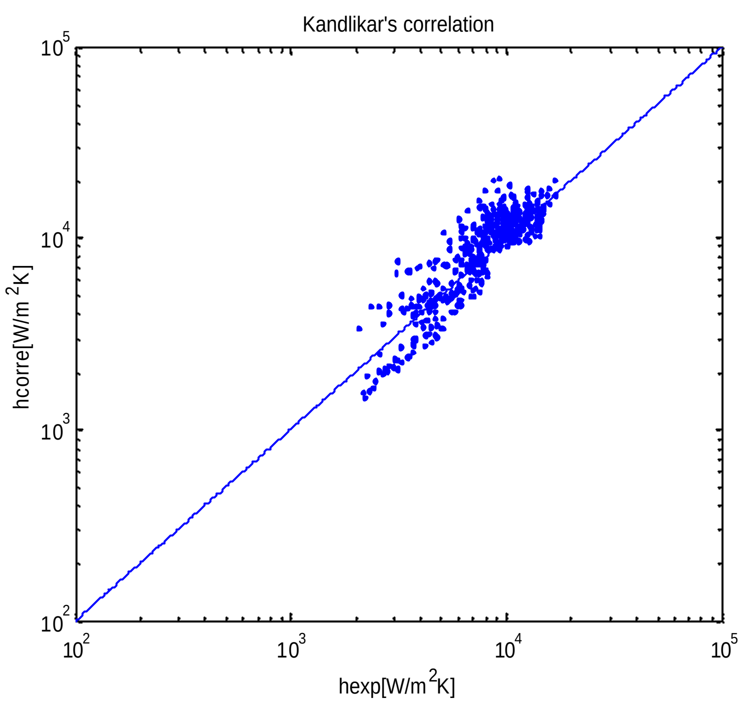


Figure 4.2: Comparison between the experimental data of Bao et al. [39] and the correlation of Kandlikar [21,22]

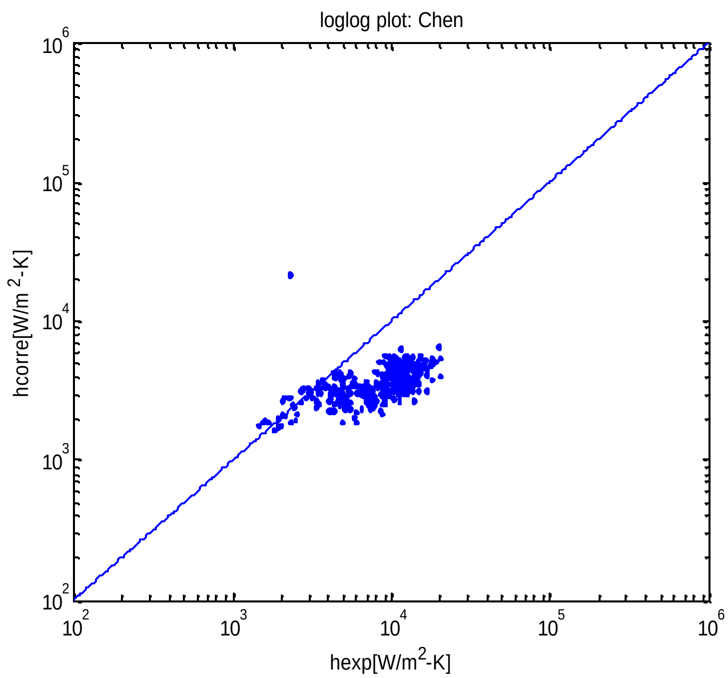


Figure 4.3: Comparison between the experimental data of Bao et al. [39] and the correlation of Chen [17]

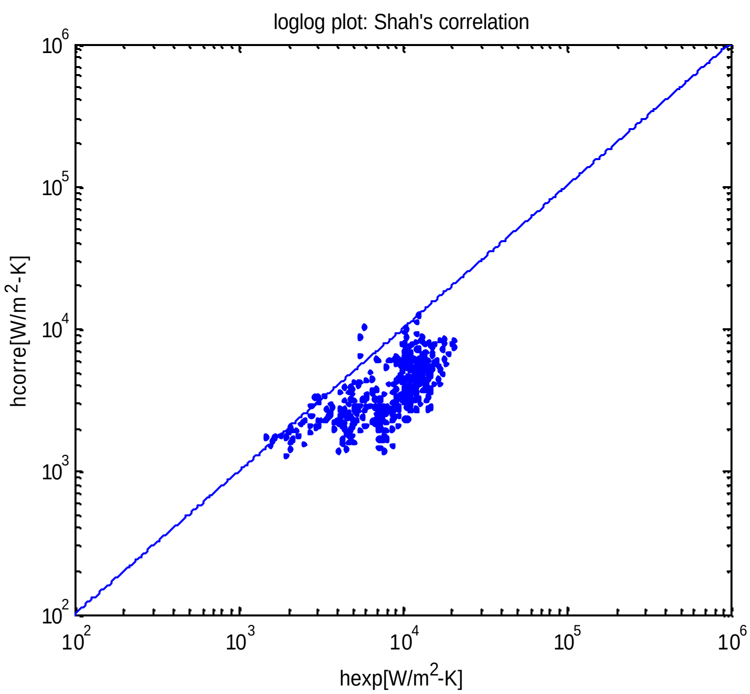


Figure 4.4: Comparison between the experimental data of Bao et al. [39] and the correlation of Shah [18]

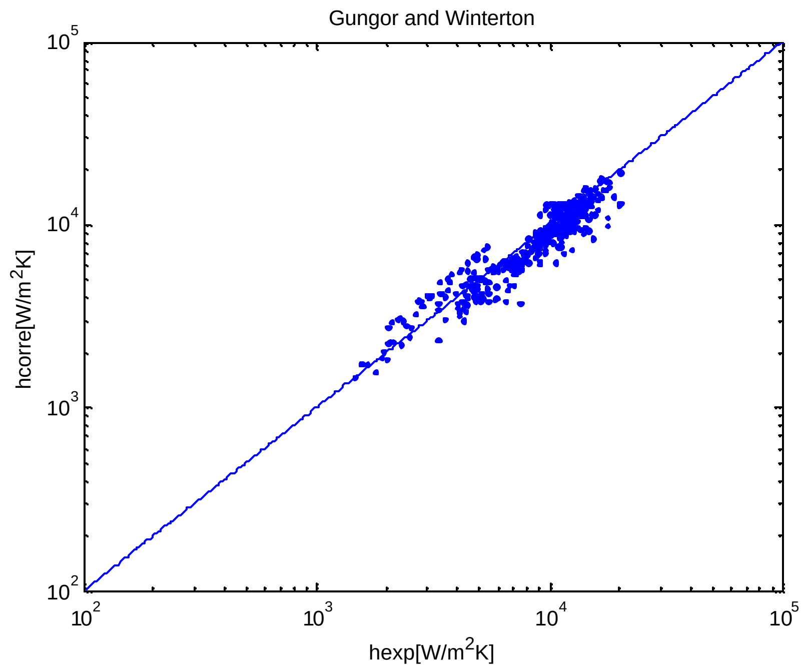


Figure 4.5: Comparison between the experimental data of Bao et al. [39] and the correlation of Gungor and Winterton [15]

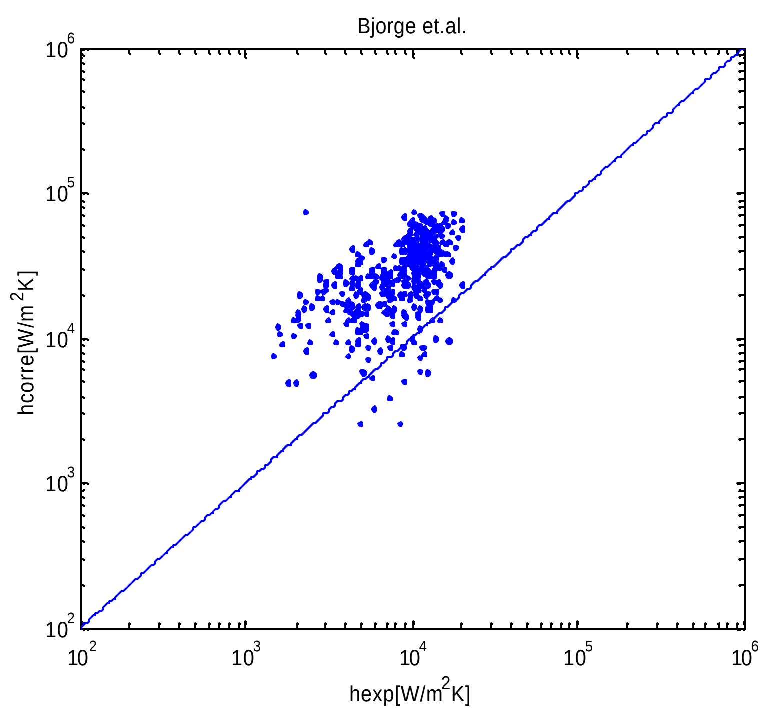


Figure 4.6: Comparison between the experimental data of Bao et al. [39] and the correlation of Bjorge et al. [19]

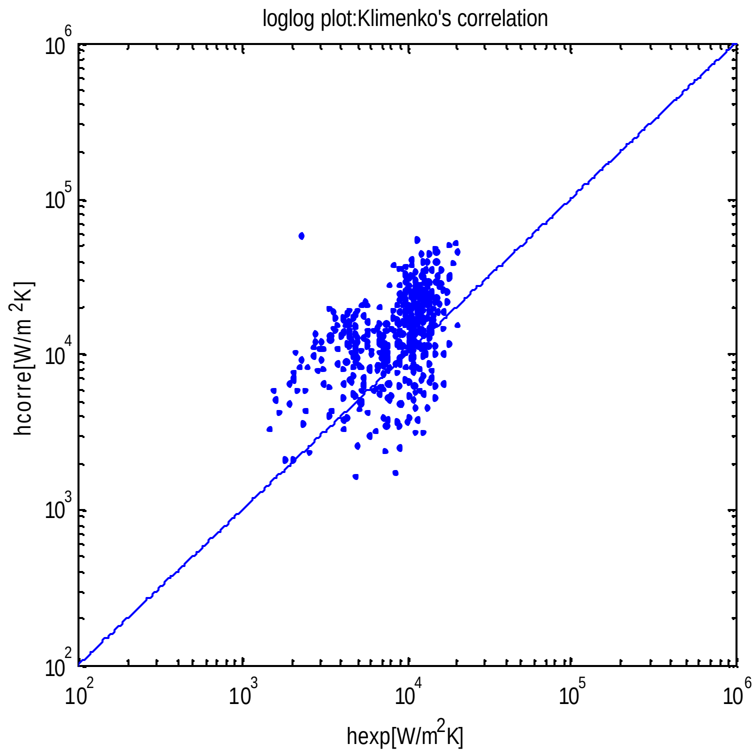


Figure 4.7: Comparison between the experimental data of Bao et al. [39] and the correlation of Klimenko [11, 12]

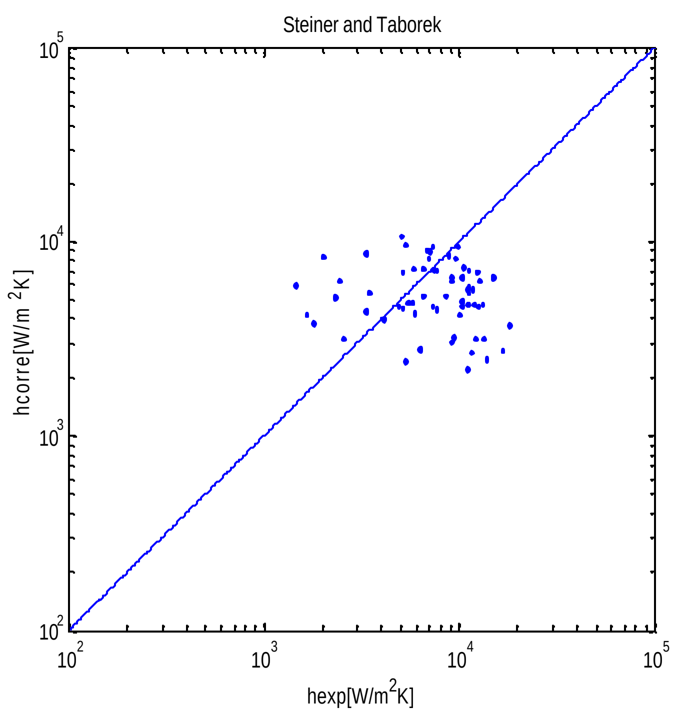


Figure 4.8: Comparison between the experimental data of Bao et al. [39] and the correlation of Steiner and Taborek [27]

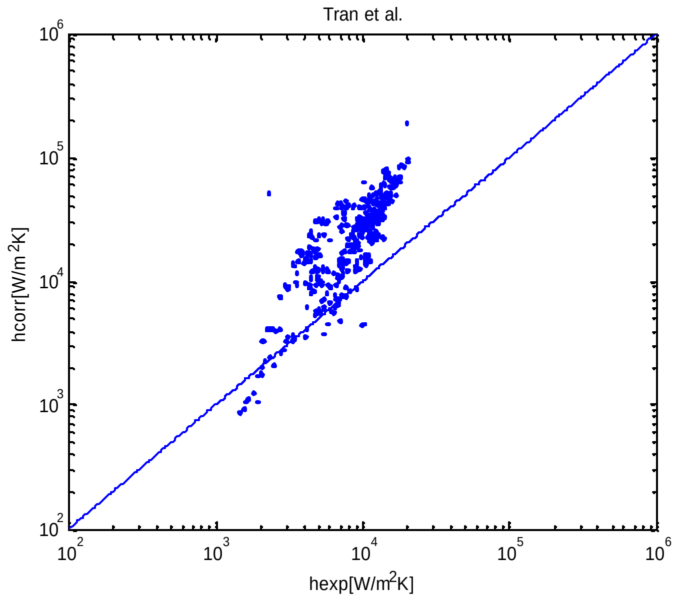


Figure 4.9: Comparison between the experimental data of Bao et al. [39] and the correlation of Tran et al. [34]

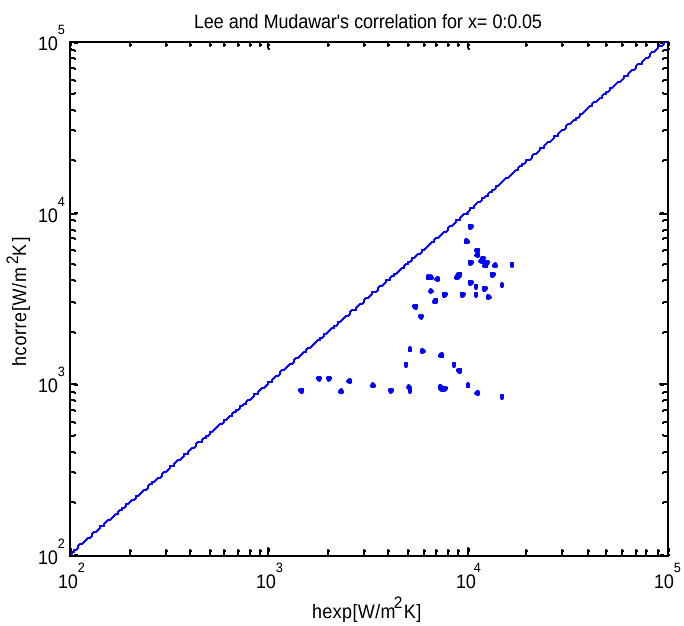


Figure 4.10: Comparison between the experimental data of Bao et al. [39] and the correlation of Lee and Mudawar [37]

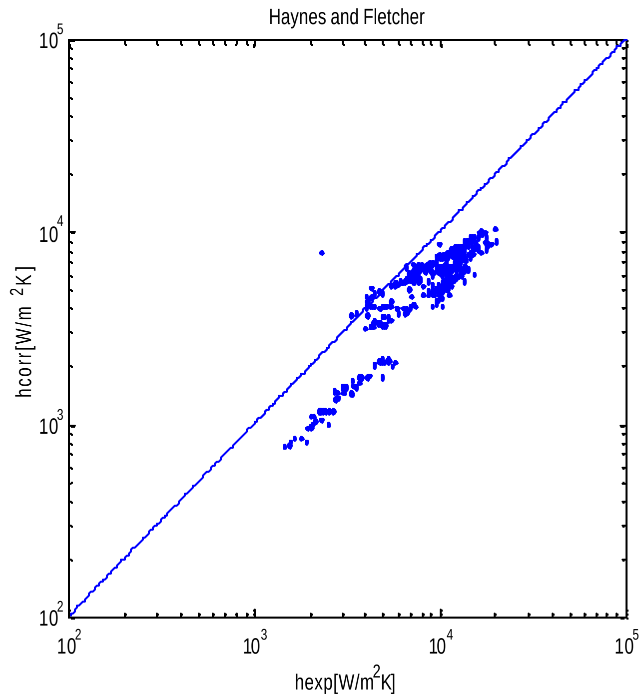


Figure 4.11: Comparison between the experimental data of Bao et al. [39] and the correlation of Haynes and Fletcher [52]

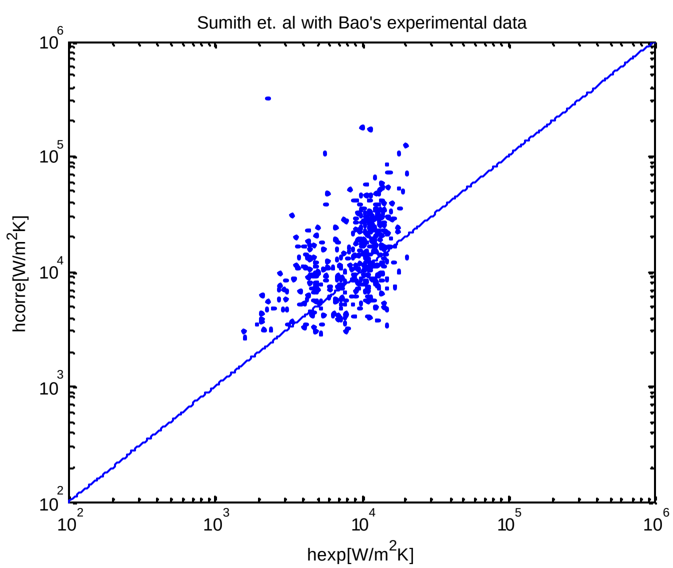


Figure 4.12: Comparison between the experimental data of Bao et al. [39] and the correlation of Sumith et al. [58]

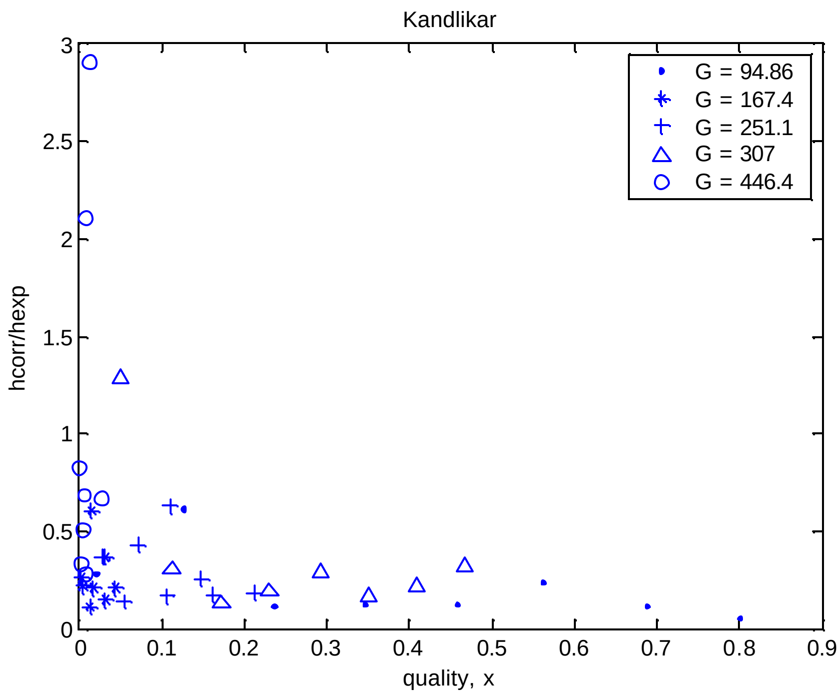


Figure 4.13: Comparison between the experimental data of Bao et al [39] and the correlation of Kandlikar and Steinke [68]: Effects of quality and Mass flux.

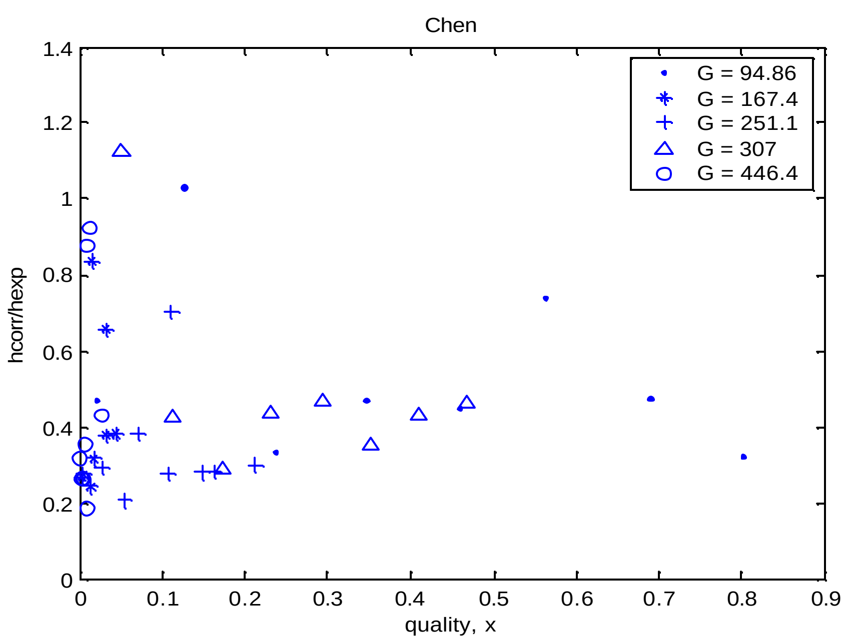


Figure 4.14: Comparison between the experimental data of Bao et al [39] and the correlation of Chen[17]: Effects of quality.

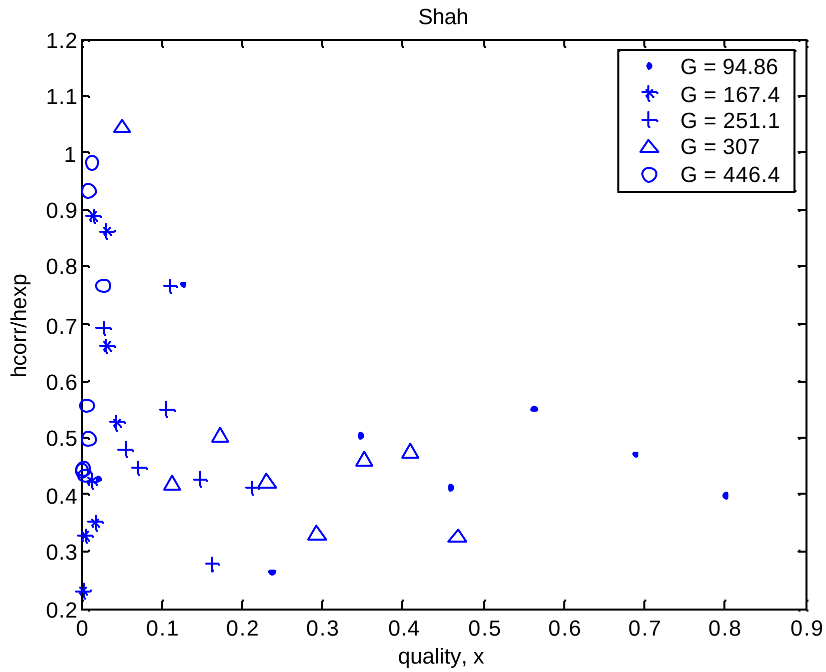


Figure 4.15: Comparison between the experimental data of Bao et al [39]and the correlation of Shah [18]: Effects of quality.

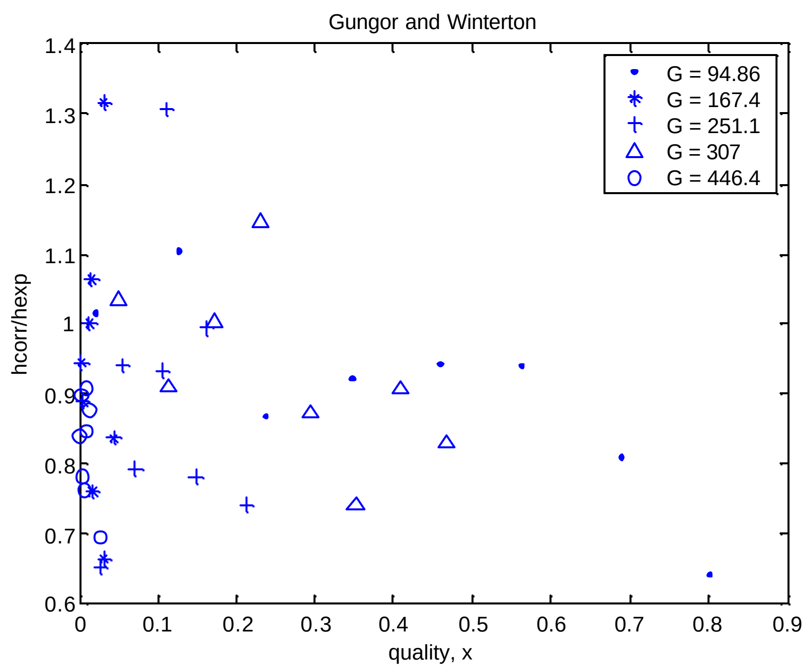


Figure 4.16: Comparison between the experimental data of Bao et al [39] and the correlation of Gungor and Winterton [15]: Effects of quality.

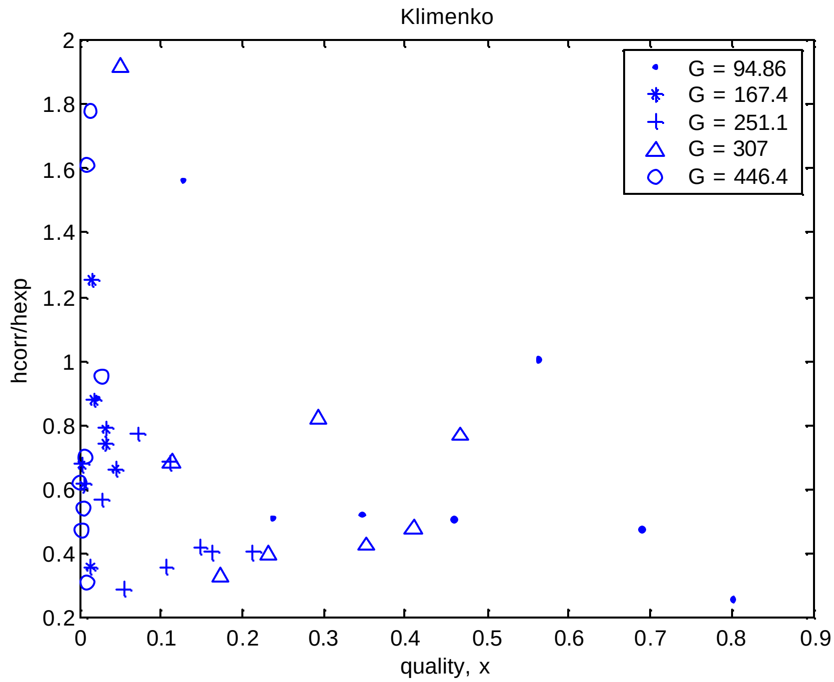


Figure 4.17: Comparison between the experimental data of Bao et al [39] and the correlation of Klimenko [11, 12]: Effects of quality.

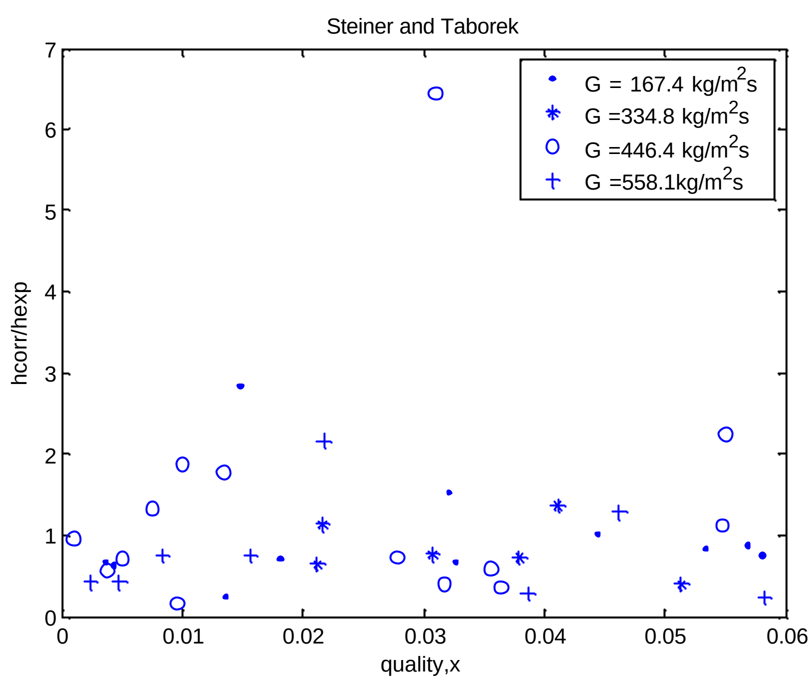


Figure 4.18: Comparison between the experimental data of Bao et al [39] and the correlation of Steiner and Taborek [27]: Effects of quality

## 4.3 The Experimental Data of Baird et al. [60]

The plots in figures 4.19 through 4.36 show the performance of aforementioned correlations in comparison with the experimental data set of Baird et al [60].

Figure 4.19 shows the predictions of the correlation of Liu and Winterton [20] as compared with the data. In this particular situation, the correlation predicts the data with large scatter, as can be seen in the plot. For this correlation $\bar{x}$ = -44.09 % and $s_?$ = 22 %.

The correlation of Kandlikar [21, 22] is compared with this data set in Figure 4.20. The correlation overall appears to under predict the data, with $\bar{x}$ = -23.40 % and $s_?$ = 42 %.

In figure 4.21, the correlation of Chen [17] is compared with the data. This correlation shows good agreement with the data with respect to average heat transfer coefficients; however, there is still considerable scatter. The statistical values are $\bar{x}$ = -41.30 % and $s_?$ = 29.90 %.

The correlation of Shah [18] is compared with the data in figure 4.22. This correlation shows similar performance with that of Chen [17] seen in figure 4.21. The statistical parameters for Shah [18] are $\bar{x}$ = -49.30 % and $s_?$ = 21.10 % .

In figure 4.23, the predictions of the correlation of Gungor and Winterton [15] are evaluated against the data. This correlation slightly under predicted the data. The values for $\bar{x}$ = -10.78 % and $s_?$ = 39.67 %. Figure 4.24 shows the performance of the correlation of Bjorge et al [19]. The correlation under predicts the data significantly ($\bar{x}$ = 58.40 % ) and $s_?$ = 20 % .

Overall, the correlation of Klimenko [11, 12], depicted in figure 4.25, shows close agreement with the data at certain points; however, there is still an over prediction trend with this correlation ($\bar{x}$ = 105 %) and ($s_?$ = 106 %).

The correlation of Steiner and Taborek [27] is displayed in Figure 4.26, and shows significant scatter with this data set. However, there were a few agreements with the data. The average error is $\bar{x}$ = 60 %, while the scatter leads to $s_?$ = 79 %.The comparison is shown in figure 4.26.

Figure 4.27 shows the comparison of the correlation of Tran et al [34] with the data. The correlation of Tran et al [34] shows an under prediction of the data. For this correlation, $\bar{x}$ = -11 % and $s_?$ = 66.80 %

Finally, the correlation of Lee and Mudawar [37] shows poor agreement with data, with wide scatter. Figure 4.28 shows the correlation's performance in comparison with the data. Statistical evaluation shows $\bar{x}$ = 125 % and $s_?$ = 181 %.

The correlation of Haynes and Fletcher [52] and Sumith et al [58] are compared with the data of Baird et al [60] in Figures 4.29 and 4.30, respectively. As noted, overall, both correlations do relatively poorly. The correlation of Haynes and Fletcher under-predicts most of the data, with large scatter (? =-40.34 and $s_?$ 62.89). On the other hand, the correlation of Sumith et al [58] over-predicts data (? = 92 %), also with relatively large scatter ($s_?$ = 86.34 %).

It must be noted that the two data sets of Bao et al [39] and Baird et al [60] were obtained under different experimental conditions. Hence, the discrepancies in the predictions of the correlations are not alarming as can be expected.

Bao et al [39] used wall heat flux 3-58 kW/m$^2$ while Baird et al [60] operated at higher heat flux range [15-110 kW/m$^2$]. The effect of the heat flux was also previously mentioned by Baird et al [60].

The effect of quality on the accuracy of the predictions of some of the depicted correlations is depicted in Figures 4.30 through 4.35. The reason and justification for the depictions were given in the previous section. As noted, the correlation of Kandlikar and Steinke [21, 22, 68], under predict the data consistently at high quality where annular-dispersed flow regime is likely, and as shown large scatter at low qualities. The correlation of Chen [17], Gungor and Winterton [15], and Steiner and Taborek [27], depicted in Figures 4.32, 4.34 and 4.36, respectively, show a relatively uniform scatter over the entire range of quality. The correlation of Shah [18] (Figure 4.33 has a fairly similar average discrepancy with average experimental data for all x range. The correlation of Klimenko [11, 12] does poorly.

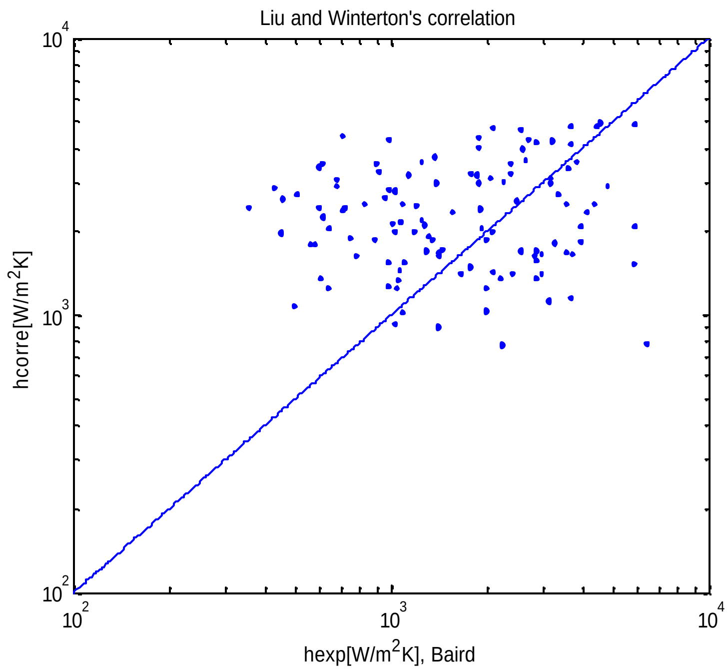


Figure 4.19: Comparison between the experimental data of Baird et al. [60] and the correlation of Liu and Winterton [20]

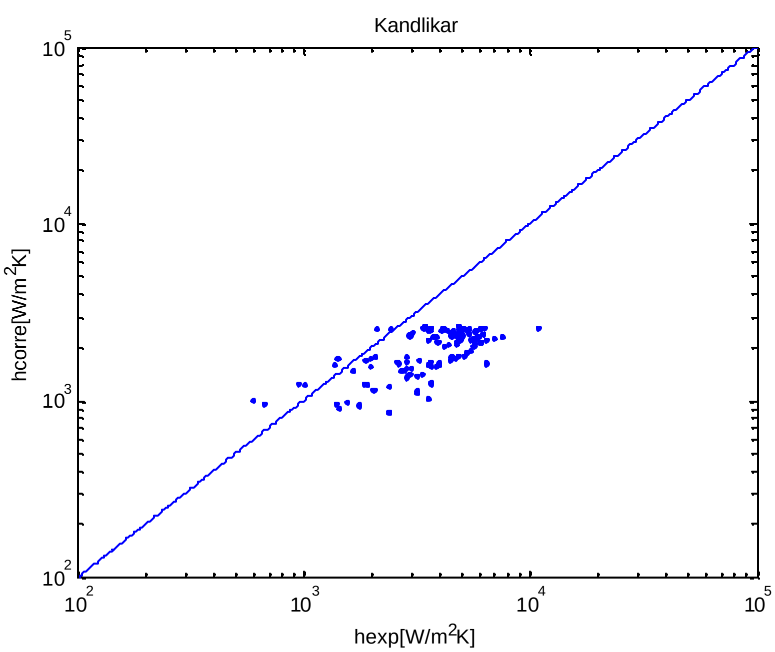


Figure 4.20: Comparison between the experimental data of Baird et al. [60] and the correlation of Kandlikar [21, 22].

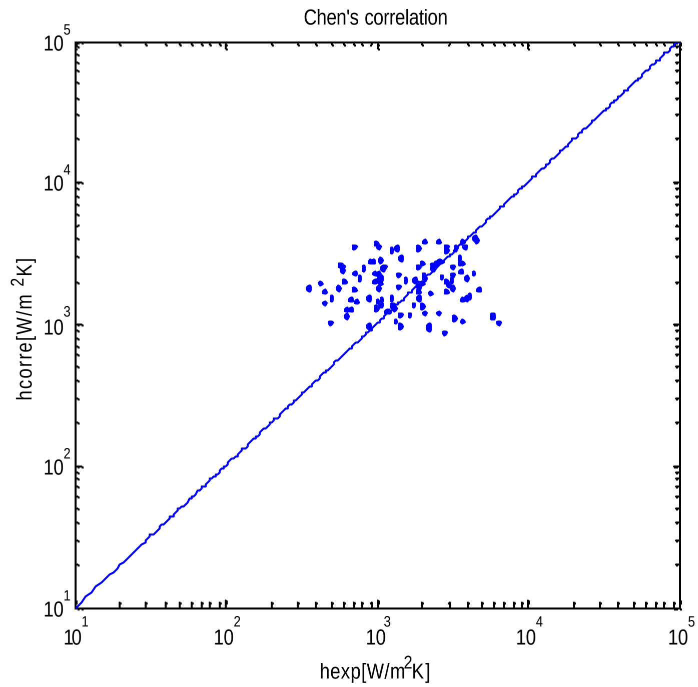


Figure 4.21: Comparison between the experimental data of Baird et al. [60] and the correlation of Chen [17]

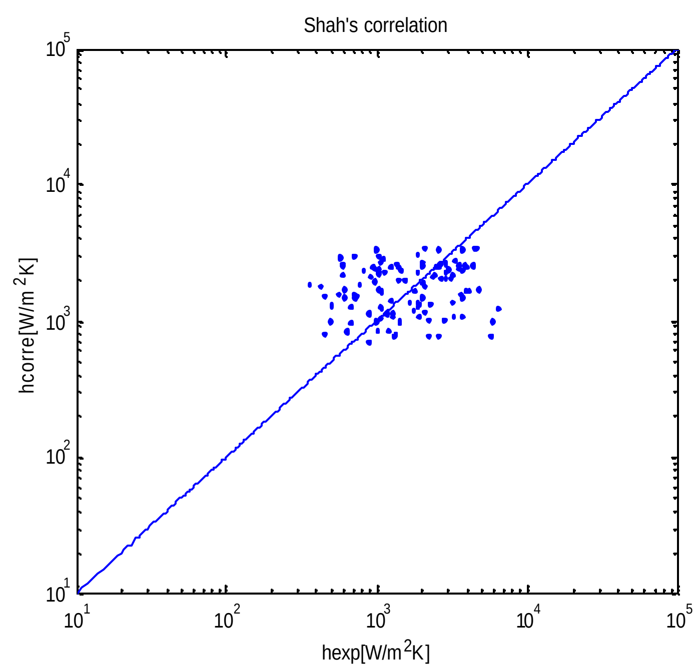


Figure 4.22: Comparison between the experimental data of Baird et al. [60] and the correlation of Shah [18].

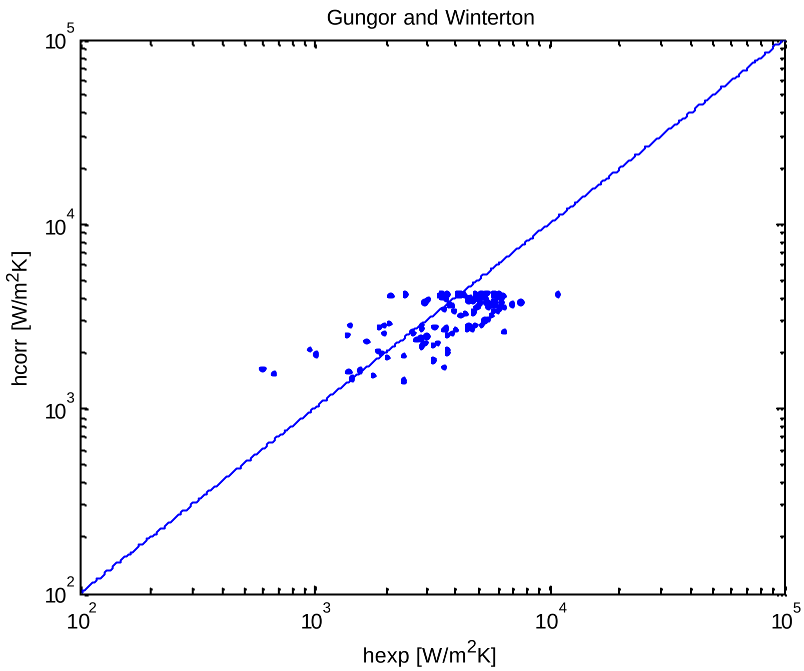


Figure 4.23: Comparison between the experimental data of Baird et al. [60] and the correlation of Gungor and Winterton [15].

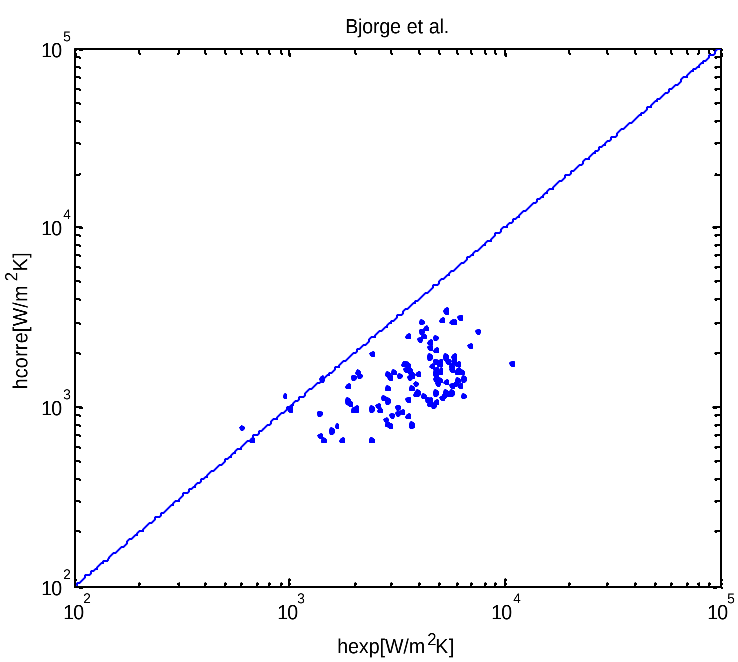


Figure 4.24: Comparison between the experimental data of Baird et al. [60] and the correlation of Bjorge et al [19]

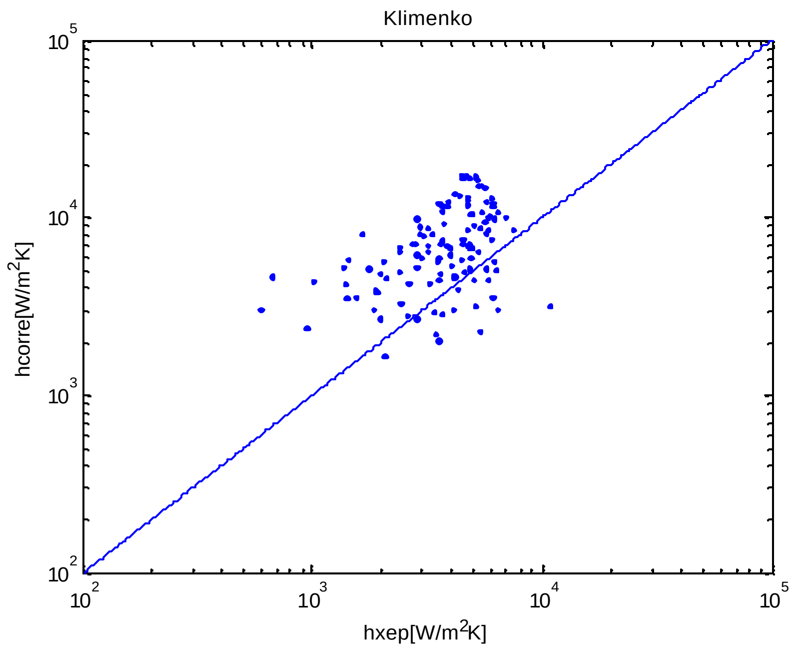


Figure 4.25: Comparison between the experimental data of Baird et al. [60] and the correlation of Klimenko [11, 12]

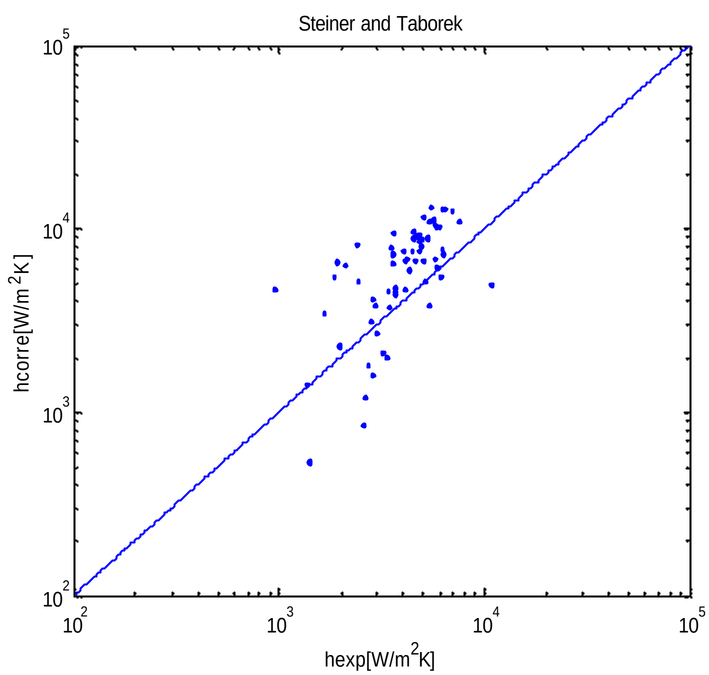


Figure 4.26: Comparison between the experimental data of Baird et al. [60] and the correlation of Steiner and Taborek [27]

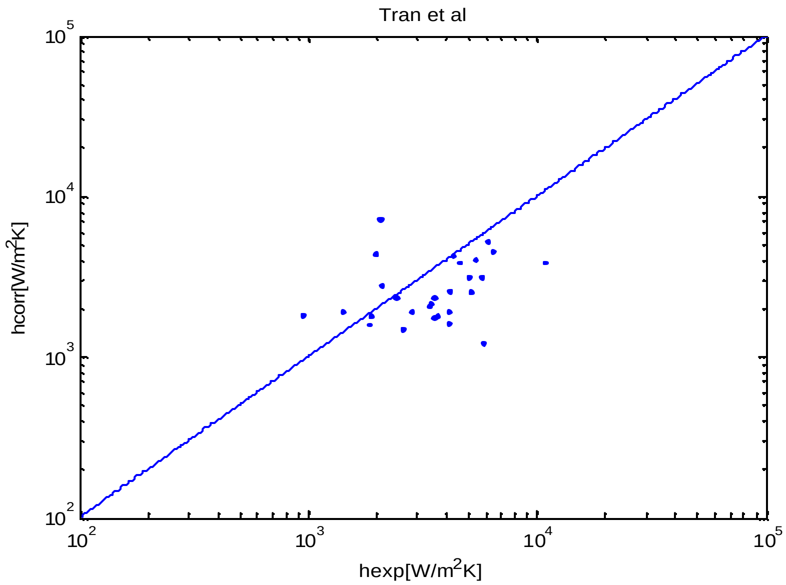


Figure 4.27: Comparison between the experimental data of Baird et al. [60] and the correlation of Tran et al [34]

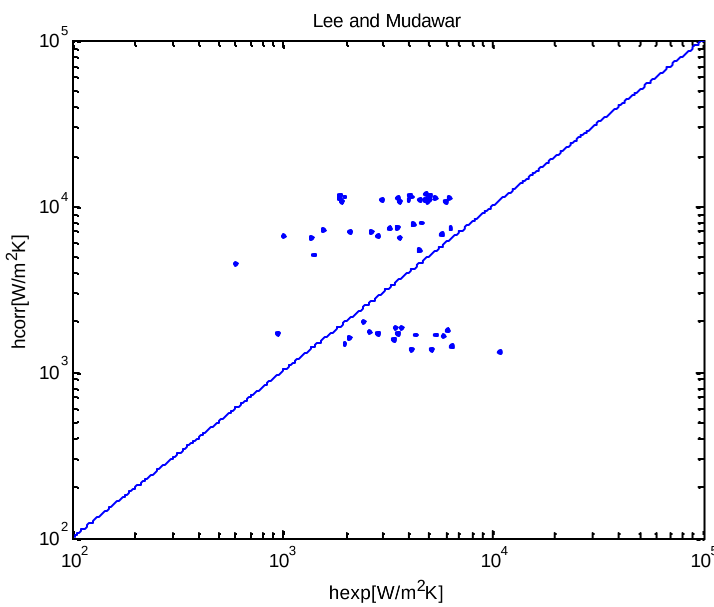


Figure 4.28: Comparison between the experimental data of Baird et al. [60] and the correlation of Lee and Mudawar [37]

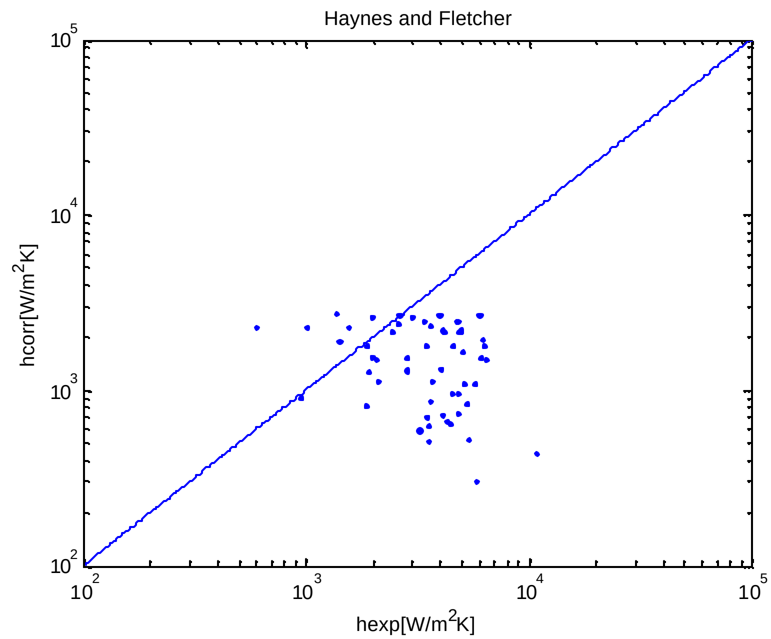


Figure 4.29: Comparison between the experimental data of Baird et al. [60] and the correlation of Haynes and Fletcher [52]

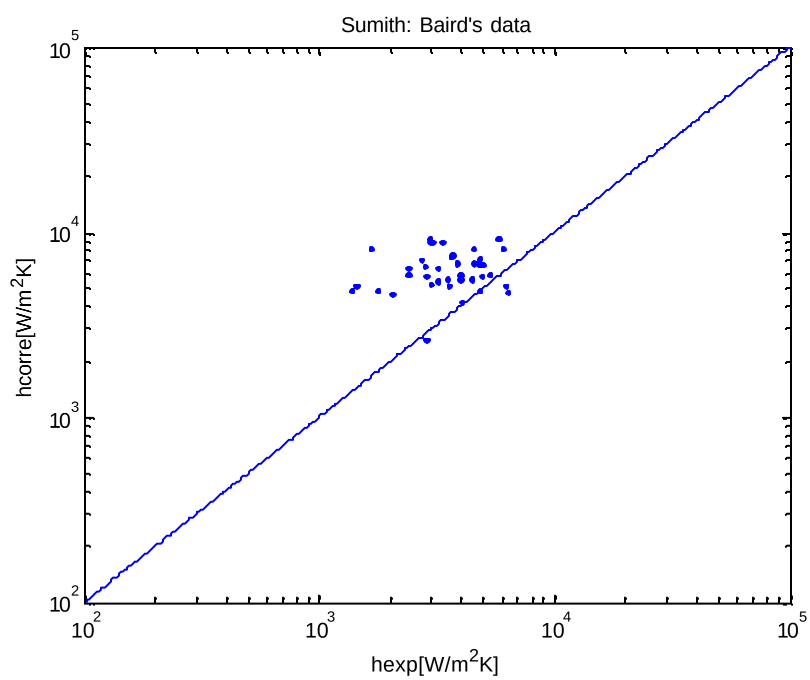


Figure 4.30: Comparison between the experimental data of Baird et al. [60] and the correlation of Sumith et al [58]

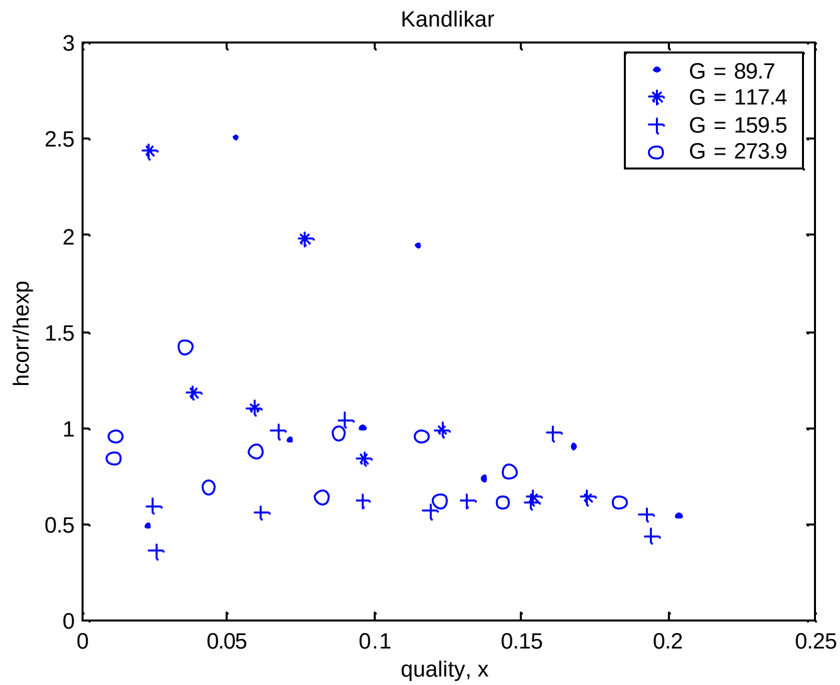


Figure 4.31: Comparison between the experimental data of Baird et al. [60]and the correlation of Kandlikar [21, 22]: Effects of quality

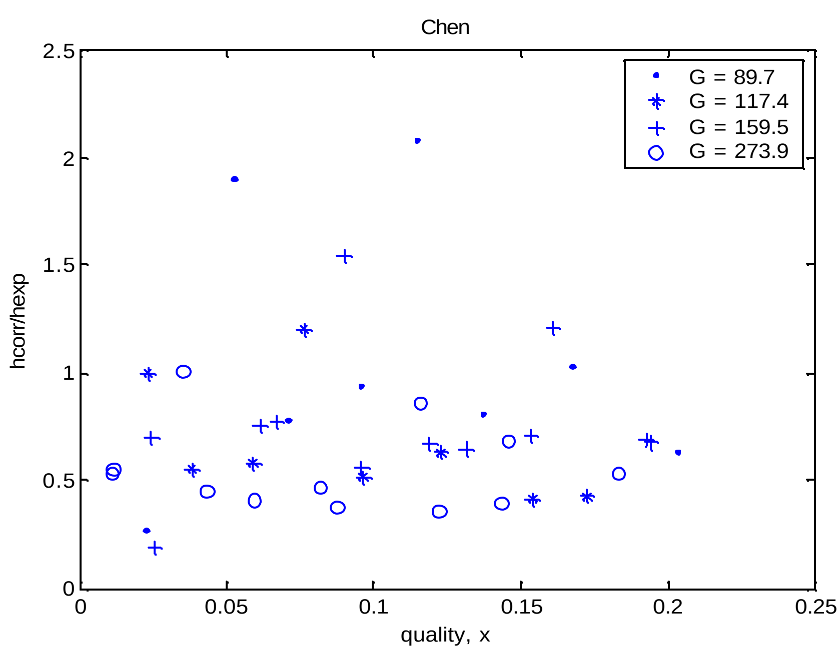


Figure 4.32: Comparison between the experimental data of Baird et al. [60]and the correlation of Chen [17]: Effects of quality

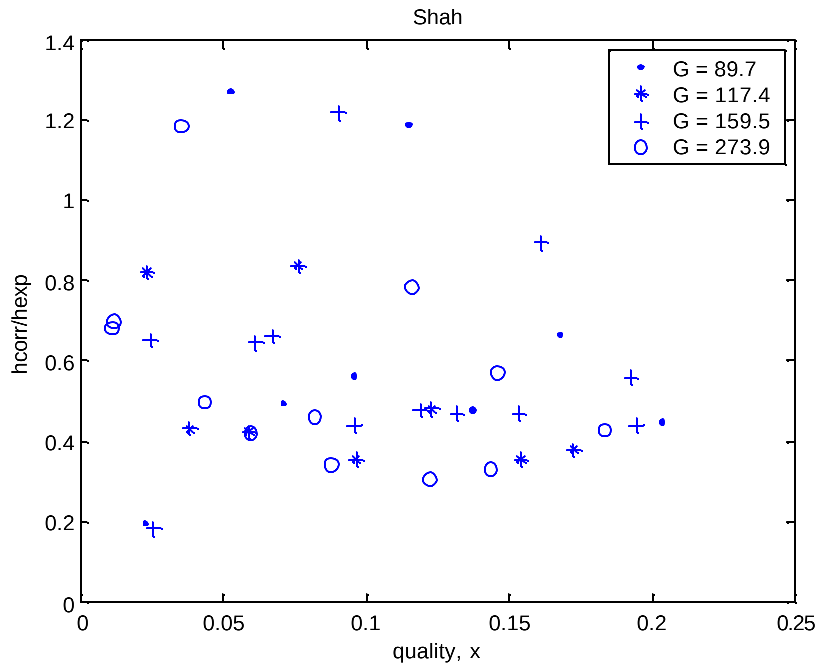


Figure 4.33: Comparison between the experimental data of Baird et al. [60]and the correlation of Shah [18]: Effects of quality

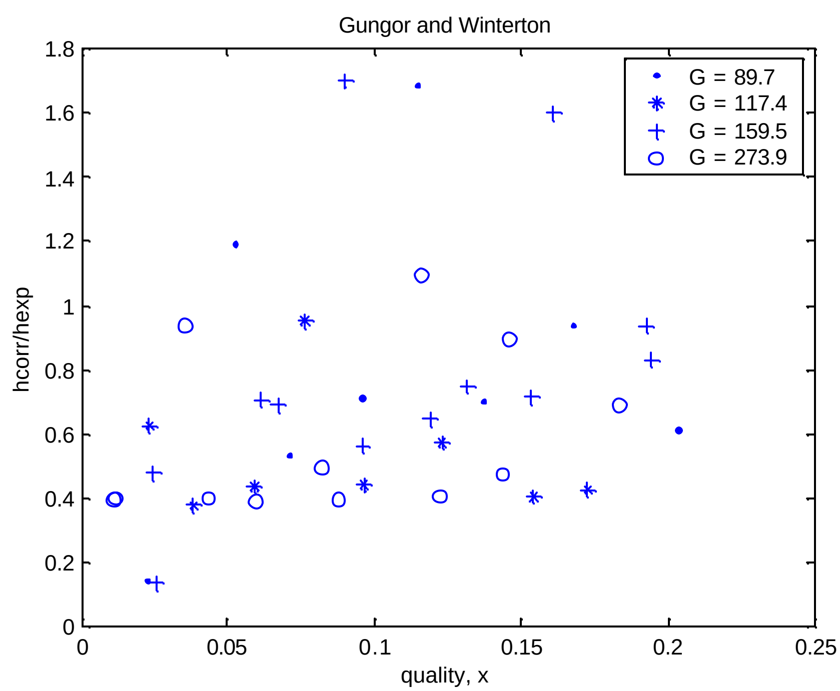


Figure 4.34: Comparison between the experimental data of Baird et al. [60] and the correlation of Gungor and Winterton [15]: Effects of quality

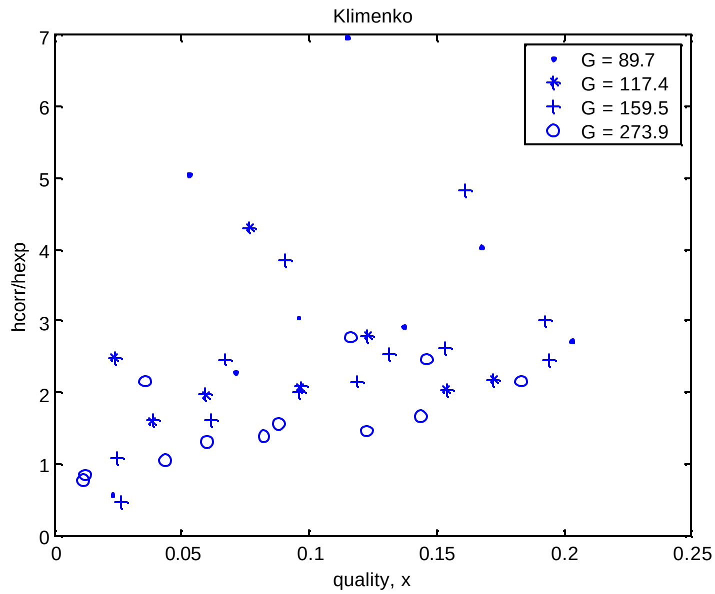


Figure 4.35: Comparison between the experimental data of Baird et al. [60]and the correlation of Klimenko [11, 12]: Effects of quality

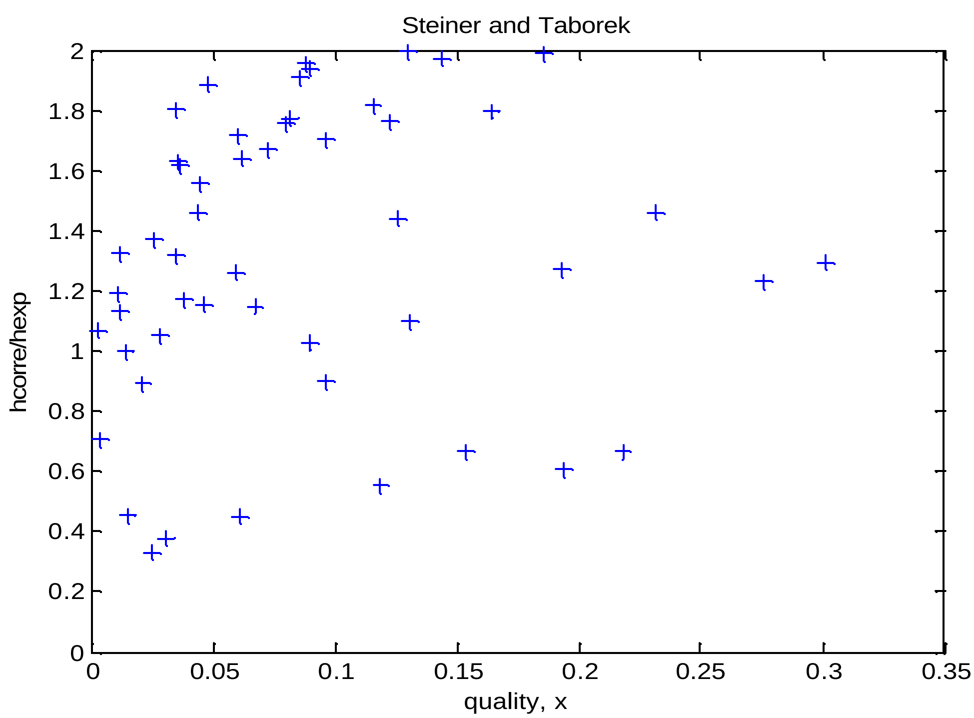


Figure 4.36: Comparison between the experimental data of Baird et al. [60]and the correlation of Steiner and Taborek [27]: Effects of quality

## 4.4 The Experimental Data of Yan and Lin [61]

The data of Yan and Lin [61] are compared with the predictions of all the aforementioned correlations in Figures 4.37 through 4.46. The effect of quality, x, on the predictions of several of these correlations, furthermore, is depicted in Figures 4.47 through 4.52. The statistical parameters $\bar{x}$ and s ? for all these comparisons are summarized in Table 4.3.

As noted, with the exception of the correlation Gungor and Winterton [15], depicted in Figure 4.41, and to a lesser extent the correlation of Lee and Mudawar [37], depicted in Figure 4.45, all the correlations disagree with the data and/or display significant scatter. The correlation of Gungor and Winterton predicts the data quite well, although a distinct effect of mass flux can be seen (Figure 4.41). The rather distinct effect of mass flux can indeed be noted in the data of Yan and Lin [61], as well as in most of the comparison with various correlations depicted in the section. Figure 4.50 provides very interesting insight into the data of Yan and Lin [61], as predicted by the correlation of Gungor and Winterton. As noted, for the data points with G = 100 kg/m$^2$s, $\frac{h_{corr}}{h_{\exp}} \approx 0.78$ is predicted for all qualities. For G = 200 kg/m$^2$s, furthermore, $\frac{h_{corr}}{h_{\exp}} \approx 1.18$ is predicted for all qualities. The $\frac{h_{corr}}{h_{\exp}} \approx$ constant trends are of course consistent with Figure 4.41, and indicates an interesting coincidence

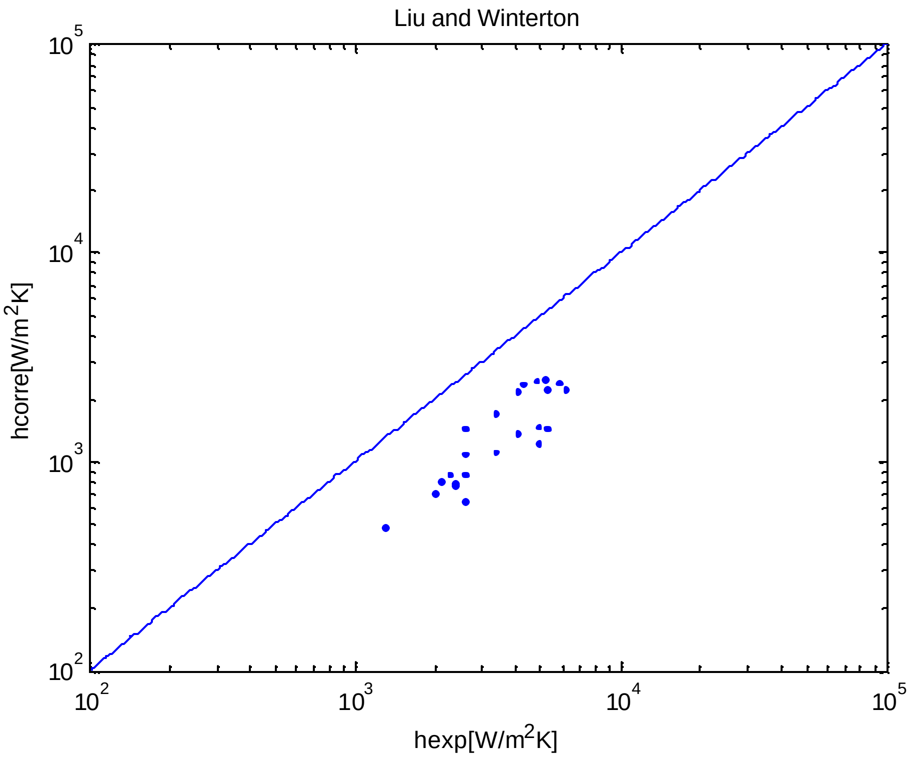


Figure 4.37: Comparison between the experimental data of Yan and Lin [61] and the correlation of Liu and Winterton [20]

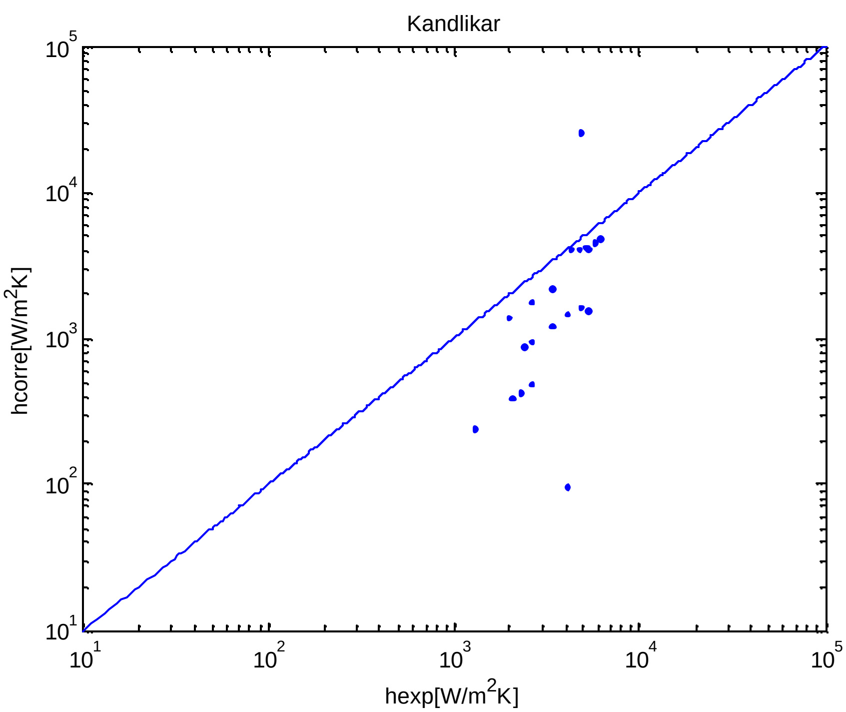


Figure 4.38: Comparison between the experimental data of Yan and Lin [61] and the correlation of Kandlikar [21, 22]

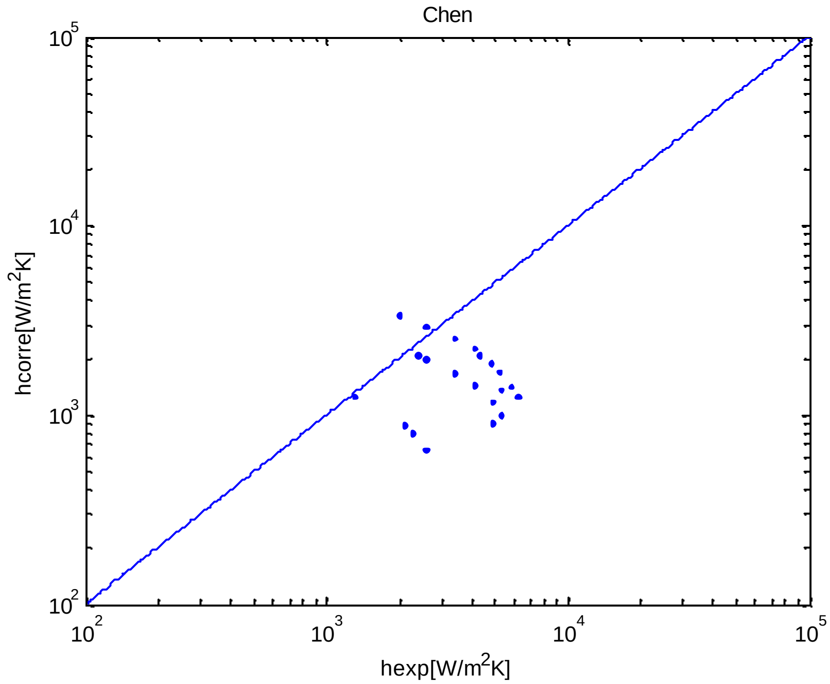


Figure 4.39: Comparison between the experimental data of Yan and Lin [61] and the correlation of Chen [17]

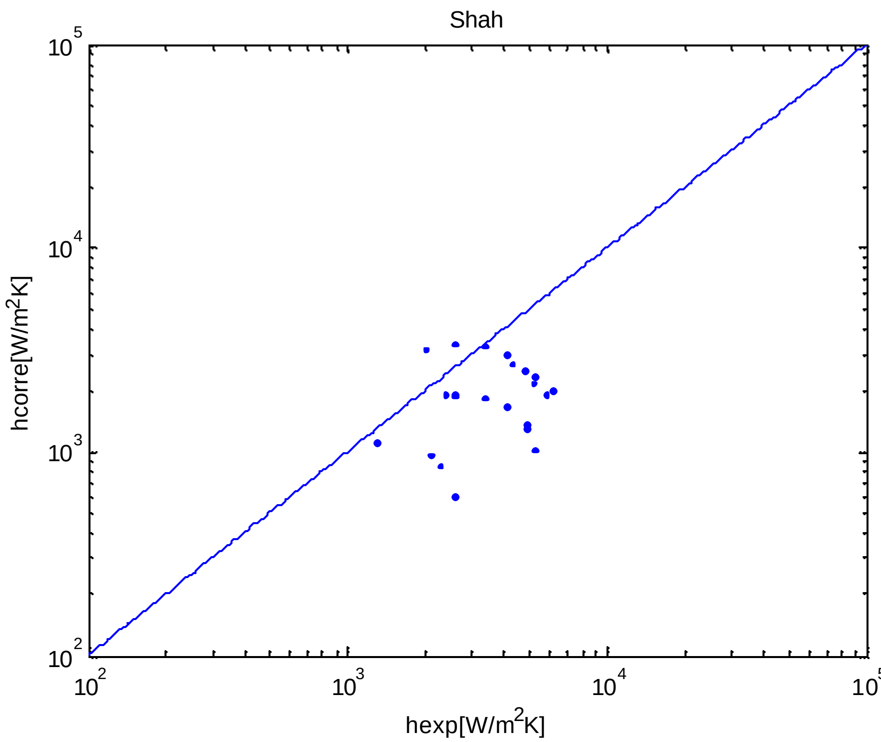


Figure 4.40: Comparison between the experimental data of Yan and Lin [61] and the correlation of Shah [18]

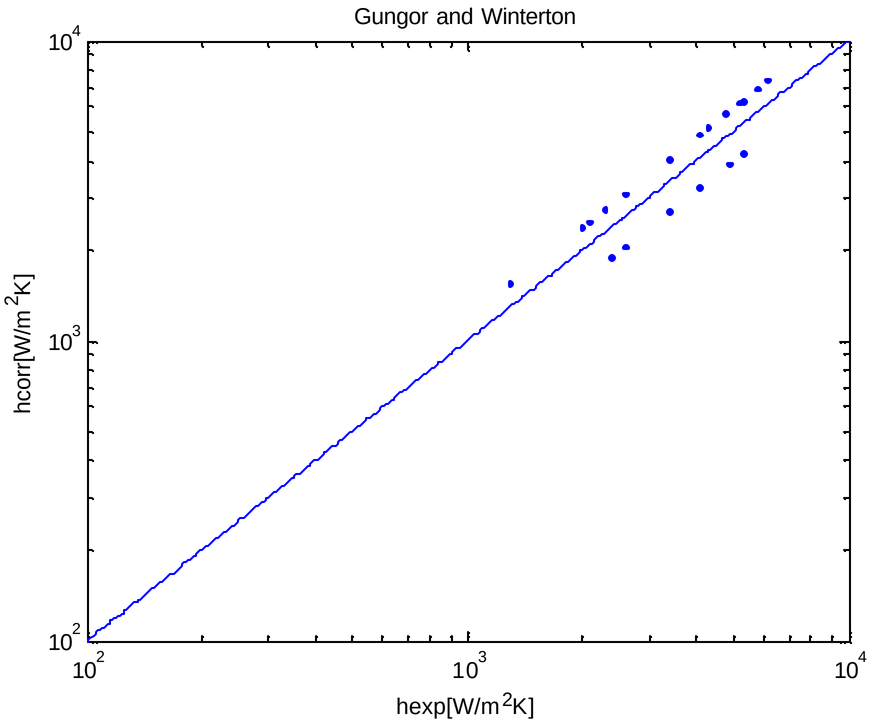

Figure 4.41: Comparison between the experimental data of Yan and Lin [61] and the correlation of Gungor and Winterton [15]

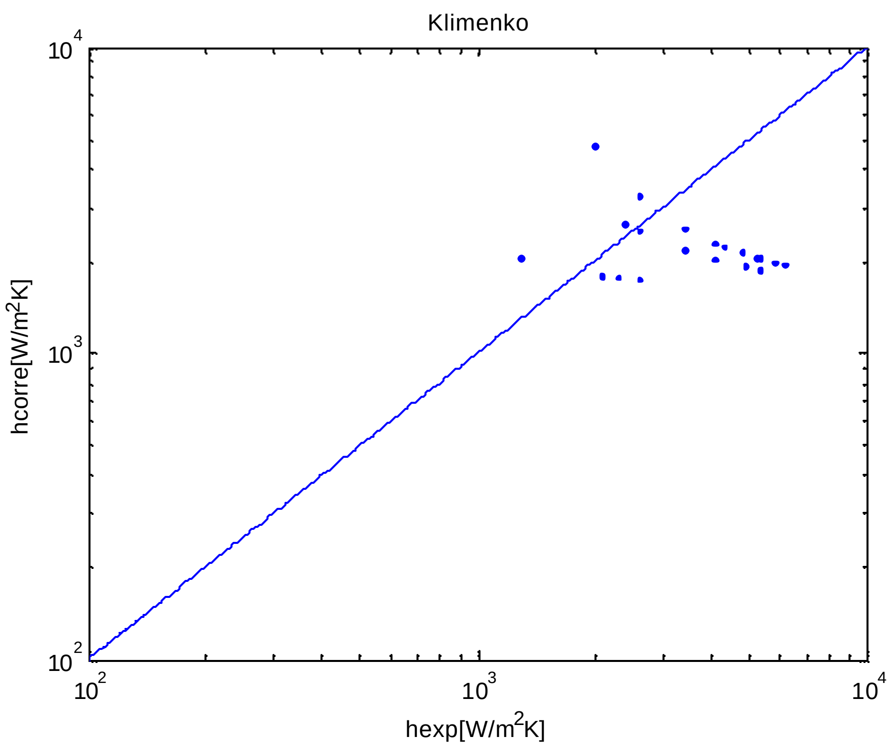

Figure 4.42: Comparison between the experimental data of Yan and Lin [61] and the correlation of Klimenko [11, 12]

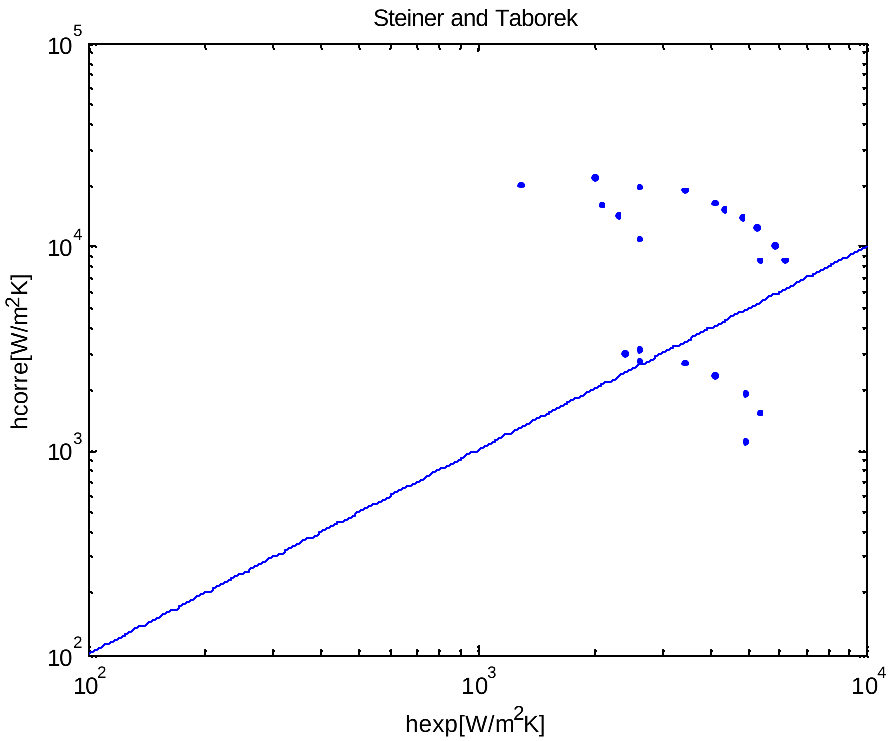

Figure 4.43: Comparison between the experimental data of Yan and Lin [61] and the correlation of Steiner and Taborek [27]

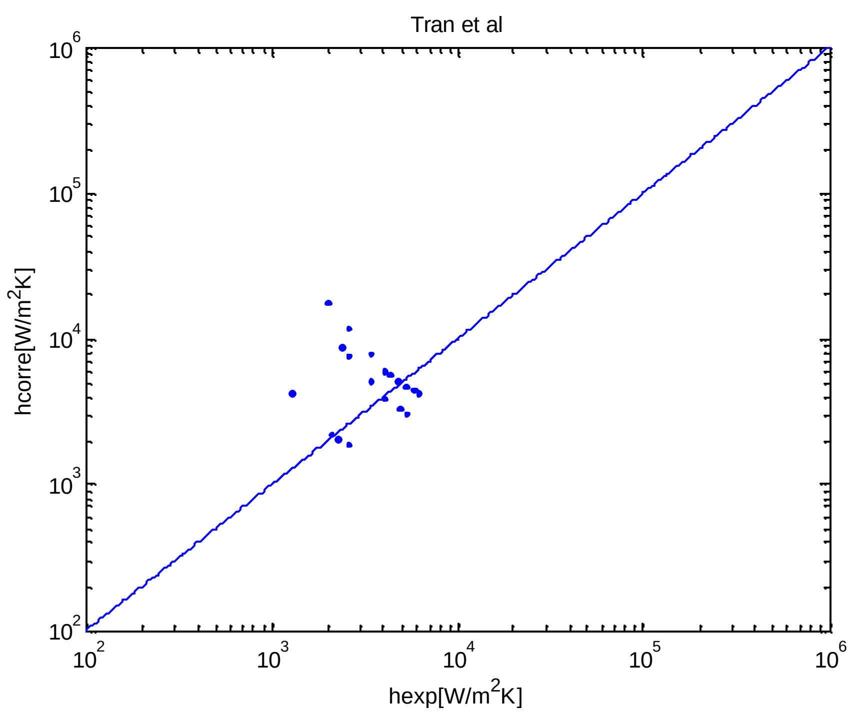

Figure 4.44: Comparison between the experimental data of Yan and Lin [61] and the correlation of Tran et al. [34]

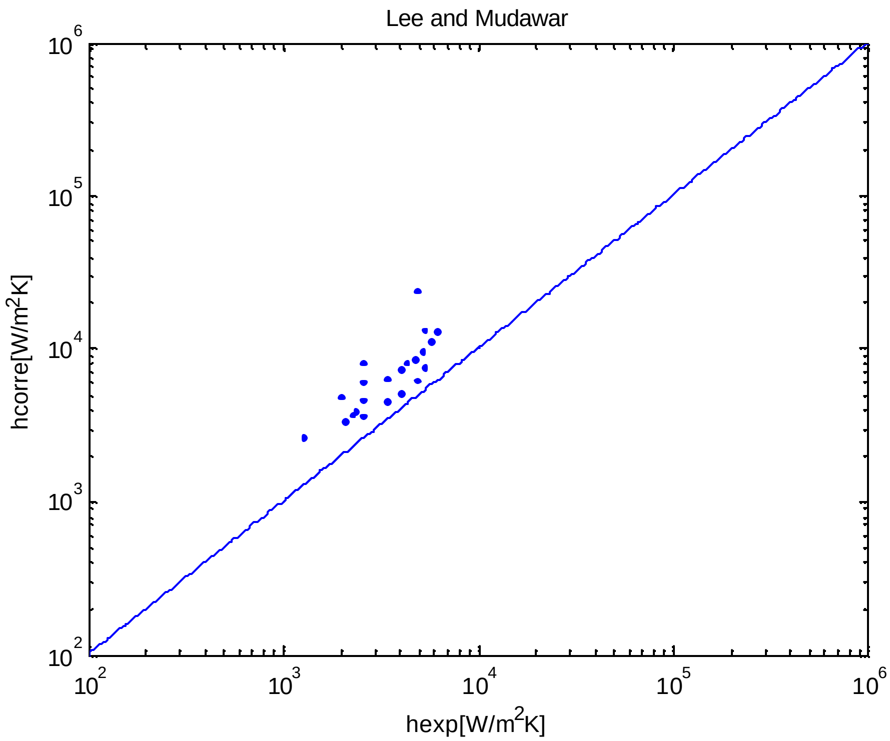


Figure 4.45: Comparison between the experimental data of Yan and Lin [61] and the correlation of Lee and Mudawar [37]

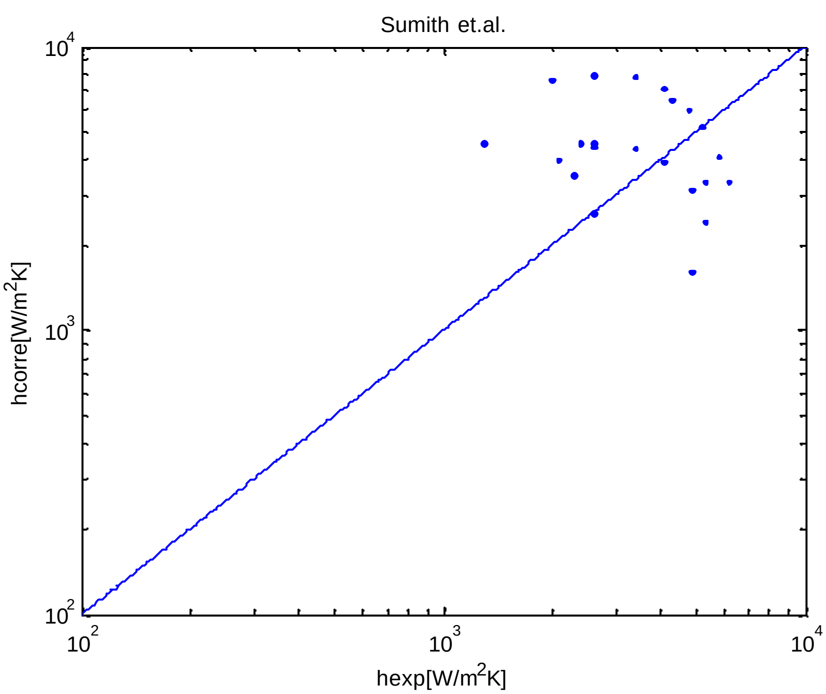


Figure 4.46: Comparison between the experimental data of Yan and Lin [61] and the correlation of Sumith et al. [58]

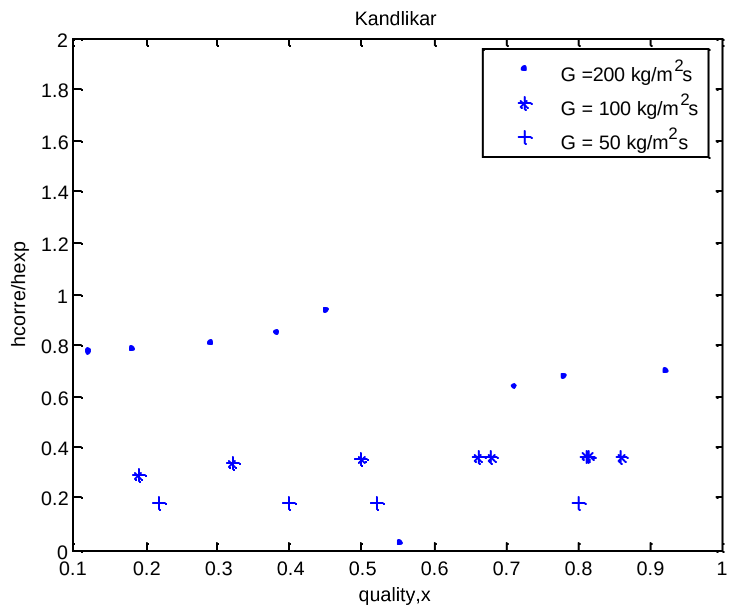


Figure 4.47: Comparison between the experimental data of Yan and Lin [61]and the correlation of Kandlikar [21, 22]: Effects of quality

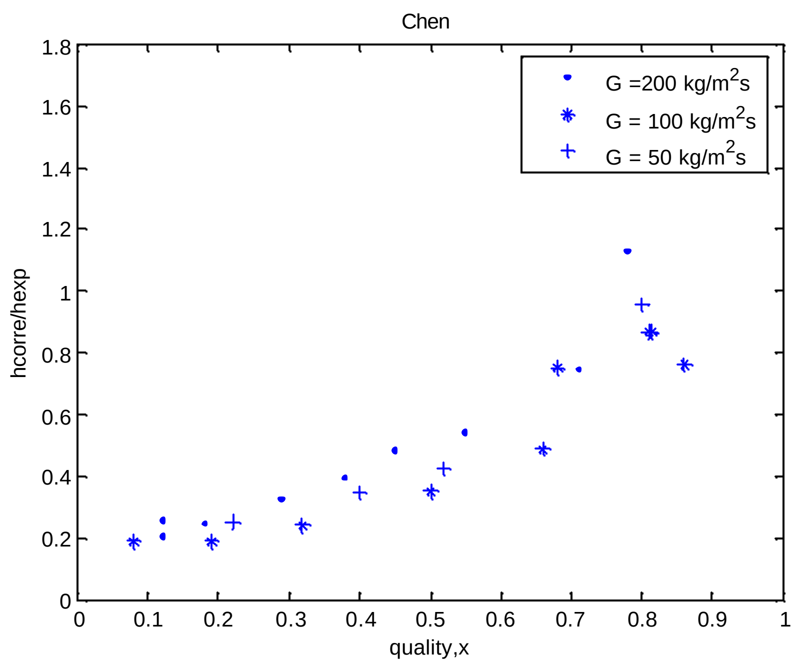


Figure 4.48: Comparison between the experimental data of Yan and Lin [61]and the correlation of Chen [17]: Effects of quality

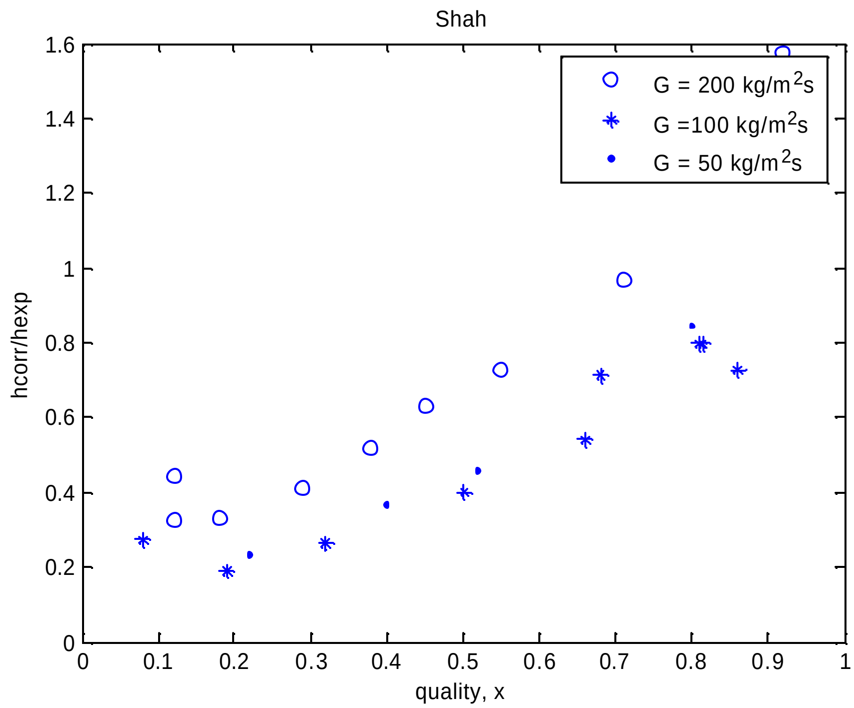


Figure 4.49: Comparison between the experimental data of Yan and Lin [61]and the correlation of Shah [18]: Effects of quality

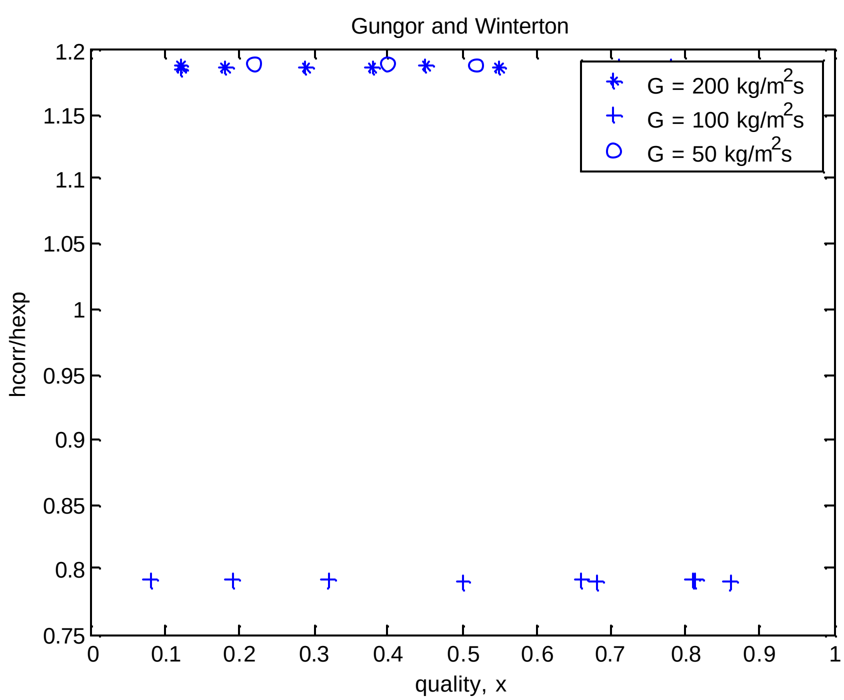


Figure 4.50: Comparison between the experimental data of Yan and Lin [61]and the correlation of Gungor and Winterton [15]: Effects of quality

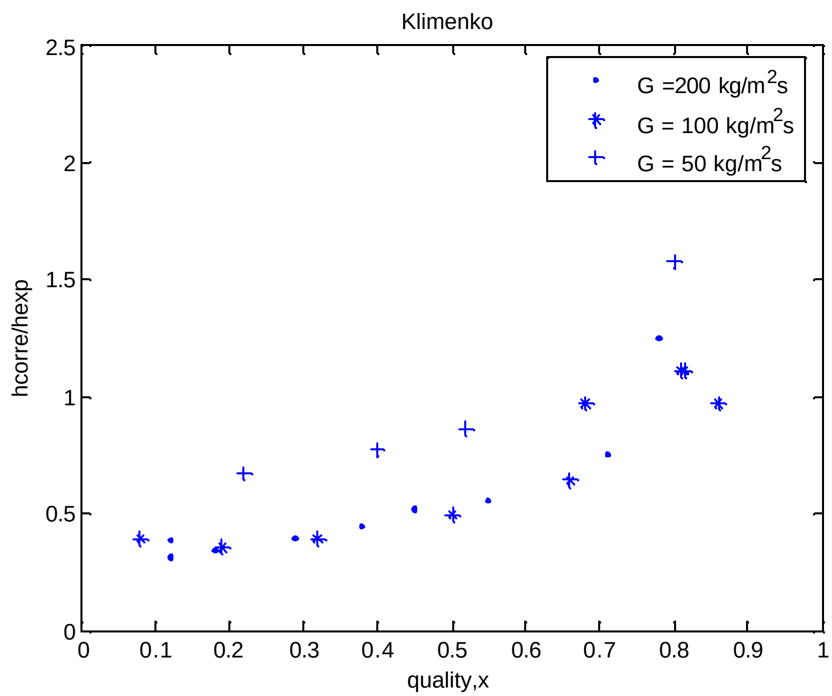


Figure 4.51: Comparison between the experimental data of Yan and Lin [61] and the correlation of Klimenko [11, 12]: Effects of quality

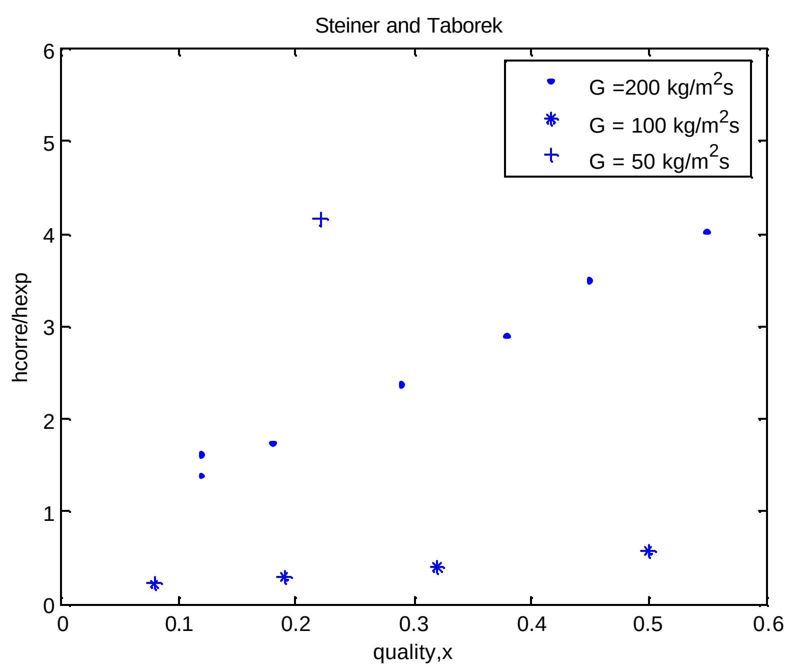


Figure 4.52: Comparison between the experimental of Yan and Lin [61] data and the correlation of Steiner and Taborek [27]: Effects of quality

## 4.5: Discussion

In the previous three sections various correlations for forced-flow boiling were compared with three separate experimental data, from three different research groups, all representing forced-flow boiling in mini and micro-channels. These comparisons lead to the following general observations.

1. Forced-flow boiling heat transfer coefficients in mini-channels can be predicted within the correct order of magnitude by several macro-scale correlations, including the correlations of Gungor and Winterton [15], Chen [17], Steiner and Taborek [27], and Liu and Winterton [20].
2. Among the tested correlations, the correlations of Gungor and Winterton [15], and the correlation of Kandlikar [21, 22] as modified by Kandlikar and Steinke [68], appear to provide the closet estimates of the experimental data.
3. The examination of the effect of quality on the $\frac{h_{corr}}{h_{\exp}}$ values for various correlations shows that the performance of some of the correlations (e.g. Kandlikar [21, 22] and Gungor and Winterton [15]) depends strongly on the flow boiling regimes, For example the correlation of Kandlikar [21, 22] appears to do better at low qualities where nucleate boiling is predominant. In the comparison, the correlation of performs rather poorly at high qualities where annular dispersed flow regime and forced convective evaporation predominates.
4. The correlations that have been developed based on one set of data, even though the data were obtained with mini channels ( Tran et al [34], Lee and Mudawar [37]), performed poorly. This observation confirms that empirical correlations for

forced flow boiling in mini and micro-channels must be based on an extensive data base.

Table 4.1: Statistical parameters for data of Bao et al [39]

| Summary of the statistical parameters related to the comparison between the data of Bao et. al [39] and various correlations. | | |
|---|---|---|
| | (%) $\bar{x}$ | s? (%) |
| Liu and Winterton [20] | -57.38% | 39.20% |
| Kandlikar [21,22] | -14.30% | 31% |
| Chen [17] | -52.40% | 22.90% |
| Shah [18] | -140% | 93% |
| Gungor and Winterton [15] | -6.44% | 17% |
| Bjorge et al [19] | 26.10% | 28.25% |
| Klimenko [11,12] | 33.93% | 33.99% |
| Steiner and Taborek [27] | -3.90% | 81.80% |
| Tran et al [34] | 88.40% | 1.60% |
| Lee and Mudawar [37] | -70% | 23.22% |
| Hayes and Fletcher [52] | -37.40% | 15.34% |
| Sumith et. al [58] | 128% | 28.70% |

Table 4.2: Statistical parameters for data of Baird et al [60]

| Summary of the statistical parameters related to the comparison between the data of Baird et al [60] and various correlations. | | |
|---|---|---|
| | $\bar{x}$ (%) | s? (%) |
| | | |
| Liu and Winterton [20] | -44.09% | 22% |
| | | |
| Kandlikar [21,22] | -23.40% | 42.00% |
| | | |
| Chen [17] | -41.30% | 29.90% |
| | | |
| Shah [18] | -49.30% | 21.10% |
| | | |
| Gungor & Winterton [15] | -11% | 39.67% |
| | | |
| Bjorge [19] | -64.90% | 20% |
| | | |
| Klimenko [11,12] | 105% | 106% |
| | | |
| Steiner & Taborek [27] | 60% | 79% |
| | | |
| Tran et al [34] | -11% | 66.80% |
| | | |
| Lee and Mudawar [37] | 125.00% | 181.00% |
| | | |
| Hayes and Fletcher [52] | -40% | 62.80% |
| | | |
| Sumith et. al [58] | 92% | 86.34% |

Table 4.3: Statistical parameters for data of Yan and Lin [61]

| Summary of the statistical parameters related to the comparison between the data of Yan and Lin [61] and various correlations. | | |
|---|---|---|
| | $\bar{x}$ (%) | s? (%) |
| | | |
| Liu and Winterton [20] | -61.84% | 9% |
| | | |
| Kandlikar [21,22] | -52.22% | 27.10% |
| | | |
| Chen [17] | -44.90% | 37.28% |
| | | |
| Shah [18] | -39.95% | 34.32% |
| | | |
| Gungor & Winterton [15] | 105% | 39.40% |
| | | |
| Klimenko [11,12] | -24% | 48% |
| | | |
| Steiner & Taborek [27] | 76% | 145% |
| | | |
| Tran et al [34] | 100% | 190.00% |
| | | |
| Lee and Mudawar [37] | 95.20% | 48.10% |
| | | |
| | | |
| Sumith et. al [58] | 53% | 94.00% |

# CHAPTER 5

## Conclusions and Recommendations

### 5.1 Concluding Remarks

Forced flow boiling in mini channels was the subject of this research. Mini and micro-channel networks can provide extremely large volumetric interfacial area concentrations. They can thus sustain enormous volumetric transfer rates. The advances in micro manufacturing has now made the manufacture of mini and micro-channel networks feasible at reasonable cost and effort. As a result, the applications of mini and micro-channels in advanced, high performance systems will undoubtedly accelerate in the future.

At present, the most important applications of mini and micro-channel networks is in miniature heat exchangers, refrigeration systems and the heat sinks of performance electronic, magnetic and infrared systems. The most efficient heat transfer method in these systems can be achieved by forced flow nucleate boiling in a mini or micro-channel.

The applicability of several widely-referenced correlations for forced flow boiling to mini and micro-channel data was thus examined in this study. Three sets of experimental data, (Bao et al [39]; Baird et al [60]; Yan and Lin [61]). The tested correlations included those proposed by Liu and Winterton [20], Chen [17]; Kandlikar [21, 22]; Gungor and Winterton [15]; Bjorge et al [19]; Klimenko [11, 12], Steiner and Taborek [27]; Tran et al [34]; Lee and Mudawar [37]; Haynes and Fletcher [52]; and Sumith et al [58]. The investigation is novel in its breadth. Previously published studies are either focused on the development of a correlation based on single set of mini channel experimental data (Tran et al [34]; Lee and Mudawar [37]; Sumith et al [58]), or are aimed at the comparison and validation of a specific correlation against data from several sources, (Kandlikar and Steinke [68]).

The following conclusions can be made on the results of this study:

1. The performance of each correlation varies from data set to set, and none of the tested correlations provides a reasonably accurate prediction of all the three data sets.
2. Overall, the correlations of Gungor and Winterton [15] and Kandlikar and Steinke [68] provide the closest agreement with data. The correlation of Gungor and Winterton [15], furthermore leads to relatively small scatter.
3. The aforementioned correlations provide a reasonable estimate of the experimental data, with a better than average order of magnitude
4. Given that the utilized experimental data all represented mini channels, ($D_h$ = 1 mm), the comparison provides a little insight about micro-channels ($D_h$ = 100 μm). The above conclusions, therefore do not apply to micro-channels

### 5.2: Recommendations for Future Research

Based on this investigation, the following follow-up studies are recommended.

1. The correlation-data comparisons reported in this study were based on micro channel data sets. More experimental data dealing with mini channel boiling are available, however, (e.g. Lee and Mudawar [37]). It is therefore recommended that more experimental data be collected and included in the data bank for comparison with correlations. Data representing various refrigerants, in particular, would be useful.
2. Flow boiling data representing micro-channels is rare, and reported studies are virtually all based on multi-channel system where various modes of instability and oscillations are likely. Experiments where forced flow boiling heat transfer in micro-channels is measured, are highly recommended.

## Appendix A: EES codes for evaluated correlations

### A.1

Liu and Winterton

$corr1_{sat}$

$D = 0.00195$

$q = \sqrt{(F \cdot h_l \cdot del_{Tb})^2 + (S \cdot h_{pool} \cdot del_{Ts})^2}$

$h_l = 0.023 \cdot Re_l^{0.8} \cdot Pr_l^{0.4} \cdot \frac{k_l}{D}$ THIS IS FROM DITTUS-BOELTER

$Re_l = \frac{G \cdot D}{miu_l}$

$Pr_l = \mathbf{Pr}('R11', P=P, x=0)$

$k_l = \mathbf{k}('R11', P=P, x=0)$

$h_f = \mathbf{h}('R11', P=P, x=0)$

$h_g = \mathbf{h}('R11', P=P, x=1)$

$h_{fg} = h_g - h_f$

$miu_l = \mathbf{Visc}('R11', P=P, x=0)$

$del_{Tb} = Tw - Tb$

$del_{Ts} = Tw - Ts$

$Ts = \mathbf{T_{sat}}('R11', P=P)$

$F = \left[1 + x \cdot Pr_l \cdot \left(\frac{\rho_l}{\rho_g} - 1\right)\right]^{0.35}$

$S = \frac{1}{1 + 0.055 \cdot F^{0.1} \cdot Re_l^{0.16}}$

Since the temperature difference is know we will do the following

$h_{pool} = 55 \cdot P_r^{0.12} \cdot PR2 \cdot M^{-0.5} \cdot qp^{0.67}$

$PR = \mathbf{log}(P_r)$

$PR1 = -PR$

$PR2 = PR1^{-0.55}$

$q = qp$

$P_r = \frac{P}{P_{cr}}$

$P_{cr} = 0.442 \cdot 10^7$ $P_r$ is the reduced pressure given by Absolute Press/Critical Pressure

$M = 137.4$

$\rho_g = \rho('R11', P=P, x=1)$

$\rho_l = \rho('R11', P=P, x=0)$

$h_{tp} = \frac{q}{del_{Ts}}$

A.2

```
"Correlation of Kandlikar"
" For this correlation the h_tp is the larger between h_NBD and h_CBD"
" for R11 the value of"
PROCEDURE lamturb(Re_l,k_l,D,Pr_l,f,:h_l)
if Re_l < 1600 THEN
h_l = (k_l/D)*4.36
else
h_l = ((Re_l-1000)*Pr_l*(f/2)*(k_l/D))/(1+12.7*(Pr_l^(2/3)-1)*(f/2)^(0.5))
ENDif
F_fl =1.30
D=0.00195
" Co is the convection number"
Co = (((rho_g/rho_l)^0.5)*(((1-x)/x))^(0.8))
h_NBD =((0.6683*(Co^(-.2))*h_l1)*(1-x)^0.8)+ ((1058*Bo_N^(0.7))*F_fl*h_l1*(1-x)^0.8)
h_CBD = (1.1360*(Co^(-0.9))*(1-x)^(0.8)*h_l1) +((667.2*Bo_C^(0.7))*(1-x)^(0.8)*F_fl*h_l1)
h_tp = max(h_NBD,h_CBD)
Re_l = (G*D)/miu_l
call lamturb(Re_l,k_l,D,Pr_l,f:h_l)
"h_l = 0.023*Re_l^(0.8)*(Pr_l^0.4)*(k_l/D)"
"h_l1= ((Re_l-1000)*Pr_l*(f/2)*(k_l/D))/(1+12.7*(Pr_l^(2/3)-1)*(f/2)^(0.5))"
f = (1.58*ln(Re_l)-3.28)^(-2)
Bo_N= (q_N/(G*h_fg))
q_N = h_NBD*(del_Ts)
q_C = h_CBD*(del_Ts)

Bo_C= q_C/(G*h_fg)

del_Ts = (T_w -Ts)

Ts = t_sat(R11,p=P)

k_l= conductivity(R11,p=P,x=0)

Pr_l =  prandtl(R11,p=P,x=0)

rho_l = density(R11,p=P,x=0)

rho_g = density(R11,p=P,x=1)

miu_g = viscosity(R11,p=P,x=1)

miu_l = viscosity(R11,p=P,x=0)
h_f = enthalpy(R11,p=P,x=0)

h_g = enthalpy(R11,p=P,x=1)

h_fg = (h_g-h_f)

cp_l = specheat(R11,p=P,x=0)

Ps = p_sat(R11,t=T_w)

M =molarmass(R11)
```

A.3

Chen's correlation

$D = 0.00195$

$$Re_l = \frac{G \cdot (1 - x) \cdot D}{miu_l}$$

$$X_{tt} = \left[\frac{1 - x}{x}\right]^{0.9} \cdot \left[\frac{\rho_g}{\rho_l}\right]^{0.5} \cdot \left[\frac{miu_l}{miu_g}\right]^{0.1}$$

$$F = \left[\frac{1}{X_{tt}} + 0.213\right]^{0.736}$$

$$Re_{tp} = Re_l \cdot F^{1.25}$$

$$S = \frac{1}{1 + 0.00000253 \cdot Re_{tp}^{1.17}}$$

$$h_l = 0.023 \cdot Re_l^{0.8} \cdot Pr_l^{0.4} \cdot \frac{k_l}{D}$$

$del_{Ts} = T_w - T_s$ this is delta $T_{sat}$

$del_{Ps} = Ps - P$ this is delta $P_{sat}$

$$h_{pool} = 0.00122 \cdot \frac{k_l^{0.79} \cdot cp_l^{0.45} \cdot \rho_l^{0.49}}{\sigma^{0.5} \cdot miu_l^{0.29} \cdot h_{fg}^{0.24} \cdot \rho_g^{0.24}} \cdot del_{Ts}^{0.24} \cdot del_{Ps}^{0.75}$$

$h_{tp} = h_{pool} \cdot S + h_l \cdot F$

$k_l = \mathbf{k}$ ( 'R11' , P = P , x = 0 )

$Pr_l = \mathbf{Pr}$ ( 'R11' , P = P , x = 0 )

$\rho_l = \rho$ ( 'R11' , P = P , x = 0 )

$\rho_g = \rho$ ( 'R11' , P = P , x = 1 )

$T_s = \mathbf{T}_{sat}$ ( 'R11' , P = P )

$miu_g = \mathbf{Visc}$ ( 'R11' , P = P , x = 1 )

$miu_l = \mathbf{Visc}$ ( 'R11' , P = P , x = 0 )

$h_f = \mathbf{h}$ ( 'R11' , P = P , x = 0 )

$h_g = \mathbf{h}$ ( 'R11' , P = P , x = 1 )

$h_{fg} = h_g - h_f$

$cp_l = \mathbf{Cp}$ ( 'R11' , P = P , x = 0 )

$Ps = \mathbf{P}_{sat}$ ( 'R11' , T = $T_w$ )

$M = \mathbf{MolarMass}$ ( 'R11' )

A.4

Shah

$$Bo = \frac{h_{tp} \cdot del_{Ts}}{G \cdot h_{fg}}$$

$$Bo_{ch} = Bo - 0.0003$$

$$h_f = \mathbf{h}\ ('R11', P=P, x=0)$$

$$h_g = \mathbf{h}\ ('R11', P=P, x=1)$$

$$h_{fg} = h_g - h_f$$

$$h_{tp} = h_l \cdot \chi$$

$$Co = \left[\frac{1}{x} - 1\right]^{0.8} \cdot \left[\frac{\rho_g}{\rho_l}\right]^{0.5}$$

$$N = Co$$

$$h_l = 0.023 \cdot Re_l^{0.8} \cdot Pr_l^{0.4} \cdot \frac{k_l}{D}$$

$$\chi = \mathbf{Max}\ (\chi_{nb}, \chi_{cb})$$

$$\chi_{nb} = 230 \cdot Bo^{0.5}$$ when Bo > 0.3 $*10^{-4}$

$$\chi_{cb} = \frac{1.8}{N^{0.8}}$$

$$grav = 9.8$$

$$Pr_l = \mathbf{Pr}\ ('R11', x=0, P=P)$$

$$k_l = \mathbf{k}\ ('R11', P=P, x=0)$$

$$\rho_l = \rho\ ('R11', P=P, x=0)$$

$$\rho_g = \rho\ ('R11', P=P, x=1)$$

$$del_{Ts} = Tw - Ts$$

$$Ts = \mathbf{T_{sat}}\ ('R11', P=P)$$

$$Re_l = \frac{G \cdot (1 - x) \cdot D}{miu_l}$$

$$miu_l = \mathbf{Visc}\ ('R11', P=P, x=0)$$

$$M = \mathbf{MolarMass}\ ('R11')$$

$$Fr_l = \frac{G^2}{\rho_l^2 \cdot grav \cdot D}$$

$$D = 0.00195$$

A.5

Gungor and Winterton

$$h_{tp} = E \cdot h_l + S \cdot h_{pool}$$

$$E = 1 + 24000 \cdot Bo^{1.16} + 1.37 \cdot \left[\frac{1}{X_{tt}}\right]^{0.86}$$

E=1

in subcooled region

$$X_{tt} = \left[\frac{1 - x}{x}\right]^{0.9} \cdot \left[\frac{\rho_g}{\rho}\right]^{0.5} \cdot \left[\frac{miu_l}{miu_g}\right]^{0.1}$$

$$S = \frac{1}{(1 + 1.15 \cdot 10^{-6}) \cdot E^2 \cdot Re_l^{1.17}}$$

$h_{pool}$ according to Cooper is given below

$$h_l = 0.023 \cdot \left[\frac{G \cdot (1 - x) \cdot D}{miu_l}\right]^{0.8} \cdot \left[\frac{cp_l \cdot miu_l}{k_l}\right]^{0.4} \cdot \frac{k_l}{D}$$

$$h_{pool} = 55 \cdot P_r^{0.12} \cdot PR2 \cdot M^{-0.5} \cdot qp^{0.67}$$

$$P_{cr} = 0.442 \cdot 10^7$$

$$P_r = \frac{P}{P_{cr}}$$

$$PR = \mathbf{log}(P_r)$$

$$PR1 = -PR$$

$$PR2 = PR1^{-0.55}$$

$$qp = h_{tp} \cdot del_{Ts}$$

$$del_{Ts} = Tw - Ts$$

$$Bo = \frac{qp}{G \cdot h_{fg}}$$

$$M = \mathbf{MolarMass}(\text{'R11'})$$

$$D = 0.00195$$

$$Re_l = \frac{G \cdot (1 - x) \cdot D}{miu_l}$$

$$k_l = \mathbf{k}(\text{'R11'}, P = P, x = 0)$$

$$\rho_l = \rho(\text{'R11'}, P = P, x = 0)$$

$$\rho_g = \rho(\text{'R11'}, P = P, x = 1)$$

$$Ts = \mathbf{T}_{sat}(\text{'R11'}, P = P)$$

$$miu_g = \mathbf{Visc}(\text{'R11'}, P = P, x = 1)$$

$$miu_l = \mathbf{Visc}(\text{'R11'}, P = P, x = 0)$$

$$h_f = \mathbf{h}(\text{'R11'}, P = P, x = 0)$$

$$h_g = \mathbf{h}(\text{'R11'}, P = P, x = 1)$$

$$h_{fg} = h_g - h_f$$

$$cp_l = \mathbf{Cp}(\text{'R11'}, P = P, x = 0)$$

**A.6. Bjorge et al**

```
"checking the T_sat,ib"
"the result of this code shows that r_tang is greater than r_max"
"then the equation that will be used for del_T_ib is the one used in this code"
B_M = 1.89*10^(-14  ) "this is really the value for water"
grav =9.8
r_max = 10^(-6)
r_tang = (4*sigma*T_s*v_fg)/(h_fg*del_Tib)
r_comp = r_tang-r_max
N=(h_FC*r_max)/k_l
Gamma = (k_l*h_fg)/(8*sigma*v_fg*h_FC*T_s)

v_f = volume(R11,x=0,t=T_f)
v_g = volume(R11,t=T_f,x=1)
v_fg=v_g-v_f
temp1=N*del_Tsc
del_Tib = (1/(1-N))*((1/(4*Gamma*N))-(((temp1))))
del_Tsc = T_s- T_b
(q_b/(miu_l*h_fg))*((sigma)/(grav*(rho_l-rho_g)))^0.5 =
B_M*(((k_l^0.5)*(rho_l^(17/8)*(cp_l^(19/8))*(rho_g^(1/8))))/(miu_l*h_fg^(7/8)*((rho_
l-rho_g)^(9/8))*((sigma)^(5/8))*((T_s)^(1/8))))*(del_Ts^3)
T=T_f
D= 1.95/1000
h_FC = ((k_b)*((0.023*(((G*D)/miu_f)^(0.8))*((miu_f*cp_b)/k_b)^(0.333)))))/D
q_FC = h_FC*(del_Ts+del_Tsc)
h_s = q/(T_w-T_s) "using T_w- T_saturation"
h_mf =q/(T_w-T_f) "this is the heat transfer coefficient"
"Finishing off this code, we will add the complete evaluation in subcooled region"
q=((q_FC)^(2)+((q_b^(2)*(1-((del_Tib/del_Ts))^3)^2)))^(0.5)
"========================================"
k_b = conductivity(R11,p=P,t=T_b) "this is conductivity when the bulk temperature is
used"
k_l = conductivity(R11,p=P,x=0)
rho_l = density(R11,p=P,x=0)
rho_g = density(R11,p=P,x=1)
T_s = t_sat(R11,p=P)
miu_f = viscosity(R11,p=P,x=1)
miu_l = viscosity(R11,p=P,t=T_f)
"enthalpy for liquid only"
h_f = enthalpy(R11,p=P,x=0)
h_g = enthalpy(R11,p=P,x=1)
h_fg = h_g-h_f
cp_l = specheat(R11,p=P,x=0)
cp_b = specheat(R11,p=P,t=T_b)
del_Ts = T_w - T_s
M =molarmass(R11)
```

## A.7

Klimenko

D=0.00195

$h_{tp} = h_{nb}$ for $N_{cb} < 1.2*10^4$

$h_{tp} = h_{cb}$ for $N_{cb} > 2*10^4$

$h_{tp} = \mathbf{Max}(h_{nb}, h_{cb})$ for $1.2*10^4 < N_{cb} <= 2*10^4$

$$N_{cb} = \frac{G \cdot h_{fg}}{h_{tp} \cdot del_{Ts}} \cdot \left[1 + x \cdot \left(\frac{\rho_l}{\rho_g} - 1\right)\right] \cdot \left[\frac{\rho_g}{\rho_l}\right]^{(1/3)}$$

$$h_{nb} = C \cdot \frac{k_l}{b} \cdot Pe_{star}^{0.6} \cdot \left[\frac{P \cdot b}{\sigma}\right]^{0.54} \cdot Pr_l^{-0.33} \cdot \left[\frac{k_w}{k_l}\right]^{0.12}$$

$$h_{cb} = 0.087 \cdot \frac{k_l}{b} \cdot Re_m^{0.6} \cdot Pr_l^{0.167} \cdot \left[\frac{\rho_g}{\rho_l}\right]^{0.2} \cdot \left[\frac{k_w}{k_l}\right]^{0.09}$$

$$Re_m = \frac{Wm \cdot b}{miu_l}$$

$$Wm = \frac{G}{\rho_l} \cdot \left[1 + x \cdot \left(\frac{\rho_l}{\rho_g} - 1\right)\right]$$

$k_w$ is for wall thermal conductivity

b is the Laplace constant given in Thesis

$$b = \left[\frac{\sigma}{grav \cdot del_\rho}\right]^{0.5}$$

$$C = 7.6 \cdot 10^{-3}$$

$$q = h_{tp} \cdot (T_w - T_s)$$

$$Pe_{star} = \frac{q \cdot b}{h_{fg} \cdot \rho_g \cdot a1}$$ this modified Peclet number as given by Klimenko

$Pr_l = 1.6$

$cp = \mathbf{Cp}('R11', x=0, P=P)$

$$a1 = \frac{k_l}{\rho_l \cdot cp_l}$$

$grav = 9.8$

$k_w = \mathbf{k}('R11', P=P, T=T_w)$

$k_l = \mathbf{k}('R11', P=P, x=0)$

$\rho_l = \rho('R11', P=P, x=0)$

$\rho_g = \rho('R11', P=P, x=1)$

$T_s = \mathbf{T}_{sat}('R11', P=P)$

$miu_l = \mathbf{Visc}('R11', P=P, x=0)$

$h_f = \mathbf{h}('R11', P=P, x=0)$

$h_g = \mathbf{h}('R11', P=P, x=1)$

$h_{fg} = h_g - h_f$

$del_{Ts} = T_w - T_s$

$del_\rho = \rho_l - \rho_g$

A.8:

```
"Steiner and Taborek"
PROCEDURE lamturb(Re_l:f)
if Re_l < 2300 THEN
f = 64/Re_l
else
f= (0.7904*ln(Re_l)-1.64)^(-2)
ENDif

h_tp = ((h_nb^n)+(abs(h_cb))^n)^(1/n)
n = 3
h_nb = h_nbo*F_nb
F_nb = F_pf *((h_nb*del_Ts)/q_o)^nf *(D/D_o)^(-0.4)*((R_a/R_a0)^(0.133))*(FM)
nf = 0.8-0.1*exp(1.75*P_r)
D_o = 0.01
R_a0 = 1*10^(-6)
R_a = 1*10^(-6) "this is according to the recommendation of Steiner and Taborek"
"q = (2*sigma*Ts*h_LO)/(r_cr*rho_g*h_fg)"
"q_ONB = (2*sigma*Ts*h_LO)/(r_cr*rho_g*del_hv)" "this is the given equation to determine the
minimum q"
r_cr = 0.3 *10^(-6)
del_Ts= abs(Tw-Ts)
Ts = t_sat(R11,p=P)
h_LO =(((((f/8)*(Re_l-1000)*(Pr_l))/(1+12.7*(f/8)^(1/2)*(Pr_l^(2/3)-1))))*k_l)/D
Re_l = (G*D)/miu_l
call lamturb(Re_l:f)
k_l = conductivity(R11,p=P,x=0)
Pr_l =  prandtl(R11,p=P,x=0)
rho_l = density(R11,p=P,x=0)
rho_g = density(R11,p=P,x=1)
miu_g = viscosity(R11,p=P,x=1)
miu_l = viscosity(R11,p=P,x=0)
h_f = enthalpy(R11,p=P,x=0)
h_g = enthalpy(R11,p=P,x=1)
h_fg = h_g-h_f
cp_l = specheat(R11,p=P,x=0)
"h_LO could be obtained from the Dittus-Boelter of Gnielinski"
"del_hv is the latent heat of vaporization"
P_r = P/P_cr  "reduced pressure value"
P_cr =0.0442*10^7
h_nbo = 2690
F_pf = (2.816*(P_r)^0.45 +(3.4+(1.7/(1-(P_r)^7)))*(P_r^(3.7)))
h_cb = h_LO*F_tp
F_M1 =0.377+0.199*(ln(M)) + 0.000028427*M^2  " this is given by Steiner and Taborek"
FM = max(F_M1,2.5)
q_o = 20000 [W/m^2]
"for x <= 0.6"
F_tp = (((1-x)^1.5)+(1.9*x^(0.6))*((rho_l/rho_g)^0.35))^1.1
M = molarmass(R11)
"otherwise Ftp for x? 1 is given by the equation below"
" F_tp =((((1-x)^(1.5))+ (1.9*(x^0.6)*((1-x)^(0.01))*(rho_l/rho_g)^(0.35)))^(-2.2))
+((h_Go/h_lo)*(x^0.01)*(1+(8*(1-x)^(0.7))*(rho_l/rho_G)^(0.67)))^(-2) "
D= 0.00195
```

A.9

The correlation of Tran et al

$$h_{tp} = 8.4 \cdot 10^{5} \cdot (Bo^{2} \cdot We_{fo})^{0.3} \cdot \left[\frac{v_g}{v_f}\right]^{-0.4}$$

$$We_{fo} = \frac{v_f \cdot G^{2} \cdot D}{\sigma}$$

$$D = 0.00195$$

$$v_f = \mathbf{v}('R11', P=P, x=0)$$

$$v_g = \mathbf{v}('R11', P=P, x=1)$$

$$Bo = \frac{h_{tp} \cdot del_{Ts}}{G \cdot h_{fg}}$$

$$del_{Ts} = Tw - Ts$$

$$Ts = \mathbf{T}_{sat}('R11', P=P)$$

$$h_f = \mathbf{h}('R11', P=P, x=0)$$

$$h_g = \mathbf{h}('R11', P=P, x=1)$$

$$h_{fg} = h_g - h_f$$

## A.10

Correlation of Lee and Mudawar

this is for $x_e$ 0 to 0.05

Procedure **myeffe** ($Re_f$, $miu_l$, $miu_g$, $\rho_l$, $\rho_g$, $x_e$, $f_f$, $Pr_l$ : $X_t$, Nuf)

If ( $Re_f < 2300$ ) Then

$$X_t := \left[\frac{miu_l}{miu_g}\right]^{0.5} \cdot \left[\frac{\rho_g}{\rho_l}\right]^{0.5} \cdot \left[\frac{1 - x_e}{x_e}\right]^{0.5}$$

$$Nuf := 4.36$$

Else

$$X_t := \left[\frac{f_f \cdot Re_f^{0.25}}{0.079}\right]^{0.5} \cdot \left[\frac{1 - x_e}{x_e}\right]^{0.5} \cdot \left[\frac{\rho_g}{\rho_l}\right]^{0.5}$$

$$Nuf := 0.023 \cdot Re_f^{0.8} \cdot Pr_l^{0.4}$$

EndIf

End **myeffe**

$$D = 0.00195$$

$$Re_g = \frac{G \cdot x_e \cdot D}{miu_g}$$

$$Re_f = \frac{G \cdot (1 - x_e) \cdot D}{miu_l}$$

Call **myeffe** ( $Re_f$, $miu_l$, $miu_g$, $\rho_l$, $\rho_g$, $x_e$, $f_f$, $Pr_l$ : $x_t$, Nuf )

$$h_{tp} = 3.85 \cdot x_t^{0.267} \cdot h_{sp,f}$$

$$h_{sp,f} = \frac{k_l \cdot Nuf}{D}$$

$$f_f = \frac{64}{Re_f}$$

$$x_e = x$$

$k_l$ = **k** ( 'R11' , P = P , x = 0 )

$Pr_l$ = **Pr** ( 'R11' , P = P , x = 0 )

$\rho_l$ = $\rho$ ( 'R11' , P = P , x = 0 )

$\rho_g$ = $\rho$ ( 'R11' , P = P , x = 1 )

$miu_g$ = **Visc** ( 'R11' , P = P , x = 1 )

$miu_l$ = **Visc** ( 'R11' , P = P , x = 0 )

enthalpy for liquid only

$h_f$ = **h** ( 'R11' , P = P , x = 0 )

$h_g$ = **h** ( 'R11' , P = P , x = 1 )

$$h_{fg} = h_g - h_f$$

$$del_{Ts} = Tw - Ts$$

Ts = $\mathbf{T}_{sat}$ ( 'R11' , P = P )

## A.11

PROCEDURE lamturb(Re,Pr,f,$k_{l,D:h,FC}$)
if $Re_l < 2300$ THEN
Nu = 4.34
else
Nu = ((Re-1000)*$Pr^{(f/2)}$)/(1.07+12.7*($Pr^{(2/3)}$-1)*($(f/2)^{(0.5)}$))
ENDif

$D = 0.00195$

$N_u$ = ((Re-1000)*$Pr^{(f/2)}$)/(1.07+12.7*($Pr^{(2/3)}$-1)*($(f/2)^{(0.5)}$))

$N_u = 4.34$

$f = 2 \cdot 0.0396 \cdot Re^{-0.25}$

$T_m = \frac{T_b + T_w}{2}$

$T_s = \mathbf{T_{sat}}('R11', P = P)$

$k_l = \mathbf{k}('R11', P = P, x = 0)$

$Re = \frac{G \cdot D}{miu}$

call lamturb(Re,Pr,f,$k_{l,D:h,FC}$)

$h = h_{FC} + h_{pb} \cdot \frac{del_{Ts}}{del_{Tm}}$

$h_{FC} = \frac{N_u \cdot k_l}{D}$

$miu = \mathbf{Visc}('R11', P = P, x = 0)$

$Pr = \mathbf{Pr}('R11', P = P, x = 0)$

$h_{pb}$ = we need Gorenflo's correlation for pool boiling

$h_{pb} = f_{gorenflo}*(q_{nb})$

see page 3677 of Haynes and Flethcer

$h_{pb} = h_o \cdot F_{PF} \cdot \left[\frac{q_{pb}}{q_o}\right]^n \cdot \left[\frac{R_p}{R_{po}}\right]^{0.133}$

$q_{pb} = h_{pb} \cdot \left[\left|T_w - T_s\right|\right] \cdot S$

$S = 1$

$F_{PF} = 1.2 \cdot P_r^{0.27} + 2.5 \cdot P_r + \frac{P_r}{1 + P_r}$

$R_p = 0.4$

$R_{po} = R_p$

$q_o = 20000$

$h_o = 2800$

$P_{ro} = 0.1 \cdot 10^6$

$P_r = \frac{P}{P_{ro}}$

$n = 0.9 - 0.3 \cdot P_r^{0.3}$

$del_{Ts} = T_w - T_s$

$del_{Tm} = T_w - T_b$

## A.12: Sumith et al

Correlation of Sumith et.al

Procedure lamturb($Re_{g,G,x,D,miu,l,miu,g,Pr,l,Re,lo,k,l,X,tt,C,3,h,lf,delta,m,Fr,G,rho,g,Re,l:h,tp}$)

if $Re_g > 2000$ THEN
$h_{tp} = 2.83*(((1/X_{tt})+0.213)^{(0.736)})*h_{lo}$
ELSE
$h_{tp} = C_3*h_{lf}$
ENDif

$$h_{tp} = 2.83 \cdot \left[\frac{1}{X_{tt}} + 0.213\right]^{0.736} \cdot h_{lo}$$

$$h_{tp} = C_3 \cdot h_{lf}$$

$$Re_g = \frac{G \cdot x \cdot D}{miu_g}$$

$$h_{lo} = 0.023 \cdot Re_l^{0.8} \cdot Pr_l^{0.4}$$

$$Re_{lo} = \frac{G \cdot D}{miu_l}$$

call lamturb($Re_{g,G,x,D,miu,l,miu,g,Pr,l,Re,lo,k,l,X,tt,C,3,h,lf,delta,m,Fr,G,rho,g,Re,l:h,tp}$)

$$X_{tt} = \left[\frac{1 - x}{x}\right]^{0.9} \cdot \left[\frac{\rho_g}{\rho_l}\right]^{0.5} \cdot \left[\frac{miu_l}{miu_g}\right]^{0.1}$$

$$C_3 = 2.36$$

$D = 0.00195$ [m]

$$h_{lf} = \frac{k_l}{\delta_m}$$

$$\delta_m = D \cdot 0.082 \cdot \mathbf{exp}\left(-0.0594 \cdot Re_l^{0.21} \cdot Fr_G^{0.25} \cdot x^{0.12}\right)$$

$$Re_l = \frac{G \cdot (1 - x) \cdot D}{miu_l}$$

$$Fr_G = \frac{G \cdot x}{\rho_g} \cdot (G \cdot D)^{0.5}$$

$G = 9.81$ [m/s$^2$]

$miu_g = \mathbf{Visc}$ ( 'R11' , P = P , x = 1 )

$Pr_l = \mathbf{Pr}$ ( 'R11' , P = P , x = 0 )

$miu_l = \mathbf{Visc}$ ( 'R11' , P = P , x = 0 )

$\rho_g = \rho$ ( 'R11' , P = P , x = 1 )

$\rho_l = \rho$ ( 'R11' , P = P , x = 0 )

$k_l = \mathbf{k}$ ( 'R11' , P = P , x = 0 )

## Appendix B: Tabulated data from Bao et al [39], Baird et al [60] and Yan and Lin [61]

### Table B.1: Tabulated data of Bao et al [39]

| | | | | Notes | |
|---|---|---|---|---|---|
| L_HT | 0.027 | m/block | | Notes | First value for $q_{wall}$ in each block is average over the test section |
| d | 0.00195 | m | | | |

| R11 | | Measured Quantities | | | | Derived Quantities | | | | |
|---|---|---|---|---|---|---|---|---|---|---|
| | | G | $q_{wall}$ | $T_{wall}$ | p | enthalpy | $T_f$ | quality | ΔT local | h |
| | | kg $m^{-2}$ $s^{-1}$ | kW $m^{-2}$ | $^oC$ | MPa | kJ $kg^{-1}$ | $^oC$ | (-) | $^oC$ | kW $m^{-2}$ $K^{-1}$ |
| p1q1g | | 167.4 | 11.07 | | 0.21518 | 226.1057 | 29.88 | -0.089 | | |
| | 1 | 167.4 | 13.09 | 50.52 | 0.21518 | 228.2710 | 32.32 | -0.076 | 18.198 | 0.719 |
| | 2 | 167.4 | 10.16 | 51.85 | 0.21517 | 232.1172 | 36.64 | -0.054 | 15.211 | 0.668 |
| | 3 | 167.4 | 12.00 | 52.66 | 0.21516 | 235.7834 | 40.74 | -0.032 | 11.925 | 1.007 |
| | 4 | 167.4 | 10.27 | 53.28 | 0.21515 | 239.4667 | 44.83 | -0.011 | 8.449 | 1.215 |
| | 5 | 167.4 | 11.78 | 53.42 | 0.21514 | 243.1137 | 46.85 | 0.010 | 6.572 | 1.793 |
| | 6 | 167.4 | 9.83 | 53.59 | 0.21512 | 246.6894 | 46.85 | 0.031 | 6.744 | 1.458 |
| | 7 | 167.4 | 11.55 | 53.77 | 0.21505 | 250.2262 | 46.84 | 0.051 | 6.939 | 1.664 |
| | 8 | 167.4 | 10.88 | 53.69 | 0.21495 | 253.9369 | 46.82 | 0.073 | 6.871 | 1.584 |
| | 9 | 167.4 | 10.15 | 53.27 | 0.21483 | 257.4159 | 46.80 | 0.093 | 6.467 | 1.569 |
| | 10 | 167.4 | 10.95 | 52.49 | 0.21470 | 260.9050 | 46.78 | 0.114 | 5.714 | 1.916 |
| | 1 | 167.4 | 16.94 | 51.99 | 0.22110 | 228.7463 | 32.85 | -0.078 | 19.141 | 0.885 |
| | 2 | 167.4 | 14.68 | 53.31 | 0.22109 | 233.9755 | 38.72 | -0.048 | 14.598 | 1.005 |
| | 3 | 167.4 | 15.50 | 54.24 | 0.22108 | 238.9672 | 44.27 | -0.019 | 9.962 | 1.556 |
| | 4 | 167.4 | 14.12 | 54.76 | 0.22107 | 243.8673 | 47.76 | 0.010 | 6.998 | 2.018 |
| | 5 | 167.4 | 16.27 | 54.75 | 0.22103 | 248.8941 | 47.76 | 0.039 | 6.994 | 2.326 |
| | 6 | 167.4 | 13.86 | 54.85 | 0.22093 | 253.8772 | 47.74 | 0.068 | 7.105 | 1.951 |
| | 7 | 167.4 | 15.74 | 55.04 | 0.22081 | 258.7723 | 47.72 | 0.097 | 7.319 | 2.150 |
| | 8 | 167.4 | 15.06 | 54.95 | 0.22066 | 263.8667 | 47.70 | 0.126 | 7.252 | 2.077 |
| | 9 | 167.4 | 13.98 | 54.52 | 0.22048 | 268.6711 | 47.67 | 0.155 | 6.843 | 2.043 |
| | 10 | 167.4 | 15.06 | 53.68 | 0.22029 | 273.4741 | 47.64 | 0.183 | 6.040 | 2.493 |
| | 1 | 167.4 | 22.06 | 53.54 | 0.21549 | 229.5978 | 33.81 | -0.069 | 19.732 | 1.118 |
| | 2 | 167.4 | 20.98 | 54.64 | 0.21548 | 236.7169 | 41.78 | -0.027 | 12.870 | 1.630 |
| | 3 | 167.4 | 21.68 | 55.38 | 0.21547 | 243.7738 | 46.90 | 0.014 | 8.484 | 2.556 |
| | 4 | 167.4 | 21.47 | 55.78 | 0.21541 | 250.9105 | 46.89 | 0.055 | 8.893 | 2.414 |
| | 5 | 167.4 | 21.75 | 56.05 | 0.21528 | 258.0584 | 46.87 | 0.097 | 9.177 | 2.370 |
| | 6 | 167.4 | 19.23 | 56.22 | 0.21511 | 264.8371 | 46.85 | 0.136 | 9.378 | 2.051 |
| | 7 | 167.4 | 21.65 | 56.43 | 0.21491 | 271.5988 | 46.81 | 0.175 | 9.620 | 2.250 |
| | 8 | 167.4 | 21.51 | 56.26 | 0.21467 | 278.7376 | 46.78 | 0.217 | 9.480 | 2.270 |
| | 9 | 167.4 | 19.09 | 55.84 | 0.21440 | 285.4541 | 46.74 | 0.256 | 9.107 | 2.097 |
| | 10 | 167.4 | 21.66 | 54.73 | 0.21411 | 292.1947 | 46.69 | 0.295 | 8.043 | 2.693 |
| | 1 | 167.4 | 32.16 | 56.51 | 0.22761 | 231.7231 | 36.19 | -0.066 | 20.321 | 1.582 |
| | 2 | 167.4 | 30.15 | 57.74 | 0.22760 | 242.0293 | 47.66 | -0.006 | 10.080 | 2.991 |
| | 3 | 167.4 | 32.86 | 58.20 | 0.22753 | 252.4520 | 48.74 | 0.055 | 9.462 | 3.473 |
| | 4 | 167.4 | 31.43 | 58.70 | 0.22737 | 263.0861 | 48.71 | 0.117 | 9.989 | 3.146 |
| | 5 | 167.4 | 31.74 | 59.01 | 0.22716 | 273.5352 | 48.68 | 0.178 | 10.329 | 3.073 |

| | | | | | | | | | |
|---|---|---|---|---|---|---|---|---|---|
| 6 | 167.4 | 28.71 | 59.14 | 0.22690 | 283.5341 | 48.64 | 0.237 | 10.498 | 2.735 |
| 7 | 167.4 | 31.97 | 59.35 | 0.22660 | 293.5706 | 48.60 | 0.295 | 10.753 | 2.973 |
| 8 | 167.4 | 31.83 | 59.14 | 0.22625 | 304.1234 | 48.54 | 0.357 | 10.599 | 3.003 |
| 9 | 167.4 | 28.48 | 58.69 | 0.22586 | 314.0988 | 48.49 | 0.415 | 10.202 | 2.792 |
| 10 | 167.4 | 31.99 | 57.39 | 0.22544 | 324.1006 | 48.42 | 0.474 | 8.970 | 3.566 |
| 1 | 167.4 | 42.89 | 57.24 | 0.22114 | 233.4322 | 38.11 | -0.051 | 19.129 | 2.242 |
| 2 | 167.4 | 42.85 | 58.17 | 0.22113 | 247.6133 | 47.77 | 0.032 | 10.395 | 4.122 |
| 3 | 167.4 | 44.75 | 58.53 | 0.22102 | 262.1032 | 47.76 | 0.116 | 10.778 | 4.152 |
| 4 | 167.4 | 43.03 | 59.02 | 0.22077 | 276.6227 | 47.72 | 0.201 | 11.306 | 3.806 |
| 5 | 167.4 | 43.71 | 59.26 | 0.22046 | 290.9693 | 47.67 | 0.284 | 11.594 | 3.770 |
| 6 | 167.4 | 39.83 | 59.30 | 0.22008 | 304.7864 | 47.61 | 0.365 | 11.689 | 3.407 |
| 7 | 167.4 | 43.84 | 59.44 | 0.21965 | 318.6256 | 47.55 | 0.445 | 11.899 | 3.685 |
| 8 | 167.4 | 43.40 | 59.10 | 0.21915 | 333.0558 | 47.47 | 0.529 | 11.627 | 3.733 |
| 9 | 167.4 | 39.77 | 58.28 | 0.21862 | 346.8120 | 47.39 | 0.610 | 10.890 | 3.652 |
| 10 | 167.4 | 45.05 | 56.54 | 0.21804 | 360.8405 | 47.30 | 0.691 | 9.240 | 4.875 |
| 1 | 167.4 | 56.97 | 58.61 | 0.22581 | 235.7883 | 40.74 | -0.041 | 17.877 | 3.187 |
| 2 | 167.4 | 58.67 | 59.35 | 0.22570 | 254.9167 | 48.46 | 0.071 | 10.890 | 5.387 |
| 3 | 167.4 | 59.46 | 59.73 | 0.22544 | 274.4570 | 48.42 | 0.185 | 11.308 | 5.259 |
| 4 | 167.4 | 57.83 | 60.22 | 0.22510 | 293.8587 | 48.37 | 0.298 | 11.845 | 4.883 |
| 5 | 167.4 | 58.62 | 60.44 | 0.22467 | 313.1212 | 48.31 | 0.410 | 12.129 | 4.833 |
| 6 | 167.4 | 53.76 | 60.37 | 0.22417 | 331.7103 | 48.23 | 0.519 | 12.139 | 4.429 |
| 7 | 167.4 | 58.09 | 60.43 | 0.22361 | 350.2119 | 48.15 | 0.627 | 12.285 | 4.729 |
| 8 | 167.4 | 58.62 | 59.65 | 0.22299 | 369.5165 | 48.05 | 0.739 | 11.596 | 5.055 |
| 9 | 167.4 | 58.89 | 58.28 | 0.22233 | 388.9524 | 47.95 | 0.853 | 10.322 | 5.705 |
| 10 | 167.4 | 56.44 | 57.95 | 0.22169 | 408.0284 | 47.86 | 0.964 | 10.089 | 5.595 |
| 1 | 309.7 | 30.72 | 54.17 | 0.22119 | 229.5810 | 33.79 | -0.073 | 20.384 | 1.507 |
| 2 | 309.7 | 30.48 | 55.24 | 0.22118 | 235.0535 | 39.92 | -0.041 | 15.319 | 1.990 |
| 3 | 309.7 | 30.38 | 56.12 | 0.22116 | 240.4951 | 45.97 | -0.010 | 10.157 | 2.991 |
| 4 | 309.7 | 29.74 | 56.67 | 0.22103 | 245.8699 | 47.76 | 0.022 | 8.916 | 3.335 |
| 5 | 309.7 | 31.01 | 56.93 | 0.22071 | 251.3011 | 47.71 | 0.053 | 9.220 | 3.363 |
| 6 | 309.7 | 27.49 | 57.21 | 0.22026 | 256.5319 | 47.64 | 0.084 | 9.573 | 2.872 |
| 7 | 309.7 | 30.33 | 57.57 | 0.21971 | 261.7014 | 47.56 | 0.115 | 10.016 | 3.028 |
| 8 | 309.7 | 30.71 | 57.44 | 0.21905 | 267.1586 | 47.45 | 0.147 | 9.981 | 3.077 |
| 9 | 309.7 | 27.16 | 57.17 | 0.21830 | 272.3331 | 47.34 | 0.177 | 9.833 | 2.763 |
| 10 | 309.7 | 30.32 | 56.07 | 0.21745 | 277.4726 | 47.21 | 0.208 | 8.863 | 3.421 |
| 1 | 307.0 | 56.34 | 58.95 | 0.23306 | 232.0882 | 36.60 | -0.068 | 22.351 | 2.521 |
| 2 | 307.0 | 55.00 | 60.13 | 0.23305 | 242.1334 | 47.78 | -0.009 | 12.351 | 4.453 |
| 3 | 307.0 | 57.57 | 60.38 | 0.23281 | 252.2889 | 49.52 | 0.050 | 10.869 | 5.296 |
| 4 | 307.0 | 55.87 | 60.79 | 0.23224 | 262.5226 | 49.43 | 0.110 | 11.363 | 4.916 |
| 5 | 307.0 | 57.02 | 60.95 | 0.23148 | 272.7066 | 49.32 | 0.170 | 11.627 | 4.904 |
| 6 | 307.0 | 52.02 | 60.94 | 0.23056 | 282.5440 | 49.18 | 0.228 | 11.756 | 4.425 |
| 7 | 307.0 | 57.44 | 61.09 | 0.22949 | 292.4198 | 49.03 | 0.287 | 12.068 | 4.760 |
| 8 | 307.0 | 57.20 | 60.88 | 0.22827 | 302.7629 | 48.85 | 0.348 | 12.032 | 4.754 |
| 9 | 307.0 | 52.13 | 60.44 | 0.22695 | 312.6264 | 48.65 | 0.406 | 11.790 | 4.422 |
| 10 | 307.0 | 56.76 | 59.09 | 0.22569 | 322.4502 | 48.46 | 0.464 | 10.624 | 5.343 |
| 1 | 170.2 | 39.11 | 68.80 | 0.34284 | 233.7857 | 38.46 | -0.137 | 30.343 | 1.289 |
| 2 | 170.2 | 40.73 | 70.00 | 0.34283 | 246.7755 | 52.85 | -0.058 | 17.150 | 2.375 |
| 3 | 170.2 | 39.52 | 71.15 | 0.34283 | 259.8317 | 63.33 | 0.021 | 7.813 | 5.058 |
| 4 | 170.2 | 39.89 | 71.58 | 0.34275 | 272.7520 | 63.33 | 0.099 | 8.250 | 4.835 |
| 5 | 170.2 | 40.47 | 71.83 | 0.34258 | 285.8269 | 63.31 | 0.178 | 8.527 | 4.746 |

| | | | | | | | | | |
|---|---|---|---|---|---|---|---|---|---|
| 6 | 170.2 | 36.52 | 71.95 | 0.34236 | 298.3525 | 63.28 | 0.254 | 8.669 | 4.212 |
| 7 | 170.2 | 41.57 | 72.29 | 0.34210 | 311.0579 | 63.25 | 0.331 | 9.040 | 4.599 |
| 8 | 170.2 | 40.31 | 72.48 | 0.34179 | 324.3808 | 63.22 | 0.411 | 9.259 | 4.354 |
| 9 | 170.2 | 36.59 | 72.44 | 0.34145 | 336.8935 | 63.18 | 0.487 | 9.253 | 3.955 |
| 10 | 170.2 | 37.60 | 71.66 | 0.34108 | 348.9652 | 63.14 | 0.560 | 8.521 | 4.413 |
| 1 | 251.1 | 36.74 | 69.59 | 0.36011 | 231.1867 | 35.54 | -0.164 | 34.050 | 1.079 |
| 2 | 251.1 | 43.13 | 70.07 | 0.36009 | 239.9943 | 45.37 | -0.110 | 24.704 | 1.746 |
| 3 | 251.1 | 41.40 | 71.30 | 0.36008 | 249.3159 | 55.63 | -0.054 | 15.677 | 2.641 |
| 4 | 251.1 | 38.07 | 72.42 | 0.36007 | 258.0793 | 65.14 | -0.001 | 7.281 | 5.228 |
| 5 | 251.1 | 40.16 | 72.76 | 0.35995 | 266.7053 | 65.17 | 0.052 | 7.595 | 5.288 |
| 6 | 251.1 | 36.20 | 72.91 | 0.35966 | 275.1251 | 65.14 | 0.103 | 7.779 | 4.654 |
| 7 | 251.1 | 41.41 | 73.22 | 0.35928 | 283.6826 | 65.10 | 0.155 | 8.125 | 5.096 |
| 8 | 251.1 | 40.67 | 73.33 | 0.35881 | 292.7331 | 65.05 | 0.211 | 8.278 | 4.913 |
| 9 | 251.1 | 37.02 | 73.35 | 0.35827 | 301.3001 | 64.99 | 0.263 | 8.363 | 4.427 |
| 10 | 251.1 | 36.67 | 72.86 | 0.35767 | 309.4264 | 64.93 | 0.313 | 7.938 | 4.620 |
| 1 | 334.8 | 35.95 | 68.21 | 0.35225 | 228.9799 | 33.07 | -0.172 | 35.142 | 1.023 |
| 2 | 334.8 | 43.14 | 68.40 | 0.35223 | 235.5209 | 40.39 | -0.132 | 28.005 | 1.540 |
| 3 | 334.8 | 42.53 | 69.31 | 0.35221 | 242.6061 | 48.26 | -0.089 | 21.053 | 2.020 |
| 4 | 334.8 | 39.38 | 70.48 | 0.35220 | 249.3806 | 55.70 | -0.048 | 14.780 | 2.664 |
| 5 | 334.8 | 38.83 | 71.25 | 0.35218 | 255.8485 | 62.73 | -0.009 | 8.524 | 4.555 |
| 6 | 334.8 | 36.36 | 71.42 | 0.35204 | 262.0669 | 64.33 | 0.029 | 7.096 | 5.124 |
| 7 | 334.8 | 41.38 | 71.80 | 0.35169 | 268.4967 | 64.29 | 0.068 | 7.509 | 5.511 |
| 8 | 334.8 | 40.70 | 71.95 | 0.35119 | 275.2850 | 64.24 | 0.109 | 7.716 | 5.275 |
| 9 | 334.8 | 36.94 | 72.04 | 0.35058 | 281.7061 | 64.17 | 0.148 | 7.865 | 4.697 |
| 10 | 334.8 | 36.71 | 71.56 | 0.34987 | 287.7975 | 64.10 | 0.186 | 7.469 | 4.915 |
| 1 | 337.6 | 51.53 | 70.25 | 0.35534 | 229.5265 | 33.68 | -0.171 | 36.576 | 1.409 |
| 2 | 337.6 | 61.99 | 70.19 | 0.35532 | 238.8376 | 44.08 | -0.114 | 26.103 | 2.375 |
| 3 | 337.6 | 56.88 | 71.47 | 0.35530 | 248.5880 | 54.83 | -0.055 | 16.635 | 3.420 |
| 4 | 337.6 | 55.65 | 72.23 | 0.35529 | 257.8182 | 64.67 | 0.001 | 7.553 | 7.368 |
| 5 | 337.6 | 56.84 | 72.50 | 0.35506 | 267.0448 | 64.65 | 0.057 | 7.851 | 7.240 |
| 6 | 337.6 | 52.38 | 72.42 | 0.35454 | 276.0031 | 64.59 | 0.112 | 7.829 | 6.690 |
| 7 | 337.6 | 58.84 | 72.66 | 0.35385 | 285.1253 | 64.52 | 0.167 | 8.143 | 7.226 |
| 8 | 337.6 | 57.63 | 72.77 | 0.35300 | 294.6785 | 64.43 | 0.226 | 8.340 | 6.910 |
| 9 | 337.6 | 53.48 | 72.70 | 0.35202 | 303.7919 | 64.33 | 0.281 | 8.371 | 6.389 |
| 10 | 337.6 | 53.44 | 72.21 | 0.35094 | 312.5618 | 64.21 | 0.335 | 7.997 | 6.683 |
| 1 | 334.8 | 82.58 | 72.46 | 0.35589 | 231.9809 | 36.43 | -0.156 | 36.029 | 2.292 |
| 2 | 334.8 | 89.15 | 72.88 | 0.35587 | 246.1829 | 52.20 | -0.070 | 20.688 | 4.309 |
| 3 | 334.8 | 86.90 | 73.42 | 0.35586 | 260.7427 | 64.73 | 0.018 | 8.684 | 10.008 |
| 4 | 334.8 | 87.14 | 73.60 | 0.35551 | 275.1369 | 64.70 | 0.106 | 8.901 | 9.791 |
| 5 | 334.8 | 87.23 | 73.77 | 0.35471 | 289.5580 | 64.61 | 0.194 | 9.157 | 9.526 |
| 6 | 334.8 | 81.26 | 73.47 | 0.35371 | 303.4922 | 64.51 | 0.279 | 8.965 | 9.064 |
| 7 | 334.8 | 89.69 | 73.77 | 0.35253 | 317.6296 | 64.38 | 0.365 | 9.385 | 9.557 |
| 8 | 334.8 | 87.80 | 73.92 | 0.35121 | 332.3080 | 64.24 | 0.455 | 9.681 | 9.069 |
| 9 | 334.8 | 82.89 | 73.64 | 0.34980 | 346.4246 | 64.09 | 0.541 | 9.551 | 8.679 |
| 10 | 334.8 | 83.59 | 73.10 | 0.34847 | 360.1937 | 63.94 | 0.625 | 9.160 | 9.126 |
| 1 | 334.8 | 101.81 | 72.53 | 0.35342 | 233.3754 | 38.00 | -0.146 | 34.531 | 2.948 |
| 2 | 334.8 | 104.67 | 73.51 | 0.35340 | 250.4516 | 56.87 | -0.043 | 16.643 | 6.289 |
| 3 | 334.8 | 105.01 | 73.75 | 0.35309 | 267.7930 | 64.44 | 0.063 | 9.315 | 11.274 |
| 4 | 334.8 | 104.98 | 73.92 | 0.35233 | 285.1598 | 64.36 | 0.168 | 9.557 | 10.985 |
| 5 | 334.8 | 104.91 | 74.14 | 0.35130 | 302.5178 | 64.25 | 0.274 | 9.893 | 10.605 |

| | | | | | | | | | |
|---|---|---|---|---|---|---|---|---|---|
| 6 | 334.8 | 98.23 | 73.81 | 0.35007 | 319.3176 | 64.12 | 0.376 | 9.695 | 10.132 |
| 7 | 334.8 | 107.38 | 74.27 | 0.34867 | 336.3225 | 63.97 | 0.480 | 10.307 | 10.419 |
| 8 | 334.8 | 105.12 | 74.47 | 0.34731 | 353.8972 | 63.82 | 0.587 | 10.652 | 9.869 |
| 9 | 334.8 | 98.07 | 73.99 | 0.34602 | 370.7013 | 63.68 | 0.689 | 10.310 | 9.512 |
| 10 | 334.8 | 103.71 | 72.47 | 0.34462 | 387.3886 | 63.53 | 0.791 | 8.946 | 11.593 |
| 1 | 449.3 | 103.12 | 71.24 | 0.34813 | 230.2463 | 34.49 | -0.162 | 36.747 | 2.806 |
| 2 | 449.3 | 105.25 | 72.54 | 0.34809 | 243.0904 | 48.79 | -0.084 | 23.743 | 4.433 |
| 3 | 449.3 | 104.00 | 73.23 | 0.34806 | 255.9886 | 62.88 | -0.006 | 10.351 | 10.047 |
| 4 | 449.3 | 105.13 | 73.39 | 0.34756 | 268.8792 | 63.85 | 0.073 | 9.546 | 11.014 |
| 5 | 449.3 | 104.72 | 73.60 | 0.34640 | 281.8147 | 63.72 | 0.151 | 9.881 | 10.598 |
| 6 | 449.3 | 98.54 | 73.11 | 0.34489 | 294.3435 | 63.56 | 0.228 | 9.554 | 10.313 |
| 7 | 449.3 | 107.88 | 73.43 | 0.34307 | 307.0670 | 63.36 | 0.306 | 10.072 | 10.711 |
| 8 | 449.3 | 105.79 | 73.57 | 0.34099 | 320.2380 | 63.13 | 0.387 | 10.433 | 10.140 |
| 9 | 449.3 | 98.88 | 73.16 | 0.33872 | 332.8543 | 62.88 | 0.464 | 10.280 | 9.619 |
| 10 | 449.3 | 103.11 | 71.97 | 0.33630 | 345.3052 | 62.62 | 0.540 | 9.355 | 11.022 |
| 1 | 446.4 | 122.83 | 72.54 | 0.35030 | 231.4363 | 35.83 | -0.156 | 36.713 | 3.346 |
| 2 | 446.4 | 126.11 | 73.60 | 0.35027 | 246.8778 | 52.96 | -0.062 | 20.637 | 6.111 |
| 3 | 446.4 | 125.35 | 73.91 | 0.35024 | 262.4757 | 64.14 | 0.032 | 9.774 | 12.825 |
| 4 | 446.4 | 126.05 | 73.99 | 0.34959 | 278.0699 | 64.07 | 0.127 | 9.924 | 12.702 |
| 5 | 446.4 | 125.61 | 74.18 | 0.34807 | 293.6801 | 63.90 | 0.222 | 10.276 | 12.224 |
| 6 | 446.4 | 118.37 | 73.57 | 0.34621 | 308.8142 | 63.70 | 0.315 | 9.874 | 11.989 |
| 7 | 446.4 | 128.93 | 73.94 | 0.34405 | 324.1538 | 63.47 | 0.409 | 10.475 | 12.307 |
| 8 | 446.4 | 126.59 | 74.04 | 0.34165 | 340.0030 | 63.21 | 0.506 | 10.835 | 11.684 |
| 9 | 446.4 | 118.61 | 73.42 | 0.33913 | 355.2122 | 62.93 | 0.599 | 10.490 | 11.307 |
| 10 | 446.4 | 124.82 | 71.87 | 0.33675 | 370.3114 | 62.67 | 0.691 | 9.200 | 13.567 |
| 1 | 447.6 | 143.46 | 73.84 | 0.35378 | 232.9221 | 37.49 | -0.149 | 36.353 | 3.946 |
| 2 | 447.6 | 147.92 | 74.73 | 0.35374 | 250.9500 | 57.41 | -0.040 | 17.315 | 8.543 |
| 3 | 447.6 | 147.11 | 74.82 | 0.35316 | 269.2036 | 64.45 | 0.071 | 10.368 | 14.190 |
| 4 | 447.6 | 147.65 | 74.87 | 0.35178 | 287.4407 | 64.30 | 0.182 | 10.572 | 13.967 |
| 5 | 447.6 | 147.01 | 75.09 | 0.34993 | 305.6717 | 64.10 | 0.294 | 10.993 | 13.374 |
| 6 | 447.6 | 138.71 | 74.39 | 0.34774 | 323.3496 | 63.87 | 0.402 | 10.521 | 13.184 |
| 7 | 447.6 | 149.84 | 74.77 | 0.34529 | 341.2024 | 63.60 | 0.511 | 11.173 | 13.411 |
| 8 | 447.6 | 149.09 | 74.51 | 0.34265 | 359.6973 | 63.31 | 0.624 | 11.199 | 13.313 |
| 9 | 447.6 | 139.92 | 73.70 | 0.34015 | 377.5785 | 63.04 | 0.733 | 10.658 | 13.128 |
| 10 | 447.6 | 146.17 | 72.20 | 0.33775 | 395.2790 | 62.78 | 0.841 | 9.422 | 15.513 |
| 1 | 446.4 | 84.52 | 70.29 | 0.35209 | 229.5922 | 33.75 | -0.168 | 36.532 | 2.314 |
| 2 | 446.4 | 86.17 | 71.77 | 0.35206 | 240.1798 | 45.57 | -0.104 | 26.198 | 3.289 |
| 3 | 446.4 | 84.22 | 72.96 | 0.35201 | 250.7490 | 57.19 | -0.040 | 15.766 | 5.342 |
| 4 | 446.4 | 84.92 | 73.40 | 0.35199 | 261.2404 | 64.32 | 0.024 | 9.077 | 9.356 |
| 5 | 446.4 | 85.18 | 73.65 | 0.35151 | 271.7916 | 64.27 | 0.088 | 9.376 | 9.086 |
| 6 | 446.4 | 79.82 | 73.31 | 0.35042 | 282.0263 | 64.15 | 0.150 | 9.160 | 8.714 |
| 7 | 446.4 | 87.77 | 73.62 | 0.34903 | 292.4216 | 64.01 | 0.214 | 9.619 | 9.125 |
| 8 | 446.4 | 86.24 | 73.71 | 0.34738 | 303.2151 | 63.83 | 0.280 | 9.878 | 8.730 |
| 9 | 446.4 | 79.91 | 73.41 | 0.34552 | 313.5208 | 63.63 | 0.344 | 9.782 | 8.170 |
| 10 | 446.4 | 83.48 | 72.26 | 0.34349 | 323.6557 | 63.41 | 0.406 | 8.852 | 9.430 |
| 1 | 449.3 | 48.76 | 67.95 | 0.35720 | 227.2318 | 31.09 | -0.186 | 36.857 | 1.323 |
| 2 | 449.3 | 53.04 | 68.72 | 0.35716 | 233.5069 | 38.14 | -0.148 | 30.583 | 1.734 |
| 3 | 449.3 | 53.43 | 69.70 | 0.35711 | 240.0699 | 45.45 | -0.108 | 24.250 | 2.204 |
| 4 | 449.3 | 51.23 | 70.85 | 0.35707 | 246.5216 | 52.57 | -0.069 | 18.288 | 2.801 |
| 5 | 449.3 | 49.68 | 71.82 | 0.35703 | 252.7418 | 59.36 | -0.031 | 12.457 | 3.988 |

| | | | | | | | | | |
|---|---|---|---|---|---|---|---|---|---|
| 6 | 449.3 | 46.77 | 72.01 | 0.35700 | 258.6871 | 64.86 | 0.005 | 7.157 | 6.535 |
| 7 | 449.3 | 52.79 | 72.43 | 0.35671 | 264.8240 | 64.82 | 0.042 | 7.605 | 6.941 |
| 8 | 449.3 | 51.72 | 72.59 | 0.35602 | 271.2657 | 64.75 | 0.082 | 7.839 | 6.597 |
| 9 | 449.3 | 47.36 | 72.52 | 0.35514 | 277.3733 | 64.66 | 0.120 | 7.862 | 6.024 |
| 10 | 449.3 | 48.52 | 71.73 | 0.35409 | 283.2837 | 64.55 | 0.156 | 7.185 | 6.753 |
| 1 | 446.4 | 28.47 | 64.29 | 0.34558 | 225.9914 | 29.70 | -0.186 | 34.588 | 0.823 |
| 2 | 446.4 | 20.02 | 66.61 | 0.34555 | 228.9994 | 33.09 | -0.167 | 33.523 | 0.597 |
| 3 | 446.4 | 27.27 | 66.79 | 0.34552 | 231.9329 | 36.38 | -0.150 | 30.409 | 0.897 |
| 4 | 446.4 | 27.11 | 67.01 | 0.34549 | 235.3065 | 40.16 | -0.129 | 26.853 | 1.010 |
| 5 | 446.4 | 26.39 | 67.50 | 0.34545 | 238.6250 | 43.85 | -0.109 | 23.650 | 1.116 |
| 6 | 446.4 | 23.49 | 68.02 | 0.34540 | 241.7184 | 47.28 | -0.090 | 20.742 | 1.132 |
| 7 | 446.4 | 26.60 | 68.91 | 0.34536 | 244.8250 | 50.71 | -0.072 | 18.207 | 1.461 |
| 8 | 446.4 | 25.70 | 69.53 | 0.34531 | 248.0691 | 54.27 | -0.052 | 15.267 | 1.683 |
| 9 | 446.4 | 22.51 | 70.03 | 0.34527 | 251.0595 | 57.53 | -0.034 | 12.499 | 1.801 |
| 10 | 446.4 | 21.85 | 69.76 | 0.34523 | 253.8108 | 60.53 | -0.017 | 9.233 | 2.366 |
| 1 | 558.1 | 125.14 | 78.47 | 0.42842 | 228.9239 | 32.97 | -0.220 | 45.502 | 2.750 |
| 2 | 558.1 | 128.42 | 80.02 | 0.42836 | 241.5056 | 47.02 | -0.142 | 33.008 | 3.890 |
| 3 | 558.1 | 126.30 | 81.06 | 0.42829 | 254.1447 | 60.86 | -0.064 | 20.196 | 6.254 |
| 4 | 558.1 | 126.69 | 81.44 | 0.42825 | 266.6981 | 71.89 | 0.014 | 9.557 | 13.257 |
| 5 | 558.1 | 127.04 | 81.59 | 0.42755 | 279.2883 | 71.82 | 0.092 | 9.769 | 13.005 |
| 6 | 558.1 | 119.71 | 80.85 | 0.42592 | 291.5320 | 71.67 | 0.168 | 9.179 | 13.042 |
| 7 | 558.1 | 131.05 | 81.11 | 0.42384 | 303.9744 | 71.48 | 0.246 | 9.632 | 13.605 |
| 8 | 558.1 | 128.73 | 81.17 | 0.42136 | 316.8645 | 71.25 | 0.327 | 9.920 | 12.976 |
| 9 | 558.1 | 121.48 | 80.65 | 0.41859 | 329.2797 | 70.99 | 0.405 | 9.661 | 12.575 |
| 10 | 558.1 | 123.77 | 79.77 | 0.41559 | 341.4492 | 70.70 | 0.481 | 9.064 | 13.655 |
| 1 | 563.6 | 125.32 | 77.03 | 0.40620 | 228.8106 | 32.85 | -0.208 | 44.178 | 2.837 |
| 2 | 563.6 | 128.37 | 78.56 | 0.40614 | 241.2750 | 46.77 | -0.131 | 31.795 | 4.038 |
| 3 | 563.6 | 126.29 | 79.54 | 0.40607 | 253.7866 | 60.48 | -0.054 | 19.055 | 6.628 |
| 4 | 563.6 | 127.01 | 79.85 | 0.40603 | 266.2315 | 69.79 | 0.023 | 10.058 | 12.628 |
| 5 | 563.6 | 127.01 | 80.02 | 0.40527 | 278.7117 | 69.72 | 0.100 | 10.297 | 12.334 |
| 6 | 563.6 | 119.87 | 79.26 | 0.40351 | 290.8412 | 69.55 | 0.175 | 9.705 | 12.352 |
| 7 | 563.6 | 131.02 | 79.51 | 0.40130 | 303.1681 | 69.34 | 0.252 | 10.175 | 12.877 |
| 8 | 563.6 | 128.85 | 79.54 | 0.39867 | 315.9359 | 69.08 | 0.332 | 10.456 | 12.322 |
| 9 | 563.6 | 121.49 | 79.00 | 0.39575 | 328.2353 | 68.80 | 0.409 | 10.204 | 11.906 |
| 10 | 563.6 | 124.17 | 78.07 | 0.39259 | 340.3047 | 68.49 | 0.484 | 9.581 | 12.960 |
| 1 | 558.1 | 125.42 | 75.00 | 0.37905 | 228.8713 | 32.93 | -0.190 | 42.067 | 2.981 |
| 2 | 558.1 | 128.42 | 76.45 | 0.37899 | 241.4666 | 46.99 | -0.113 | 29.457 | 4.360 |
| 3 | 558.1 | 126.33 | 77.31 | 0.37893 | 254.1074 | 60.84 | -0.036 | 16.469 | 7.671 |
| 4 | 558.1 | 127.50 | 77.53 | 0.37834 | 266.7025 | 67.06 | 0.041 | 10.464 | 12.184 |
| 5 | 558.1 | 126.95 | 77.72 | 0.37694 | 279.3280 | 66.92 | 0.119 | 10.800 | 11.754 |
| 6 | 558.1 | 120.16 | 76.93 | 0.37500 | 291.5893 | 66.73 | 0.195 | 10.205 | 11.775 |
| 7 | 558.1 | 131.02 | 77.19 | 0.37261 | 304.0526 | 66.48 | 0.272 | 10.705 | 12.239 |
| 8 | 558.1 | 129.04 | 77.18 | 0.36982 | 316.9567 | 66.19 | 0.352 | 10.989 | 11.742 |
| 9 | 558.1 | 121.46 | 76.64 | 0.36673 | 329.3864 | 65.87 | 0.429 | 10.766 | 11.281 |
| 10 | 558.1 | 124.74 | 75.63 | 0.36342 | 341.6030 | 65.53 | 0.505 | 10.100 | 12.351 |
| 1 | 558.1 | 125.46 | 73.02 | 0.35069 | 228.8792 | 32.95 | -0.172 | 40.071 | 3.131 |
| 2 | 558.1 | 128.36 | 74.37 | 0.35062 | 241.4737 | 47.01 | -0.095 | 27.366 | 4.691 |
| 3 | 558.1 | 126.57 | 75.07 | 0.35057 | 254.1236 | 60.86 | -0.019 | 14.209 | 8.908 |
| 4 | 558.1 | 127.83 | 75.22 | 0.34989 | 266.7471 | 64.10 | 0.058 | 11.120 | 11.496 |
| 5 | 558.1 | 127.05 | 75.41 | 0.34828 | 279.3941 | 63.92 | 0.136 | 11.484 | 11.063 |

| | | | | | | | | | | |
|---|---|---|---|---|---|---|---|---|---|---|
| | 6 | 558.1 | 120.33 | 74.61 | 0.34615 | 291.6691 | 63.69 | 0.211 | 10.915 | 11.024 |
| | 7 | 558.1 | 131.03 | 74.85 | 0.34356 | 304.1415 | 63.41 | 0.288 | 11.434 | 11.459 |
| | 8 | 558.1 | 129.21 | 74.81 | 0.34056 | 317.0543 | 63.09 | 0.368 | 11.721 | 11.024 |
| | 9 | 558.1 | 121.40 | 74.24 | 0.33726 | 329.4895 | 62.72 | 0.444 | 11.518 | 10.540 |
| | 10 | 558.1 | 125.41 | 73.12 | 0.33372 | 341.7364 | 62.33 | 0.520 | 10.789 | 11.624 |
| | 1 | 558.1 | 125.69 | 70.29 | 0.32021 | 228.8913 | 32.98 | -0.151 | 37.317 | 3.368 |
| | 2 | 558.1 | 128.40 | 71.57 | 0.32015 | 241.4994 | 47.05 | -0.075 | 24.523 | 5.236 |
| | 3 | 558.1 | 126.94 | 72.14 | 0.32010 | 254.1691 | 60.79 | 0.001 | 11.354 | 11.180 |
| | 4 | 558.1 | 128.04 | 72.29 | 0.31931 | 266.8212 | 60.70 | 0.078 | 11.588 | 11.049 |
| | 5 | 558.1 | 127.04 | 72.50 | 0.31747 | 279.4786 | 60.49 | 0.155 | 12.016 | 10.573 |
| | 6 | 558.1 | 120.69 | 71.68 | 0.31510 | 291.7712 | 60.21 | 0.230 | 11.468 | 10.524 |
| | 7 | 558.1 | 130.91 | 71.93 | 0.31226 | 304.2557 | 59.88 | 0.306 | 12.055 | 10.860 |
| | 8 | 558.1 | 129.33 | 71.84 | 0.30899 | 317.1692 | 59.50 | 0.385 | 12.343 | 10.478 |
| | 9 | 558.1 | 121.39 | 71.20 | 0.30542 | 329.6103 | 59.07 | 0.461 | 12.128 | 10.009 |
| | 10 | 558.1 | 126.30 | 69.93 | 0.30159 | 341.9009 | 58.61 | 0.537 | 11.311 | 11.166 |
| | 1 | 558.1 | 125.15 | 68.29 | 0.29027 | 228.8711 | 32.97 | -0.129 | 35.328 | 3.542 |
| | 2 | 558.1 | 128.75 | 69.28 | 0.29020 | 241.4694 | 47.02 | -0.054 | 22.256 | 5.785 |
| | 3 | 558.1 | 127.56 | 69.62 | 0.29016 | 254.1875 | 57.22 | 0.021 | 12.405 | 10.283 |
| | 4 | 558.1 | 128.20 | 69.76 | 0.28925 | 266.8786 | 57.11 | 0.097 | 12.648 | 10.136 |
| | 5 | 558.1 | 127.09 | 69.97 | 0.28715 | 279.5462 | 56.85 | 0.174 | 13.124 | 9.684 |
| | 6 | 558.1 | 120.94 | 69.12 | 0.28450 | 291.8534 | 56.51 | 0.249 | 12.602 | 9.597 |
| | 7 | 558.1 | 130.78 | 69.36 | 0.28137 | 304.3440 | 56.12 | 0.325 | 13.236 | 9.880 |
| | 8 | 558.1 | 129.46 | 69.17 | 0.27780 | 317.2572 | 55.66 | 0.403 | 13.507 | 9.585 |
| | 9 | 558.1 | 121.28 | 68.43 | 0.27390 | 329.6989 | 55.16 | 0.479 | 13.267 | 9.142 |
| | 10 | 558.1 | 127.33 | 66.93 | 0.26974 | 342.0351 | 54.62 | 0.554 | 12.306 | 10.347 |
| | 1 | 167.4 | 36.02 | 78.04 | 0.46110 | 228.0469 | 31.97 | -0.245 | 46.072 | 0.782 |
| | 2 | 167.4 | 18.09 | 81.87 | 0.46109 | 236.9975 | 42.00 | -0.189 | 39.865 | 0.454 |
| | 3 | 167.4 | 32.70 | 81.13 | 0.46108 | 245.3995 | 51.30 | -0.136 | 29.827 | 1.096 |
| | 4 | 167.4 | 35.42 | 80.44 | 0.46107 | 256.6673 | 63.59 | -0.066 | 16.854 | 2.102 |
| | 5 | 167.4 | 30.31 | 81.02 | 0.46107 | 267.5385 | 74.83 | 0.002 | 6.195 | 4.892 |
| | 6 | 167.4 | 27.40 | 81.18 | 0.46101 | 277.0834 | 74.82 | 0.062 | 6.356 | 4.311 |
| | 7 | 167.4 | 32.16 | 81.58 | 0.46088 | 286.9355 | 74.81 | 0.123 | 6.768 | 4.752 |
| | 8 | 167.4 | 30.98 | 81.71 | 0.46072 | 297.3800 | 74.80 | 0.188 | 6.915 | 4.480 |
| | 9 | 167.4 | 27.88 | 81.65 | 0.46055 | 307.1167 | 74.78 | 0.249 | 6.870 | 4.059 |
| | 10 | 167.4 | 26.61 | 80.98 | 0.46036 | 316.1305 | 74.77 | 0.306 | 6.213 | 4.283 |
| | 1 | 167.4 | 49.98 | 82.05 | 0.47728 | 230.3679 | 34.58 | -0.239 | 47.472 | 1.053 |
| | 2 | 167.4 | 62.61 | 81.86 | 0.47727 | 248.9921 | 55.24 | -0.122 | 26.628 | 2.351 |
| | 3 | 167.4 | 57.47 | 83.00 | 0.47727 | 268.8543 | 76.22 | 0.002 | 6.774 | 8.484 |
| | 4 | 167.4 | 57.77 | 83.37 | 0.47717 | 287.9145 | 76.22 | 0.122 | 7.154 | 8.074 |
| | 5 | 167.4 | 57.31 | 83.67 | 0.47698 | 306.9486 | 76.20 | 0.241 | 7.473 | 7.669 |
| | 6 | 167.4 | 53.36 | 83.49 | 0.47675 | 325.2546 | 76.18 | 0.356 | 7.311 | 7.299 |
| | 7 | 167.4 | 59.85 | 83.94 | 0.47648 | 343.9807 | 76.16 | 0.474 | 7.781 | 7.692 |
| | 8 | 167.4 | 57.68 | 84.22 | 0.47616 | 363.4208 | 76.13 | 0.596 | 8.088 | 7.131 |
| | 9 | 167.4 | 53.30 | 84.09 | 0.47582 | 381.7777 | 76.10 | 0.711 | 7.986 | 6.674 |
| | 10 | 167.4 | 53.55 | 83.22 | 0.47546 | 399.4509 | 76.07 | 0.822 | 7.153 | 7.486 |
| | 1 | 279.0 | 32.95 | 73.24 | 0.45264 | 225.6430 | 29.26 | -0.255 | 43.976 | 0.749 |
| | 2 | 279.0 | 22.85 | 76.29 | 0.45262 | 231.1805 | 35.50 | -0.220 | 40.788 | 0.560 |
| | 3 | 279.0 | 30.69 | 76.94 | 0.45261 | 236.4934 | 41.44 | -0.187 | 35.495 | 0.865 |
| | 4 | 279.0 | 29.93 | 77.39 | 0.45259 | 242.5095 | 48.12 | -0.150 | 29.271 | 1.023 |
| | 5 | 279.0 | 30.77 | 77.85 | 0.45258 | 248.5340 | 54.74 | -0.112 | 23.104 | 1.332 |

| | | | | | | | | | |
|---|---|---|---|---|---|---|---|---|---|
| 6 | 279.0 | 26.13 | 78.58 | 0.45256 | 254.1809 | 60.90 | -0.077 | 17.685 | 1.477 |
| 7 | 279.0 | 30.27 | 79.63 | 0.45255 | 259.7780 | 66.94 | -0.042 | 12.687 | 2.386 |
| 8 | 279.0 | 28.18 | 80.33 | 0.45254 | 265.5792 | 73.14 | -0.006 | 7.186 | 3.922 |
| 9 | 279.0 | 26.33 | 80.47 | 0.45245 | 270.9899 | 74.07 | 0.028 | 6.403 | 4.113 |
| 10 | 279.0 | 24.46 | 80.05 | 0.45226 | 276.0314 | 74.05 | 0.059 | 5.993 | 4.082 |
| 1 | 279.0 | 47.01 | 79.95 | 0.46449 | 227.1825 | 31.00 | -0.252 | 48.954 | 0.960 |
| 2 | 279.0 | 59.16 | 79.65 | 0.46447 | 237.7190 | 42.80 | -0.186 | 36.849 | 1.605 |
| 3 | 279.0 | 58.04 | 80.47 | 0.46446 | 249.3507 | 55.63 | -0.113 | 24.836 | 2.337 |
| 4 | 279.0 | 53.07 | 81.72 | 0.46444 | 260.3780 | 67.58 | -0.044 | 14.136 | 3.754 |
| 5 | 279.0 | 53.49 | 82.28 | 0.46443 | 270.9537 | 75.12 | 0.022 | 7.162 | 7.468 |
| 6 | 279.0 | 49.93 | 82.16 | 0.46427 | 281.2176 | 75.11 | 0.086 | 7.057 | 7.075 |
| 7 | 279.0 | 57.15 | 82.41 | 0.46387 | 291.8452 | 75.07 | 0.153 | 7.337 | 7.790 |
| 8 | 279.0 | 54.78 | 82.63 | 0.46335 | 302.9543 | 75.03 | 0.222 | 7.603 | 7.205 |
| 9 | 279.0 | 51.14 | 82.47 | 0.46274 | 313.4667 | 74.97 | 0.288 | 7.493 | 6.825 |
| 10 | 279.0 | 50.16 | 81.85 | 0.46205 | 323.5212 | 74.92 | 0.351 | 6.936 | 7.232 |
| 1 | 290.2 | 58.53 | 81.09 | 0.45939 | 228.0296 | 31.95 | -0.244 | 49.138 | 1.191 |
| 2 | 290.2 | 75.85 | 80.17 | 0.45937 | 240.8523 | 46.28 | -0.164 | 33.891 | 2.238 |
| 3 | 290.2 | 68.97 | 81.34 | 0.45935 | 254.6709 | 61.43 | -0.077 | 19.914 | 3.463 |
| 4 | 290.2 | 67.37 | 82.06 | 0.45934 | 267.6808 | 74.68 | 0.004 | 7.379 | 9.130 |
| 5 | 290.2 | 67.81 | 82.36 | 0.45915 | 280.5802 | 74.66 | 0.084 | 7.698 | 8.809 |
| 6 | 290.2 | 63.20 | 82.07 | 0.45869 | 293.0818 | 74.62 | 0.163 | 7.450 | 8.483 |
| 7 | 290.2 | 71.28 | 82.32 | 0.45808 | 305.9142 | 74.57 | 0.243 | 7.750 | 9.197 |
| 8 | 290.2 | 68.56 | 82.59 | 0.45735 | 319.2580 | 74.50 | 0.326 | 8.082 | 8.483 |
| 9 | 290.2 | 64.23 | 82.40 | 0.45654 | 331.9294 | 74.43 | 0.406 | 7.968 | 8.061 |
| 10 | 290.2 | 63.97 | 81.73 | 0.45567 | 344.1627 | 74.36 | 0.482 | 7.374 | 8.676 |
| 1 | 279.0 | 78.66 | 82.30 | 0.46677 | 230.1686 | 34.36 | -0.234 | 47.945 | 1.641 |
| 2 | 279.0 | 92.12 | 82.02 | 0.46675 | 247.1177 | 53.19 | -0.128 | 28.839 | 3.194 |
| 3 | 279.0 | 86.29 | 82.97 | 0.46674 | 264.8239 | 72.34 | -0.018 | 10.634 | 8.114 |
| 4 | 279.0 | 87.09 | 83.19 | 0.46653 | 282.0311 | 75.30 | 0.090 | 7.891 | 11.036 |
| 5 | 279.0 | 86.49 | 83.44 | 0.46603 | 299.2580 | 75.26 | 0.198 | 8.180 | 10.573 |
| 6 | 279.0 | 80.99 | 83.03 | 0.46537 | 315.8799 | 75.20 | 0.302 | 7.832 | 10.342 |
| 7 | 279.0 | 90.18 | 83.37 | 0.46459 | 332.8683 | 75.14 | 0.409 | 8.239 | 10.945 |
| 8 | 279.0 | 87.08 | 83.73 | 0.46382 | 350.4607 | 75.07 | 0.519 | 8.659 | 10.057 |
| 9 | 279.0 | 81.70 | 83.50 | 0.46309 | 367.2120 | 75.01 | 0.624 | 8.492 | 9.621 |
| 10 | 279.0 | 82.74 | 82.66 | 0.46230 | 383.5326 | 74.94 | 0.726 | 7.723 | 10.714 |
| 1 | 334.8 | 49.38 | 78.41 | 0.46491 | 226.6286 | 30.37 | -0.256 | 48.036 | 1.028 |
| 2 | 334.8 | 55.14 | 79.06 | 0.46489 | 235.2729 | 40.08 | -0.201 | 38.984 | 1.414 |
| 3 | 334.8 | 57.58 | 79.72 | 0.46487 | 244.5954 | 50.41 | -0.143 | 29.309 | 1.965 |
| 4 | 334.8 | 53.65 | 80.94 | 0.46485 | 253.7943 | 60.47 | -0.086 | 20.470 | 2.621 |
| 5 | 334.8 | 51.94 | 81.88 | 0.46483 | 262.5271 | 69.88 | -0.031 | 11.998 | 4.329 |
| 6 | 334.8 | 48.95 | 81.92 | 0.46482 | 270.8716 | 75.16 | 0.021 | 6.761 | 7.241 |
| 7 | 334.8 | 56.09 | 82.24 | 0.46461 | 279.5589 | 75.14 | 0.075 | 7.099 | 7.901 |
| 8 | 334.8 | 54.18 | 82.44 | 0.46411 | 288.6784 | 75.09 | 0.133 | 7.345 | 7.376 |
| 9 | 334.8 | 50.22 | 82.33 | 0.46348 | 297.3127 | 75.04 | 0.187 | 7.293 | 6.887 |
| 10 | 334.8 | 49.44 | 81.70 | 0.46274 | 305.5549 | 74.98 | 0.239 | 6.727 | 7.350 |
| 1 | 334.8 | 62.40 | 79.63 | 0.46243 | 227.7939 | 31.69 | -0.247 | 47.943 | 1.302 |
| 2 | 334.8 | 73.55 | 79.73 | 0.46241 | 239.0372 | 44.27 | -0.177 | 35.457 | 2.074 |
| 3 | 334.8 | 70.25 | 80.94 | 0.46239 | 250.9297 | 57.36 | -0.102 | 23.583 | 2.979 |
| 4 | 334.8 | 67.28 | 81.98 | 0.46237 | 262.3040 | 69.65 | -0.031 | 12.335 | 5.455 |
| 5 | 334.8 | 68.01 | 82.39 | 0.46218 | 273.4927 | 74.93 | 0.039 | 7.467 | 9.107 |

| | | | | | | | | | |
|---|---|---|---|---|---|---|---|---|---|
| 6 | 334.8 | 63.62 | 82.13 | 0.46175 | 284.3781 | 74.89 | 0.107 | 7.241 | 8.785 |
| 7 | 334.8 | 71.67 | 82.38 | 0.46112 | 295.5668 | 74.83 | 0.177 | 7.550 | 9.494 |
| 8 | 334.8 | 69.27 | 82.61 | 0.46033 | 307.2230 | 74.77 | 0.250 | 7.847 | 8.827 |
| 9 | 334.8 | 64.69 | 82.45 | 0.45942 | 318.3012 | 74.69 | 0.320 | 7.769 | 8.326 |
| 10 | 334.8 | 64.46 | 81.80 | 0.45842 | 328.9815 | 74.60 | 0.387 | 7.199 | 8.954 |
| 1 | 334.8 | 79.81 | 81.12 | 0.46331 | 229.1483 | 33.21 | -0.239 | 47.910 | 1.666 |
| 2 | 334.8 | 93.10 | 81.00 | 0.46329 | 243.4485 | 49.15 | -0.150 | 31.853 | 2.923 |
| 3 | 334.8 | 86.44 | 82.30 | 0.46328 | 258.2973 | 65.34 | -0.057 | 16.956 | 5.098 |
| 4 | 334.8 | 86.79 | 82.76 | 0.46327 | 272.6244 | 75.02 | 0.033 | 7.744 | 11.208 |
| 5 | 334.8 | 86.72 | 83.02 | 0.46296 | 286.9747 | 74.99 | 0.123 | 8.024 | 10.808 |
| 6 | 334.8 | 81.41 | 82.56 | 0.46224 | 300.8795 | 74.93 | 0.210 | 7.631 | 10.669 |
| 7 | 334.8 | 90.58 | 82.84 | 0.46134 | 315.1031 | 74.85 | 0.299 | 7.989 | 11.338 |
| 8 | 334.8 | 87.83 | 83.12 | 0.46030 | 329.8584 | 74.76 | 0.391 | 8.361 | 10.505 |
| 9 | 334.8 | 82.40 | 82.93 | 0.45916 | 343.9369 | 74.66 | 0.480 | 8.263 | 9.971 |
| 10 | 334.8 | 82.88 | 82.23 | 0.45795 | 357.6060 | 74.56 | 0.565 | 7.675 | 10.799 |
| 1 | 337.6 | 97.44 | 82.13 | 0.46031 | 230.5412 | 34.78 | -0.229 | 47.348 | 2.058 |
| 2 | 337.6 | 109.12 | 82.14 | 0.46029 | 247.4834 | 53.59 | -0.123 | 28.552 | 3.822 |
| 3 | 337.6 | 104.23 | 82.92 | 0.46027 | 264.9823 | 72.51 | -0.014 | 10.411 | 10.012 |
| 4 | 337.6 | 105.14 | 83.07 | 0.45996 | 282.1549 | 74.73 | 0.094 | 8.339 | 12.608 |
| 5 | 337.6 | 104.44 | 83.29 | 0.45923 | 299.3446 | 74.67 | 0.201 | 8.625 | 12.109 |
| 6 | 337.6 | 98.19 | 82.75 | 0.45829 | 315.9641 | 74.59 | 0.306 | 8.167 | 12.022 |
| 7 | 337.6 | 108.42 | 83.10 | 0.45717 | 332.9101 | 74.49 | 0.412 | 8.607 | 12.596 |
| 8 | 337.6 | 105.45 | 83.40 | 0.45593 | 350.4522 | 74.38 | 0.522 | 9.020 | 11.690 |
| 9 | 337.6 | 99.13 | 83.11 | 0.45476 | 367.2327 | 74.28 | 0.627 | 8.834 | 11.221 |
| 10 | 337.6 | 100.81 | 82.26 | 0.45367 | 383.6323 | 74.18 | 0.729 | 8.077 | 12.481 |
| 1 | 334.8 | 121.08 | 83.17 | 0.46439 | 232.5112 | 36.99 | -0.218 | 46.182 | 2.622 |
| 2 | 334.8 | 131.50 | 83.34 | 0.46437 | 253.4004 | 60.05 | -0.088 | 23.294 | 5.645 |
| 3 | 334.8 | 128.16 | 83.72 | 0.46436 | 274.8753 | 75.12 | 0.046 | 8.603 | 14.897 |
| 4 | 334.8 | 128.90 | 83.76 | 0.46393 | 296.1348 | 75.08 | 0.179 | 8.687 | 14.838 |
| 5 | 334.8 | 128.03 | 83.99 | 0.46296 | 317.3830 | 74.99 | 0.312 | 8.995 | 14.233 |
| 6 | 334.8 | 120.69 | 83.35 | 0.46180 | 337.9528 | 74.89 | 0.441 | 8.455 | 14.276 |
| 7 | 334.8 | 131.80 | 83.82 | 0.46051 | 358.8350 | 74.78 | 0.572 | 9.036 | 14.587 |
| 8 | 334.8 | 130.03 | 84.01 | 0.45926 | 380.4895 | 74.67 | 0.708 | 9.336 | 13.928 |
| 9 | 334.8 | 128.97 | 83.75 | 0.45806 | 401.9101 | 74.57 | 0.842 | 9.185 | 14.042 |
| 10 | 334.8 | 116.20 | 86.01 | 0.45693 | 422.1866 | 74.47 | 0.969 | 11.547 | 10.063 |
| 1 | 446.4 | 50.99 | 77.18 | 0.46239 | 225.8260 | 29.47 | -0.259 | 47.710 | 1.069 |
| 2 | 446.4 | 51.95 | 78.40 | 0.46235 | 232.2114 | 36.65 | -0.219 | 41.750 | 1.244 |
| 3 | 446.4 | 57.39 | 78.64 | 0.46231 | 238.9934 | 44.22 | -0.177 | 34.419 | 1.667 |
| 4 | 446.4 | 54.30 | 79.53 | 0.46226 | 245.9210 | 51.87 | -0.134 | 27.653 | 1.964 |
| 5 | 446.4 | 53.54 | 80.42 | 0.46222 | 252.6099 | 59.19 | -0.092 | 21.228 | 2.522 |
| 6 | 446.4 | 48.24 | 81.01 | 0.46218 | 258.9227 | 66.02 | -0.052 | 14.989 | 3.218 |
| 7 | 446.4 | 54.58 | 81.73 | 0.46214 | 265.3003 | 72.84 | -0.012 | 8.892 | 6.139 |
| 8 | 446.4 | 53.80 | 81.93 | 0.46191 | 272.0228 | 74.90 | 0.030 | 7.025 | 7.658 |
| 9 | 446.4 | 50.13 | 81.79 | 0.46138 | 278.4691 | 74.86 | 0.070 | 6.931 | 7.232 |
| 10 | 446.4 | 49.10 | 81.20 | 0.46067 | 284.6242 | 74.79 | 0.109 | 6.405 | 7.666 |
| 1 | 446.4 | 64.14 | 78.44 | 0.46495 | 226.6264 | 30.37 | -0.256 | 48.075 | 1.334 |
| 2 | 446.4 | 70.18 | 79.22 | 0.46492 | 234.9576 | 39.73 | -0.203 | 39.492 | 1.777 |
| 3 | 446.4 | 71.09 | 80.11 | 0.46487 | 243.7198 | 49.45 | -0.149 | 30.661 | 2.318 |
| 4 | 446.4 | 67.97 | 81.30 | 0.46483 | 252.3455 | 58.90 | -0.095 | 22.401 | 3.034 |
| 5 | 446.4 | 66.61 | 82.20 | 0.46479 | 260.6938 | 67.92 | -0.043 | 14.276 | 4.666 |

| | | | | | | | | | |
|---|---|---|---|---|---|---|---|---|---|
| 6 | 446.4 | 62.50 | 82.18 | 0.46476 | 268.7024 | 75.15 | 0.007 | 7.031 | 8.888 |
| 7 | 446.4 | 70.69 | 82.48 | 0.46444 | 276.9636 | 75.12 | 0.059 | 7.354 | 9.612 |
| 8 | 446.4 | 68.68 | 82.59 | 0.46369 | 285.6081 | 75.06 | 0.114 | 7.537 | 9.112 |
| 9 | 446.4 | 64.57 | 82.28 | 0.46272 | 293.8733 | 74.97 | 0.166 | 7.312 | 8.831 |
| 10 | 446.4 | 64.00 | 81.62 | 0.46156 | 301.8484 | 74.87 | 0.216 | 6.746 | 9.487 |
| 1 | 446.4 | 85.18 | 79.82 | 0.46510 | 227.7215 | 31.60 | -0.249 | 48.219 | 1.767 |
| 2 | 446.4 | 93.11 | 80.60 | 0.46507 | 238.7805 | 43.98 | -0.180 | 36.617 | 2.543 |
| 3 | 446.4 | 90.11 | 81.93 | 0.46502 | 250.1451 | 56.50 | -0.109 | 25.426 | 3.544 |
| 4 | 446.4 | 88.24 | 82.84 | 0.46498 | 261.2079 | 68.47 | -0.039 | 14.373 | 6.140 |
| 5 | 446.4 | 88.84 | 83.21 | 0.46496 | 272.1923 | 75.17 | 0.029 | 8.041 | 11.049 |
| 6 | 446.4 | 83.54 | 82.77 | 0.46454 | 282.8848 | 75.13 | 0.096 | 7.635 | 10.941 |
| 7 | 446.4 | 92.64 | 83.02 | 0.46354 | 293.8130 | 75.04 | 0.165 | 7.972 | 11.622 |
| 8 | 446.4 | 90.38 | 83.11 | 0.46227 | 305.1658 | 74.93 | 0.236 | 8.177 | 11.054 |
| 9 | 446.4 | 85.19 | 82.72 | 0.46079 | 316.0560 | 74.81 | 0.305 | 7.912 | 10.767 |
| 10 | 446.4 | 85.46 | 81.98 | 0.45915 | 326.6412 | 74.66 | 0.372 | 7.324 | 11.670 |
| 1 | 446.4 | 100.25 | 80.85 | 0.46284 | 228.7642 | 32.78 | -0.241 | 48.066 | 2.086 |
| 2 | 446.4 | 107.82 | 81.70 | 0.46281 | 241.6701 | 47.19 | -0.160 | 34.516 | 3.124 |
| 3 | 446.4 | 104.00 | 82.89 | 0.46276 | 254.8089 | 61.57 | -0.078 | 21.319 | 4.879 |
| 4 | 446.4 | 104.02 | 83.37 | 0.46273 | 267.7125 | 74.97 | 0.002 | 8.400 | 12.384 |
| 5 | 446.4 | 104.37 | 83.57 | 0.46230 | 280.6389 | 74.94 | 0.083 | 8.635 | 12.087 |
| 6 | 446.4 | 98.04 | 83.00 | 0.46129 | 293.1942 | 74.85 | 0.162 | 8.150 | 12.029 |
| 7 | 446.4 | 108.16 | 83.27 | 0.45998 | 305.9845 | 74.73 | 0.243 | 8.533 | 12.676 |
| 8 | 446.4 | 105.49 | 83.41 | 0.45840 | 319.2370 | 74.60 | 0.326 | 8.815 | 11.968 |
| 9 | 446.4 | 99.77 | 82.95 | 0.45663 | 331.9691 | 74.44 | 0.406 | 8.512 | 11.721 |
| 10 | 446.4 | 100.62 | 82.18 | 0.45473 | 344.3986 | 74.27 | 0.484 | 7.912 | 12.718 |
| 1 | 457.6 | 123.28 | 81.79 | 0.45666 | 229.8864 | 34.05 | -0.231 | 47.743 | 2.582 |
| 2 | 457.6 | 130.76 | 82.60 | 0.45662 | 245.2589 | 51.15 | -0.135 | 31.452 | 4.157 |
| 3 | 457.6 | 127.25 | 83.38 | 0.45657 | 260.8717 | 68.11 | -0.037 | 15.272 | 8.332 |
| 4 | 457.6 | 128.28 | 83.52 | 0.45613 | 276.3345 | 74.40 | 0.059 | 9.123 | 14.062 |
| 5 | 457.6 | 128.02 | 83.65 | 0.45506 | 291.8437 | 74.30 | 0.157 | 9.344 | 13.700 |
| 6 | 457.6 | 120.61 | 82.90 | 0.45361 | 306.8886 | 74.17 | 0.251 | 8.722 | 13.828 |
| 7 | 457.6 | 132.20 | 83.20 | 0.45185 | 322.1869 | 74.02 | 0.347 | 9.186 | 14.392 |
| 8 | 457.6 | 129.39 | 83.38 | 0.44984 | 338.0164 | 73.84 | 0.446 | 9.541 | 13.562 |
| 9 | 457.6 | 122.52 | 82.91 | 0.44769 | 353.2598 | 73.65 | 0.542 | 9.257 | 13.235 |
| 10 | 457.6 | 124.03 | 82.17 | 0.44546 | 368.1789 | 73.45 | 0.636 | 8.719 | 14.225 |
| 1 | 558.1 | 81.94 | 78.40 | 0.46562 | 226.8069 | 30.57 | -0.255 | 47.831 | 1.713 |
| 2 | 558.1 | 85.04 | 79.77 | 0.46556 | 235.0927 | 39.88 | -0.203 | 39.898 | 2.131 |
| 3 | 558.1 | 86.59 | 80.75 | 0.46549 | 243.6090 | 49.33 | -0.150 | 31.426 | 2.755 |
| 4 | 558.1 | 84.01 | 81.92 | 0.46543 | 252.0741 | 58.60 | -0.097 | 23.315 | 3.603 |
| 5 | 558.1 | 82.73 | 82.80 | 0.46536 | 260.3475 | 67.55 | -0.045 | 15.257 | 5.422 |
| 6 | 558.1 | 77.79 | 82.71 | 0.46532 | 268.3124 | 75.20 | 0.005 | 7.509 | 10.360 |
| 7 | 558.1 | 86.95 | 83.04 | 0.46485 | 276.4870 | 75.16 | 0.056 | 7.879 | 11.036 |
| 8 | 558.1 | 85.00 | 83.13 | 0.46374 | 285.0197 | 75.06 | 0.110 | 8.067 | 10.537 |
| 9 | 558.1 | 80.17 | 82.75 | 0.46231 | 293.2156 | 74.94 | 0.162 | 7.816 | 10.257 |
| 10 | 558.1 | 80.02 | 82.08 | 0.46061 | 301.1641 | 74.79 | 0.212 | 7.291 | 10.975 |
| 1 | 558.1 | 124.38 | 80.93 | 0.46029 | 228.8320 | 32.86 | -0.239 | 48.076 | 2.587 |
| 2 | 558.1 | 128.78 | 82.37 | 0.46022 | 241.3941 | 46.88 | -0.161 | 35.490 | 3.629 |
| 3 | 558.1 | 126.45 | 83.46 | 0.46016 | 254.0588 | 60.76 | -0.082 | 22.703 | 5.570 |
| 4 | 558.1 | 126.27 | 83.95 | 0.46011 | 266.5986 | 74.22 | -0.003 | 9.725 | 12.983 |
| 5 | 558.1 | 126.84 | 84.10 | 0.45948 | 279.1582 | 74.69 | 0.075 | 9.407 | 13.483 |

| | | | | | | | | | |
|---|---|---|---|---|---|---|---|---|---|
| 6 | 558.1 | 119.61 | 83.33 | 0.45802 | 291.3875 | 74.56 | 0.152 | 8.771 | 13.637 |
| 7 | 558.1 | 130.98 | 83.61 | 0.45611 | 303.8221 | 74.39 | 0.231 | 9.221 | 14.205 |
| 8 | 558.1 | 128.52 | 83.69 | 0.45380 | 316.6985 | 74.19 | 0.312 | 9.504 | 13.523 |
| 9 | 558.1 | 121.50 | 83.17 | 0.45120 | 329.1043 | 73.96 | 0.390 | 9.210 | 13.192 |
| 10 | 558.1 | 123.20 | 82.36 | 0.44838 | 341.2465 | 73.71 | 0.467 | 8.647 | 14.248 |
| 1 | 558.1 | 167.06 | 83.12 | 0.45699 | 230.9991 | 35.30 | -0.224 | 47.829 | 3.493 |
| 2 | 558.1 | 173.54 | 84.16 | 0.45693 | 247.8998 | 54.05 | -0.118 | 30.115 | 5.763 |
| 3 | 558.1 | 170.78 | 84.60 | 0.45688 | 264.9853 | 72.51 | -0.012 | 12.089 | 14.127 |
| 4 | 558.1 | 171.73 | 84.61 | 0.45609 | 281.9808 | 74.39 | 0.095 | 10.217 | 16.809 |
| 5 | 558.1 | 171.69 | 84.64 | 0.45423 | 299.0213 | 74.23 | 0.202 | 10.408 | 16.495 |
| 6 | 558.1 | 162.09 | 83.57 | 0.45185 | 315.5832 | 74.02 | 0.306 | 9.556 | 16.961 |
| 7 | 558.1 | 176.56 | 83.86 | 0.44905 | 332.3870 | 73.77 | 0.412 | 10.096 | 17.489 |
| 8 | 558.1 | 173.79 | 83.95 | 0.44593 | 349.7715 | 73.49 | 0.521 | 10.458 | 16.618 |
| 9 | 558.1 | 164.32 | 83.32 | 0.44267 | 366.5486 | 73.20 | 0.626 | 10.122 | 16.234 |
| 10 | 558.1 | 168.11 | 82.36 | 0.43937 | 383.0439 | 72.90 | 0.730 | 9.460 | 17.771 |
| 1 | 558.1 | 141.34 | 81.74 | 0.45666 | 229.7084 | 33.85 | -0.232 | 47.892 | 2.951 |
| 2 | 558.1 | 145.32 | 83.17 | 0.45660 | 243.9328 | 49.69 | -0.143 | 33.479 | 4.341 |
| 3 | 558.1 | 143.63 | 83.88 | 0.45653 | 258.2707 | 65.32 | -0.054 | 18.564 | 7.737 |
| 4 | 558.1 | 144.23 | 84.08 | 0.45650 | 272.5544 | 74.43 | 0.036 | 9.650 | 14.946 |
| 5 | 558.1 | 144.27 | 84.19 | 0.45569 | 286.8699 | 74.36 | 0.125 | 9.835 | 14.670 |
| 6 | 558.1 | 135.93 | 83.34 | 0.45383 | 300.7733 | 74.19 | 0.213 | 9.149 | 14.856 |
| 7 | 558.1 | 148.67 | 83.61 | 0.45153 | 314.8950 | 73.99 | 0.302 | 9.622 | 15.451 |
| 8 | 558.1 | 146.02 | 83.69 | 0.44885 | 329.5174 | 73.75 | 0.394 | 9.941 | 14.688 |
| 9 | 558.1 | 138.02 | 83.12 | 0.44593 | 343.6115 | 73.49 | 0.483 | 9.627 | 14.336 |
| 10 | 558.1 | 140.70 | 82.21 | 0.44283 | 357.4418 | 73.21 | 0.570 | 8.998 | 15.638 |
| 1 | 558.1 | 99.37 | 79.58 | 0.46402 | 227.7858 | 31.68 | -0.248 | 47.899 | 2.075 |
| 2 | 558.1 | 102.91 | 81.08 | 0.46395 | 237.8231 | 42.92 | -0.185 | 38.165 | 2.697 |
| 3 | 558.1 | 102.11 | 82.32 | 0.46389 | 247.9963 | 54.15 | -0.121 | 28.173 | 3.624 |
| 4 | 558.1 | 100.43 | 83.24 | 0.46382 | 258.0460 | 65.07 | -0.059 | 18.168 | 5.528 |
| 5 | 558.1 | 100.64 | 83.68 | 0.46378 | 268.0230 | 75.07 | 0.004 | 8.619 | 11.677 |
| 6 | 558.1 | 94.84 | 83.21 | 0.46326 | 277.7227 | 75.02 | 0.065 | 8.190 | 11.580 |
| 7 | 558.1 | 104.83 | 83.48 | 0.46201 | 287.6305 | 74.91 | 0.127 | 8.571 | 12.231 |
| 8 | 558.1 | 102.47 | 83.58 | 0.46036 | 297.9168 | 74.77 | 0.192 | 8.816 | 11.622 |
| 9 | 558.1 | 96.77 | 83.14 | 0.45840 | 307.8032 | 74.60 | 0.255 | 8.548 | 11.322 |
| 10 | 558.1 | 97.43 | 82.39 | 0.45616 | 317.4397 | 74.40 | 0.316 | 7.995 | 12.187 |
| 1 | 920.8 | 66.59 | 65.70 | 0.43526 | 227.7585 | 31.66 | -0.232 | 34.045 | 1.956 |
| 2 | 920.8 | 45.01 | 73.77 | 0.43510 | 231.1146 | 35.43 | -0.211 | 38.342 | 1.174 |
| 3 | 920.8 | 46.74 | 76.71 | 0.43494 | 233.8737 | 38.53 | -0.194 | 38.188 | 1.224 |
| 4 | 920.8 | 49.58 | 76.74 | 0.43479 | 236.7704 | 41.76 | -0.175 | 34.987 | 1.417 |
| 5 | 920.8 | 59.40 | 74.57 | 0.43463 | 240.0478 | 45.40 | -0.155 | 29.173 | 2.036 |
| 6 | 920.8 | 52.02 | 75.31 | 0.43448 | 243.3987 | 49.11 | -0.134 | 26.207 | 1.985 |
| 7 | 920.8 | 54.88 | 76.26 | 0.43433 | 246.6135 | 52.64 | -0.114 | 23.614 | 2.324 |
| 8 | 920.8 | 54.51 | 77.38 | 0.43417 | 249.9030 | 56.25 | -0.094 | 21.132 | 2.579 |
| 9 | 920.8 | 52.01 | 78.35 | 0.43402 | 253.1063 | 59.74 | -0.074 | 18.617 | 2.794 |
| 10 | 920.8 | 46.18 | 79.34 | 0.43386 | 256.0591 | 62.94 | -0.055 | 16.400 | 2.816 |
| 1 | 837.1 | 66.65 | 67.94 | 0.43533 | 227.8587 | 31.77 | -0.231 | 36.172 | 1.843 |
| 2 | 837.1 | 43.66 | 76.06 | 0.43519 | 231.5078 | 35.87 | -0.208 | 40.185 | 1.086 |
| 3 | 837.1 | 45.10 | 78.30 | 0.43506 | 234.4438 | 39.16 | -0.190 | 39.142 | 1.152 |
| 4 | 837.1 | 53.15 | 76.67 | 0.43493 | 237.6939 | 42.79 | -0.170 | 33.886 | 1.568 |
| 5 | 837.1 | 58.92 | 74.37 | 0.43480 | 241.4013 | 46.90 | -0.147 | 27.471 | 2.145 |

| | | | | | | | | | | |
|---|---|---|---|---|---|---|---|---|---|---|
| | 6 | 837.1 | 54.36 | 74.57 | 0.43467 | 245.1486 | 51.03 | -0.123 | 23.539 | 2.309 |
| | 7 | 837.1 | 55.44 | 75.93 | 0.43454 | 248.7808 | 55.02 | -0.101 | 20.913 | 2.651 |
| | 8 | 837.1 | 55.01 | 77.52 | 0.43441 | 252.4349 | 59.00 | -0.078 | 18.520 | 2.970 |
| | 9 | 837.1 | 50.48 | 79.03 | 0.43428 | 255.9248 | 62.79 | -0.056 | 16.239 | 3.109 |
| | 10 | 837.1 | 47.33 | 79.60 | 0.43415 | 259.1606 | 66.28 | -0.036 | 13.321 | 3.553 |
| | 1 | 759.0 | 66.69 | 71.25 | 0.42849 | 228.1021 | 32.05 | -0.226 | 39.205 | 1.701 |
| | 2 | 759.0 | 41.84 | 79.67 | 0.42838 | 232.0619 | 36.50 | -0.201 | 43.169 | 0.969 |
| | 3 | 759.0 | 43.03 | 81.46 | 0.42827 | 235.1584 | 39.96 | -0.182 | 41.497 | 1.037 |
| | 4 | 759.0 | 55.23 | 78.43 | 0.42816 | 238.7434 | 43.95 | -0.159 | 34.475 | 1.602 |
| | 5 | 759.0 | 59.70 | 75.77 | 0.42805 | 242.9369 | 48.60 | -0.133 | 27.175 | 2.197 |
| | 6 | 759.0 | 54.13 | 76.03 | 0.42794 | 247.0903 | 53.17 | -0.108 | 22.863 | 2.368 |
| | 7 | 759.0 | 55.17 | 77.38 | 0.42783 | 251.0785 | 57.53 | -0.083 | 19.852 | 2.779 |
| | 8 | 759.0 | 54.24 | 78.87 | 0.42772 | 255.0705 | 61.87 | -0.058 | 16.998 | 3.191 |
| | 9 | 759.0 | 49.87 | 79.91 | 0.42761 | 258.8689 | 65.97 | -0.035 | 13.944 | 3.576 |
| | 10 | 759.0 | 48.78 | 79.76 | 0.42751 | 262.4682 | 69.83 | -0.012 | 9.929 | 4.913 |
| | 1 | 502.3 | 49.79 | 77.34 | 0.42866 | 228.9591 | 33.01 | -0.220 | 44.331 | 1.123 |
| | 2 | 502.3 | 45.87 | 78.11 | 0.42860 | 234.2332 | 38.93 | -0.188 | 39.183 | 1.171 |
| | 3 | 502.3 | 66.23 | 74.41 | 0.42855 | 240.4136 | 45.81 | -0.149 | 28.600 | 2.316 |
| | 4 | 502.3 | 52.01 | 76.59 | 0.42850 | 246.9329 | 53.00 | -0.109 | 23.592 | 2.205 |
| | 5 | 502.3 | 54.10 | 77.55 | 0.42844 | 252.7835 | 59.39 | -0.073 | 18.164 | 2.978 |
| | 6 | 502.3 | 51.60 | 78.66 | 0.42839 | 258.6114 | 65.69 | -0.037 | 12.972 | 3.978 |
| | 7 | 502.3 | 53.69 | 79.75 | 0.42835 | 264.4167 | 71.89 | -0.001 | 7.860 | 6.831 |
| | 8 | 502.3 | 54.52 | 80.26 | 0.42805 | 270.3830 | 71.87 | 0.036 | 8.399 | 6.492 |
| | 9 | 502.3 | 51.76 | 80.54 | 0.42735 | 276.2431 | 71.80 | 0.073 | 8.736 | 5.925 |
| | 10 | 502.3 | 48.35 | 80.58 | 0.42645 | 281.7627 | 71.72 | 0.108 | 8.862 | 5.456 |
| | 1 | 591.6 | 52.03 | 73.20 | 0.42860 | 227.9244 | 31.85 | -0.227 | 41.355 | 1.258 |
| | 2 | 591.6 | 54.05 | 74.43 | 0.42853 | 232.8905 | 37.43 | -0.196 | 37.002 | 1.461 |
| | 3 | 591.6 | 58.08 | 74.57 | 0.42846 | 238.1396 | 43.28 | -0.163 | 31.285 | 1.857 |
| | 4 | 591.6 | 53.19 | 76.54 | 0.42839 | 243.3482 | 49.05 | -0.131 | 27.489 | 1.935 |
| | 5 | 591.6 | 54.51 | 77.60 | 0.42832 | 248.3897 | 54.59 | -0.100 | 23.007 | 2.369 |
| | 6 | 591.6 | 51.83 | 78.72 | 0.42825 | 253.3676 | 60.02 | -0.069 | 18.697 | 2.772 |
| | 7 | 591.6 | 54.29 | 79.62 | 0.42818 | 258.3354 | 65.39 | -0.038 | 14.224 | 3.817 |
| | 8 | 591.6 | 55.35 | 79.94 | 0.42812 | 263.4681 | 70.90 | -0.006 | 9.041 | 6.122 |
| | 9 | 591.6 | 52.66 | 80.13 | 0.42779 | 268.5243 | 71.84 | 0.025 | 8.284 | 6.357 |
| | 10 | 591.6 | 48.81 | 80.23 | 0.42703 | 273.2742 | 71.77 | 0.055 | 8.454 | 5.773 |
| | 1 | 421.3 | 44.77 | 78.17 | 0.43563 | 228.4919 | 32.48 | -0.227 | 45.692 | 0.980 |
| | 2 | 421.3 | 59.94 | 76.30 | 0.43561 | 235.3740 | 40.20 | -0.185 | 36.101 | 1.660 |
| | 3 | 421.3 | 60.27 | 76.25 | 0.43557 | 243.2746 | 48.97 | -0.136 | 27.283 | 2.209 |
| | 4 | 421.3 | 51.93 | 79.09 | 0.43553 | 250.6488 | 57.06 | -0.090 | 22.037 | 2.356 |
| | 5 | 421.3 | 50.77 | 80.50 | 0.43550 | 257.3989 | 64.38 | -0.048 | 16.115 | 3.151 |
| | 6 | 421.3 | 53.47 | 80.28 | 0.43547 | 264.2501 | 71.73 | -0.005 | 8.555 | 6.250 |
| | 7 | 421.3 | 55.27 | 80.55 | 0.43522 | 271.3967 | 72.52 | 0.039 | 8.022 | 6.889 |
| | 8 | 421.3 | 55.48 | 80.78 | 0.43466 | 278.6758 | 72.47 | 0.084 | 8.312 | 6.675 |
| | 9 | 421.3 | 52.36 | 80.98 | 0.43390 | 285.7642 | 72.40 | 0.129 | 8.574 | 6.107 |
| | 10 | 421.3 | 48.96 | 80.96 | 0.43299 | 292.4239 | 72.32 | 0.170 | 8.634 | 5.671 |
| | 1 | 312.5 | 54.38 | 71.83 | 0.43565 | 230.3592 | 34.58 | -0.216 | 37.243 | 1.460 |
| | 2 | 312.5 | 56.70 | 74.04 | 0.43563 | 240.2022 | 45.57 | -0.155 | 28.467 | 1.992 |
| | 3 | 312.5 | 54.49 | 76.32 | 0.43562 | 250.0547 | 56.41 | -0.094 | 19.906 | 2.737 |
| | 4 | 312.5 | 50.98 | 78.84 | 0.43560 | 259.4006 | 66.54 | -0.036 | 12.298 | 4.146 |
| | 5 | 312.5 | 52.87 | 79.45 | 0.43559 | 268.6038 | 72.56 | 0.022 | 6.891 | 7.673 |

| | | | | | | | | | |
|---|---|---|---|---|---|---|---|---|---|
| 6 | 312.5 | 53.72 | 79.44 | 0.43539 | 278.0492 | 72.54 | 0.080 | 6.902 | 7.782 |
| 7 | 312.5 | 54.62 | 80.05 | 0.43491 | 287.6495 | 72.50 | 0.140 | 7.555 | 7.230 |
| 8 | 312.5 | 56.91 | 80.26 | 0.43430 | 297.5325 | 72.44 | 0.202 | 7.820 | 7.277 |
| 9 | 312.5 | 50.33 | 81.15 | 0.43357 | 307.0354 | 72.37 | 0.261 | 8.772 | 5.738 |
| 10 | 312.5 | 49.68 | 80.78 | 0.43276 | 315.8975 | 72.30 | 0.316 | 8.485 | 5.855 |
| 1 | 195.3 | 57.23 | 72.85 | 0.43567 | 233.6775 | 38.31 | -0.195 | 34.543 | 1.657 |
| 2 | 195.3 | 53.49 | 76.51 | 0.43566 | 249.3749 | 55.67 | -0.098 | 20.844 | 2.566 |
| 3 | 195.3 | 50.75 | 78.76 | 0.43565 | 264.1541 | 71.63 | -0.006 | 7.129 | 7.119 |
| 4 | 195.3 | 54.03 | 79.51 | 0.43555 | 279.0107 | 72.55 | 0.086 | 6.951 | 7.773 |
| 5 | 195.3 | 52.90 | 79.83 | 0.43529 | 294.1724 | 72.53 | 0.180 | 7.304 | 7.243 |
| 6 | 195.3 | 54.17 | 79.57 | 0.43500 | 309.3534 | 72.50 | 0.275 | 7.063 | 7.670 |
| 7 | 195.3 | 54.72 | 80.11 | 0.43470 | 324.7926 | 72.48 | 0.370 | 7.637 | 7.166 |
| 8 | 195.3 | 54.95 | 80.32 | 0.43434 | 340.3427 | 72.44 | 0.467 | 7.877 | 6.976 |
| 9 | 195.3 | 57.78 | 80.17 | 0.43393 | 356.3260 | 72.41 | 0.566 | 7.768 | 7.439 |
| 10 | 195.3 | 44.00 | 82.49 | 0.43349 | 370.7570 | 72.37 | 0.656 | 10.123 | 4.347 |
| 1 | 150.7 | 58.95 | 73.63 | 0.43568 | 236.4435 | 41.39 | -0.178 | 32.237 | 1.829 |
| 2 | 150.7 | 48.06 | 78.20 | 0.43567 | 256.1113 | 62.99 | -0.056 | 15.206 | 3.161 |
| 3 | 150.7 | 54.26 | 78.83 | 0.43562 | 274.9167 | 72.56 | 0.061 | 6.273 | 8.650 |
| 4 | 150.7 | 53.99 | 79.60 | 0.43548 | 294.8112 | 72.55 | 0.184 | 7.055 | 7.653 |
| 5 | 150.7 | 52.89 | 79.92 | 0.43530 | 314.4546 | 72.53 | 0.306 | 7.387 | 7.161 |
| 6 | 150.7 | 54.38 | 79.63 | 0.43506 | 334.1698 | 72.51 | 0.428 | 7.125 | 7.633 |
| 7 | 150.7 | 54.83 | 80.27 | 0.43479 | 354.2398 | 72.48 | 0.553 | 7.790 | 7.038 |
| 8 | 150.7 | 54.78 | 80.63 | 0.43448 | 374.3840 | 72.46 | 0.678 | 8.171 | 6.705 |
| 9 | 150.7 | 53.21 | 80.56 | 0.43415 | 394.2312 | 72.43 | 0.801 | 8.132 | 6.543 |
| 10 | 150.7 | 48.74 | 80.69 | 0.43383 | 412.9686 | 72.40 | 0.917 | 8.290 | 5.880 |
| 1 | 1841.6 | 93.68 | 58.46 | 0.35145 | 226.0816 | 29.80 | -0.189 | 28.663 | 3.268 |
| 2 | 1841.6 | 84.35 | 62.61 | 0.35092 | 228.7585 | 32.82 | -0.173 | 29.794 | 2.831 |
| 3 | 1841.6 | 89.95 | 63.29 | 0.35040 | 231.3794 | 35.76 | -0.156 | 27.524 | 3.268 |
| 4 | 1841.6 | 86.95 | 64.92 | 0.34988 | 234.0394 | 38.74 | -0.140 | 26.182 | 3.321 |
| 5 | 1841.6 | 89.74 | 65.27 | 0.34935 | 236.6961 | 41.71 | -0.123 | 23.568 | 3.808 |
| 6 | 1841.6 | 86.94 | 66.30 | 0.34883 | 239.3528 | 44.66 | -0.107 | 21.641 | 4.017 |
| 7 | 1841.6 | 89.06 | 67.97 | 0.34831 | 241.9992 | 47.59 | -0.091 | 20.384 | 4.369 |
| 8 | 1841.6 | 89.85 | 69.12 | 0.34779 | 244.6894 | 50.56 | -0.074 | 18.569 | 4.838 |
| 9 | 1841.6 | 86.16 | 69.82 | 0.34728 | 247.3359 | 53.46 | -0.058 | 16.360 | 5.266 |
| 10 | 1841.6 | 82.21 | 70.60 | 0.34676 | 249.8676 | 56.23 | -0.042 | 14.363 | 5.724 |
| 1 | 1573.8 | 88.90 | 61.74 | 0.35181 | 226.8013 | 30.61 | -0.185 | 31.126 | 2.856 |
| 2 | 1573.8 | 88.03 | 63.83 | 0.35142 | 229.9145 | 34.12 | -0.166 | 29.716 | 2.962 |
| 3 | 1573.8 | 90.80 | 64.29 | 0.35102 | 233.0612 | 37.65 | -0.147 | 26.642 | 3.408 |
| 4 | 1573.8 | 87.21 | 66.10 | 0.35062 | 236.1935 | 41.14 | -0.127 | 24.959 | 3.494 |
| 5 | 1573.8 | 89.37 | 66.79 | 0.35023 | 239.3008 | 44.60 | -0.108 | 22.192 | 4.027 |
| 6 | 1573.8 | 86.68 | 68.00 | 0.34983 | 242.3986 | 48.03 | -0.089 | 19.967 | 4.341 |
| 7 | 1573.8 | 88.42 | 69.80 | 0.34944 | 245.4798 | 51.42 | -0.070 | 18.373 | 4.813 |
| 8 | 1573.8 | 89.26 | 70.78 | 0.34904 | 248.6063 | 54.85 | -0.051 | 15.927 | 5.604 |
| 9 | 1573.8 | 85.94 | 71.06 | 0.34865 | 251.6892 | 58.22 | -0.032 | 12.846 | 6.690 |
| 10 | 1573.8 | 83.10 | 71.36 | 0.34826 | 254.6637 | 61.45 | -0.014 | 9.908 | 8.387 |
| 1 | 1300.3 | 84.03 | 66.02 | 0.35214 | 228.3891 | 32.40 | -0.176 | 33.624 | 2.499 |
| 2 | 1300.3 | 91.91 | 66.10 | 0.35186 | 232.1361 | 36.61 | -0.153 | 29.494 | 3.116 |
| 3 | 1300.3 | 91.46 | 66.49 | 0.35157 | 236.0413 | 40.97 | -0.129 | 25.511 | 3.585 |
| 4 | 1300.3 | 87.16 | 68.57 | 0.35129 | 239.8454 | 45.20 | -0.106 | 23.369 | 3.730 |
| 5 | 1300.3 | 88.61 | 69.57 | 0.35101 | 243.5887 | 49.34 | -0.083 | 20.227 | 4.381 |

| | | | | | | | | | |
|---|---|---|---|---|---|---|---|---|---|
| 6 | 1300.3 | 85.95 | 70.77 | 0.35073 | 247.3061 | 53.43 | -0.060 | 17.343 | 4.956 |
| 7 | 1300.3 | 87.59 | 72.26 | 0.35044 | 251.0019 | 57.47 | -0.037 | 14.786 | 5.924 |
| 8 | 1300.3 | 89.59 | 72.56 | 0.35016 | 254.7753 | 61.57 | -0.014 | 10.988 | 8.153 |
| 9 | 1300.3 | 86.22 | 72.39 | 0.35002 | 258.5194 | 64.11 | 0.008 | 8.281 | 10.411 |
| 10 | 1300.3 | 83.53 | 72.41 | 0.34856 | 262.1346 | 63.95 | 0.031 | 8.459 | 9.875 |
| 1 | 591.6 | 89.62 | 71.44 | 0.42171 | 231.2304 | 35.57 | -0.202 | 35.876 | 2.498 |
| 2 | 591.6 | 88.64 | 74.63 | 0.42164 | 239.5748 | 44.88 | -0.151 | 29.748 | 2.980 |
| 3 | 591.6 | 87.24 | 76.65 | 0.42157 | 247.8079 | 53.96 | -0.100 | 22.694 | 3.844 |
| 4 | 591.6 | 86.11 | 78.67 | 0.42150 | 255.9224 | 62.79 | -0.049 | 15.882 | 5.422 |
| 5 | 591.6 | 86.16 | 79.37 | 0.42145 | 263.9867 | 71.25 | 0.000 | 8.118 | 10.614 |
| 6 | 591.6 | 85.83 | 79.40 | 0.42092 | 272.0377 | 71.20 | 0.050 | 8.193 | 10.475 |
| 7 | 591.6 | 88.44 | 79.69 | 0.41969 | 280.1956 | 71.09 | 0.101 | 8.597 | 10.288 |
| 8 | 591.6 | 89.56 | 79.48 | 0.41805 | 288.5281 | 70.94 | 0.154 | 8.545 | 10.481 |
| 9 | 591.6 | 85.25 | 79.01 | 0.41607 | 296.7112 | 70.75 | 0.205 | 8.256 | 10.326 |
| 10 | 591.6 | 83.88 | 78.41 | 0.41380 | 304.6287 | 70.54 | 0.255 | 7.875 | 10.652 |
| 1 | 390.7 | 91.11 | 73.40 | 0.42185 | 233.1059 | 37.67 | -0.191 | 35.730 | 2.550 |
| 2 | 390.7 | 84.22 | 77.46 | 0.42182 | 245.5343 | 51.46 | -0.114 | 25.999 | 3.239 |
| 3 | 390.7 | 87.25 | 78.35 | 0.42179 | 257.6889 | 64.70 | -0.039 | 13.652 | 6.391 |
| 4 | 390.7 | 87.55 | 79.24 | 0.42151 | 270.0797 | 71.26 | 0.038 | 7.977 | 10.976 |
| 5 | 390.7 | 87.10 | 79.49 | 0.42085 | 282.4603 | 71.20 | 0.115 | 8.290 | 10.506 |
| 6 | 390.7 | 86.08 | 79.52 | 0.41992 | 294.7367 | 71.11 | 0.191 | 8.411 | 10.235 |
| 7 | 390.7 | 88.44 | 79.95 | 0.41876 | 307.1080 | 71.00 | 0.268 | 8.951 | 9.881 |
| 8 | 390.7 | 89.59 | 79.88 | 0.41741 | 319.7276 | 70.88 | 0.347 | 9.009 | 9.944 |
| 9 | 390.7 | 85.08 | 79.57 | 0.41592 | 332.1087 | 70.73 | 0.424 | 8.831 | 9.634 |
| 10 | 390.7 | 83.66 | 79.04 | 0.41432 | 344.0699 | 70.58 | 0.498 | 8.458 | 9.892 |
| 1 | 362.7 | 89.54 | 73.41 | 0.42185 | 234.5481 | 39.28 | -0.182 | 34.131 | 2.623 |
| 2 | 362.7 | 85.39 | 76.69 | 0.42183 | 247.9021 | 54.06 | -0.099 | 22.633 | 3.773 |
| 3 | 362.7 | 87.64 | 77.35 | 0.42181 | 261.1114 | 68.38 | -0.018 | 8.974 | 9.766 |
| 4 | 362.7 | 87.41 | 78.15 | 0.42152 | 274.4751 | 71.26 | 0.065 | 6.892 | 12.683 |
| 5 | 362.7 | 87.12 | 78.20 | 0.42083 | 287.7991 | 71.20 | 0.148 | 7.009 | 12.431 |
| 6 | 362.7 | 86.81 | 78.02 | 0.41990 | 301.0779 | 71.11 | 0.230 | 6.914 | 12.557 |
| 7 | 362.7 | 89.16 | 78.53 | 0.41878 | 314.5127 | 71.00 | 0.314 | 7.530 | 11.841 |
| 8 | 362.7 | 89.06 | 78.88 | 0.41750 | 328.1187 | 70.88 | 0.398 | 7.994 | 11.141 |
| 9 | 362.7 | 88.98 | 78.63 | 0.41610 | 341.7108 | 70.75 | 0.483 | 7.877 | 11.296 |
| 10 | 362.7 | 79.53 | 80.08 | 0.41464 | 354.5752 | 70.61 | 0.563 | 9.471 | 8.397 |
| 1 | 446.4 | 89.38 | 72.14 | 0.42183 | 232.9693 | 37.52 | -0.191 | 34.624 | 2.582 |
| 2 | 446.4 | 87.25 | 75.24 | 0.42179 | 243.9254 | 49.69 | -0.124 | 25.549 | 3.415 |
| 3 | 446.4 | 86.74 | 76.55 | 0.42174 | 254.7177 | 61.49 | -0.057 | 15.064 | 5.758 |
| 4 | 446.4 | 87.06 | 77.58 | 0.42171 | 265.4984 | 71.28 | 0.010 | 6.300 | 13.820 |
| 5 | 446.4 | 87.05 | 77.68 | 0.42130 | 276.2984 | 71.24 | 0.077 | 6.443 | 13.511 |
| 6 | 446.4 | 86.77 | 77.51 | 0.42033 | 287.0801 | 71.15 | 0.144 | 6.361 | 13.641 |
| 7 | 446.4 | 89.11 | 77.99 | 0.41908 | 297.9896 | 71.03 | 0.212 | 6.956 | 12.810 |
| 8 | 446.4 | 89.18 | 78.26 | 0.41759 | 309.0491 | 70.89 | 0.281 | 7.368 | 12.104 |
| 9 | 446.4 | 88.56 | 77.99 | 0.41589 | 320.0743 | 70.73 | 0.349 | 7.260 | 12.199 |
| 10 | 446.4 | 80.16 | 79.20 | 0.41405 | 330.5396 | 70.56 | 0.415 | 8.644 | 9.273 |
| 1 | 457.6 | 35.17 | 63.90 | 0.42184 | 228.9609 | 33.02 | -0.216 | 30.879 | 1.139 |
| 2 | 457.6 | 23.03 | 68.20 | 0.42180 | 232.4826 | 36.97 | -0.194 | 31.228 | 0.737 |
| 3 | 457.6 | 33.12 | 68.38 | 0.42175 | 235.8801 | 40.77 | -0.173 | 27.608 | 1.200 |
| 4 | 457.6 | 29.33 | 69.90 | 0.42171 | 239.6590 | 44.97 | -0.150 | 24.926 | 1.177 |
| 5 | 457.6 | 31.92 | 70.72 | 0.42166 | 243.3651 | 49.07 | -0.127 | 21.652 | 1.474 |

| | | | | | | | | | |
|---|---|---|---|---|---|---|---|---|---|
| 6 | 457.6 | 29.24 | 72.23 | 0.42162 | 247.0662 | 53.14 | -0.104 | 19.086 | 1.532 |
| 7 | 457.6 | 30.26 | 74.10 | 0.42157 | 250.6670 | 57.08 | -0.082 | 17.017 | 1.778 |
| 8 | 457.6 | 30.89 | 75.57 | 0.42153 | 254.3676 | 61.11 | -0.059 | 14.461 | 2.136 |
| 9 | 457.6 | 26.75 | 77.07 | 0.42148 | 257.8558 | 64.88 | -0.038 | 12.196 | 2.194 |
| 10 | 457.6 | 24.10 | 77.31 | 0.42144 | 260.9331 | 68.19 | -0.018 | 9.118 | 2.643 |
| 1 | 251.1 | 28.96 | 71.30 | 0.42187 | 229.2192 | 33.31 | -0.215 | 37.997 | 0.762 |
| 2 | 251.1 | 25.97 | 73.21 | 0.42186 | 235.2761 | 40.10 | -0.177 | 33.111 | 0.784 |
| 3 | 251.1 | 36.56 | 72.58 | 0.42184 | 242.1714 | 47.75 | -0.135 | 24.826 | 1.473 |
| 4 | 251.1 | 28.25 | 74.99 | 0.42183 | 249.3178 | 55.61 | -0.090 | 19.383 | 1.457 |
| 5 | 251.1 | 27.68 | 76.33 | 0.42182 | 255.4851 | 62.32 | -0.052 | 14.010 | 1.976 |
| 6 | 251.1 | 29.24 | 76.50 | 0.42181 | 261.7617 | 69.08 | -0.014 | 7.421 | 3.940 |
| 7 | 251.1 | 30.65 | 76.90 | 0.42173 | 268.3652 | 71.28 | 0.027 | 5.623 | 5.450 |
| 8 | 251.1 | 30.04 | 77.25 | 0.42153 | 275.0573 | 71.26 | 0.069 | 5.984 | 5.020 |
| 9 | 251.1 | 29.09 | 77.26 | 0.42127 | 281.5780 | 71.24 | 0.109 | 6.021 | 4.831 |
| 10 | 251.1 | 24.77 | 77.20 | 0.42094 | 287.5174 | 71.21 | 0.146 | 5.994 | 4.133 |
| 1 | 178.6 | 28.33 | 71.94 | 0.42189 | 229.8430 | 34.01 | -0.211 | 37.926 | 0.747 |
| 2 | 178.6 | 28.68 | 73.57 | 0.42187 | 238.6851 | 43.89 | -0.156 | 29.673 | 0.967 |
| 3 | 178.6 | 34.16 | 73.94 | 0.42186 | 248.4309 | 54.64 | -0.096 | 19.298 | 1.770 |
| 4 | 178.6 | 25.90 | 76.27 | 0.42186 | 257.7449 | 64.76 | -0.038 | 11.511 | 2.250 |
| 5 | 178.6 | 29.72 | 76.40 | 0.42185 | 266.3708 | 71.29 | 0.015 | 5.110 | 5.817 |
| 6 | 178.6 | 30.09 | 76.38 | 0.42178 | 275.6471 | 71.28 | 0.072 | 5.100 | 5.900 |
| 7 | 178.6 | 30.07 | 77.02 | 0.42161 | 284.9768 | 71.27 | 0.130 | 5.751 | 5.228 |
| 8 | 178.6 | 30.25 | 77.27 | 0.42140 | 294.3307 | 71.25 | 0.188 | 6.024 | 5.021 |
| 9 | 178.6 | 29.08 | 77.30 | 0.42117 | 303.5312 | 71.23 | 0.245 | 6.071 | 4.790 |
| 10 | 178.6 | 24.79 | 77.25 | 0.42096 | 311.8851 | 71.21 | 0.297 | 6.039 | 4.105 |
| 1 | 122.8 | 27.75 | 73.91 | 0.42190 | 231.3275 | 35.68 | -0.202 | 38.234 | 0.726 |
| 2 | 122.8 | 30.30 | 75.39 | 0.42189 | 244.4194 | 50.23 | -0.121 | 25.158 | 1.204 |
| 3 | 122.8 | 29.22 | 76.42 | 0.42188 | 257.8432 | 64.87 | -0.038 | 11.559 | 2.528 |
| 4 | 122.8 | 29.76 | 77.10 | 0.42186 | 271.1444 | 71.29 | 0.044 | 5.810 | 5.121 |
| 5 | 122.8 | 29.16 | 77.47 | 0.42179 | 284.4325 | 71.29 | 0.127 | 6.186 | 4.715 |
| 6 | 122.8 | 30.08 | 77.42 | 0.42169 | 297.7945 | 71.28 | 0.209 | 6.148 | 4.893 |
| 7 | 122.8 | 30.09 | 78.05 | 0.42156 | 311.3651 | 71.26 | 0.293 | 6.782 | 4.436 |
| 8 | 122.8 | 30.22 | 78.31 | 0.42141 | 324.9668 | 71.25 | 0.377 | 7.065 | 4.278 |
| 9 | 122.8 | 28.71 | 78.37 | 0.42124 | 338.2584 | 71.23 | 0.459 | 7.132 | 4.026 |
| 10 | 122.8 | 24.97 | 78.18 | 0.42105 | 350.3646 | 71.22 | 0.534 | 6.959 | 3.588 |
| 1 | 94.9 | 26.38 | 74.67 | 0.42190 | 232.1206 | 36.57 | -0.197 | 38.103 | 0.692 |
| 2 | 94.9 | 30.84 | 75.56 | 0.42189 | 248.8260 | 55.07 | -0.094 | 20.487 | 1.505 |
| 3 | 94.9 | 29.68 | 76.28 | 0.42189 | 266.4951 | 71.30 | 0.016 | 4.986 | 5.954 |
| 4 | 94.9 | 30.15 | 76.85 | 0.42186 | 283.9619 | 71.29 | 0.124 | 5.561 | 5.422 |
| 5 | 94.9 | 29.11 | 77.30 | 0.42179 | 301.2624 | 71.29 | 0.231 | 6.012 | 4.843 |
| 6 | 94.9 | 30.07 | 77.29 | 0.42169 | 318.5383 | 71.28 | 0.337 | 6.016 | 4.997 |
| 7 | 94.9 | 29.86 | 77.95 | 0.42157 | 336.0334 | 71.27 | 0.446 | 6.687 | 4.466 |
| 8 | 94.9 | 30.23 | 78.14 | 0.42144 | 353.5774 | 71.25 | 0.554 | 6.884 | 4.392 |
| 9 | 94.9 | 29.81 | 78.10 | 0.42129 | 371.1065 | 71.24 | 0.662 | 6.864 | 4.343 |
| 10 | 94.9 | 24.01 | 78.37 | 0.42113 | 386.8185 | 71.22 | 0.759 | 7.145 | 3.360 |
| 1 | 446.4 | 34.80 | 64.81 | 0.42184 | 228.4197 | 32.41 | -0.220 | 32.408 | 1.074 |
| 2 | 446.4 | 22.87 | 69.02 | 0.42181 | 231.9971 | 36.43 | -0.197 | 32.591 | 0.702 |
| 3 | 446.4 | 32.01 | 69.06 | 0.42177 | 235.4010 | 40.24 | -0.176 | 28.822 | 1.111 |
| 4 | 446.4 | 31.25 | 69.90 | 0.42173 | 239.3249 | 44.60 | -0.152 | 25.302 | 1.235 |
| 5 | 446.4 | 30.94 | 70.99 | 0.42169 | 243.1824 | 48.87 | -0.128 | 22.123 | 1.398 |

| | | | | | | | | | |
|---|---|---|---|---|---|---|---|---|---|
| 6 | 446.4 | 29.80 | 72.29 | 0.42164 | 246.9496 | 53.02 | -0.105 | 19.278 | 1.546 |
| 7 | 446.4 | 30.18 | 74.23 | 0.42160 | 250.6700 | 57.09 | -0.082 | 17.143 | 1.761 |
| 8 | 446.4 | 30.23 | 75.72 | 0.42156 | 254.4173 | 61.16 | -0.059 | 14.561 | 2.076 |
| 9 | 446.4 | 27.29 | 76.92 | 0.42151 | 257.9853 | 65.02 | -0.037 | 11.898 | 2.294 |
| 10 | 446.4 | 24.21 | 77.11 | 0.42147 | 261.1799 | 68.45 | -0.017 | 8.659 | 2.796 |
| 1 | 446.4 | 39.62 | 70.80 | 0.42184 | 227.9837 | 31.92 | -0.222 | 38.883 | 1.019 |
| 2 | 446.4 | 38.80 | 72.22 | 0.42180 | 232.8476 | 37.38 | -0.192 | 34.843 | 1.113 |
| 3 | 446.4 | 47.63 | 71.54 | 0.42176 | 238.2087 | 43.36 | -0.159 | 28.173 | 1.691 |
| 4 | 446.4 | 40.48 | 73.66 | 0.42171 | 243.6744 | 49.41 | -0.125 | 24.244 | 1.670 |
| 5 | 446.4 | 41.84 | 74.91 | 0.42167 | 248.7805 | 55.02 | -0.094 | 19.885 | 2.104 |
| 6 | 446.4 | 38.50 | 76.17 | 0.42163 | 253.7639 | 60.45 | -0.063 | 15.722 | 2.449 |
| 7 | 446.4 | 41.46 | 76.75 | 0.42158 | 258.7236 | 65.81 | -0.032 | 10.934 | 3.792 |
| 8 | 446.4 | 43.21 | 76.75 | 0.42155 | 263.9755 | 71.26 | 0.000 | 5.489 | 7.872 |
| 9 | 446.4 | 41.04 | 77.07 | 0.42133 | 269.2017 | 71.24 | 0.033 | 5.828 | 7.043 |
| 10 | 446.4 | 35.04 | 77.64 | 0.42083 | 273.9210 | 71.20 | 0.062 | 6.442 | 5.439 |
| 1 | 457.6 | 44.74 | 74.54 | 0.42183 | 228.6310 | 32.65 | -0.218 | 41.890 | 1.068 |
| 2 | 457.6 | 62.20 | 72.46 | 0.42180 | 235.1022 | 39.90 | -0.178 | 32.554 | 1.911 |
| 3 | 457.6 | 58.33 | 73.10 | 0.42175 | 242.3960 | 48.00 | -0.133 | 25.094 | 2.324 |
| 4 | 457.6 | 51.20 | 75.58 | 0.42171 | 249.0242 | 55.29 | -0.092 | 20.290 | 2.524 |
| 5 | 457.6 | 54.28 | 76.08 | 0.42166 | 255.4076 | 62.23 | -0.053 | 13.850 | 3.919 |
| 6 | 457.6 | 53.34 | 76.48 | 0.42162 | 261.9203 | 69.25 | -0.012 | 7.233 | 7.375 |
| 7 | 457.6 | 54.61 | 77.20 | 0.42138 | 268.4526 | 71.25 | 0.028 | 5.954 | 9.172 |
| 8 | 457.6 | 56.15 | 77.36 | 0.42079 | 275.1549 | 71.19 | 0.070 | 6.166 | 9.106 |
| 9 | 457.6 | 53.42 | 77.64 | 0.41999 | 281.7852 | 71.12 | 0.111 | 6.524 | 8.188 |
| 10 | 457.6 | 48.29 | 78.07 | 0.41901 | 287.9401 | 71.03 | 0.150 | 7.047 | 6.853 |
| 1 | 446.4 | 55.91 | 78.35 | 0.42184 | 229.4579 | 33.58 | -0.213 | 44.774 | 1.249 |
| 2 | 446.4 | 85.13 | 74.44 | 0.42180 | 238.2064 | 43.36 | -0.159 | 31.078 | 2.739 |
| 3 | 446.4 | 67.87 | 76.59 | 0.42176 | 247.6967 | 53.84 | -0.100 | 22.751 | 2.983 |
| 4 | 446.4 | 67.56 | 77.86 | 0.42171 | 256.0974 | 62.98 | -0.049 | 14.885 | 4.539 |
| 5 | 446.4 | 70.45 | 77.52 | 0.42169 | 264.6579 | 71.28 | 0.004 | 6.247 | 11.277 |
| 6 | 446.4 | 69.22 | 77.46 | 0.42135 | 273.3212 | 71.24 | 0.058 | 6.218 | 11.132 |
| 7 | 446.4 | 70.58 | 78.02 | 0.42055 | 281.9925 | 71.17 | 0.112 | 6.853 | 10.299 |
| 8 | 446.4 | 72.35 | 78.14 | 0.41951 | 290.8578 | 71.07 | 0.167 | 7.065 | 10.241 |
| 9 | 446.4 | 68.38 | 78.50 | 0.41825 | 299.5868 | 70.95 | 0.222 | 7.545 | 9.063 |
| 10 | 446.4 | 63.81 | 78.93 | 0.41683 | 307.7864 | 70.82 | 0.273 | 8.111 | 7.867 |
| 1 | 446.4 | 84.22 | 75.64 | 0.42184 | 231.4319 | 35.79 | -0.201 | 39.849 | 2.113 |
| 2 | 446.4 | 94.58 | 75.94 | 0.42180 | 242.5225 | 48.14 | -0.132 | 27.797 | 3.402 |
| 3 | 446.4 | 88.02 | 77.41 | 0.42176 | 253.8490 | 60.54 | -0.062 | 16.865 | 5.219 |
| 4 | 446.4 | 87.15 | 78.63 | 0.42173 | 264.7149 | 71.28 | 0.005 | 7.349 | 11.859 |
| 5 | 446.4 | 88.95 | 78.39 | 0.42132 | 275.6382 | 71.24 | 0.072 | 7.150 | 12.441 |
| 6 | 446.4 | 88.13 | 78.22 | 0.42037 | 286.6218 | 71.15 | 0.141 | 7.069 | 12.467 |
| 7 | 446.4 | 89.98 | 78.81 | 0.41912 | 297.6696 | 71.04 | 0.210 | 7.776 | 11.571 |
| 8 | 446.4 | 91.95 | 79.01 | 0.41762 | 308.9545 | 70.90 | 0.280 | 8.111 | 11.336 |
| 9 | 446.4 | 86.56 | 79.46 | 0.41593 | 320.0271 | 70.74 | 0.349 | 8.729 | 9.916 |
| 10 | 446.4 | 83.02 | 79.82 | 0.41408 | 330.5461 | 70.56 | 0.415 | 9.261 | 8.965 |
| 1 | 446.4 | 100.68 | 77.59 | 0.42183 | 232.5747 | 37.08 | -0.194 | 40.517 | 2.485 |
| 2 | 446.4 | 110.60 | 77.67 | 0.42178 | 245.6804 | 51.62 | -0.113 | 26.047 | 4.246 |
| 3 | 446.4 | 106.67 | 78.19 | 0.42175 | 259.1575 | 66.28 | -0.030 | 11.909 | 8.957 |
| 4 | 446.4 | 104.84 | 79.20 | 0.42135 | 272.2769 | 71.25 | 0.052 | 7.951 | 13.186 |
| 5 | 446.4 | 106.09 | 78.88 | 0.42041 | 285.3606 | 71.16 | 0.133 | 7.725 | 13.734 |

| | | | | | | | | | | |
|---|---|---|---|---|---|---|---|---|---|---|
| | 6 | 446.4 | 105.09 | 78.66 | 0.41912 | 298.4601 | 71.04 | 0.215 | 7.622 | 13.788 |
| | 7 | 446.4 | 107.48 | 79.27 | 0.41753 | 311.6460 | 70.89 | 0.297 | 8.379 | 12.828 |
| | 8 | 446.4 | 109.53 | 79.51 | 0.41571 | 325.1069 | 70.72 | 0.381 | 8.793 | 12.456 |
| | 9 | 446.4 | 102.25 | 79.97 | 0.41372 | 338.2430 | 70.53 | 0.462 | 9.445 | 10.826 |
| | 10 | 446.4 | 101.40 | 79.81 | 0.41161 | 350.8746 | 70.33 | 0.541 | 9.488 | 10.687 |
| | 1 | 446.4 | 119.16 | 79.75 | 0.42183 | 233.6785 | 38.31 | -0.187 | 41.435 | 2.876 |
| | 2 | 446.4 | 132.35 | 78.95 | 0.42179 | 249.2795 | 55.57 | -0.091 | 23.385 | 5.660 |
| | 3 | 446.4 | 128.15 | 78.91 | 0.42176 | 265.4382 | 71.28 | 0.009 | 7.632 | 16.791 |
| | 4 | 446.4 | 125.67 | 79.85 | 0.42120 | 281.1821 | 71.23 | 0.107 | 8.615 | 14.586 |
| | 5 | 446.4 | 126.67 | 79.45 | 0.41992 | 296.8339 | 71.11 | 0.204 | 8.341 | 15.186 |
| | 6 | 446.4 | 125.44 | 79.19 | 0.41829 | 312.4719 | 70.96 | 0.301 | 8.230 | 15.243 |
| | 7 | 446.4 | 128.48 | 79.86 | 0.41638 | 328.2224 | 70.78 | 0.400 | 9.081 | 14.149 |
| | 8 | 446.4 | 129.59 | 80.22 | 0.41426 | 344.2303 | 70.58 | 0.499 | 9.642 | 13.440 |
| | 9 | 446.4 | 120.26 | 80.24 | 0.41203 | 359.7280 | 70.37 | 0.596 | 9.874 | 12.180 |
| | 10 | 446.4 | 125.26 | 78.64 | 0.40996 | 374.9573 | 70.17 | 0.690 | 8.469 | 14.790 |
| | 1 | 446.4 | 142.06 | 80.93 | 0.42183 | 235.1395 | 39.94 | -0.178 | 40.990 | 3.466 |
| | 2 | 446.4 | 156.43 | 79.94 | 0.42179 | 253.6546 | 60.33 | -0.064 | 19.605 | 7.979 |
| | 3 | 446.4 | 151.86 | 79.69 | 0.42130 | 272.7774 | 71.24 | 0.055 | 8.449 | 17.973 |
| | 4 | 446.4 | 149.29 | 80.63 | 0.42012 | 291.4570 | 71.13 | 0.171 | 9.496 | 15.720 |
| | 5 | 446.4 | 150.09 | 80.19 | 0.41848 | 310.0267 | 70.98 | 0.286 | 9.216 | 16.285 |
| | 6 | 446.4 | 148.43 | 79.94 | 0.41652 | 328.5435 | 70.79 | 0.401 | 9.146 | 16.230 |
| | 7 | 446.4 | 150.99 | 80.66 | 0.41432 | 347.1162 | 70.58 | 0.517 | 10.079 | 14.981 |
| | 8 | 446.4 | 151.95 | 80.41 | 0.41198 | 365.9069 | 70.36 | 0.634 | 10.052 | 15.116 |
| | 9 | 446.4 | 155.82 | 78.89 | 0.40976 | 384.9971 | 70.15 | 0.752 | 8.744 | 17.821 |
| | 10 | 446.4 | 138.63 | 82.08 | 0.40769 | 403.2610 | 69.95 | 0.865 | 12.130 | 11.428 |
| | 1 | 446.4 | 163.64 | 81.16 | 0.42183 | 236.4598 | 41.42 | -0.170 | 39.742 | 4.117 |
| | 2 | 446.4 | 178.07 | 80.22 | 0.42179 | 257.6553 | 64.66 | -0.039 | 15.555 | 11.448 |
| | 3 | 446.4 | 173.44 | 79.83 | 0.42117 | 279.4591 | 71.23 | 0.096 | 8.600 | 20.167 |
| | 4 | 446.4 | 170.86 | 80.78 | 0.41971 | 300.8155 | 71.09 | 0.229 | 9.688 | 17.636 |
| | 5 | 446.4 | 170.51 | 80.31 | 0.41781 | 321.9900 | 70.91 | 0.360 | 9.401 | 18.137 |
| | 6 | 446.4 | 168.93 | 79.62 | 0.41561 | 343.0447 | 70.71 | 0.491 | 8.910 | 18.959 |
| | 7 | 446.4 | 182.08 | 79.50 | 0.41321 | 364.8174 | 70.48 | 0.627 | 9.020 | 20.186 |
| | 8 | 446.4 | 255.32 | 83.04 | 0.41075 | 391.9488 | 70.25 | 0.795 | 12.796 | 19.953 |
| | 9 | 446.4 | 131.72 | 127.05 | 0.40853 | 415.9561 | 70.03 | 0.943 | 57.015 | 2.310 |
| | 10 | 446.4 | 101.80 | 153.01 | 0.40693 | 430.4405 | 64.20 | 1.033 | 75.102 | 1.355 |

Table B.2: Baird et al [60]

| **R11** | | | **Measured Quantities** | | | | **Derived Quantities** | | | | |
|---|---|---|---|---|---|---|---|---|---|---|---|
| | | | G | $q_{wall}$ | $T_{wall}$ | p | enthalpy | $T_f$ | quality | $\Delta$T local | h |
| | | | kg $m^{-2}$ $s^{-1}$ | kW $m^{-2}$ | $^oC$ | MPa | kJ $kg^{-1}$ | $^oC$ | (-) | $^oC$ | kW $m^{-2}$ $K^{-1}$ |
| csub_002 | csub_002 | . | | 20.03 | 46.09 | 0.18257 | 221.2685 | 24.41 | -0.090 | 21.682 | |
| | | 1 | 159.6 | 23.76 | 46.09 | 0.18257 | 225.3915 | 29.08 | -0.067 | 17.009 | 1.397 |
| | | 2 | 159.6 | 19.19 | 46.17 | 0.18255 | 232.8452 | 37.47 | -0.024 | 8.704 | 2.205 |
| | | 3 | 159.6 | 30.33 | 46.18 | 0.18246 | 241.4384 | 41.44 | 0.026 | 4.738 | 6.401 |
| | | 4 | 159.6 | 11.16 | 47.05 | 0.18228 | 248.6375 | 41.41 | 0.067 | 5.641 | 1.978 |
| | | 5 | 159.6 | 17.67 | 47.31 | 0.18207 | 253.6403 | 41.37 | 0.096 | 5.938 | 2.976 |
| | | 6 | 159.6 | 17.92 | 47.68 | 0.18181 | 259.8166 | 41.33 | 0.131 | 6.353 | 2.821 |
| | | 7 | 159.6 | 11.42 | 48.16 | 0.18150 | 264.9081 | 41.27 | 0.161 | 6.890 | 1.657 |
| | | 8 | 159.6 | 20.17 | 48.03 | 0.18116 | 270.3901 | 41.21 | 0.193 | 6.816 | 2.960 |
| | | 9 | 159.6 | 19.08 | 47.86 | 0.18076 | 277.2016 | 41.14 | 0.232 | 6.721 | 2.839 |
| | | 10 | 159.6 | 24.81 | 47.78 | 0.18031 | 284.8180 | 41.06 | 0.276 | 6.722 | 3.691 |
| | | 11 | 159.6 | 24.81 | 47.77 | 0.18008 | 289.1234 | 41.02 | 0.301 | 6.751 | 3.675 |
| csub_003 | csub_003 | . | | 11.37 | 43.92 | 0.18245 | 220.9188 | 24.01 | -0.092 | 19.907 | |
| | | 1 | 175.1 | 16.55 | 43.92 | 0.18244 | 223.5365 | 26.98 | -0.077 | 16.936 | 0.977 |
| | | 2 | 175.1 | 10.85 | 44.14 | 0.18243 | 227.8705 | 31.88 | -0.052 | 12.259 | 0.885 |
| | | 3 | 175.1 | 16.79 | 44.34 | 0.18241 | 232.2423 | 36.79 | -0.027 | 7.550 | 2.224 |
| | | 4 | 175.1 | 4.56 | 45.01 | 0.18237 | 235.6190 | 40.56 | -0.008 | 4.444 | 1.026 |
| | | 5 | 175.1 | 7.99 | 45.24 | 0.18233 | 237.6030 | 41.42 | 0.004 | 3.822 | 2.090 |
| | | 6 | 175.1 | 7.98 | 45.43 | 0.18223 | 240.1277 | 41.40 | 0.018 | 4.026 | 1.982 |
| | | 7 | 175.1 | 5.84 | 45.52 | 0.18212 | 242.3131 | 41.38 | 0.031 | 4.138 | 1.412 |
| | | 8 | 175.1 | 12.82 | 45.30 | 0.18200 | 245.2639 | 41.36 | 0.048 | 3.935 | 3.257 |
| | | 9 | 175.1 | 11.00 | 45.18 | 0.18181 | 249.0310 | 41.33 | 0.070 | 3.855 | 2.854 |
| | | 10 | 175.1 | 15.37 | 45.15 | 0.18157 | 253.2009 | 41.29 | 0.094 | 3.869 | 3.972 |
| | | 11 | 175.1 | 15.37 | 45.15 | 0.18146 | 255.6308 | 41.26 | 0.108 | 3.887 | 3.954 |
| csub_004 | csub_004 | . | | 12.28 | 42.87 | 0.18115 | 220.2808 | 23.29 | -0.095 | 19.580 | |
| | | 1 | 284.1 | 18.81 | 42.87 | 0.18114 | 222.1140 | 25.37 | -0.084 | 17.497 | 1.075 |
| | | 2 | 284.1 | 10.78 | 43.28 | 0.18111 | 224.9985 | 28.64 | -0.068 | 14.645 | 0.736 |
| | | 3 | 284.1 | 16.11 | 43.60 | 0.18108 | 227.6205 | 31.60 | -0.053 | 11.997 | 1.343 |
| | | 4 | 284.1 | 5.09 | 44.20 | 0.18105 | 229.6879 | 33.93 | -0.041 | 10.275 | 0.496 |
| | | 5 | 284.1 | 9.12 | 44.36 | 0.18102 | 231.0737 | 35.48 | -0.033 | 8.884 | 1.027 |
| | | 6 | 284.1 | 8.81 | 44.54 | 0.18094 | 232.8219 | 37.44 | -0.023 | 7.096 | 1.242 |
| | | 7 | 284.1 | 6.11 | 44.63 | 0.18084 | 234.2761 | 39.07 | -0.014 | 5.561 | 1.098 |
| | | 8 | 284.1 | 13.75 | 44.29 | 0.18062 | 236.2118 | 41.12 | -0.003 | 3.173 | 4.333 |
| | | 9 | 284.1 | 12.20 | 44.03 | 0.18036 | 238.7411 | 41.07 | 0.012 | 2.965 | 4.113 |
| | | 10 | 284.1 | 17.15 | 43.93 | 0.17991 | 241.6019 | 40.99 | 0.029 | 2.937 | 5.839 |
| | | 11 | 284.1 | 17.15 | 43.91 | 0.17968 | 243.2738 | 40.95 | 0.038 | 2.965 | 5.785 |
| csub_005 | csub_005 | . | | 11.98 | 42.71 | 0.18553 | 220.0836 | 23.06 | -0.099 | 19.647 | |

| | | | | | | | | | | |
|---|---|---|---|---|---|---|---|---|---|---|
| | | 1 | 455.1 | 19.88 | 42.71 | 0.18543 | 221.2931 | 24.44 | -0.092 | 18.271 | 1.088 |
| | | 2 | 455.1 | 10.60 | 43.24 | 0.18524 | 223.1475 | 26.54 | -0.082 | 16.700 | 0.635 |
| | | 3 | 455.1 | 15.93 | 43.65 | 0.18506 | 224.7620 | 28.37 | -0.072 | 15.279 | 1.043 |
| | | 4 | 455.1 | 5.17 | 44.31 | 0.18477 | 226.0459 | 29.82 | -0.065 | 14.493 | 0.356 |
| | | 5 | 455.1 | 8.41 | 44.57 | 0.18448 | 226.8722 | 30.75 | -0.060 | 13.820 | 0.609 |
| | | 6 | 455.1 | 7.46 | 44.80 | 0.18420 | 227.8383 | 31.84 | -0.054 | 12.962 | 0.576 |
| | | 7 | 455.1 | 6.10 | 44.84 | 0.18392 | 228.6638 | 32.77 | -0.049 | 12.071 | 0.505 |
| | | 8 | 455.1 | 13.30 | 44.52 | 0.18365 | 229.8444 | 34.10 | -0.042 | 10.416 | 1.277 |
| | | 9 | 455.1 | 11.88 | 44.27 | 0.18338 | 231.3766 | 35.82 | -0.033 | 8.451 | 1.406 |
| | | 10 | 455.1 | 16.50 | 44.19 | 0.18172 | 233.1036 | 37.75 | -0.022 | 6.433 | 2.565 |
| | | 11 | 455.1 | 16.50 | 44.18 | 0.18079 | 234.1076 | 38.88 | -0.015 | 5.301 | 3.113 |
| csub_006 | csub_006 | . | | 12.46 | 41.89 | 0.18490 | 219.8343 | 22.78 | -0.100 | 19.112 | |
| | | 1 | 564.8 | 21.45 | 41.89 | 0.18490 | 220.8860 | 23.97 | -0.094 | 17.915 | 1.197 |
| | | 2 | 564.8 | 10.03 | 42.55 | 0.18490 | 222.4296 | 25.73 | -0.085 | 16.823 | 0.596 |
| | | 3 | 564.8 | 16.18 | 42.92 | 0.18490 | 223.7146 | 27.18 | -0.078 | 15.736 | 1.028 |
| | | 4 | 564.8 | 6.81 | 43.50 | 0.18489 | 224.8418 | 28.46 | -0.072 | 15.040 | 0.453 |
| | | 5 | 564.8 | 10.06 | 43.77 | 0.18489 | 225.6691 | 29.39 | -0.067 | 14.377 | 0.700 |
| | | 6 | 564.8 | 8.13 | 44.12 | 0.18489 | 226.5612 | 30.40 | -0.062 | 13.721 | 0.593 |
| | | 7 | 564.8 | 5.60 | 44.32 | 0.18489 | 227.2344 | 31.16 | -0.058 | 13.158 | 0.425 |
| | | 8 | 564.8 | 12.86 | 44.06 | 0.18489 | 228.1395 | 32.18 | -0.053 | 11.879 | 1.083 |
| | | 9 | 564.8 | 12.03 | 43.76 | 0.18489 | 229.3601 | 33.56 | -0.046 | 10.208 | 1.179 |
| | | 10 | 564.8 | 16.93 | 43.65 | 0.18489 | 230.7803 | 35.15 | -0.038 | 8.495 | 1.993 |
| | | 11 | 564.8 | 16.93 | 43.63 | 0.18452 | 231.6105 | 36.08 | -0.032 | 7.550 | 2.243 |
| csub_007 | csub_007 | . | | 13.34 | 41.43 | 0.18202 | 219.8565 | 22.80 | -0.098 | 18.627 | |
| | | 1 | 672.2 | 22.90 | 41.43 | 0.18184 | 220.7999 | 23.88 | -0.092 | 17.554 | 1.305 |
| | | 2 | 672.2 | 10.56 | 42.16 | 0.18148 | 222.1781 | 25.44 | -0.084 | 16.718 | 0.631 |
| | | 3 | 672.2 | 16.71 | 42.54 | 0.18113 | 223.3011 | 26.72 | -0.077 | 15.821 | 1.056 |
| | | 4 | 672.2 | 8.40 | 43.05 | 0.18079 | 224.3352 | 27.89 | -0.071 | 15.162 | 0.554 |
| | | 5 | 672.2 | 11.91 | 43.31 | 0.18046 | 225.1719 | 28.83 | -0.066 | 14.471 | 0.823 |
| | | 6 | 672.2 | 9.34 | 43.73 | 0.18013 | 226.0475 | 29.82 | -0.061 | 13.905 | 0.672 |
| | | 7 | 672.2 | 6.08 | 44.04 | 0.17980 | 226.6826 | 30.54 | -0.057 | 13.498 | 0.450 |
| | | 8 | 672.2 | 12.99 | 43.87 | 0.17948 | 227.4680 | 31.43 | -0.052 | 12.442 | 1.044 |
| | | 9 | 672.2 | 12.43 | 43.57 | 0.17917 | 228.5153 | 32.61 | -0.046 | 10.960 | 1.134 |
| | | 10 | 672.2 | 17.74 | 43.42 | 0.17886 | 229.7583 | 34.01 | -0.039 | 9.413 | 1.885 |
| | | 11 | 672.2 | 17.74 | 43.40 | 0.17872 | 230.4891 | 34.83 | -0.034 | 8.572 | 2.069 |
| csub_008 | csub_008 | . | | 10.10 | 44.66 | 0.18452 | 221.6462 | 24.84 | -0.090 | 19.825 | |
| | | 1 | 117.9 | 15.47 | 44.66 | 0.18452 | 225.2793 | 28.95 | -0.069 | 15.709 | 0.985 |
| | | 2 | 117.9 | 9.14 | 44.90 | 0.18451 | 231.0585 | 35.46 | -0.036 | 9.433 | 0.969 |
| | | 3 | 117.9 | 15.42 | 45.03 | 0.18449 | 236.8266 | 41.80 | -0.002 | 3.230 | 4.774 |
| | | 4 | 117.9 | 3.64 | 45.62 | 0.18447 | 241.3042 | 41.80 | 0.023 | 3.824 | 0.953 |
| | | 5 | 117.9 | 7.48 | 45.80 | 0.18444 | 243.9161 | 41.79 | 0.038 | 4.005 | 1.867 |
| | | 6 | 117.9 | 8.08 | 45.98 | 0.18438 | 247.5689 | 41.78 | 0.059 | 4.200 | 1.923 |
| | | 7 | 117.9 | 4.49 | 46.22 | 0.18431 | 250.5191 | 41.77 | 0.076 | 4.453 | 1.008 |
| | | 8 | 117.9 | 10.62 | 46.18 | 0.18424 | 254.0659 | 41.76 | 0.097 | 4.423 | 2.400 |
| | | 9 | 117.9 | 8.94 | 46.13 | 0.18413 | 258.6594 | 41.74 | 0.123 | 4.391 | 2.037 |
| | | 10 | 117.9 | 13.89 | 46.08 | 0.18399 | 264.0222 | 41.71 | 0.154 | 4.372 | 3.177 |
| | | 11 | 117.9 | 13.89 | 46.08 | 0.18392 | 267.2846 | 41.70 | 0.173 | 4.377 | 3.174 |

| | | | | | | | | | | | |
|---|---|---|---|---|---|---|---|---|---|---|---|
| csub_009 | csub_009 | . | | 9.15 | 45.43 | 0.18499 | 222.4632 | 25.77 | -0.085 | 19.669 | |
| | | 1 | 89.9 | 15.26 | 45.43 | 0.18499 | 227.1634 | 31.08 | -0.058 | 14.353 | 1.063 |
| | | 2 | 89.9 | 8.28 | 45.71 | 0.18498 | 234.4154 | 39.22 | -0.017 | 6.494 | 1.275 |
| | | 3 | 89.9 | 14.17 | 45.86 | 0.18496 | 241.3333 | 41.88 | 0.023 | 3.983 | 3.558 |
| | | 4 | 89.9 | 2.75 | 46.44 | 0.18492 | 246.5458 | 41.87 | 0.053 | 4.564 | 0.602 |
| | | 5 | 89.9 | 7.35 | 46.60 | 0.18487 | 249.6582 | 41.87 | 0.071 | 4.732 | 1.554 |
| | | 6 | 89.9 | 6.92 | 46.85 | 0.18482 | 254.0553 | 41.86 | 0.096 | 4.994 | 1.385 |
| | | 7 | 89.9 | 3.54 | 47.13 | 0.18476 | 257.2776 | 41.85 | 0.115 | 5.285 | 0.670 |
| | | 8 | 89.9 | 9.40 | 47.15 | 0.18468 | 261.2642 | 41.83 | 0.138 | 5.322 | 1.766 |
| | | 9 | 89.9 | 7.65 | 47.15 | 0.18459 | 266.5163 | 41.82 | 0.168 | 5.331 | 1.435 |
| | | 10 | 89.9 | 12.69 | 47.12 | 0.18448 | 272.7832 | 41.80 | 0.204 | 5.320 | 2.385 |
| | | 11 | 89.9 | 12.69 | 47.11 | 0.18442 | 276.6932 | 41.79 | 0.226 | 5.324 | 2.384 |
| csub_010 | csub_010 | . | | 15.30 | 51.21 | 0.23710 | 222.0466 | 25.27 | -0.130 | 25.937 | |
| | | 1 | 172.3 | 20.37 | 51.21 | 0.23709 | 225.3213 | 28.98 | -0.110 | 22.227 | 0.916 |
| | | 2 | 172.3 | 10.31 | 52.00 | 0.23707 | 230.2536 | 34.54 | -0.082 | 17.459 | 0.591 |
| | | 3 | 172.3 | 22.35 | 52.99 | 0.23706 | 235.5041 | 40.42 | -0.051 | 12.569 | 1.778 |
| | | 4 | 172.3 | 6.56 | 54.70 | 0.23704 | 240.1520 | 45.58 | -0.024 | 9.122 | 0.719 |
| | | 5 | 172.3 | 12.34 | 55.41 | 0.23701 | 243.1901 | 48.94 | -0.006 | 6.468 | 1.907 |
| | | 6 | 172.3 | 15.54 | 55.59 | 0.23692 | 247.6720 | 50.11 | 0.020 | 5.480 | 2.836 |
| | | 7 | 172.3 | 10.10 | 55.48 | 0.23682 | 251.7949 | 50.10 | 0.045 | 5.382 | 1.877 |
| | | 8 | 172.3 | 15.90 | 54.50 | 0.23665 | 255.9756 | 50.07 | 0.069 | 4.422 | 3.596 |
| | | 9 | 172.3 | 14.84 | 54.22 | 0.23645 | 260.9173 | 50.04 | 0.098 | 4.178 | 3.551 |
| | | 10 | 172.3 | 19.98 | 55.22 | 0.23620 | 266.5149 | 50.01 | 0.131 | 5.210 | 3.835 |
| | | 11 | 172.3 | 19.98 | 55.43 | 0.23607 | 269.7273 | 49.99 | 0.150 | 5.440 | 3.673 |
| csub_011 | csub_011 | . | | 17.86 | 54.26 | 0.25001 | 222.5284 | 25.81 | -0.137 | 28.442 | |
| | | 1 | 159.0 | 21.55 | 54.26 | 0.25000 | 226.2826 | 30.06 | -0.115 | 24.193 | 0.891 |
| | | 2 | 159.0 | 13.78 | 54.93 | 0.24998 | 232.4376 | 36.98 | -0.079 | 17.943 | 0.768 |
| | | 3 | 159.0 | 27.24 | 55.96 | 0.24996 | 239.5832 | 44.95 | -0.037 | 11.017 | 2.473 |
| | | 4 | 159.0 | 7.73 | 57.86 | 0.24992 | 245.6741 | 51.67 | -0.001 | 6.186 | 1.249 |
| | | 5 | 159.0 | 17.08 | 58.55 | 0.24982 | 249.9955 | 51.94 | 0.025 | 6.608 | 2.585 |
| | | 6 | 159.0 | 18.52 | 58.94 | 0.24965 | 256.1975 | 51.92 | 0.061 | 7.027 | 2.636 |
| | | 7 | 159.0 | 9.84 | 59.10 | 0.24944 | 261.1382 | 51.89 | 0.090 | 7.213 | 1.364 |
| | | 8 | 159.0 | 17.82 | 58.10 | 0.24920 | 265.9560 | 51.85 | 0.119 | 6.244 | 2.854 |
| | | 9 | 159.0 | 16.19 | 57.81 | 0.24891 | 271.8805 | 51.81 | 0.154 | 5.997 | 2.701 |
| | | 10 | 159.0 | 23.36 | 58.81 | 0.24857 | 278.7697 | 51.77 | 0.194 | 7.042 | 3.317 |
| | | 11 | 159.0 | 23.36 | 59.02 | 0.24840 | 282.8381 | 51.74 | 0.218 | 7.277 | 3.210 |
| csub_012 | csub_012 | . | | 25.11 | 55.42 | 0.25923 | 222.2031 | 25.44 | -0.146 | 29.981 | |
| | | 1 | 274.0 | 27.62 | 55.42 | 0.25921 | 224.9944 | 28.60 | -0.129 | 26.818 | 1.030 |
| | | 2 | 274.0 | 15.94 | 56.34 | 0.25918 | 229.3964 | 33.57 | -0.103 | 22.770 | 0.700 |
| | | 3 | 274.0 | 34.40 | 57.54 | 0.25915 | 234.4847 | 39.27 | -0.073 | 18.267 | 1.883 |
| | | 4 | 274.0 | 14.51 | 59.50 | 0.25913 | 239.4290 | 44.77 | -0.044 | 14.727 | 0.985 |
| | | 5 | 274.0 | 26.60 | 59.81 | 0.25897 | 243.5849 | 49.37 | -0.020 | 10.441 | 2.548 |
| | | 6 | 274.0 | 25.35 | 60.04 | 0.25866 | 248.8366 | 53.15 | 0.011 | 6.890 | 3.679 |
| | | 7 | 274.0 | 14.89 | 60.19 | 0.25824 | 252.9040 | 53.09 | 0.036 | 7.097 | 2.098 |
| | | 8 | 274.0 | 24.65 | 58.59 | 0.25773 | 256.9000 | 53.02 | 0.060 | 5.570 | 4.425 |
| | | 9 | 274.0 | 22.46 | 57.87 | 0.25711 | 261.6615 | 52.94 | 0.088 | 4.933 | 4.553 |
| | | 10 | 274.0 | 34.92 | 58.79 | 0.25636 | 267.4615 | 52.84 | 0.123 | 5.954 | 5.865 |

| | | | | | | | | | | | |
|---|---|---|---|---|---|---|---|---|---|---|---|
| | | 11 | 274.0 | 34.92 | 59.00 | 0.25597 | 270.9914 | 52.78 | 0.144 | 6.215 | 5.619 |
| csub_013 | csub_013 | . | | 17.56 | 55.28 | 0.26734 | 221.8809 | 25.07 | -0.154 | 30.205 | |
| | | 1 | 284.2 | 26.28 | 55.28 | 0.26732 | 224.4412 | 27.97 | -0.139 | 27.302 | 0.963 |
| | | 2 | 284.2 | 12.96 | 56.24 | 0.26727 | 228.2643 | 32.29 | -0.116 | 23.949 | 0.541 |
| | | 3 | 284.2 | 27.57 | 57.39 | 0.26723 | 232.2134 | 36.73 | -0.093 | 20.664 | 1.334 |
| | | 4 | 284.2 | 8.74 | 59.21 | 0.26719 | 235.7511 | 40.68 | -0.072 | 18.525 | 0.472 |
| | | 5 | 284.2 | 18.10 | 59.57 | 0.26715 | 238.3658 | 43.59 | -0.056 | 15.984 | 1.132 |
| | | 6 | 284.2 | 18.48 | 59.72 | 0.26712 | 241.9292 | 47.54 | -0.035 | 12.182 | 1.517 |
| | | 7 | 284.2 | 8.35 | 59.80 | 0.26700 | 244.5428 | 50.42 | -0.020 | 9.382 | 0.890 |
| | | 8 | 284.2 | 14.99 | 58.63 | 0.26674 | 246.8172 | 52.92 | -0.006 | 5.710 | 2.626 |
| | | 9 | 284.2 | 19.44 | 57.98 | 0.26641 | 250.1719 | 54.18 | 0.014 | 3.796 | 5.121 |
| | | 10 | 284.2 | 19.10 | 58.65 | 0.26582 | 253.9270 | 54.11 | 0.036 | 4.545 | 4.203 |
| | | 11 | 284.2 | 19.10 | 58.81 | 0.26550 | 255.7883 | 54.06 | 0.048 | 4.744 | 4.027 |
| csub_014 | csub_014 | . | | 16.71 | 55.54 | 0.27364 | 221.8641 | 25.05 | -0.159 | 30.490 | |
| | | 1 | 279.8 | 26.44 | 55.54 | 0.27362 | 224.4807 | 28.02 | -0.143 | 27.523 | 0.961 |
| | | 2 | 279.8 | 11.77 | 56.60 | 0.27357 | 228.2618 | 32.29 | -0.121 | 24.312 | 0.484 |
| | | 3 | 279.8 | 26.87 | 57.79 | 0.27353 | 232.0849 | 36.58 | -0.098 | 21.205 | 1.267 |
| | | 4 | 279.8 | 7.84 | 59.63 | 0.27349 | 235.5191 | 40.42 | -0.078 | 19.215 | 0.408 |
| | | 5 | 279.8 | 16.64 | 60.03 | 0.27346 | 237.9414 | 43.12 | -0.063 | 16.917 | 0.984 |
| | | 6 | 279.8 | 17.71 | 60.14 | 0.27342 | 241.3407 | 46.89 | -0.043 | 13.251 | 1.337 |
| | | 7 | 279.8 | 8.28 | 60.19 | 0.27331 | 243.9125 | 49.72 | -0.028 | 10.461 | 0.791 |
| | | 8 | 279.8 | 13.79 | 59.07 | 0.27307 | 246.0962 | 52.13 | -0.015 | 6.943 | 1.986 |
| | | 9 | 279.8 | 18.42 | 58.44 | 0.27277 | 249.2837 | 55.02 | 0.004 | 3.424 | 5.380 |
| | | 10 | 279.8 | 18.01 | 59.12 | 0.27224 | 252.8890 | 54.95 | 0.026 | 4.175 | 4.314 |
| | | 11 | 279.8 | 18.01 | 59.28 | 0.27196 | 254.6713 | 54.91 | 0.037 | 4.371 | 4.120 |
| csub_015 | csub_015 | . | | 11.67 | 56.67 | 0.28344 | 224.5813 | 28.13 | -0.150 | 28.544 | |
| | | 1 | 282.4 | 25.42 | 56.67 | 0.28340 | 227.0743 | 30.94 | -0.135 | 25.727 | 0.988 |
| | | 2 | 282.4 | 0.44 | 58.35 | 0.28334 | 229.6107 | 33.80 | -0.120 | 24.548 | 0.018 |
| | | 3 | 282.4 | 20.82 | 59.47 | 0.28327 | 231.6956 | 36.14 | -0.108 | 23.333 | 0.892 |
| | | 4 | 282.4 | 7.28 | 60.71 | 0.28322 | 234.4510 | 39.22 | -0.091 | 21.481 | 0.339 |
| | | 5 | 282.4 | 11.60 | 61.21 | 0.28316 | 236.3024 | 41.29 | -0.080 | 19.921 | 0.582 |
| | | 6 | 282.4 | 11.44 | 61.56 | 0.28311 | 238.5618 | 43.80 | -0.067 | 17.757 | 0.644 |
| | | 7 | 282.4 | 3.28 | 61.86 | 0.28306 | 240.0059 | 45.40 | -0.058 | 16.457 | 0.200 |
| | | 8 | 282.4 | 9.30 | 61.24 | 0.28301 | 241.2405 | 46.77 | -0.051 | 14.473 | 0.643 |
| | | 9 | 282.4 | 14.88 | 60.13 | 0.28292 | 243.6118 | 49.39 | -0.037 | 10.743 | 1.385 |
| | | 10 | 282.4 | 11.96 | 60.68 | 0.28276 | 246.2432 | 52.28 | -0.021 | 8.395 | 1.424 |
| | | 11 | 282.4 | 11.96 | 60.84 | 0.28260 | 247.4159 | 53.57 | -0.014 | 7.265 | 1.646 |
| csub_016 | csub_016 | . | | 11.72 | 56.54 | 0.28322 | 224.2479 | 27.75 | -0.152 | 28.795 | |
| | | 1 | 284.9 | 24.81 | 56.54 | 0.28318 | 226.6592 | 30.48 | -0.137 | 26.069 | 0.952 |
| | | 2 | 284.9 | 0.17 | 58.06 | 0.28311 | 229.0872 | 33.21 | -0.123 | 24.850 | 0.007 |
| | | 3 | 284.9 | 19.42 | 58.81 | 0.28305 | 230.9920 | 35.35 | -0.112 | 23.456 | 0.828 |
| | | 4 | 284.9 | 8.13 | 59.85 | 0.28298 | 233.6705 | 38.35 | -0.096 | 21.495 | 0.378 |
| | | 5 | 284.9 | 11.09 | 60.80 | 0.28292 | 235.5390 | 40.44 | -0.085 | 20.363 | 0.545 |
| | | 6 | 284.9 | 11.56 | 61.27 | 0.28287 | 237.7407 | 42.89 | -0.071 | 18.375 | 0.629 |
| | | 7 | 284.9 | 3.15 | 61.45 | 0.28282 | 239.1704 | 44.48 | -0.063 | 16.976 | 0.186 |
| | | 8 | 284.9 | 10.80 | 60.45 | 0.28276 | 240.5267 | 45.98 | -0.055 | 14.466 | 0.747 |
| | | 9 | 284.9 | 14.81 | 59.68 | 0.28271 | 243.0164 | 48.73 | -0.040 | 10.949 | 1.353 |

| | | | | | | | | | | | |
|---|---|---|---|---|---|---|---|---|---|---|---|
| | | 10 | 284.9 | 12.47 | 60.42 | 0.28255 | 245.6679 | 51.65 | -0.024 | 8.767 | 1.422 |
| | | 11 | 284.9 | 12.47 | 60.60 | 0.28239 | 246.8796 | 52.98 | -0.017 | 7.614 | 1.637 |
| csub_017 | csub_017 | . | | 13.07 | 56.09 | 0.28310 | 224.1000 | 27.58 | -0.153 | 28.506 | |
| | | 1 | 284.8 | 24.29 | 56.09 | 0.28308 | 226.4614 | 30.25 | -0.138 | 25.836 | 0.940 |
| | | 2 | 284.8 | 0.86 | 57.53 | 0.28303 | 228.9062 | 33.01 | -0.124 | 24.518 | 0.035 |
| | | 3 | 284.8 | 31.93 | 58.45 | 0.28299 | 232.0944 | 36.59 | -0.105 | 21.857 | 1.461 |
| | | 4 | 284.8 | 7.73 | 59.96 | 0.28295 | 235.9511 | 40.90 | -0.082 | 19.057 | 0.406 |
| | | 5 | 284.8 | 11.23 | 60.67 | 0.28291 | 237.7946 | 42.95 | -0.071 | 17.716 | 0.634 |
| | | 6 | 284.8 | 12.62 | 60.93 | 0.28288 | 240.1139 | 45.52 | -0.057 | 15.407 | 0.819 |
| | | 7 | 284.8 | 5.39 | 61.06 | 0.28284 | 241.8655 | 47.46 | -0.047 | 13.593 | 0.397 |
| | | 8 | 284.8 | 10.05 | 60.12 | 0.28275 | 243.3664 | 49.12 | -0.038 | 10.999 | 0.913 |
| | | 9 | 284.8 | 14.84 | 59.35 | 0.28253 | 245.7861 | 51.78 | -0.023 | 7.565 | 1.962 |
| | | 10 | 284.8 | 12.42 | 60.07 | 0.28226 | 248.4370 | 54.69 | -0.008 | 5.384 | 2.307 |
| | | 11 | 284.8 | 12.42 | 60.25 | 0.28212 | 249.6448 | 56.01 | 0.000 | 4.240 | 2.930 |
| csub_018 | csub_018 | . | | 21.33 | 57.57 | 0.28236 | 223.8666 | 27.32 | -0.153 | 30.257 | |
| | | 1 | 277.3 | 24.63 | 57.57 | 0.28234 | 226.3264 | 30.10 | -0.139 | 27.475 | 0.896 |
| | | 2 | 277.3 | 4.69 | 58.67 | 0.28231 | 229.2549 | 33.40 | -0.121 | 25.269 | 0.186 |
| | | 3 | 277.3 | 48.15 | 59.32 | 0.28229 | 234.5330 | 39.32 | -0.090 | 20.004 | 2.407 |
| | | 4 | 277.3 | 12.99 | 61.06 | 0.28226 | 240.6394 | 46.11 | -0.054 | 14.949 | 0.869 |
| | | 5 | 277.3 | 22.35 | 61.52 | 0.28221 | 244.1693 | 50.00 | -0.033 | 11.515 | 1.941 |
| | | 6 | 277.3 | 23.82 | 61.69 | 0.28205 | 248.7814 | 55.07 | -0.005 | 6.620 | 3.598 |
| | | 7 | 277.3 | 13.88 | 61.87 | 0.28176 | 252.5474 | 56.17 | 0.017 | 5.700 | 2.436 |
| | | 8 | 277.3 | 16.61 | 60.79 | 0.28140 | 255.5929 | 56.12 | 0.035 | 4.669 | 3.557 |
| | | 9 | 277.3 | 22.97 | 59.79 | 0.28095 | 259.5464 | 56.07 | 0.059 | 3.721 | 6.175 |
| | | 10 | 277.3 | 22.29 | 60.69 | 0.28040 | 264.0672 | 56.00 | 0.086 | 4.694 | 4.748 |
| | | 11 | 277.3 | 22.29 | 60.91 | 0.28013 | 266.2933 | 55.96 | 0.100 | 4.952 | 4.501 |
| csub_019 | csub_019 | . | | 29.24 | 57.48 | 0.28403 | 223.7976 | 27.24 | -0.155 | 30.243 | |
| | | 1 | 278.3 | 25.67 | 57.48 | 0.28401 | 226.3523 | 30.13 | -0.140 | 27.354 | 0.938 |
| | | 2 | 278.3 | 13.65 | 58.54 | 0.28398 | 230.2651 | 34.54 | -0.117 | 24.002 | 0.569 |
| | | 3 | 278.3 | 31.60 | 59.98 | 0.28395 | 234.7679 | 39.58 | -0.090 | 20.399 | 1.549 |
| | | 4 | 278.3 | 21.76 | 62.57 | 0.28392 | 240.0778 | 45.48 | -0.058 | 17.085 | 1.273 |
| | | 5 | 278.3 | 35.50 | 63.02 | 0.28386 | 245.7755 | 51.77 | -0.024 | 11.249 | 3.156 |
| | | 6 | 278.3 | 40.78 | 63.05 | 0.28362 | 253.3662 | 56.40 | 0.021 | 6.651 | 6.131 |
| | | 7 | 278.3 | 24.29 | 63.29 | 0.28312 | 259.8416 | 56.34 | 0.059 | 6.955 | 3.492 |
| | | 8 | 278.3 | 26.73 | 61.82 | 0.28248 | 264.9189 | 56.26 | 0.090 | 5.559 | 4.808 |
| | | 9 | 278.3 | 32.94 | 60.56 | 0.28169 | 270.8570 | 56.16 | 0.126 | 4.404 | 7.479 |
| | | 10 | 278.3 | 34.37 | 61.96 | 0.28074 | 277.5553 | 56.04 | 0.166 | 5.920 | 5.805 |
| | | 11 | 278.3 | 34.37 | 62.29 | 0.28026 | 280.9755 | 55.98 | 0.187 | 6.313 | 5.444 |
| csub_020 | csub_020 | . | | 33.44 | 58.79 | 0.28351 | 224.0213 | 27.49 | -0.153 | 31.298 | |
| | | 1 | 280.8 | 27.30 | 58.79 | 0.28350 | 226.7136 | 30.54 | -0.137 | 28.254 | 0.966 |
| | | 2 | 280.8 | 17.25 | 59.62 | 0.28346 | 231.1066 | 35.48 | -0.111 | 24.142 | 0.714 |
| | | 3 | 280.8 | 34.82 | 60.85 | 0.28344 | 236.2413 | 41.22 | -0.081 | 19.632 | 1.774 |
| | | 4 | 280.8 | 26.90 | 63.21 | 0.28341 | 242.3282 | 47.97 | -0.045 | 15.235 | 1.766 |
| | | 5 | 280.8 | 40.47 | 63.55 | 0.28321 | 248.9718 | 55.27 | -0.005 | 8.281 | 4.887 |
| | | 6 | 280.8 | 46.01 | 63.57 | 0.28272 | 257.4998 | 56.29 | 0.046 | 7.285 | 6.317 |
| | | 7 | 280.8 | 28.05 | 63.93 | 0.28206 | 264.8032 | 56.21 | 0.090 | 7.725 | 3.631 |
| | | 8 | 280.8 | 30.25 | 62.51 | 0.28127 | 270.5517 | 56.11 | 0.124 | 6.399 | 4.727 |

| | | | | | | | | | | | |
|---|---|---|---|---|---|---|---|---|---|---|---|
| | | 9 | 280.8 | 36.17 | 61.21 | 0.28033 | 277.1010 | 55.99 | 0.164 | 5.223 | 6.926 |
| | | 10 | 280.8 | 40.32 | 62.45 | 0.27923 | 284.6442 | 55.85 | 0.209 | 6.602 | 6.108 |
| | | 11 | 280.8 | 40.32 | 62.75 | 0.27867 | 288.6206 | 55.78 | 0.233 | 6.974 | 5.782 |
| csub_021 | csub_021 | . | | 32.56 | 60.85 | 0.28198 | 225.0800 | 28.69 | -0.146 | 32.154 | |
| | | 1 | 273.5 | 42.26 | 60.85 | 0.28197 | 229.3582 | 33.52 | -0.121 | 27.328 | 1.546 |
| | | 2 | 273.5 | 30.73 | 61.27 | 0.28194 | 236.7475 | 41.79 | -0.077 | 19.485 | 1.577 |
| | | 3 | 273.5 | 47.05 | 61.57 | 0.28191 | 244.6219 | 50.50 | -0.030 | 11.064 | 4.252 |
| | | 4 | 273.5 | 22.12 | 62.66 | 0.28172 | 251.6250 | 56.16 | 0.012 | 6.498 | 3.405 |
| | | 5 | 273.5 | 30.63 | 62.75 | 0.28135 | 256.9658 | 56.12 | 0.044 | 6.630 | 4.620 |
| | | 6 | 273.5 | 33.27 | 62.90 | 0.28084 | 263.4347 | 56.05 | 0.082 | 6.850 | 4.857 |
| | | 7 | 273.5 | 21.97 | 63.47 | 0.28020 | 269.0273 | 55.97 | 0.116 | 7.500 | 2.930 |
| | | 8 | 273.5 | 27.40 | 63.23 | 0.27946 | 274.0259 | 55.88 | 0.146 | 7.350 | 3.728 |
| | | 9 | 273.5 | 34.42 | 62.83 | 0.27860 | 280.2844 | 55.77 | 0.184 | 7.063 | 4.873 |
| | | 10 | 273.5 | 34.13 | 62.78 | 0.27760 | 287.2247 | 55.64 | 0.225 | 7.139 | 4.781 |
| | | 11 | 273.5 | 34.13 | 62.78 | 0.27710 | 290.6804 | 55.57 | 0.246 | 7.206 | 4.737 |
| csub_022 | csub_022 | . | | 34.82 | 59.84 | 0.28185 | 224.6391 | 28.19 | -0.148 | 31.647 | |
| | | 1 | 282.2 | 38.99 | 59.84 | 0.28184 | 228.4660 | 32.51 | -0.126 | 27.327 | 1.427 |
| | | 2 | 282.2 | 30.37 | 60.73 | 0.28181 | 235.2739 | 40.14 | -0.085 | 20.588 | 1.475 |
| | | 3 | 282.2 | 48.86 | 61.49 | 0.28179 | 243.0508 | 48.77 | -0.039 | 12.721 | 3.841 |
| | | 4 | 282.2 | 22.58 | 62.67 | 0.28161 | 250.0630 | 56.15 | 0.003 | 6.520 | 3.463 |
| | | 5 | 282.2 | 32.35 | 62.49 | 0.28125 | 255.4547 | 56.10 | 0.035 | 6.384 | 5.068 |
| | | 6 | 282.2 | 32.08 | 62.12 | 0.28075 | 261.7783 | 56.04 | 0.073 | 6.083 | 5.273 |
| | | 7 | 282.2 | 22.11 | 63.20 | 0.28014 | 267.0970 | 55.96 | 0.105 | 7.234 | 3.057 |
| | | 8 | 282.2 | 36.10 | 63.02 | 0.27942 | 272.8101 | 55.87 | 0.139 | 7.152 | 5.047 |
| | | 9 | 282.2 | 32.74 | 62.31 | 0.27857 | 279.5664 | 55.76 | 0.179 | 6.543 | 5.004 |
| | | 10 | 282.2 | 43.42 | 62.70 | 0.27758 | 287.0418 | 55.64 | 0.224 | 7.067 | 6.145 |
| | | 11 | 282.2 | 43.42 | 62.81 | 0.27708 | 291.3037 | 55.57 | 0.250 | 7.241 | 5.997 |
| csub_023 | csub_023 | . | | 47.06 | 60.65 | 0.28056 | 225.2792 | 28.92 | -0.144 | 31.732 | |
| | | 1 | 276.6 | 52.43 | 60.65 | 0.28055 | 230.5287 | 34.83 | -0.113 | 25.816 | 2.031 |
| | | 2 | 276.6 | 46.21 | 61.55 | 0.28051 | 240.4052 | 45.85 | -0.054 | 15.703 | 2.943 |
| | | 3 | 276.6 | 69.83 | 62.44 | 0.28032 | 252.0249 | 55.99 | 0.015 | 6.453 | 10.821 |
| | | 4 | 276.6 | 39.51 | 63.84 | 0.27978 | 262.9735 | 55.92 | 0.080 | 7.921 | 4.987 |
| | | 5 | 276.6 | 43.96 | 63.94 | 0.27901 | 271.3312 | 55.82 | 0.130 | 8.117 | 5.416 |
| | | 6 | 276.6 | 49.21 | 63.37 | 0.27800 | 280.6605 | 55.69 | 0.186 | 7.676 | 6.411 |
| | | 7 | 276.6 | 36.47 | 64.81 | 0.27678 | 289.2403 | 55.53 | 0.238 | 9.279 | 3.931 |
| | | 8 | 276.6 | 39.56 | 64.88 | 0.27539 | 296.8535 | 55.35 | 0.284 | 9.522 | 4.154 |
| | | 9 | 276.6 | 48.47 | 64.23 | 0.27380 | 305.6676 | 55.15 | 0.337 | 9.080 | 5.338 |
| | | 10 | 276.6 | 46.02 | 65.02 | 0.27201 | 315.1293 | 54.92 | 0.394 | 10.101 | 4.557 |
| | | 11 | 276.6 | 46.02 | 65.21 | 0.27140 | 319.7377 | 54.84 | 0.421 | 10.370 | 4.438 |
| csub_024 | csub_024 | . | | 47.63 | 60.61 | 0.28175 | 225.2861 | 28.92 | -0.144 | 31.682 | |
| | | 1 | 279.0 | 45.89 | 60.61 | 0.28173 | 229.8414 | 34.06 | -0.117 | 26.546 | 1.729 |
| | | 2 | 279.0 | 38.99 | 61.37 | 0.28169 | 238.2677 | 43.48 | -0.067 | 17.895 | 2.179 |
| | | 3 | 279.0 | 69.86 | 62.96 | 0.28166 | 249.0740 | 55.39 | -0.003 | 7.571 | 9.228 |
| | | 4 | 279.0 | 41.05 | 64.46 | 0.28121 | 260.0845 | 56.10 | 0.062 | 8.359 | 4.911 |
| | | 5 | 279.0 | 49.04 | 64.50 | 0.28048 | 269.0282 | 56.01 | 0.116 | 8.497 | 5.772 |
| | | 6 | 279.0 | 49.40 | 64.19 | 0.27949 | 278.8004 | 55.88 | 0.174 | 8.313 | 5.942 |
| | | 7 | 279.0 | 35.66 | 65.72 | 0.27827 | 287.2443 | 55.72 | 0.225 | 9.997 | 3.567 |

| | | | | | | | | | | | |
|---|---|---|---|---|---|---|---|---|---|---|---|
| | | 8 | 279.0 | 43.43 | 65.48 | 0.27685 | 295.0963 | 55.54 | 0.272 | 9.938 | 4.370 |
| | | 9 | 279.0 | 51.09 | 64.73 | 0.27520 | 304.4796 | 55.33 | 0.329 | 9.399 | 5.436 |
| | | 10 | 279.0 | 49.75 | 65.45 | 0.27333 | 314.4896 | 55.09 | 0.389 | 10.363 | 4.800 |
| | | 11 | 279.0 | 49.75 | 65.63 | 0.27270 | 319.4281 | 55.01 | 0.419 | 10.624 | 4.683 |
| csub_025 | csub_025 | . | | 47.74 | 60.19 | 0.28182 | 225.1296 | 28.75 | -0.145 | 31.438 | |
| | | 1 | 287.0 | 43.89 | 60.19 | 0.28180 | 229.3653 | 33.52 | -0.120 | 26.661 | 1.646 |
| | | 2 | 287.0 | 36.68 | 61.01 | 0.28177 | 237.1412 | 42.22 | -0.074 | 18.783 | 1.953 |
| | | 3 | 287.0 | 66.07 | 62.60 | 0.28174 | 247.0573 | 53.18 | -0.015 | 9.423 | 7.011 |
| | | 4 | 287.0 | 38.77 | 64.10 | 0.28139 | 257.1749 | 56.12 | 0.045 | 7.980 | 4.859 |
| | | 5 | 287.0 | 49.41 | 64.26 | 0.28081 | 265.6848 | 56.05 | 0.096 | 8.210 | 6.018 |
| | | 6 | 287.0 | 53.51 | 64.51 | 0.28000 | 275.6174 | 55.95 | 0.155 | 8.565 | 6.248 |
| | | 7 | 287.0 | 36.92 | 65.42 | 0.27900 | 284.3449 | 55.82 | 0.207 | 9.604 | 3.844 |
| | | 8 | 287.0 | 44.70 | 65.12 | 0.27782 | 292.2220 | 55.67 | 0.255 | 9.449 | 4.731 |
| | | 9 | 287.0 | 53.14 | 64.92 | 0.27646 | 301.6640 | 55.49 | 0.312 | 9.423 | 5.639 |
| | | 10 | 287.0 | 51.04 | 65.08 | 0.27490 | 311.7179 | 55.29 | 0.372 | 9.787 | 5.216 |
| | | 11 | 287.0 | 51.04 | 65.12 | 0.27413 | 316.6440 | 55.19 | 0.402 | 9.925 | 5.143 |

Table B.3: Yan and Lin [61]

| | | | | | | | |
|---|---|---|---|---|---|---|---|
| Yan and Lin [61 ] | | | | | | | |
| R-134a, D = 2.0 mm | | | | | | | |
| T_sat = 31 C | | | | | | | |
| | | | | | 15 kW/m^2 | | |
| | **G = 200 kg/m^2s** | | | **G = 100 kg/m^2s** | | **G = 50 kg/m^2s** | |
| | **x** | **h** | | **x** | **h** | **x** | **h** |
| | 0.12 | 6200 | | 0.08 | 4900 | 0.22 | 2600 |
| | 0.18 | 5800 | | 0.19 | 5300 | 0.4 | 2300 |
| | 0.29 | 5200 | | 0.32 | 4900 | 0.52 | 2100 |
| | 0.38 | 4800 | | 0.5 | 4100 | 0.8 | 1300 |
| 20 kW/m^2 | 0.45 | 4300 | | 0.66 | 3400 | | |
| | 0.55 | 4100 | | 0.68 | 2600 | h | q |
| | 0.71 | 3400 | | 0.81 | 2400 | | |
| | 0.78 | 2600 | | 0.815 | 2400 | 2600 | 5000 |
| | 0.92 | 2000 | | 0.86 | 2600 | 2300 | 5000 |
| | 0.12 | 5300 | | | | 2100 | 5000 |
| | | | | | | 1300 | 5000 |
| h | q | | | h | q | | |
| | | | | | | | |
| 6200 | 20000 | | | 4900 | 15000 | | |
| 5800 | 20000 | | | 5300 | 15000 | | |
| 5200 | 20000 | | | 4900 | 15000 | | |
| 4800 | 20000 | | | 4100 | 15000 | | |
| 4300 | 20000 | | | 3400 | 15000 | | |
| 4100 | 20000 | | | 2600 | 15000 | | |
| 3400 | 20000 | | | 2400 | 15000 | | |
| 2600 | 20000 | | | 2400 | 15000 | | |
| 2000 | 20000 | | | 2600 | 15000 | | |
| 5300 | 20000 | | | | | | |
| | | | | | | | |
| | | | | | | | |
| | | | | | | | |

## References

[1] D.C. Lowe and K.S.Rezkalla, Flow Regime identification in microgravity two-phase flow using void fraction signals. Int. J. Multiphase flow 25, 433-457 (99)

[2] Ghiaasiaan, S.M., Abdul-Khalik, S.I., 2001. Two Phase flow in micro-channels. Advances in Heat Transfer 34, 145-254.

[3] S.G. Kandlikar, Fundamental issues related to flow boiling in minichannels and micro channels, Experimental Thermal and Fluid Science 26 (2002 389-407

[4] S. Lin, P.A. Kew, K.Cornwell, Two-phase heat transfer to a refrigerant in a 1 mm diameter tube, International Journal of Refrigeration 24 (2001) 51-56.

[5] J.G. Collier and J.R. Thome, Convective Boiling and Condensation, third ed., Oxford University Press, Inc., N.Y. 1996

[6] V.P. Carey, Liquid phase Change Phenomena: An introduction to the thermophysics of vaporization and condensation process in Heat transfer equipment. 1992

[7] G.F. Hewitt, D.N. Robert, Studies in two phase flow patterns by simultaneous x-ray and flash photography AERE-M-2159 HMSO.

[8] D. Baker, "Simultaneous Flow of Oil and Gas," *Oil and Gas J*, 53, pp 183-195 1954.

[9] T. Som, Satyendra Kumar, Vishwas N. Kulkarni, $H^+$ ion induced hydrogen depletion from a-C: H films, Nuclear Instruments and methods in Physics Research B 156 (1999) 212-216

[10] D.A. Butterworth, A comparison of some void-fraction relationships for co-current gas-liquid flow, Int. J. Multiphase Flow, v1, pp 845-850. 1975

[11] V.V. Klimenko, A generalized correlation for two phase forced flow heat transfer, International Journal of Heat and Mass transfer, 31 (1988) 541-552

[12] Klimenko, V.V. 1990 A generalized correlation for two phase flow heat transfer, second assessment. Int. J. Heat and Mass Trans. 33: 2073-2088

[13] S.G. Kandlikar," Heat Transfer Characteristics in Partial Boiling, Fully Developed Boiling, and Significant Void Flow Regions of Sub cooled Flow Boiling, Journal of Heat Transfer, May 1998, Vol. 120 p395

[14] L.S. Tong, Y.S. Tang, Boiling Heat transfer and two phase flow ed. 2 1997

[15] K.E. Gungor, R.H.S Winterton, “Simplified general Correlation for saturated flow Boiling and comparisons of correlations with data, Chem. Eng. Res Des, Vol. 65, March 1987

[16] Thome, J.R., “Boiling in micro-channels: a review of experiment and theory, Int. J. of Heat and Fluid flow (25) 2004 128-139.

[17] J.C. Chen, “Correlation for Boiling heat Transfer to Saturated fluids in convective Flow”, I & EC Process Design and Development vol. 5 no. 3 July 1966.

[18] M.M. Shah, “A General Correlation for Heat Transfer During Subcooled Boiling in Pipes and Annuli,” ASHRAE Trans., 83, pp. 202–215.1977

[19] R.W. Bjorge, G.R. Hall, W.M. Rohsenow, 1982 Correlations of forced convective boiling heat transfer data. Int. J. Heat Mass Transfer 25, 753-757

[20] Liu and Winterton 1991, A general correlation for saturated and subcooled flow boiling in tubes and annuli, based on a nucleate pool boiling equation, Int. J. Heat Mass transfer vol. 34, no 11, p. 2759-2766

[21] Kandlikar, S.G. 1990, “A General Correlation for Saturated Two-Phase Flow Boiling Heat Transfer Inside Horizontal and Vertical Tubes,” ASME Journal of Heat Transfer, Vol. 112, pp. 219-228

[22] Kandlikar, S.G., “Development of a flow boiling map for subcooled and saturated flow boiling of different fluids inside circular tubes, ASME Journal of Heat transfer 113 (1991) 190-200

[23] Dittus, F.W., Boelter, L.M.K, 1930, “Heat Transfer in automobile radiators of tubular type. University of California Pub. Eng. Vol. 2 pp.443-461

[24] V. Gnielinski, New equations for hear and Mass transfer in turbulent pipe and Channel flow, International Chemical Energy 16 (1970) 359-368

[25] Petukov, B.S., 1970 Heat Transfer and friction in turbulent pipe flow with variable physical Properties. Adv Heat Transfer 6. 503-565

[26] H.K. Forster and N. Zuber, “Bubble dynamics and boiling in heat transfer” AIChE J. 1 532-535, 1955

[27] D. Steiner and J. Taborek, 1992. Flow boiling heat transfer in vertical tubes correlated by asymptotic model. Heat Transfer Eng. 13, 43-69.

[28] J. R. Thome, Laboratory of Heat and Mass Transfer Faculty of Engineering Science Swiss Federal Institute of Technology Lausanne, Switzerland.

[29] Agostini, B., Watel, B., Bontemps, A., Thonon, B., Liquid flow friction factor and heat transfer coefficients in small channels: an experimental investigation. Experimental Thermal and Fluid Science (28) (2004) 97-103.

[30] M. Suo, and P. Griffith, "Two-phase flow in capillary tubes". J. Basic Eng. Vol. 86, 576-582 (1964)

[31] Ghiaasiaan and Abdul-Khalik 2001 (See #2)

[32] S.S. Mehendale, A. M. Jacobi, Evaporative heat transfer in mesoscale heat exchanger, ASHRAE trans. 106 (1) 2000 446-452

[33] C. Vlassie, H. Macchi, J. Guilpart, B. Agostini, Flow boiling in small diameter channels, Int. J. of Refrigeration 27 (2002) 191-201.

[34] T.N. Tran, M.W. Wambsganss, D.M. France, Small Circular and rectangular-channel boiling with two refrigerants, Int. J. Multiphase Flow 22 (3) (1996) 485-498

[35] S.Lin, P.A. Kew, K. Cornwell, Two phase flow regimes and heat transfer in small tubes and channels", Heat Transfer 1998 Proceedings of 11P$^{thP}$ IHTC, vol.2 Aug. 23-28 1998.

[36] B. Agostini, B. Watel, A. Bontemps, B. Thonon, " Friction factor and heat transfer coefficient of R134a liquid flow in mini-channels", Applied Thermal Engineering, 22 (2002) 1821-1834

[37] J. Lee, I Mudawar, "Two phase flow in high-heat micro-channel heat sink for refrigeration cooling applications: Part II- heat transfer characteristics" Int. Journal of Heat and Mass Transfer (2004)

[38] G.M. Lazarek, S.H. Black , Evaporative heat transfer pressure drop and critical heat flux in a small vertical tube with R113, International of Heat and mass transfer (25) 7 (1982) 945-960

[39] Z.Y. Bao, D.F. Fletcher, B.S. Haynes, Flow boiling heat transfer of Freon R11 and HCFC123 in narrow passages, Int. J. Heat Mass Transfer 43 (2000) 3347–3358

[40] W. Yu, D.M. France, M.W. Wambsganss, J.R. Hull, Two-phase pressure drop, boiling heat transfer, and critical heat flux to water in a small-diameter horizontal tube, Int. J. Multiphase Flow 28 (2002) 927–941

[41] P.A. Kew, K. Cornwell, Correlations for the prediction of boiling heat transfer in small-diameter channels, App. Therm. Eng. 17 (1997) 705–715.

[42] T.S. Ravigururajan, Impact of channel geometry on two-phase flow heat transfer characteristics of refrigerants in micro-channels heat exchangers, J. Heat Transfer 120 (1998) 485–491.

[43] H.J. Lee, S.Y. Lee, Heat transfer correlation for boiling flows in small rectangular horizontal channels with low aspect ratios, Int. J. Multiphase Flow 27 (2001) 2043–2062.

[44] S. Lin, P.A. Kew, K. Cornwell, Two-phase heat transfer to a refrigerant in a 1 mm diameter tube, Int. J. Refrige. 24 (2001) 51–56.

[45] G.R. Warrier, V.K. Dhir, L.A. Momoda, Heat transfer and pressure drop in narrow rectangular channels, Exp. Therm. Fluid Sci. 26 (2002) 53–64

[46] Wen, D.S, Y.Yan, D.B.R, Kenning, Saturated flow boiling of water in a narrow channel: time-averaged heat transfer coefficient and correlations, App. Therm. Eng. 24 (2004) 1207-1223

[47] X. Huo, L. Chen, Y.S. Tian, T.G. Karayiannis, Flow boiling and flow regimes in small diameter tubes, App. Therm. Eng. 24 (2004) 1225–1239.

[48] Ingo Hapke, Hartwig Boye, Jurgen Schmidt, "Onset of Nucleate boiling in mini channels" Int. J. Therm. Sci. (2000) 39 505-513

[49] Kennedy, J.E., Roach, Dowling, M.F., G.M, Adel-Khalik, S.I, Ghiaasiaan, S.M., Jeter, S.M., Quershi, Z.H., " The Onset of Flow Instability in Uniformly Heated Horizontal Microchannels", Transactions of the ASME, Vol. 122 Feb. 2000, pp. 118-125.

[50] Chedester, R.C., Ghiaasiaan, S.M., A Proposed mechanism for hydro-dynamically-controlled onset of significant void in microtubes", International Journal of Heat and Fluid Flow 23 (2002) 769-775.

[51] Davis, E.J., Anderson, G.H., 1966. The incipience of nucleate Boiling in forced convection flow "AICHEJ. Vol.12 pp.774-780

[52] Haynes, B.S., Fletcher, D.F., Sub cooled flow boiling heat transfer in narrow passages, Int. J. of Heat and Mass Transfer 46 (2003) 3673-3882

53 D. Gorenflo, Pool Boiling, in: Chapter Ha in VDI Heat Atlas, VDI Vela, Dusseldof, 1993.

54 Jae-Mo Koo, Linan Jiang, Lian Zhang, Peng Zhou, Shilajeet S. Banerjee, Thomas W.Kenny, Juan G. Santiago, Kenneth E. Goodson, "Modeling of two-phase microchannel heat sinks for VLSI chips. IEEE 2001.

55 Zhang, L., Wang, E.N., Koo, J., " Enhanced nucleate boiling in microchannels" 2002 IEEE, Int. conf., Micro Electro Mechanical Systems, Las Vegas, pp.89-92.

56 Yen T., Kasagi, N., Suzuki, Y., "Forced convective boiling heat transfer in microtubes at low mass and heat fluxes", Int. J. of Multiphase Flow 29 (2003) 1771-1792.

57 Roach, G.M, Abdel-Khalik, S.I, Ghiaasiaan, S.M., Jeter, S.M., 1999, Low-flow onset of flow instability in heated microchannels Source: Nuclear science and engineering [0029-5639] Roach yr: 1999 vol: 133 iss: 1 pg: 106

58 B. Sumith, F. Kaminaga, K. Matsumura "Saturated flow boiling of water in a vertical small diameter tube", Experimental Thermal and Fluid Science 27 (2003) 789–801

59 K. Stephan and M. Abdulsalam "Heat Transfer Correlations for Natural Convection Boiling, Int. J. Heat Mass Transfer (23) 1980; p.73-87

60 Baird, J.R., Bao, Z.Y., Fletcher ,D.F., Haynes, B.S, "Local flow boiling heat transfer coefficients in narrow conduits", Multiphase Sci. Technol. 12 (2000) 129-144

61 Y. Yan and T. Lin "Evaporation heat transfer and pressure drop of refrigerant R-134a in a small pipe" International Journal of Heat and Mass Transfer (41) 1998; p.4183-4194

62 Kew PA, Cornwell K. Correlations for prediction of boiling heat transfer in small-diameter channels. Applied Thermal Eng. 1997; 17:705-715

63 M.G. Cooper, Saturated Nucleate pool boiling- a simple correlation. 1st UK National Heat Transfer Conf. IchemE Symp. Series no 86, vol 2, 1984. p. 785-793

64 V. Dupont, J.R. Thome, A.M. Jacobi, Heat transfer model for evaporation in microchannels. Part II: Comparison with the database, International Journal of Mass and Heat Transfer 47 (2004) 3387-3401

65 M.S. Plesset, S.A. Zwick, The growth of vapour bubble in superheated liquid, J Appl. Phys. 25 (1954) 493-500.

$\boxed{66}$ S. S. Kutateladze, Boiling Heat transfer, Int. J. Heat Mass Transfer 4, 31-45 (1961)

$\boxed{67}$ S.W Churchill," Friction-factor equation spans all fluid flow regimes," Chem. Eng., November, pp 91-92, 1977 (1974)

$\boxed{68}$ S.G.,Kandlikar, and M.E. Steinke. "Flow Boiling Heat Transfer Coefficient in Minichannels – Correlation and Trends." Proceedings of 12th International Heat Transfer Conference, Aug 2002, Grenoble, France, Paper # 1178, 2002.

[69] www.pe.utexas.edu/2phaseweb